BIOSENSING OF ORGANOPHOSPHORUS COMPOUNDS USING RECOMBINANT ORGANOPHOSPHATE DEGRADING ENZYMES

Ph.D. Thesis

By
MONIKA JAIN

DEPARTMENT OF BIOSCIENCES AND BIOMEDICAL ENGINEERING
INDIAN INSTITUTE OF TECHNOLOGY INDORE
FEBRUARY 2021

BIOSENSING OF ORGANOPHOSPHORUS COMPOUNDS USING RECOMBINANT ORGANOPHOSPHATE DEGRADING ENZYMES

A THESIS

Submitted in partial fulfillment of the requirements for the award of the degree
of
DOCTOR OF PHILOSOPHY

by

MONIKA JAIN

DEPARTMENT OF BIOSCIENCES AND BIOMEDICAL ENGINEERING
INDIAN INSTITUTE OF TECHNOLOGY INDORE

FEBRUARY 2021

INDIAN INSTITUTE OF TECHNOLOGY INDORE

CANDIDATE'S DECLARATION

I hereby certify that the work which is being presented in the thesis entitled **Biosensing of organophosphorus compounds using recombinant organophosphate degrading enzymes** in the partial fulfillment of the requirements for the award of the degree of **DOCTOR OF PHILOSOPHY** and submitted in the **DEPARTMENT OF BIOSCIENCES AND BIOMEDICAL ENGINEERING, Indian Institute of Technology Indore**, is an authentic record of my own work carried out during the time period from July 2015 to February 2021 under the supervision of Dr. Prashant Kodgire, Associate Professor, Department of Biosciences and Biomedical Engineering, Indian Institute of Technology Indore.

The matter presented in this thesis has not been submitted by me for the award of any other degree of this or any other institute.

Monika 09.07.2021

MONIKA JAIN

This is to certify that the above statement made by the candidate is correct to the best of my knowledge.

P.V. Kodgire

Dr. Prashant Kodgire

(Thesis Supervisor)

MONIKA JAIN has successfully given her Ph.D. Oral Examination held on **09/07/2021**

Signature of Chairperson (OEB)
Date: 09/07/2021

Signature of External Examiner
Date: 09/07/2021

P.V. Kodgire

Signature of Thesis Supervisor
Date: 09/07/2021

Signature of PSPC Member #1
Date: 09/07/2021

Debasis Nayak

Signature of PSPC Member #2
Date: 09/07/2021

ACKNOWLEDGEMENTS

"Success is stumbling from failure to failure with no loss of enthusiasm."

Firstly, I would like to thank God for all His blessings throughout my life. Secondly, I would like to state my deepest sense of gratitude to my parents. Words are not enough to express my gratitude to the source of my life, my parents. Throughout my life my mother, Mrs. Sarita Jain and my father, Mr. Ramesh Kumar Jain, have showered their unconditional love, timely encouragement, endless patience and affection towards me which have always given me the motivation to stand up again when I got weary in all circumstances of life. Without them, I would never be able to reach where I am today. I deeply express my thanks to my brother Mr. Sourabh Jain and my sister-in-law Mrs. Surbhi Jain for their love and moral support through every step of my PhD. Their patience and love have upheld me, particularly in those days when I could hardly find time for them. They have been a pillar of strength, my joy and my guiding light. I also wish to thank my brother Sulabh Jain for his constant love, understanding, motivation and unconditional support all along. I could not have come this far without them.

I am highly grateful to my PhD supervisor, Dr. Prashant Kodgire, to supervise my work and provide invaluable guidance and encouragement throughout my research. His consistent advice and efforts elevated my research work to a higher standard and quality level and ensured that my scientific output is always up to the best possible standards. Without his invariable leadership and motivation, this research work could not have been completed. The combination of his expertise, enthusiasm, and encouragement has been a significant factor in my development as a researcher. On the academic level, Dr. Prashant Kodgire encouraged me to learn the fundamentals of conducting scientific research. Under his supervision, I got the opportunity to learn how to define a research problem, organize the literature search and data, plan experiments and manage time to find a solution, and finally, translate the benchwork into the publication.

I am honoured to be his first female student to prepare and submit the PhD thesis. I would like to express my sincere thanks to Dr. Abhijeet Joshi to give me the opportunity to work with him and provide such a great podium to broaden my knowledge and exposure. I am indebted to him for always finding time between their busy schedule to discuss my results and clear my doubts. I am obliged to my PSPC members Dr. Debasis Nayak (HOD) and Dr. Amit Kumar, for their support, and constant inspiration throughout my IIT Indore stay.

I further take this opportunity to thank the institute authorities at IIT Indore for facilitating a conducive research atmosphere and thank the Director IIT Indore, Prof. Neelesh Kumar Jain, the HoD of BSBE and all the faculty members of the BSBE department at IIT Indore for their constant encouragement and support to help me advance my research and career. I also want to thank the Honorable BOG Chairman Prof. Deepak Phatak sir and the Dean of Academic Affairs, Dr. Devendra Deshmukh, and Dean of Student Affairs, Dr. Santosh Kumar Vishvakarma, for facilitating me to complete my PhD smoothly.

I also want to thank the Chemistry department and the Sophisticated Instrumentation Centre (SIC) at IIT Indore for allowing access to various departmental and institutional instrumental facilities, as well as the BSBE non-teaching staff, academic office staff, student affairs office staff, library staff, health centre staff and other technical and non-technical staff of IIT Indore for their support to complete my PhD.

I thank the Department of Biotechnology, Govt. of India, for research grants (BT/PR20319/BBE/117/189/2016 and BT/PR24652/NER/95/795/2017).

I show my deepest gratitude to Prof. Steven Harvey from the U. S. Army Edgewood Chemical Biological Center and Prof. Dayananda Siddavattam from the Department of Life Sciences at the University of Hyderabad, and

Dr. Debasis Nayak from IIT Indore for a kind gift of OPAA-FL, OPH and mTFP1 gene respectively.

I would like to express my thanks to my labmates Mr. Amit Kumar Singh, Mr. Anubhav Tamrakar, Mr. Ankit Jaiswal, Mr. Rahul, Mr. Tuhin Sarkar, Ms. Sakshi Gorey, Ms Kanika and, my project collaborator Ms. Priyanka Yadav, Mr. Vinay Singh and Bhavna Joshi for their support in my project work, and my colleagues from the research group of Dr. Debasis Nayak, Dr. Abhijeet Joshi and Dr. Amit Kumar, and my colleagues Kaushik Natarajan, Shanu Shukla, Altaf A, Satyam Singh, Charu Sonkar and Chanchal Sonkar and Rahul Chouhan for their valuable time, patience, support and competent advice. I would like to thank my hostel roommate Ms. Kanchan Samadhiya for her support and sisterly love, who has saved me on several occasions from skipping meals by her undulating concern for my well-being after shifting inside the campus.

I further extend my gratitude to my lifelong best friend Rucha Kavishwar and my sister Trishala Jain for their unconditional love, inimitable support and care while also many times being a cook of yummy food, being a stressbuster, and never leaving my side. Also, my friend Arti Thakur and Sonia Yadav, whose continuous support and encouragement helped me a lot throughout my work. This section would be incomplete without mentioning my cutie Arohi, who is my magic mood refresher and the most wonderful child in the world. I also wish to thank all my other friends who directly and indirectly supported me to complete my PhD.

At last, I acknowledge the Ministry of Education (Formerly MHRD), Govt. Of India for providing me a fellowship and its financial support during my PhD.

MONIKA JAIN

DEDICATION

This thesis is wholeheartedly dedicated to my parents, who have been my source of inspiration and gave me strength and provides their moral, spiritual, emotional and financial support. I also dedicate this thesis to my brother, sister and friends who encouraged me to finish the study. This thesis is also dedicated to my supervisor Dr. Prashant Kodgire who encouraged me to build my motivation towards the field of biosensors development and also strengthened my knowledge and concepts in molecular biology.

At last, this thesis is dedicated to the almighty God, by whose support I have gained all my successes in life and whose blessings have enlightened my life.

Jai Jinendra!

SYNOPSIS

1. Introduction

Agricultural advancements focusing on increasing crop production have led to excessive usage of insecticides and pesticides, resulting in leaching and accumulation of these highly toxic chemicals in soil, water, and food-chain. Organophosphorus (OP) compounds are the most commonly used insecticides and pesticides, which cause a wide range of long-lasting and life-threatening conditions. OP compounds were introduced as pesticides mainly in the 1950s and 1960s, and are widely used as insecticides, herbicides, nematicides as well as acaricides. Several derivatives of OPs are commercially marketed and they show prolonged half-life in the soil. For example, methyl parathion shows half-life in the soil for 25-130 days, whereas another OP compound, coumaphos, shows half-life in the soil for 24-1400 days (Singh and Walker 2006).

Continuous or prolonged exposure of the OPs leads to deposition of these compounds at the human organ depot sites, from where they are uninterruptedly released into the blood. Subsequently, from blood, they reach the nervous system where one of their targets is the AChE enzyme. (Masson et al. 1998) **Figure 1** represents the bioavailability and metabolism of OPs in humans. Once a person is exposed to OPs, these compounds may get deposited into sites like liver, kidney, muscles, adipose tissue or they may get distributed to the central nervous system via blood circulation. The amount that remains in the blood is eliminated out via urine, expired air, or in faeces (Masson et al. 1998; Paraíba et al. 2009). In addition to AChE, these compounds target some important enzymes like lipases and esterases that are crucial for proper functioning of the human body. Due to the acute toxicity and long-term side effects of OP compounds, their timely, on-the-spot, and rapid detection has gained importance for efficient healthcare management.

In this respect, several OP degrading enzymes have gained the spotlight in developing enzyme-based biosensors, owing to their high

activity and broad specificity. Among these enzymes, Organophosphorus acid anhydrolase (OPAA) and organophosphorus hydrolase (OPH) have emerged as a promising candidate for the detection of OP compounds, due to their ability to act on a broad range of substrates having a variety of bonds, like P-F, P-O, P-S, and P-CN, as well as chemical warfare agents and nerve agents (Kang et al. 2008). Enzymatic hydrolysis is reportedly 40-2450 times faster compared to chemical hydrolysis (Shimazu et al. 2003), and thus attracts great interest from a scientific viewpoint for the remediation as well as detection of organophosphorus compounds in the environment. The catalytic action of OPH and OPAA is shown in **Figure 2**. OPH and OPAA, in presence of metal ion (Vyas et al. 2010), hydrolyses methyl parathion and ethyl paraoxon into dimethyl thiophosphate and diethyl phosphoric acid, respectively, and a *p*-nitrophenol, a yellow-colored product, which can be detected calorimetrically (**Fig. 2**). This reaction also releases two protons, which eventually decreases pH and in conjunction with a pH-sensitive fluorophore or fluorescent protein like fluorescein isothiocyanate (FITC) and monomeric Teal Fluorescent Protein1 (mTFP1), respectively can be used for indirect fluorometric detection of OP substrates.

There are several reports on the sensing of organophosphorus compounds using OPAA and OPH through electrochemical, optical, and other methods (Xiong et al. 2018). However, an optimal sensor that achieves good enzymatic catalytic activity and low enough detection limits to detect organophosphorus compounds in practical use cases remains elusive; primarily due to reproducibility and cost concerns. In this study, we report colorimetric, as well as fluorescence-based sensing using a known fluorescent dye FITC and fluorescent protein, mTFP1 of organophosphorus compounds, by the interaction of OPAA and OPH with OP compounds such as methyl parathion and ethyl paraoxon.

Thus, the main objectives of this study are:

1. Expression and purification of recombinant organophosphorus acid anhydrolase (OPAA)-FL variant, organophosphorus hydrolase (OPH), and OPAA-FL-mTFP1 fusion protein in *E. coli*.
2. Development of recombinant OPAA-FL variant, OPH, and OPAA-FL-mTFP1 fusion protein-based biosensors for detection of OP compounds.
3. Detection and quantification of pesticides using the recombinant OPAA-FL variant, OPH, and OPAA-FL-mTFP1 fusion protein-based biosensor.

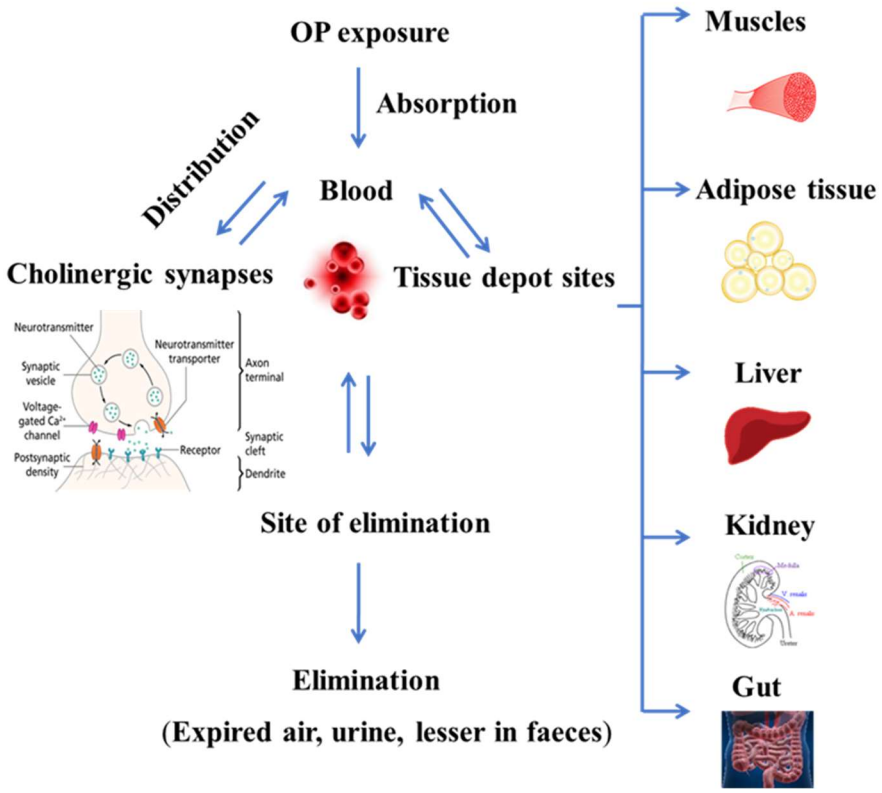

Figure 1. Representation of the bioavailability and metabolism of OPs in the human body. When a person accidendently or deliberately inhales, ingests or absorbs the OPs, it reaches either to its depot sites like muscles, adipose tissue, liver, kidney, or gut or it may get distributed to the central nervous system through the blood circulation. Excess amount that remained in the blood is eliminated out via urine, expelled air, or in faeces (Jain et al. 2019). Modified from (Masson et al. 1998).

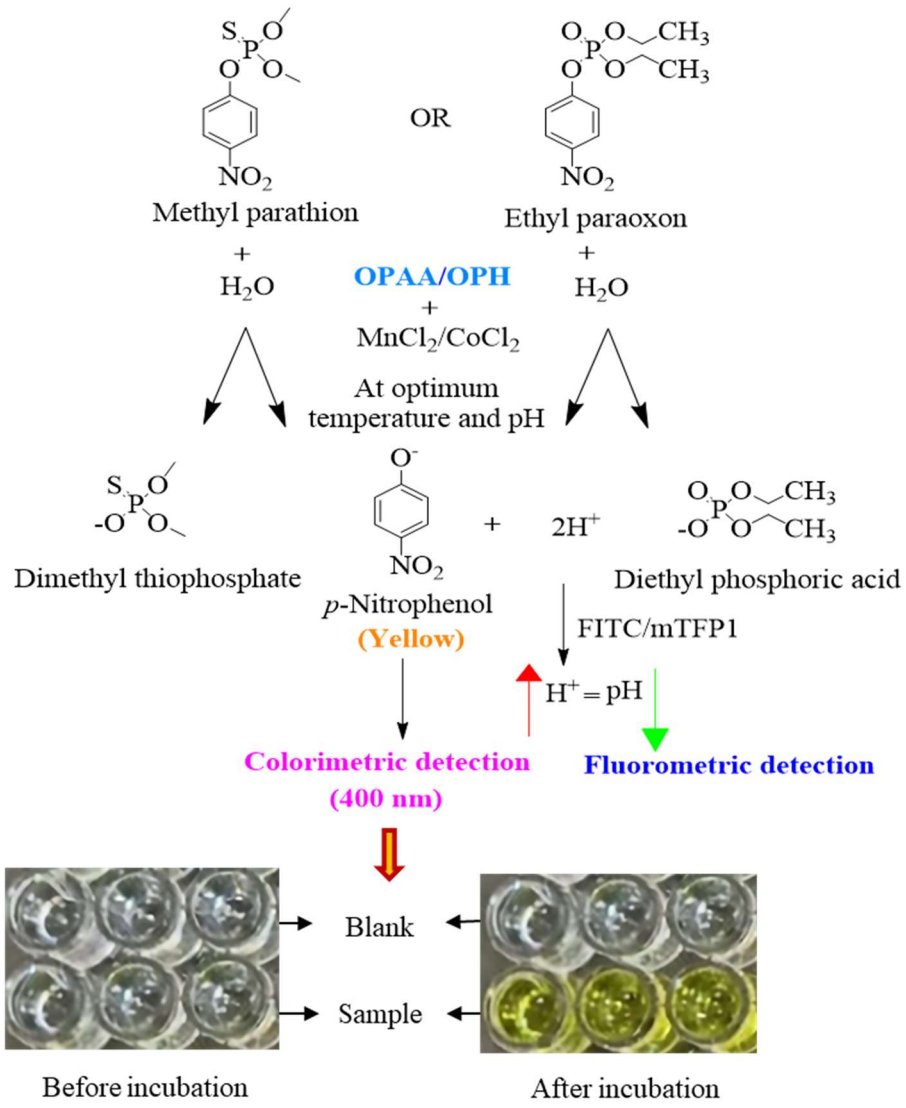

Figure 2. OPAA and OPH reaction mechanism. Depiction of hydrolysis of OP compounds in presence of OP degrading enzymes with p-nitrophenol and H^+ as a product which can be detected by colorimetric and fluorometric detection methods, respectively (Jain et al. 2021).

2. A novel biosensor for the detection of organophosphorus (OP) based pesticides using Organophosphorus acid anhydrolase (OPAA) -FL variant

Indiscriminate use of organophosphorus (OP) based insecticides is a great concern to human health because of bioaccumulation induced health hazards. Potentially fatal consequences and limited treatment methods of OP poisoning necessitate the need for development of reliable, selective, cost-effective, and sensitive methods of OP detection. To tackle this issue, the development of effective devices and methods is required to sensitively detect as well as degrade OPs. Enzymatic sensor systems have gained popularity due to high catalytic activity, enhanced detection limits, and high sensitivity with the environmentally benign operation. OPAA-FL variant (Daczkowski et al. 2015) with mutations Y212F and V343L which is a 50.8 kDa monomeric enzyme obtained from *Alteromonas sp.* JD6.5 is capable of hydrolyzing the P-F, P-O, P-S, and P-CN bonds, in OPs, including nerve agents of the G/V-series. Several mutants of OPAA are reported which have greater activity against various OPs. In this study, recombinant expression of the OPAA-FL variant in *E. coli* was performed, recombinant OPAA-FL variant was purified, and subsequently tested for activity against ethyl paraoxon and methyl parathion. OPAA-FL variant showed its optimum activity at pH 8.5 and 50°C. It is found that OPAA-FL mutations enhance the specific activity towards paraoxon which is 1.96 U/mg, which is 1.2 fold higher when compared to OPAA from marine bacterium *Pseudoalteromonas* sp. SCSIO 04301 (1.6 U/mg) reported by Xiao Yunzhu and his group (Xiao et al. 2017) but diminish the specific activity towards methyl parathion, 0.149 U/mg. Colorimetric and fluorometric assays were used for the estimation of ethyl paraoxon based on *p*-nitrophenol and FITC fluorescence intensity, respectively. OPAA-FL variant conjugated with FITC dye as a sensor for the detection of OPs. Furthermore, the OPAA-FL variant was immobilized into the sodium alginate microspheres to enhance the sensitivity for colorimetric detection of ethyl paraoxon.

The colorimetric detection method developed using purified unencapsulated and alginate-encapsulated OPAA-FL variant exhibited detection limits of 0.04 and 0.036 mM, with the linear range of 0.01 to 1 mM and 0.025 to 1 mM, respectively, for ethyl paraoxon **(Fig. 3A-B).** The fluorometric detection method using purified OPAA-FL variant, with ethyl paraoxon as the substrate, reveals the lower limit of detection as 0.038 mM with the linear range of 0.1 to 0.5 mM **(Fig. 3C)**. This is the first study on alginate encapsulation of the OPAA-FL variant for biosensing of paraoxon. This work is expected to be of interest to researchers across the biological and environmental sciences while providing insight into the structure-function relationship of the mutant OPAA-FL variant enzyme.

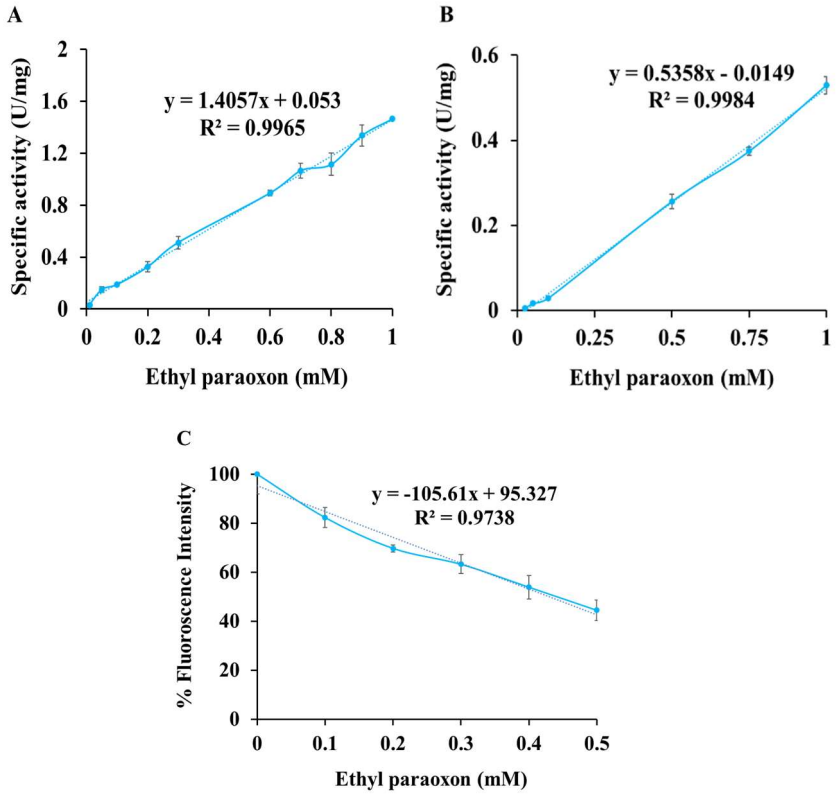

Figure 3. Biosensing of ethyl paraoxon using the OPAA-FL variant enzyme. Colorimetric biosensing of ethyl paraoxon with Bis-Tris propane buffer pH 8.5, at 50 °C for 15 minutes. **(A)** Colorimetric biosensing of 0.01-1 mM ethyl paraoxon using the purified unencapsulated OPAA-FL variant enzyme. **(B)** Colorimetric biosensing of 0.025-1 mM ethyl paraoxon using encapsulated OPAA-FL variant enzyme. **(C)** Bio-sensing of ethyl paraoxon using the OPAA-FL variant via fluorescence assay. 1:1 ratio of OPAA-FL variant and FITC-dextran were used with 0.1 to 0.5 mM ethyl paraoxon as the substrate at 50 ºC, for 3 minutes without activity buffer. Fluorescence intensity of FITC decreased linearly with an increase in the concentration of ethyl paraoxon. The values are an average of duplicate samples and error bars represent standard deviation. At least three independent experiments were performed, and a representative result is shown.

3. Recombinant organophosphorus hydrolase (OPH) expression in *E. coli* for the effective detection of organophosphate pesticides

Organophosphorus Hydrolase (OPH), an organophosphotriester-hydrolyzing enzyme originally isolated from *Pseudomonas diminuta* MG and *Flavobacterium sp*., has attracted the attention of researchers for potential biosensing applications for pesticide products due to its broad substrate scope and specificity. OPH has been proved to be an effective biocatalyst for hydrolysis of OPs, owing to which it has been considered for the purpose of detection and/or remediation of OPs. In this regard, a novel biosensor based on the enzymatic action of OPH is developed by recombinant expression in *E. coli*. In this chapter, I report the development of colorimetric and fluorometric biosensors made of His-Nus-OPH for OPs detection. I have cloned, expressed, and purified recombinant His-Nus-OPH fusion protein, and also encapsulated His-Nus-OPH into alginate microspheres. A colorimetric method developed using solution-phase and alginate-encapsulated His-Nus-OPH for OPs detection, and a fluorometric method using pH-sensitive FITC dye was employed for OPs detection. The colorimetric detection method developed using solution-phase and alginate-encapsulated His-Nus-OPH exhibited detection limits of 0.034 and 0.024 mM, respectively, for ethyl paraoxon, and 0.06 and 0.049 mM, respectively, for methyl parathion **(Fig. 4A-D).** The fluorometric detection method using solution-phase His-Nus-OPH, with ethyl paraoxon and methyl parathion as the substrate, reveals the lower limit of detection as 0.014 mM and 0.044 mM, respectively **(Fig. 4E-F)**. The results demonstrate the viability of His-Nus-OPH for OPs detection with good sensitivity, LOD, and linear range. Biosensing parameters show better results for ethyl paraoxon over methyl parathion. I report the first use of N-terminal His-NusA-tagged OPH, which enhances solubility significantly and presents a significant advance for the scientific community and also the first report on alginate encapsulation of His-Nus-OPH for biosensing of OPs.

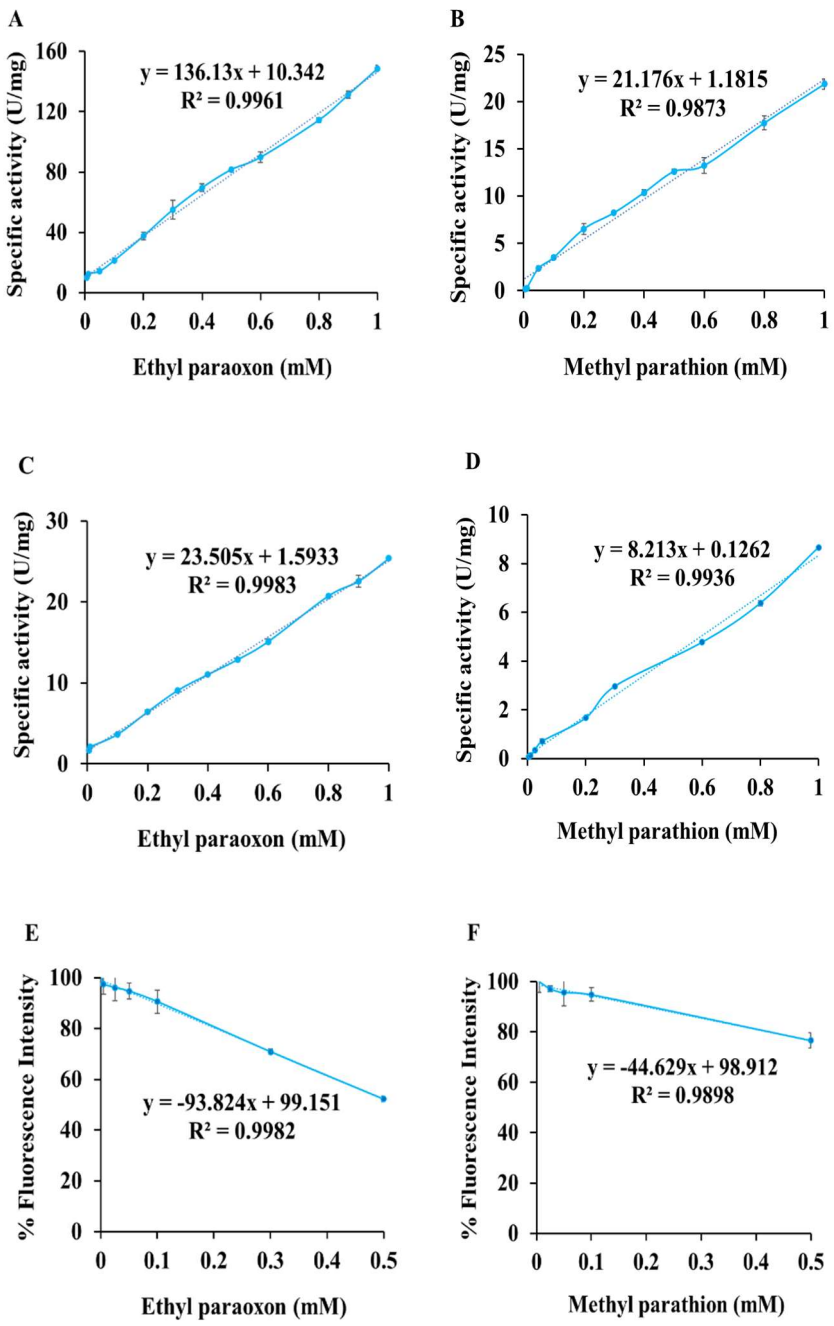

Figure 4. Biosensing of OPs using the His-Nus-OPH enzyme. Colorimetric activity assay of solution-phase His-Nus-OPH with 0.005 to 1 mM of the substrate with CHES buffer pH 9.0, at 37 ºC for 5 minutes. **(A)** With ethyl paraoxon **(B)** With methyl parathion. Colorimetric activity assay of encapsulated His-Nus-OPH with different substrate concentrations with CHES buffer pH 9.0, at 37 ºC. **(C)** Activity assay of His-Nus-OPH with 0.005 to 1 mM of ethyl paraoxon, for 10 minutes. **(D)** Activity assay of His-Nus-OPH with 0.005 to 1 mM of methyl parathion, for 20 minutes. Bio-sensing of ethyl paraoxon using solution-phase His-Nus-OPH via fluorescence assay. The 1:12 ratio of

His-Nus-OPH and FITC-dextran was used at 37 ºC for 5 minutes, without activity buffer. **(E)** Fluorescence assay of His-Nus-OPH with 0.001 to 0.5 mM of ethyl paraoxon. **(F)** Fluorescence assay of His-Nus-OPH with 0.005 to 0.5 mM of methyl parathion. The values are represented as the average of duplicate samples and the standard deviation is indicated by error bars. A representative result is shown based on at least three separate experiments.

4. Fluorometric biosensing of organophosphates using a recombinant organophosphorus acid anhydrolase (OPAA)-FL variant with monomeric teal fluorescent (mTFP) fusion protein expressed in *E. coli*.

In continuous efforts to explore enzymatic systems and sensing platforms for the detection of organophosphorus compounds, fusion proteins have often been employed in the literature, comprised of a protein of interest and a fluorescent protein, to obtain enhanced interactions between the fluorescent molecule and the enzyme for sensing applications. To tackle this problem, effective devices and methods are required to sensitively detect and degrade organophosphorus compounds. In this chapter, we explore the use of mTFP1 as the pH-sensitive fluorophore to evaluate the enzymatic activity of OPAA-FL-mTFP1 as a biosensing platform based on the OPAA-FL-mTFP1 fusion protein for the sensitive detection of paraoxon, which is found to detect paraoxon in fluorometric assay. As per colorimetric assay specific activity of OPAA-FL-mTFP1 fusion protein was 0.668 U/mg. The colorimetric detection method developed using purified OPAA-FL-mTFP1 exhibited detection limits of 0.0254 mM, with the linear range of 0.005 to 1 mM and good sensitivity for ethyl paraoxon **(Fig. 5A).** The fluorometric detection method using purified OPAA-FL-mTFP1, with ethyl paraoxon as the substrate, reveals the lower limit of detection as 0.066 mM with the linear range of 0.1 to 1 mM **(Fig. 5B)**. This chapter represents one of the first studies with potential mTFP1 for enzymatic sensing applications and is expected to further drive research efforts towards the development of sensitive probes for the estimation of organophosphorus pesticides.

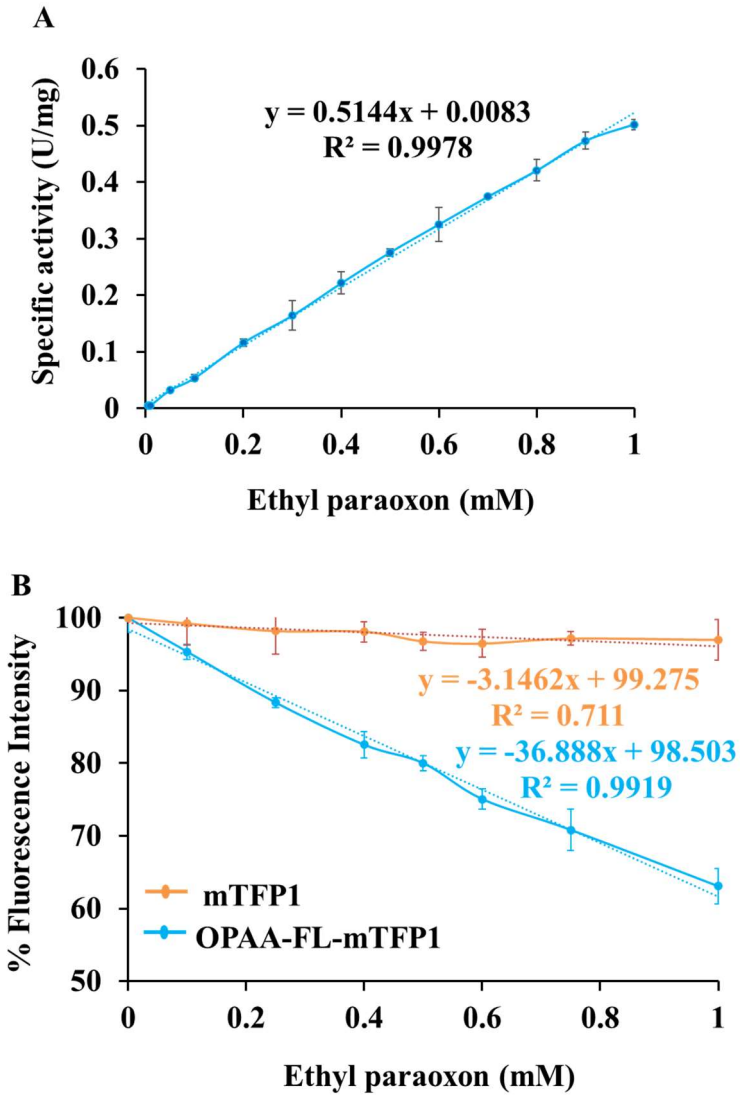

Figure 5. Biosensing of ethyl paraoxon using the OPAA-FL-mTFP1 enzyme. (A) Colorimetric activity assay of OPAA-FL-mTFP1 with 0.005 to 1 mM of the substrate with Bis-Tris propane buffer pH 8.5, at 65 °C for 15 minutes. **(B)** Bio-sensing of ethyl paraoxon using the OPAA-FL-mTFP1 and mTFP1 as a control via fluorescence assay with 0.1 to 1 mM ethyl paraoxon as the substrate at 50 ºC, for 10 minutes with activity buffer. The fluorescence intensity of mTFP1 decreased linearly with an increase in the concentration of ethyl paraoxon. The values are an average of duplicate samples and error bars represent standard deviation. At least three independent experiments were performed, and a representative result is shown.

5. Scope of the thesis

The thesis is presented in six chapters. A review of the relevant literature leading to the focus and objectives of this research are presented in Chapter 1. Chapter 2 presents the methodologies used during experiments. The results of the studies showed biosensing of OPs with OPAA-FL variant, His-Nus-OPH, and OPAA-FL-mTFP1 fusion proteins are presented in the next three chapters. Chapter 3 covers the work carried out for biosensing of ethyl paraoxon using the OPAA-FL variant enzyme. Chapter 4 describes the biosensing of ethyl paraoxon and methyl parathion using His-Nus-OPH enzyme. Chapter 5 addresses the biosensing of ethyl paraoxon using OPAA-FL-mTFP1 fusion protein. The thesis concludes in Chapter 6, with a summary and scope for future work.

The present thesis thus explores the use of recombinant OPAA-FL variant, His-Nus-OPH, and OPAA-FL-mTFP1 as enzymatic sensing elements for the detection and potential remediation of organophosphorus compounds, while using fluorescent dyes such as FITC or proteins such as mTFP1 as the fluorophore. The results are discussed in details along with the potential for future improvements and enhancements to the detection mechanism, linear range, sensitivity, and limits of detection. Synergistic approaches with complementary enzymes and nanomaterials are also discussed.

References

Daczkowski CM, Pegan SD, Harvey SP (2015) Engineering the Organophosphorus Acid Anhydrolase Enzyme for Increased Catalytic Efficiency and Broadened Stereospecificity on Russian VX. Biochemistry 54:6423–6433 . https://doi.org/10.1021/acs.biochem.5b00624

Jain M, Yadav P, Joshi A, Kodgire P (2019) Advances in detection of hazardous organophosphorus compounds using organophosphorus hydrolase based biosensors. Crit Rev Toxicol 49. https://doi.org/10.1080/10408444.2019.1626800

Jain M, Yadav P, Joshi B, Joshi A, Kodgire P (2021) A novel biosensor for the detection of organophosphorus (OP)-based pesticides using organophosphorus acid anhydrolase (OPAA)-FL variant. Appl Microbiol Biotechnol 105:389–400. https://doi.org/10.1007/s00253-020-11008-w

Kang DG, Li L, Ha JH, Choi SS, Cha HJ (2008) Efficient cell surface display of organophosphorous hydrolase using N-terminal domain of ice nucleation protein in Escherichia coli. Korean J Chem Eng 25:804–807. https://doi.org/10.1007/s11814-008-0132-0

Masson P, Josse D, Lockridge O, Viguié N, Taupin C, Buhler C (1998) Enzymes hydrolyzing organophosphates as potential catalytic scavengers against organophosphate poisoning. J Physiol Paris 92:357–362. https://doi.org/10.1016/S0928-4257(99)80005-9

Paraíba LC, de Castro VLSS, de Holanda A, Maia N (2009) Insecticide distribution model in human tissues viewing worker's health monitoring programs. Brazilian Arch Biol Technol 52:875–881. https://doi.org/10.1590/S1516-89132009000400011

Shimazu M, Chen W, Mulchandani A (2003) Biological Detoxification of Organophosphate Pesticides. ACS Symp Ser 863:25–36. https://doi.org/10.1021/bk-2004-0863.ch003

Singh BK, Walker A (2006) Microbial degradation of organophosphorus compounds. FEMS Microbiol Rev 30:428–471. https://doi.org/10.1111/j.1574-6976.2006.00018.x

Vyas NK, Nickitenko A, Rastogi VK, Shah SS, Quiocho FA (2010) Structural insights into the dual activities of the nerve agent degrading organophosphate anhydrolase/prolidase. Biochemistry 49:547–559. https://doi.org/10.1021/bi9011989

Xiao Y, Yang J, Tian X, Wang X, Li J, Zhang S, Long L (2017) Biochemical basis for hydrolysis of organophosphorus by a marine bacterial prolidase. Process Biochem 52:141–148. https://doi.org/10.1016/j.procbio.2016.10.008

Xiong S, Deng Y, Zhou Y, Gong D, Xu Y, Yang L, Chen H, Chen L, Song T, Luo A, Deng X, Zhang C, Jiang Z (2018) Current progress in biosensors for organophosphorus pesticides based on enzyme functionalized nanostructures: A review. Anal Methods 10:5468–5479. https://doi.org/10.1039/c8ay01851k

LIST OF PUBLICATIONS

A) Publications from PhD thesis work:

1) **Jain, M**., Yadav, P., Joshi, A*., Kodgire, P*., Advances in detection of hazardous organophosphorus compounds using organophosphorus hydrolase based biosensors. *Critical Reviews in Toxicology* **2019**, *49,* 387-410. https://doi.org/10.1080/10408444.2019.1626800

2) **Jain, M.**, Yadav, P., Joshi, B., Joshi, A*., Kodgire, P*., A novel biosensor for the detection of organophosphorus (OP) based pesticides using organophosphorus acid anhydrolase (OPAA) variant. *Applied Microbiology and Biotechnology* **2021***, 105, 389-400.* https://doi.org/10.1007/s00253-020-11008-w

3) **Jain, M.**, Yadav, P., Joshi, B., Joshi, A*., Kodgire, P*., Recombinant organophosphorus hydrolase (OPH) expression in *E. coli* for the effective detection of organophosphate pesticides. *Protein Expression and Purification* **2021,** 186, *105929*. https://doi.org/10.1016/j.pep.2021.105929

4) **Jain, M.,** Singh V, Joshi, A*., Kodgire, P*., Fluorometric biosensing of organophosphates using recombinant organophosphorus acid anhydrolase-FL variant with monomeric teal fluorescent (mTFP) fusion protein expressed in E. coli. 2021, (Manuscript in preparation)

B) Publication apart from PhD thesis work:

1) Choudhary, M., Tamrakar, A., Singh, A.K., **Jain, M.**, Jaiswal, A., Kodgire, P*., AID Biology: A pathological and clinical perspective. *International Reviews of Immunology* **2017**, *37,* 37-56. https://doi.org/10.1080/08830185.2017.1369980

C) List of International conferences:

1) **Jain M.** and Kodgire P*., (2018) "Structural and functional studies of Activation Induced Cytidine Deaminase (AID) and somatic hypermutation of immunoglobulin genes" in Symposium on ***Emerging areas in Biosciences and Biomedical Technologies*** held on 5-6 Jan at Indian Institute of Technology, Indore. Pg. 63

2) **Jain, M.**, Yadav, P., Joshi, B., Joshi, A*., Kodgire P*., (2020) "Detection and quantification of organophosphorus compounds using recombinant organophosphorus acid anhydrolase variant based biosensor" in Symposium on ***Emerging areas in Biosciences and Biomedical Technologies2*** held on 7-9 Feb at Indian Institute of Technology, Indore. Pg. 81

Table of contents

LIST OF FIGURES

LIST OF TABLES

ABBREVIATION

AChE	Acetyl cholinesterase
BChE	Butrylcholinesterase
bp	Base pair
Bis-Tris propane	Bis[tris(hydroxymethyl)methylamino]propane
BSA	Bovine serum albumin
CFP	Cyan Fluorescent Protein
CHES	2-(Cyclohexylamino)ethanesulfonic acid
CLSM	Confocal laser scanning microscope
DDT	Dichlorodiphenyltrichloroethane
DFP	Diisopropyl fluorophosphate
DFPase	Diisopropyl-fluorophosphatase
dNTP	Deoxyribonucleoside triphosphate
EDTA	Ethylene diamine tetra acetic acid
FITC	Fluorescein isothiocyanate
GFP	Green fluorescent protein
His	Histidine
IPCCA	Intelligent Polymerized Crystalline Colloidal Array
KDa	Kilo dalton
LB	Luria broth
LD50	Lethal Dose 50
LOD	Limit of detection
MPH	Methyl parathion hydrolase
mTFP1	Monomeric teal fluorescent protein 1

Ni NTA	Nickel nitriloacetic acid
Nus-A	N-utilization substance protein A
OC	Organochlorine
OCPs	Organochlorine pesticides
OD	Optical density
OPAA	Organophosphorus acid anhydrases
OPH	Organophosphorus hydrolase
OPs	Organophosphorus compounds
PAGE	Polyacrylamide gel electrophoresis
PNP	*p*-nitrophenol
PON	Paraoxonase
Pa-pepP	Aminopeptidase P
PTE	Phosphotriesterase
rpm	Rotations per minute
SDS	Sodium dodecyl sulfate
SEM	Scanning electron microscopy
UV	Ultraviolet

Chapter 1

Chapter 1
Introduction and literature review

1.1. The global pesticide problem

Pesticides have been widely used in the agriculture industry since the beginning of the 19th century when sulphur compounds were developed as fungicides (Lamberth 2004). Later on, arsenic-based compounds were introduced mainly to target insects attacking fruit and vegetable crops like apples and grapes (Strekopytov et al. 2017). Meanwhile, mercuric compounds were utilised to protect artifacts and objects in museums from pest infestation (Strekopytov et al. 2017). These all were widely used until the 1940s before organochlorine pesticides (OCPs) such as dichlorodiphenyltrichloroethane (DDT) were introduced. This latest class of OCPs was considered safer because of low immediate toxicity (Chattopadhyay and Chattopadhyay 2015).

After World War II, pesticide use was bolstered by many organophosphate compounds derived or inspired from nerve agents initially for use as chemical weapons such as sarin, soman, tabun, etc. (Porzio et al. 2018). These became popular due to short-term effectiveness and relative ease of manufacture, and have become ubiquitous in pesticide products today. A representative figure for the consumption of pesticides in India and in the world is presented in **Fig. 1.1** (Aktar et al. 2009).

The use of pesticides has resulted in positive and visible gains across the world for crop productivity and yield, as well as has also contributed to food security for many countries (Cooper and Dobson 2007). Pesticides are also regularly used for the preservation of museum samples, control of vector-borne diseases such as malaria/dengue, etc.,

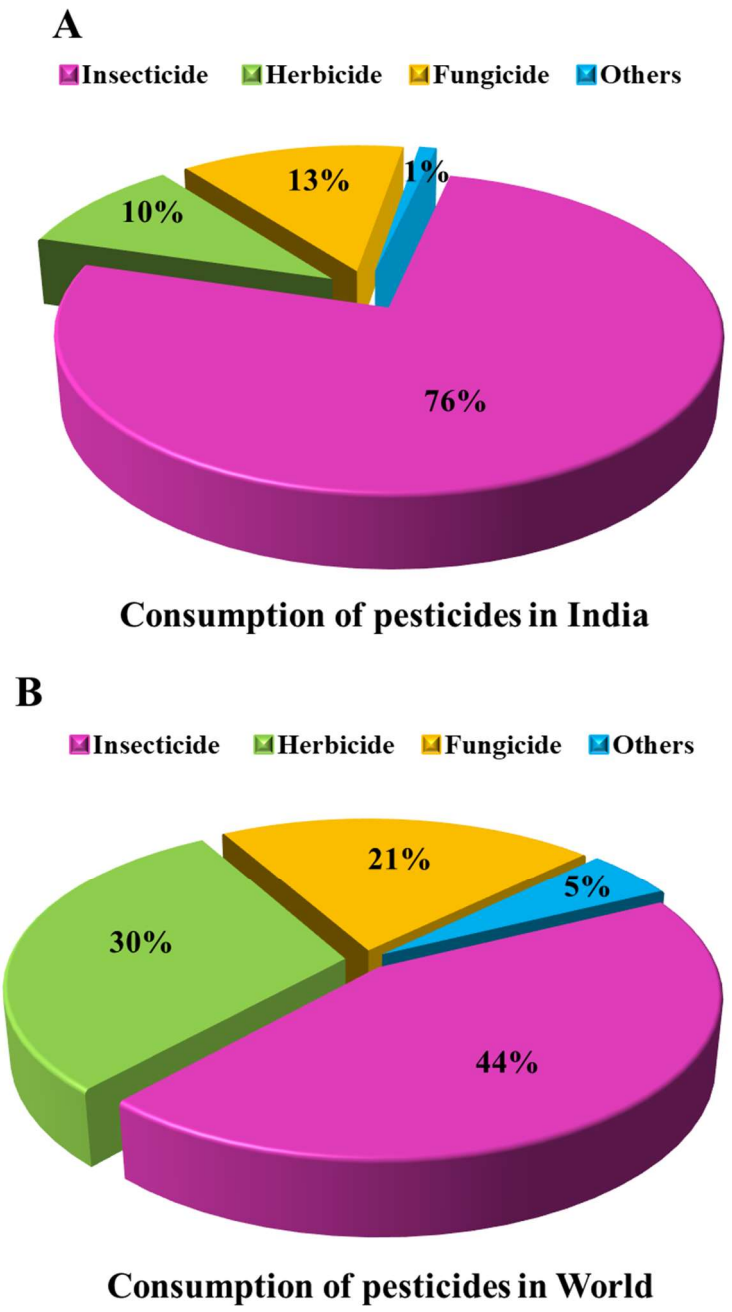

Figure 1.1: Pesticide usage by category. (A) In India and **(B)** In the world. In India, the pattern of pesticide use is distinct from that of the world in general. 76% of the pesticide used in India is in the form of insecticide, as opposed to 44% globally. Accordingly, the use of herbicides and fungicides is less prevalent. Cotton crops (45 %) are the main use of pesticides in India, followed by paddy and wheat. Reproduced from (Aktar et al. 2009)

and unwanted plants such as weeds and grass in gardening and landscaping (Gilden et al. 2010). However, it was only in the 1960s that adverse effects of these pesticides were first brought to light, and it was not until the 1980s that global organizations such as Food and Agriculture Organization issued guidelines on the distribution and handling of pesticides (Murray and Taylor 2000). It is estimated that the majority of pesticide residue is actually found in areas and items other than their intended targets due to inappropriate handling and excessive spraying. For example, in cases of agriculture, the sprayed pesticides often reach water bodies via agricultural and stormwater runoffs, (Weston et al. 2009; Arora et al. 2010; Rasmussen et al. 2011; Birch et al. 2011) and tend to accumulate on soils, in air and forests (Daly et al. 2007; Syed et al. 2013; Lupi et al. 2016) **(Fig. 1.2)**. They also tend to linger on where they are sprayed, especially at public places such as museums (Behrooz et al. 2009; Holt et al. 2017; Deering et al. 2019).

Today, pesticides pose numerous problems for all living beings the humans, plants as well as animals. Several dangers and risks of pesticide accumulation, contamination, and poisoning have surfaced consistently over recent times. Pesticides are now regularly found in water bodies, where they are difficult to assess and remediate in a cost-effective and non-disruptive manner (Silva et al. 2015; Lorenz et al. 2017). They are known to affect the biodiversity of insects and bacteria along with aquatic life (Cycoń and Piotrowska-Seget 2009; Beketov et al. 2013; Dudley et al. 2017) causing a threat to birds (Smith et al. 2010; Chiron et al. 2014) and endangered species (Macneale et al. 2010; Belenguer et al. 2014; Forbes et al. 2016). Pesticides are highly prone to bioaccumulation inside living organisms. Humans are not exempted from this, and children are especially prone to the harmful effects of pesticides (Abdel Rasoul et al. 2008; Harari et al. 2010; Muñoz-Quezada et al. 2013). Pesticide use and prevalence are linked to a number of diseases in humans such as asthma, cancer, hormone disruption, allergies, neurological disorders, and hypersensitivity (Kim et al. 2017). In some cases, just a few micromoles of certain pesticides are enough to cause significant damage to humans

(Bjørling-Poulsen et al. 2008; Ekinci and Beydemir 2010; Meijer et al. 2014).

1.2 Importance of pesticides detection

The rise of chemical synthesis techniques has led to the use of new highly specific and active pesticides with good success rates against a variety of pests for crop protection. However, particularly from the 20th century onwards, pesticide residues, accumulation, and contamination have emerged as significant problems causing harm not only to humans but also to animals in the environment. Moreover, the presence of pesticides in the food chain has created alarming situations for human health in many parts of the world. Governments across the world have formulated guidelines and regulations for the use, accumulation, remediation, and detection of pesticides in food and environment samples. These guidelines are based on medical data of mortality and lethality accumulated over the years through animal tests and human patient reports. To comply with the regulations and also to ensure total environmental health, measures are necessary to effectively and precisely detect the presence of pesticides in soil, water, or food samples. In terms of human health, pesticide contamination can only be mitigated in food samples if the concentration is below certain specified thresholds such that adverse health effects do not occur. Considering these factors, precise, portable, and accurate methods of pesticide estimation and detection are necessitated.

Detection of pesticides is traditionally done using techniques like High-Performance Liquid Chromatography and Gas Chromatography-Mass Spectroscopy. However, these techniques often require intensive sample collection, preparation and/or purification and, experienced operators, high costs, with general inability to deliver on-site detection. The proliferation of pesticide residues in the environment and the massive effects on the biosphere hence necessitates the development of a more advanced, portable, and on-site detection methodology for detecting pesticides across food, water, soil, air, etc.

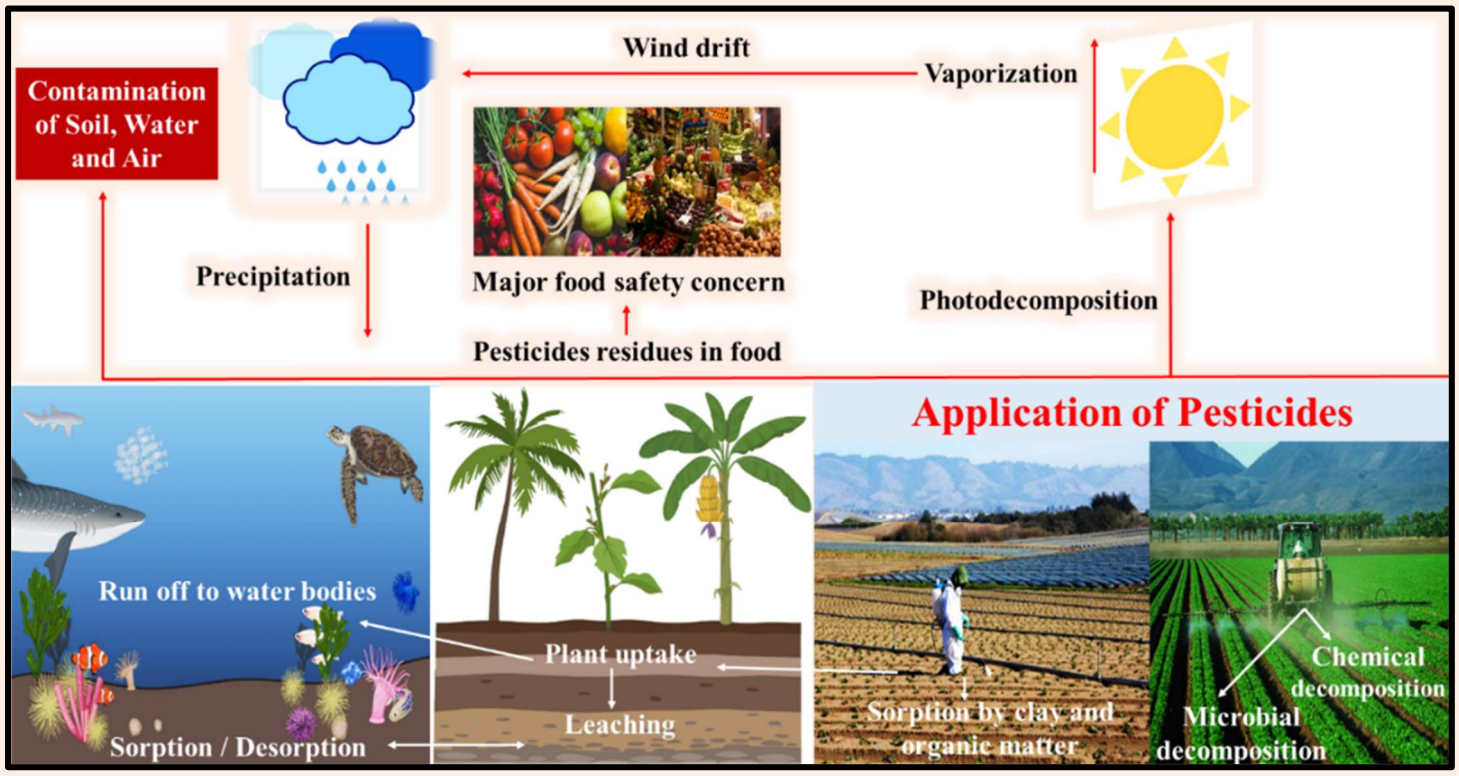

Figure 1.2: Schematic representation of exposure of pesticides: Possible sources of environmental exposure of pesticides and their residues that contaminate soil, water, air, and food and also affects human and wildlife. Adapted and modified from (Pirsaheb and Moradi 2020). RSC Adv 10:7396–7423 - Published by the Royal Society of Chemistry.

1.3 Classes of pesticide compounds

1.3.1 Organophosphorus Compounds (OPs)

Organophosphates - also called phosphotriesters due to the presence of three phosphodiester bonds **(Fig. 1.3)** (Barr et al. 2004), are of substantial interest due to their low-cost of synthesis and high efficacy. Some examples of OPs are paraoxon, malathion, Dementon-S, Diisopropyl fluorophosphate (DFP), Sarin, Tabun, Hexadeuterio Tabun. Strikingly, OP-based compounds today constitute anywhere between 33% of available pesticides in the developed countries and 50-60% in developing countries (Atwood and Paisley-Jones 2017).

Incidentally, a trace amounts of these compounds exhibit toxicity when absorbed through the skin, ingested, or inhaled. World Health Organization reports show that around 200,000 people suffer annually from pesticide-related poisoning due to direct or indirect exposure to organophosphorus compounds (OPs) (Theriot and Grunden 2011).

For researchers in medical and environmental sciences, the use of OPs has been of particular concern due to its lower biodegradability compared to the newer pesticides, as well as their tendency to block the active site of important enzymes in neurons, such as acetylcholinesterase (AChE), which breaks down and removes acetylcholine from the nerve synapse. The inability to break down acetylcholine results in neurological problems, such as convulsions, tremors, and even death (Zimmer et al. 1998). Although the OP poisoning is treatable using a combination of atropine and pralidoxime(Eddleston et al. 2008), such medication has several side effects (Headley 1982) and are not as effective in patients with prolonged exposure due to a phenomenon known as the aging effect, in which a non-enzymatic loss of alkyl chain from the phosphate group in the OP compound renders the inhibited/blocked AChE into a non-reactivatable form (Masson et al. 2010). Strikingly, poisoning by the OPs has a high rate of mortality (Eddleston 2000) that exceeds the normal expectations for exposure to toxic chemicals, such as mercury, cyanide, and cadmium. These higher mortality rates are a cause of concern for

healthcare professionals to this day (Muley et al. 2014), necessitating measures to facilitate a convenient and accurate detection of OPs in human samples as well as the environment.

1.3.1.1 Nerve agents

Nerve agents are organic chemicals most known for their use in wars and terrorist attacks as chemical warfare agents. Nerve agents are divided into two categories, the V-series (VE, VG, VM, VR, and VX) where V stands for Victory, Venomous, or Viscous, based on the source (Pita et al. 2013; Hayoun et al. 2020) and the G-series (GA, GB, GD, GF, and GV), which are are highly toxic G-nerve agents (Sidell and Borak 1992). The G series is named because they were first synthesized by the German scientist, Gerhard Schrader. Nerve agents work by blocking the active site of essential enzymes in neurons, such as acetylcholinesterase (AChE), which is responsible for the breakdown and release of acetylcholine from the nerve synapse. The inability to break down acetylcholine results in neurological problems, such as tremors, convulsions, and even death (Zimmer et al. 1998). In general, nerve agents are tasteless, colourless to amber-coloured, and liquid that can vaporize into a gas. Agents such as soman have an odour like camphor, tabun has a faint fruity scent, VX and sarin are odourless (Moshiri et al. 2012).

Poisoning is reported to begin within seconds of exposure to nerve agents. In the human body, OPs and nerve agent metabolism meet the same fate. Owing to the difficulty of detection, nerve agents are specifically hazardous. There are few reports on OP compound detection in blood/serum or human samples, but human serum Paraoxonase 1 may be used for the detection of nerve agents as it has shown potential for degradation of nerve agent VX (Peterson et al. 2011). OPAA has the strongest activity against G-agents but has no activity against V-agents (Cheng et al. 1999).

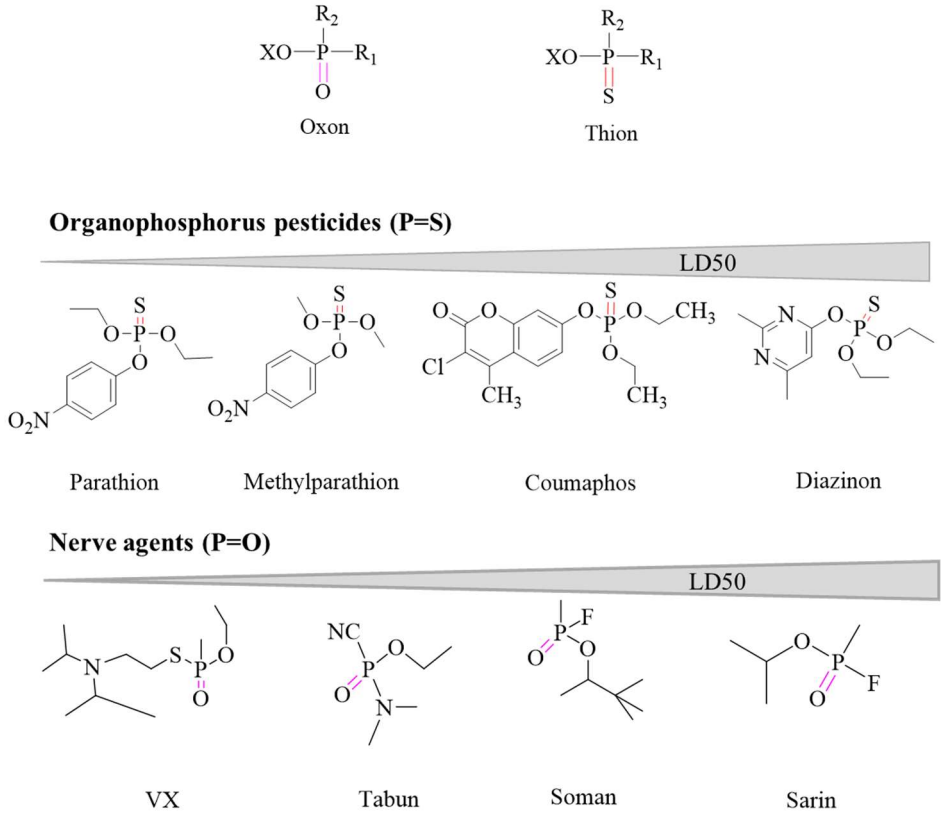

Figure 1.3. The general structure of OPs: R_1 and R_2 are aryl or alkyl groups that are either bonded to phosphorus via the oxygen or sulfur link or they are directly bonded to the phosphorus. X group attached to the phosphorus may be an aromatic group, halogen, aliphatic or heterologous cyclic group (Vilanova and Sogorb 1999; Barr et al. 2004).

1.3.2 Carbamates

Carbamates act similarly to organophosphorus compounds in terms of AChE inhibition and resistance characteristics. The symptoms of exposure are largely similar, however, carbamate compounds like methomyl, carbaryl, and carbofuran have been known to accumulate in aquatic environments (Tien et al. 2013). They tend to have half-lives of a few days to a month or more, making them some of the most dangerous pesticides known today. In this case, the AChE active site serine residue hydroxyl is carbamylated rather than phosphorylated as in the case of OP compounds (Van Dyk and Pletschke 2011).

1.3.3 Organochlorines

An organochlorine (OC) also known as organochloride, chlorinated hydrocarbon, chlorocarbon, OCPs are chlorinated hydrocarbons used extensively from the 1940s through the 1960s in agriculture and mosquito control. This class of compounds is comprised of chemicals such as polychlorinated biphenyls, polychlorinated dibenzofurans, DDT, heptachlor, mirex, dieldrin, chlordecone, etc. These compounds have a long half-life of a few years to up to 20 years or more. The Stockholm Convention on persistent organic pollutants has mandated the reduction or complete phase-out of organochlorine compounds in view of the threat to human health and effects on the immune system (Van Dyk and Pletschke 2011).

1.3.4 Pyrethrin

Pyrethrins are the active compound(s) from the pyrethrum flower extract, which are harmless to mammals under normal conditions and an effective insecticide with proven efficacy in grain protection. It is usually deployed to protect food items and warehouses from the infestation of fleas, mosquitoes, ants, moths, and other pests. Pyrethrins, unfortunately, are limited by poor stability under visible light and hence only see limited use in agriculture (Chen and Wang 1996). However, the commercial

preparations of pyrethrins contain piperonyl butoxide, which limits the metabolic degradation of pyrethrins in mammals. As a result, the accumulation of pyrethrins causes nervous problems, hypersensitivity, dermatitis, and corneal erosions (Proudfoot 2005). The biodegradability of pyrethrins makes them preferable to pyrethroids, which are synthetic derivatives of pyrethrins (Barimani et al. 2013).

1.3.5 Pyrethroids

Pyrethroids are synthetic derivatives of pyrethrins developed for high biological activity and photo-cum-chemical stability (Ding et al. 2012). Though they are nonpersistent and less toxic than organophosphate or carbamate compounds, they are known to cause changes in dopamine expression levels, leukaemia, abnormal glucose regulation, and hormonal problems in humans (Meeker et al. 2009; Wang et al. 2011; Ding et al. 2012; Wagner-Schuman et al. 2015). They are prone to toxicity changes based on stereochemistry – for example, a *cis*-isomer would likely be more toxic than a *trans*-isomer (Mueller-Beilschmidt 1990). Cypermethrin, allethrin, cismethrin, permethrin, fenvalerate, resmethrin, phenothrin, and fenpropathrin are some examples of pyrethroids.

1.4 Effects of OP compounds on health

Organophosphorus compounds were introduced as pesticides mainly in the 1950s and 1960s, and are widely used as insecticides, herbicides, nematicides as well as acaricides. Several derivatives of OPs are commercially marketed and they show prolonged half-life in the soil. For example, parathion shows half-life in the soil of 30-180 days, methyl parathion in the soil of 25-130 days, whereas another OP compound, coumaphos, in the soil of 24-1400 days (Singh and Walker 2006).

Continuous or long exposure of the OPs leads to the deposition of these compounds at the depot site, from where they are uninterruptedly released into the blood. Subsequently, from blood, they reach the nervous system where one of their targets is the AChE enzyme (Masson et al. 1998). **Fig. 1.4** represents the routes of exposure; **Fig. 1.5** represents the

bioavailability and metabolism of OPs in the human body. Once a person is exposed to the OPs, these compounds may get deposited into the site like liver, kidney, muscles, adipose tissue or they may get distributed to the central nervous system via blood circulation. The amount that remains in the blood is eliminated out via urine, expired air, or faeces (Masson et al. 1998; Paraíba et al. 2009). In addition to AChE, these compounds target some important enzymes like lipases and esterases that are crucial for the proper functioning of the human body.

1.4.1 Effect of OPs on acetylcholinesterase (AChE)

AChE is an enzyme that catalyses the hydrolysis of acetylcholine, a neurotransmitter that is involved in the transfer of nerve impulses to the effector cells at cholinergic, synaptic as well as neuromuscular junctions **(Fig. 1.6)**. Several studies have indicated that OPs mainly interact with the AChE active sites (residues Ser203, His447, and Glu334) through phosphorylation **(Fig. 1.7)**, wherein a covalent bond between the central phosphorous atom of the ligand and an oxygen atom from the side chain of a serine residue is formed (Guo et al. 2006). In some cases, the reaction may continue further, causing the loss of an alkyl chain from the resulting phosphyl alkoxy substituent. This process is known as 'aging' and prevents reactivation of AChE by conventional therapy. Once AChE is inactivated, the enzyme loses its ability to hydrolyze acetylcholine, and the build-up of acetylcholine causes continuous stimulation of muscle or nerve fibers, resulting in exhaustion and/or tetany (Fukuto 1990). A schematic of the inhibition mechanism of AChE by paraoxon, a well-known OP compound, is given in **Fig. 1.6**. The aging process is caused by a dealkylation reaction (Barak et al. 1997) which causes the resultant adduct to be remarkably unreactive and hence results in the irreversible inactivation of AChE.

Quinn et al., proposed that the inherent unreactivity and irreversibility caused by the aging is attributed to the structural similarity of the aged adducts to the tetrahedral intermediate of AChE in the deacylation stage of catalysis (Quinn et al. 2017). It is speculated that the

overstimulation of glutamate receptors caused by inhibition of AChE as well as non-AChE targets, leads to cardiac collapse, convulsions, and respiratory arrest, whereas massive histamine release may be responsible for anaphylactic shocks (Duysen et al. 2001). Thus, OPs target not only AChE but also other enzymes, which make them a severe health hazard and thus warrants urgent development of detection as well as remediation techniques (Duysen et al. 2001).

1.4.2 Organophosphorus compounds induced neuropathy

OP-induced delayed polyneuropathy is also a severe toxic effect of OPs exerted on the central nervous system and peripheral nervous system. The root cause of this neuropathy is the modification and phosphorylation of the neuropathy target esterase enzyme in the central nervous system. An increase in autophosphorylation has been observed in the calmodulin kinases due to the presence of OPs. This increases the phosphorylation of cytoskeletal proteins, such as myelin basic protein, α and β tubulin, neurofilament protein, microtubule-associated protein-2. Consequently, the transport rate of cytoskeletal protein is decreased down the axon compared to their entry rate resulting in their accumulation in the distal part of the axon. Thus, the delayed OP-induced polyneuropathy is marked by bulging in the axons of the central and peripheral nervous system with subsequent ataxia and paralysis (Abou-Donia 1995).

Additionally, OPs shows other cellular effects such as inhibition of catecholamine released in chromaffin cells, inhibition of brain of rats, alteration in the level of inositol phosphate in SH-SY5Y cells, inhibition of pig kidney Na^+/K^+ ATPase, alteration in the hindbrain of the chicken on the ganglioside profile, change in the fluidity of the membrane, and biochemical changes in the bovine chromaffin cell's mitochondria (Vilanova and Sogorb 1999; Sogorb and Vilanova 2002).

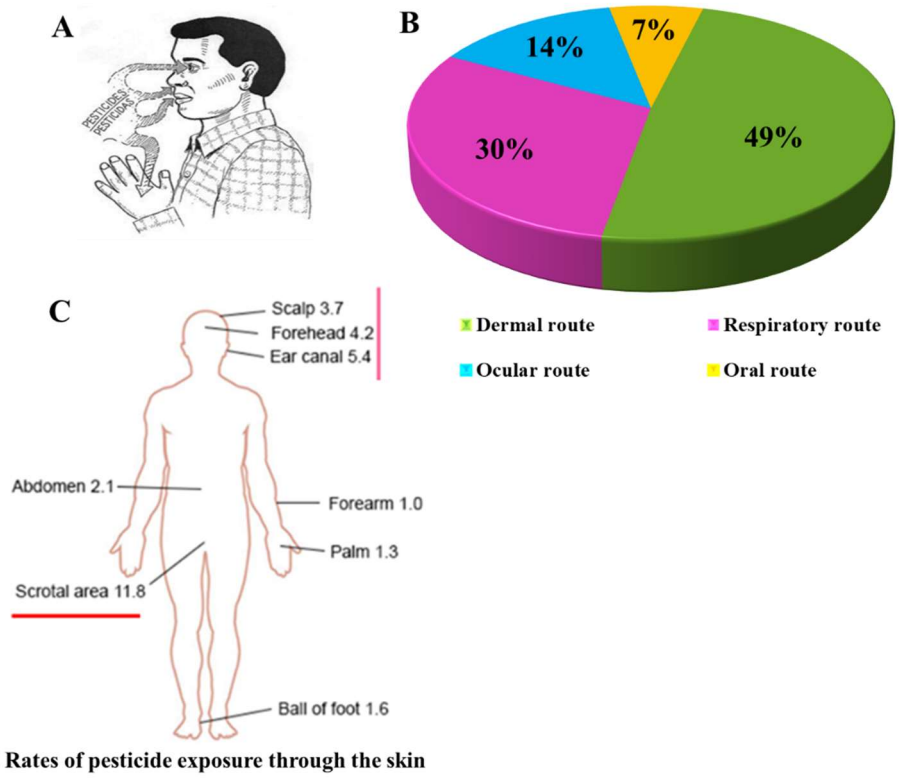

Figure 1.4. Representation of the routes and rates of exposure, of OPs in the human body: (A) Probable routes of pesticide exposure. Reproduced from the U. S. Environmental Protection Agency (US EPA 2015) **(B)** Routes of pesticide exposure reported by surveyed farmers presented in percentage (Toe et al. 2013). **(C)** Rates of pesticide exposure through dermal uptake: Pesticides are absorbed by various parts of the body through the skin at different rates. Marked places indicate places of highest exposure rate relative to places of lowest exposure rate. Adapted from the U.S. Department of Agriculture (https://www.ars.usda.gov/northeast-area/docs/safety-health-and-environmental-training/field-pesticide-work/)

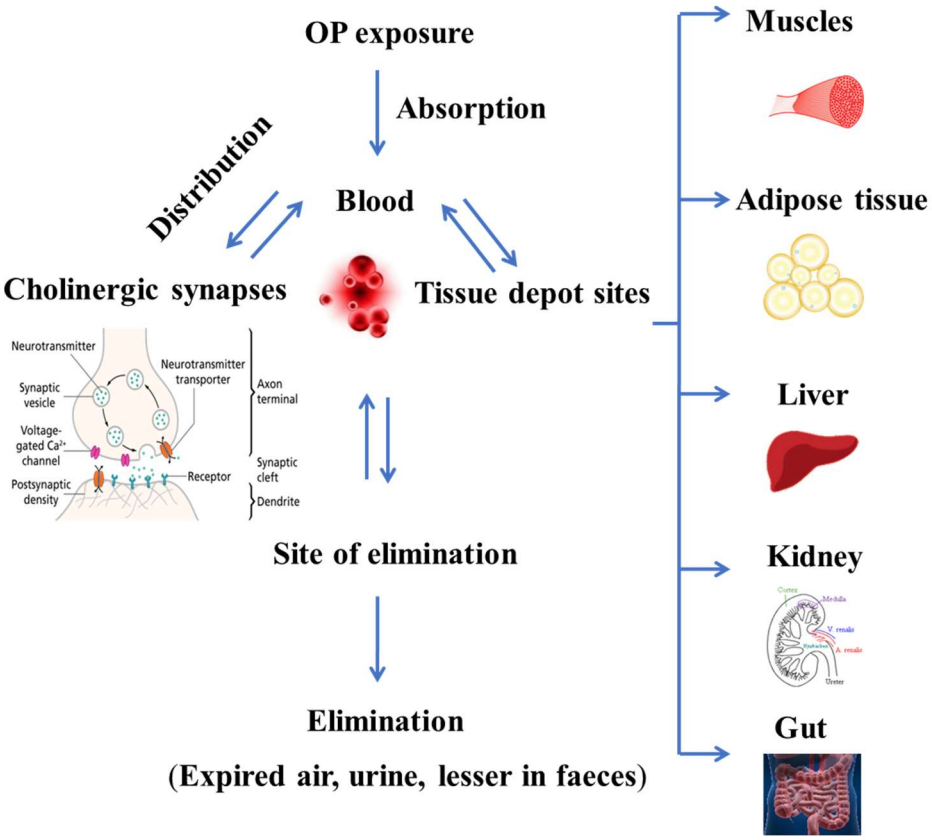

Figure 1.5. Representation of the bioavailability and metabolism of OPs in the human body: When a person accidentally or deliberately inhales, ingests, or absorbs the OPs, it reaches either to its depot site like muscles, adipose tissue, liver, kidney, or gut or it may get distributed to the central nervous system through the blood circulation. The amount that remains in the blood is eliminated out via urine, expired air, or faeces (Jain et al. 2019). Modified from (Masson et al. 1998).

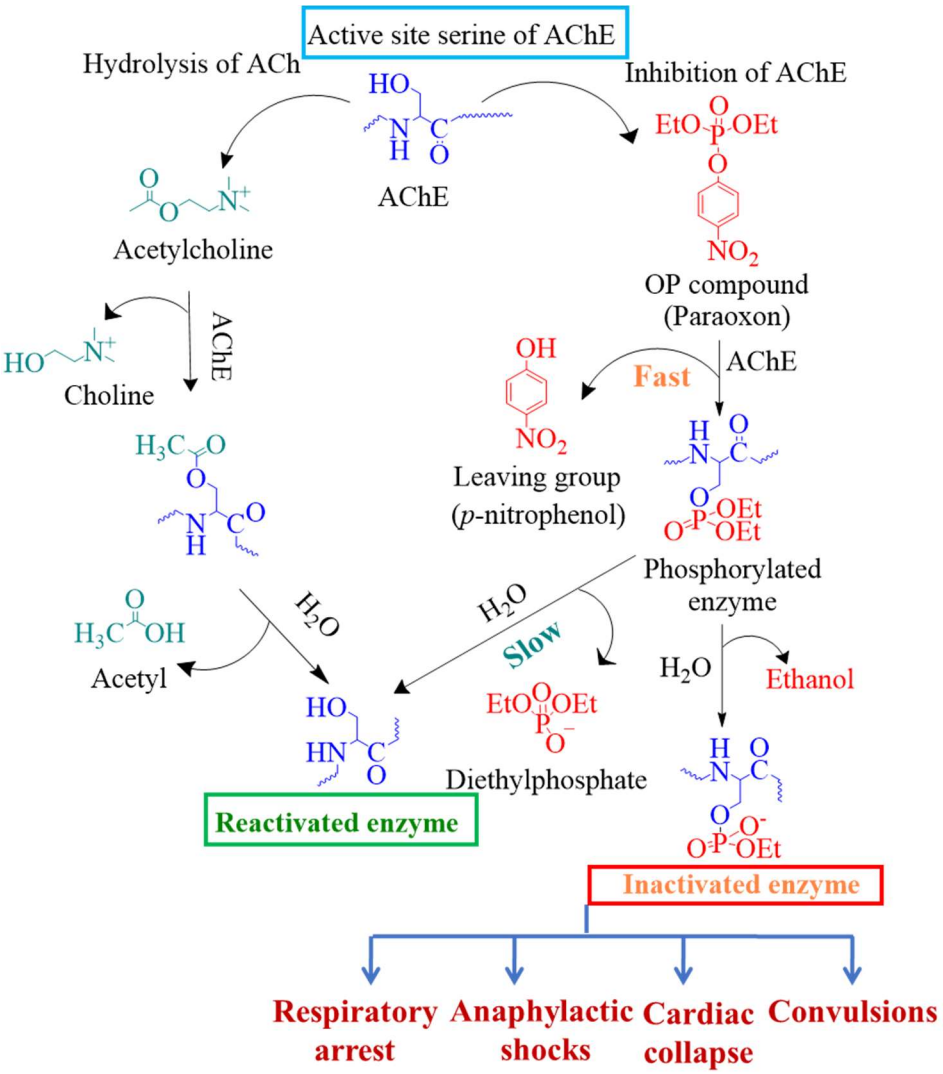

Figure 1.6. Inhibition of AChE by OPs: OPs bind to the hydroxyl group of the serine at the active site to form the phosphorylated enzyme resulting in the accumulation of the Acetylcholine at the synapses because inactivated AChE is unable to hydrolyze acetylcholine. Modified from (Raushel 2002).

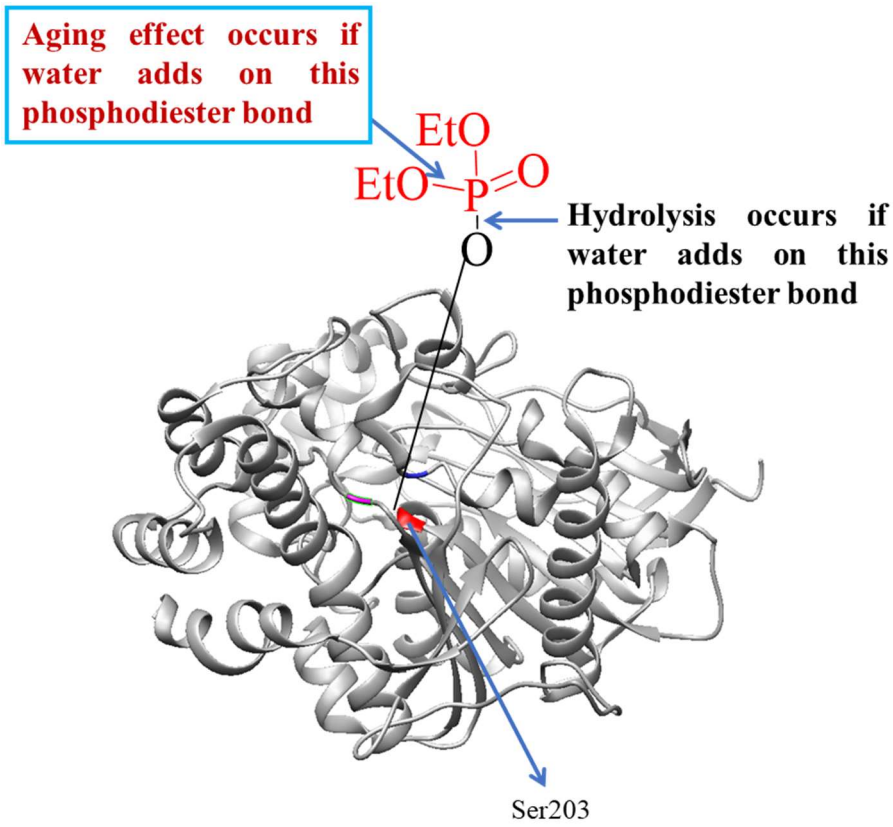

Figure 1.7. Structure of human Acetylcholinesterase (PDB ID-4PQE). Inhibition of AChE enzyme in the presence of OP compounds. In case of water addition at active site serine residue (203) P-EtO bond, AChE is inactivated through the aging effect.

1.5 Biodegradation of OPs

In general, since bacteria do not have AChE, OP compounds are either benign or an energy source to these microorganisms. Several studies have suggested increased biodegradation caused by repeated application of pesticides, which is dependent on the soil properties and chemical nature of the OPs. Some groups have explored the use of microorganisms as a sustainable option for the detoxification and decontamination of organophosphorus compounds. The use of bio-remedial microorganisms includes an understanding of the physiological, ecological, biochemical, and molecular aspects of OP degradation (Iranzo et al. 2001). In recent years, a significant number of reports have explored the use of various bacteria for organophosphate degradation (Pang et al. 2018; Santillan et al. 2020). Many bacterial strains have been identified for the degradation of commonly used organophosphorus pesticides such as parathion, methyl parathion, diazinon, dichlorvos, malathion, and others (Kumar et al. 2018). Microbial degradation usually involves hydrolysis, oxidation, alkylation, and dealkylation (Sidhu et al. 2019). A large gene diversity has been observed among microorganisms, which depend on the form, function, location, and host organism in question. Some of the more frequently reported microorganisms displaying activity for organophosphate degradation are Arthrobacter, Burkholderia, Enterobacter, Flavobacterium, Pseudomonas, and Serratia (Sidhu et al. 2019). Recent efforts have focused on the construction of bioreactors with bacterial isolates for functional applications, such as water decontamination (Santillan et al. 2020) and decontamination efforts in sewage sludge (Pang et al. 2018).

1.6 Organophosphate-hydrolyzing enzymes

There are several methods known for the degradation of OPs like incineration and chemical neutralization but, among all the advanced technologies known microbial enzyme mode of degradation is the safest. Although several OPs degrading enzymes have been identified in numbers of organisms including mammals, however, the microbial enzymes have

caught more attention and be more potent in degrading OPs (Siddavattam 2017). OPs degrading enzymes were first time reported in 1946 by Mazur. These enzymes were later categorized in the category of phosphotriester hydrolase by the Nomenclature Committee of the International Union of Biochemistry and Molecular Biology. These enzymes were further classified based on their substrate specificity (Raushel 2002). Although OPH is the most studied and well-categorized among all OP degrading enzymes, other enzymes have also been reported which are capable of detoxifying OPs (Theriot and Grunden 2011). **Table 1.1** shows the comparison of known organophosphorus degrading enzymes.

1.6.1 Organophosphorus Hydrolase (OPH)

The hazardous OPs can be degraded naturally by enzymes, such as OPH and methyl parathion hydrolase (MPH), into less toxic or non-toxic compounds like *p*-nitrophenol (PNP) and diethyl phosphate (Orbulescu et al. 2006). OPH enzyme is isolated from soil microorganisms, such as *Pseudomonas diminuta* and *Flavobacterium* species. OPH is also known as phosphotriesterase (PTE), organophosphorus degrading enzyme, and parathion hydrolase. This enzyme is encoded by the phosphate degrading gene (*opd)* located on the extrachromosomal plasmid (Raushel 2002). It has a broad substrate specificity and can hydrolyse P-O, P-CN, P-F, and P-S bonds (Orbulescu et al. 2006). On hydrolysis of the bond, it generates 2 protons and one alcohol, which are often electroactive or chromophoric (Mulchandani et al. 2001a; Theriot and Grunden 2011). Thus, OPH can be combined with a pH electrode or a field-effect transistor-based pH indicator to measure the protons produced or optical transducer to quantify the amount of PNP produced during hydrolysis based on the chromophore produced (Mulchandani et al. 2001a). OPH has been proved to be an effective biocatalyst for hydrolysis of OPs, owing to which it has been considered for detection and/or remediation of OPs **(Fig. 1.8 A)** (Jacquet et al. 2016).

Table 1.1: Features of OP compound degrading enzymes

Enzyme	Isolated from microorganism	Bonds cleaved by the enzyme					Metal ion	Active form of enzyme	Size	Substrate specificity	Reference
		P-O	P-F	P-CN	P-S	P-C					
Organophosphorus Hydrolase (OPH)	*Pseudomonas diminuta, Flavobacterium, Agrobacterium radiobacter*	✓	✓	✓	✓	×	Zn	Dimer	37 kDa	Paraoxon, DFP, VX, Soman, Mipafox, Dursban, Parathion, Coumaphos, Diazinon, Fensulfothion, Methyl parathion, Cyanophos, Acephate, Azinophos-ethyl demethon-S, Malathion, Phosalone, Methamidophos, tetriso, (Sp)-EPN	(Vilanova and Sogorb 1999; Di Sioudi et al. 1999; Benning et al. 2001; Karpouzas and Singh 2006)
Organophosphorus Acid Anhydrolase (OPAA)	*Alteromonas* sp. JD6.5, *Pseudoalteromonas haloplanktis*	✓	✓	✓	✓	×	Mn	Monomer	58 kDa	Paraoxon, DFP, Soman, Sarin, Mipafox	(Vilanova and Sogorb 1999; Di Sioudi et al. 1999; Karpouzas and Singh 2006; Daczkowski et al. 2015)
Paraoxonase (PON)	Human	✓	✓	✓	×	✓	Ca	Monomer	43 kDa	Alkyl fluorophosphate, Paraoxon, Soman, DDVP, Glyphosate	(Di Sioudi et al. 1999)
Methyl Parathion Hydrolase (MPH)	*Pseudomonas* sp. WBC 3	✓	×	×	×	×	Zn	Dimer	34 kDa	Methyl parathion, Parathion, Paraoxon	(Chu et al. 2003; Liu et al. 2007; Farnoosh and Latifi 2014)

Di-isofluoro-phosphatase (DFPase)	*Loligo vulgaris*	×	✓	×	×	×	Ca	Monomer	35 kDa	DFP, Tabun	(Di Sioudi et al. 1999)
Aminopeptidase P (Pa-pepP)	*Escherichia coli*	Amino-terminal X-pro peptide bond					Mn	Tetramer	49.65 kDa	p-nitrophenyl methyl phosphonates, Paraoxon, Substrate consisting of methyl isopropyl and methyl isobutyl group	(Yoshimoto et al. 1989; Jao et al. 2004; Graham et al. 2005; Farnoosh and Latifi 2014)

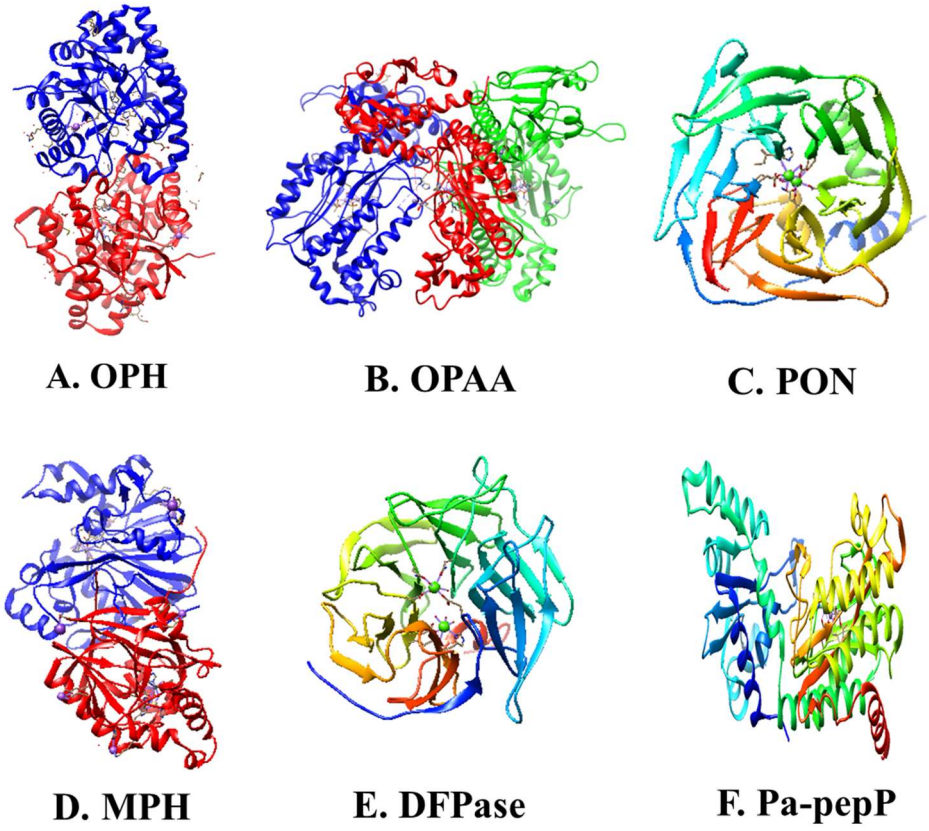

Figure 1.8. Structure of OP degrading enzymes. (A) PTE from Pseudomonas diminuta (OPH) "1HZY": Two chain metalloprotein with 46 helices and 6 sheets and the Zinc as its central atom. It belongs to the alpha and beta protein class having a TIM beta/alpha barrel-fold (Benning et al. 2001) **(B)** OPAA "3L7G": It is a three chain metalloprotein having 54 helices and 6 sheets with central atom Manganese in its structure. The protein is capable of performing biological processes like dephosphorylation, proteolysis and respond to toxic substances (Vyas et al. 2010). **(C)** Serum PON "1V04": Single-chain beta class metalloprotein with the central calcium-binding site, 4 helices, 5 sheets, and 6 bladed beta-propeller fold (Harel et al. 2004). **(D)** MPH "1P9E": It is two chain metalloprotein with 20 helices, 7 sheets, and Zinc central atom. It belongs to the class of alpha and beta proteins (Dong et al. 2005). **(E)** DFPase "1E1A": It is a single chain Calcium-dependent PTE with 1 helix and 4 sheets in its structure, that belongs to the class of beta protein having 6-bladed beta-propeller (Scharff et al. 2001a). **(F)** Pa-pepP "1WL9" from *E. coli*, a protease with manganese at its center comprising of two domains. The C-terminal domain with the characteristic "pita-bread" fold is versatile, with the ability to execute a variety of catalytic functions. It belongs to the class of alpha and beta proteins and is capable of performing molecular functions such as peptidase activity, hydrolase activity, and biological functions like proteolysis (Graham et al. 2005).

1.6.1.1 Structure of OPH

Phosphotriesterase (PTE)/OPH, a homodimer metalloprotein, is a member of the superfamily amidohydrolase. It utilizes a divalent ion, such as Co^{2+}, Zn^{2+}, Mg^{2+}, Ca^{2+}, and Fe^{2+}, etc., for the nucleophilic attack by activating the hydrolytic water molecules (Ghanem and Raushel 2005). With respect to the normal activity, enzymes supplemented with these ions show 121%, 86%, 81%, 74%, and 48% activity, respectively. The high-resolution X-ray structure showed that the protein folds into αβ barrel motif also known as TIM Barrel (Raushel 2002). OPH adopts TIM barrel fold where the active site is located at the C terminal of the β barrel (Ghanem and Raushel 2005). Two Zn^{2+} are bound to the histidine residues at the binuclear metallic center. One zinc cation is bound to two histidine residues, H201 from β strand 5 and H206 from β strand 6. Another zinc cation is bound to two histidine residues (H55, H57) and one aspartic acid (D301) (Ghanem and Raushel 2005; Bigley and Raushel 2013). Carboxylated lysine from β strand 4 and hydroxide ion form the bridge between the two cations (Bigley and Raushel 2013).

1.6.1.2 Reaction mechanism of OPH

The enzymatic reaction mechanism of hydrolysis for organophosphate triesters involves the binding of substrate to the binuclear metal ion at the active site of the enzyme. The binding occurs via the coordination of phosphoryl oxygen to one of the metal ions that weaken the hydroxide bridging between the metal ions. The distance between the metal and phosphoryl oxygen of the substrate is 2.5 Å. The bond between the metal and the oxygen polarizes the P=O bond and gives more electrophilicity to the phosphorus center. The hydroxide ion acts as a nucleophile and attacks the phosphorous center resulting in the weakening of the bond to the leaving group (Raushel 2002; Ghanem and Raushel 2005; Nath et al. 2016). The nucleophilic attack of hydroxide ion at the phosphorous center with the release of the leaving group is believed to be assisted by H254 by transferring a proton from D301 to the solvent and away from the active site. With the release of proton in the solvent the pH

of the solvent decreases, this can be exploited for the detection of OPs. The formation of phosphorylated intermediate does not take place during the reaction mechanism because it proceeds by an SN2 mechanism which involves the inversion of stereochemistry at the phosphorous center (Ghanem and Raushel 2005). The rupturing of the phosphorous oxygen bond is the rate-limiting step of the hydrolytic mechanism. Substrates with leaving group that possess a pKa value under 7 are all hydrolyzed at the same rate, while substrates with the leaving group, that have pKa over 7, are hydrolyzed slower as pKa increases (Vilanova and Sogorb 1999).

The central metal ion plays three major roles in the hydrolysis reaction of organophosphate. The metal ion reduces the negative charge development on the leaving group by the process of neutralization. The metal ion increases the polarization of the P=O bond and thus enhances the electrophilicity at the phosphorous center, thereby it accelerates the attack of the hydroxyl ion. The metal ion may also increase the nucleophilicity of the attacking hydroxide ion and decrease the pKa of the bound water molecule (Raushel and Holden 2000).

1.6.1.3 Substrate specificity of OPH

OPH has quite a broad substrate specificity implying a plastic active site (Reeves et al. 2008; Wales and Reeves 2012). The broad substrate specificity is due to the non-specific substrate binding site (Bigley and Raushel 2013). The rate-limiting step and the catalytic efficiency are dependent on the pKa of the leaving group (Ghanem and Raushel 2005). The enzyme is found to have the highest efficiency for hydrolyzing the electron withdrawing phenolic leaving groups, but it also cleaves the halide bond and thiol linkage (Bigley and Raushel 2013). The surface of the enzyme has three hydrophobic pockets, to which the three esters groups of substrates interact. The leaving group pocket is made up of the residues W131, F132, F306, and Y309. These residues largely govern the specificity of the leaving group. The other ester groups interact with the large and small pockets. This determines the specificity of the side ester groups of the substrate. In the hydrolysis reaction of organophosphate, the

enzyme exhibits a significant amount of stereoselectivity. In the hydrolysis reaction of the racemic mixture, the enzyme prefers the S_p enantiomer over the R_p enantiomer. When the actual bond cleavage is the rate-limiting step, the corresponding phosphate esters are found to be hydrolyzed slower than the thiophosphate esters. And when the rate-limiting step is associated with the conformational step or product release then the hydrolysis of phosphate esters is found to be faster than the thiophosphate esters (Raushel and Holden 2000; Bigley and Raushel 2013).

1.6.1.4 Enzyme activity of OPH

The enzymatic activity of OPH is influenced by temperature, pH, and substrate concentration. The activity of the enzyme varies with varying temperatures. Initially, with the rise in temperature, the reaction rate also increases because of the increasing kinetic energy of the reacting molecule. Eventually, the kinetic energy of the reacting molecules crosses the threshold energy required for the breaking of hydrophobic and hydrogen bonds that maintain the secondary structure. At this temperature the structure of the active site changes resulting in the loss of catalytic activity because of the denaturation of the enzyme. Therefore, the OPH enzyme shows its maximum activity at an optimal temperature of 35 °C and pH of 7.5. Enzyme activity increases with increasing substrate concentration but once all the active site of the enzyme is occupied by the substrate no further increase in the activity of the enzyme is observed (Maheshwari et al. 2017).

1.6.2 Organophosphorus Acid Anhydrolase (OPAA)

OPAA is an enzyme isolated from the extract of halophilic *Alteromonas* species and is found to be able to hydrolyze a large number of OPs. **Fig. 1.8 B** shows the crystal structure of OPAA (Jacquet et al. 2016). It is a monomeric 58 kDa polypeptide metalloprotein having Mn in its natural form. It can hydrolyze organophosphate triesters and the protein appears to be dipeptidase (Raushel 2002). It displays stereospecificity similar to PTE, but the rate of hydrolysis is slightly less than that of PTE.

It also shows high activity in hydrolyzing the P-F bond in OPs like sarin, soman, and DFP, among others. However, it is less effective in hydrolyzing P-CN, P-O, P-S and is unable to hydrolyse P-C bonds (Raushel 2002).

Among the OP compound degrading enzymes, OPH demonstrates wider substrate activity that includes P-O, P-F, P-CN, and P-S bonds **(Table 1.1)**. OPH shows its activity on substrates such as Paraoxon, DFP, VX, Soman, Mipafox, Dursban, Ethyl parathion, Coumaphos, Diazinon, Fensulfothion, Methyl parathion, Cyanophos, Acephate, Azinophos-ethyl demethon-S, Malathion, Phosalone, Methamidophos, Tetriso, O-ethyl O-(4-nitrophenyl) phenylphosphonothioate, making it a favorable candidate for biosensor and bioremediation studies. Similar to OPH, OPAA also shows wider substrate specificity and thus can be used for detection as well as for bioremediation applications. Interestingly, human PON is the only reported enzyme that can cleave P-C bond compounds and reported to be more efficient for the degradation of some OPs like cyclosarin and soman than OPH and DFPase (Amitai et al. 2006).

1.6.2.1 Structure of OPAA

OPAA enzymes were first identified in *Alteromonas* species (Matula et al. 2020), of which *Alteromonas* sp. JD6.5 is most well evaluated. Other strains, like *Alteromonas haloplanktis* or *Alteromonas undina*, also produce the enzyme which is active for the hydrolysis of organophosphate compounds. These OPAAs have a striking similarity in terms of structure and function to each other – represented by a molecular weight of 50–60 kDa, optimal operation at pH 7.5-8.5, and 40 to 55 ˚C, with the requirement of Mn^{2+} to maximize the activity. OPAA is a polypeptide comprised of 517 amino acids when isolated from *Alteromonas sp.* JD 6.5, while the enzyme isolated from *Alteromonas haloplanktis* contains 440 amino acids and lower molecular weight. Both enzymes have 77–80% amino acid homology, and the difference between them was found to be due to the presence of an extended C-terminal region in the JD 6.5 enzyme (Chishti et al. 2013). OPAA from *Alteromonas* sp.

JD6.5 has been classified into the prolidase family of enzymes based on its functionality. OPAA was initially believed to be a monomer but was later determined to be a dimer of dimers, and hence a tetramer (Matula et al. 2020).

The OPAA structure comprises a small N and a large C-terminal domain, with an active site having binuclear Mn^{2+} ions (Cheng and Defrank 2000; Vyas et al. 2010; Theriot and Grunden 2011; Daczkowski et al. 2015). Six β-sheets with an antiparallel central pair of strands and parallel flanking pairs are found in the N-terminal domain. In the C-domain, all five β-strands are antiparallel. The N-domain β-sheet is twisted while tightly curved in the C-domain, displaying a "pita bread" style (Vyas et al. 2010). In the two domains, there are variations in the composition and topological structures of alpha-helices. There are four helices in the N-domain, while the C-domain with the pita bread structure has eight (Vyas et al. 2010). The C-terminal region houses the binuclear metal center, and it has amino acid residues Asp244, Asp255, His336, Glu381, and Glu420 (Cheng et al. 1997; Vyas et al. 2010). For full catalytic action, two bridging Mn^{2+} ions are required (Theriot and Grunden 2011). In the enzyme's active site, a non-proteinaceous density was found, but not definitively characterized. A bonded glycolate whose three oxygen atoms coordinate the two Mn^{2+} ions is presumed to be (Cheng et al. 1997; Cheng and Defrank 2000; Vyas et al. 2010).

1.6.2.2 Reaction mechanism of OPAA

Three pockets represent the substrate-binding pocket of OPAA. Tyr212, Val342, His343, and Asp45 make up the small pocket, and the large pocket is made of Leu225, His226 His332, and Arg418 residues. The leaving group is composed of residues Tyr292 and Leu366 (Bigley and Raushel 2013). The OP compound cleaving ability in OPAA largely arises from the bridging water molecule or hydroxide ion in the metal center that facilitates a nucleophilic attack on either the carbonyl oxygen of the scissile peptide bond of the dipeptide [Xaa-Pro] or the phosphorus center of NA (Vyas et al. 2010; Theriot and Grunden 2011; Bigley and Raushel

2013; Daczkowski et al. 2015). In the C-terminal domain, the binuclear Mn^{2+} site is found in the central cleft of the fold, with a more solvent-exposed A-metal ligated to H336 and E381 and the B-metal ligated in a bidentate manner to D244. Structural studies have suggested that the free phosphoryl oxygen binds to the solvent-exposed A-metal of OPAA, as well as the ester oxygen extending to the small pocket, ligates to the B-metal. This bidentate ligation of the substrate possibly allows the hydroxide to attack the phosphorus center without dissociation from either of the metals. The leaving group is then expelled, and the phosphoryl product gets bound in a tridentate fashion (Bigley and Raushel 2013).

1.6.2.3 Substrate specificity of OPAA

OPAA is a bimetalloenzyme that responds to different toxic OP compounds. It is prolidase cleaving dipeptides with C-terminal proline (Hoskin and Prusch 1983; Blum et al. 2008; Wymore et al. 2014). Because of this aspect, the physiological function of the enzyme may be correlated with the metabolism of cellular dipeptides (Kitchener and Grunden 2012). For OP compounds with P-F bonds, a high degree of hydrolysis activity was observed, but rather limited activity for P-O or P-C bonds and no activity against P-S bonds. Similar activity with substrate from *Alteromonas undina* and *Alteromonas haloplanktis* was later seen for the OPAA (DeFrank and Cheng 1991; Cheng et al. 1993; DeFrank et al. 1993; Cheng et al. 1996; Cheng et al. 1997; Cheng et al. 1999). Nerve agent soman is the ideal substrate for OPAA hydrolysis. OPAA can also act on other nerve agent analogs containing a PNP leaving group, such as sarin, tabun, DFP, and nerve agents. Additionally, it is less active toward V-nerve agents (DeFrank et al. 1993; Cheng et al. 1999; Hill et al. 2000; Hill et al. 2001; Richardt and Blum 2008; Theriot and Grunden 2011; Harvey et al. 2020) and mipafox a relative analogue of DFP, a competitive inhibitor and not a substrate under normal assay conditions (DeFrank et al. 1993; Vyas et al. 2010). Normally, OPAA shows a preference towards hydrolysis of less toxic stereoisomers of nerve agents like sarin and soman (Hill et al. 2001) OPAA is stereoselective for Rp-enantiomers of methyl

phosphonates (Hill et al. 2000). OPAA is less active towards paraoxon but highly active towards G-nerve agents when compared to OPH.

1.6.2.4 Enzyme activity of OPAA

OPAA can perform biological processes such as depshosphorylation, proteolysis and act on toxic substances. OPAA has good activity against G-agents (GD> GF~ DFP> GB> GA), unlike OPH, but less active for OPs. While this enzyme does not show any activity against V-agents (Cheng et al. 1999), site-directed mutagenesis will change this in the future (Daczkowski et al. 2015). OPAA is catalytically active on broad pH, ranging from 6.5-9.5, with 7.5-8.5 being optimal, and temperature ranging from 10-65 °C, with an optimal range of 40-55 °C optimum. Furthermore, OPAA requires manganese for the highest activity.

1.6.3 Other OP compound degrading enzymes

1.6.3.1 Paraoxonase (PON)

PON enzyme in human serum has the ability to degrade paraoxons and nerve agents. Its structure revealed that it is a Ca-containing monomer enzyme **(Fig. 1.8 C)**. It is a single chain beta class metalloprotein with central Calcium binding site, 4 helices, 5 sheets, and 6 bladed beta-propeller (Harel et al. 2004). Human PON preferably cleaves bonds like P-O, P-C, P-F, P-CN (Di Sioudi et al. 1999). A variant of mammalian PON is found to be more efficient for the degradation of some OPs like cyclosarin and soman than OPH and DFPase (Amitai et al. 2006).

1.6.3.2 Methyl parathion hydrolase (MPH)

MPH belongs to a family of metallo beta-lactamase and is an aryldialkyl phosphatase **(Fig. 1.8 D)**. The first *mpd* encoding gene for MPH was identified in *Plesiomonas sp.* strain M6 (Jacquet et al. 2016). Another closely related gene was identified and sequenced from *Pseudomonas sp*. WBC3. Its structure revealed that it is a Zn-containing

homodimer enzyme. It catalyzes the degradation of methyl parathion. Each subunit consists of hybrid binuclear Zn in which most solvent-exposed β metal cation is replaced with Cd. It is found to be homologous to other metal β lactamases but does not show any similarity to PTE (Jacquet et al. 2016).

1.6.3.3 Diisopropyl-fluorophosphatase (DFPase)

DFPase is a 35 kDa monomer protein obtained from the brain of *Lolilgo vulgaris* squid **(Fig. 1.8 E)**. DFP is the main substrate and hydrolyze P-F bond releasing isopropyl phosphate and fluoride. Two highly effective Calcium sites are required for its stabilization and catalysis function. To identify the residues important for the active site and to decipher the reaction mechanism of the enzyme, site-directed mutagenesis and kinetic studies were performed (Scharff et al. 2001a; Scharff et al. 2001b; Hartleib and Rüterjans 2001; Katsemi et al. 2005). Three histidine residues were found to play an important role at the active site, in which two histidine H274 and H174 have the role of stabilization and residue H287 was found to act as a general base catalyst (Jacquet et al. 2016).

1.6.3.4 Aminopeptidase P (Pa-pepP)

It is an exopeptidase of 49.65 kDa that cleaves the N-terminal residue from a polypeptide when the second residue is proline. It is a tetrameric metalloprotein in *E. coli* that consists of 4 Pep monomers and requires two Mn ions for its activity (Farnoosh and Latifi 2014). The enzyme adopts 'pita bread' fold like creatinase and methionine aminopeptidase that functions as a tetramer (Ghanem and Raushel 2005) The two Manganese ions in the active site at the C terminal of the β sheet are separated by 33Å. The two ions bridge together via a hydroxide ion which acts as the nucleophile in the attack of the peptide bond **(Fig. 1.8 F)** (Karpouzas and Singh 2006). Its substrate for degradation includes methyl isobutyl and methyl isopropyl groups (Farnoosh and Latifi 2014).

Incidentally, it shows only 31% sequence similarity with OPAA (Theriot and Grunden 2011).

1.7 Enzymatic Biosensor

1.7.1 Basic mechanism of biosensing with enzymes

Typically, the detection systems used in conjunction with biological components can be classified into electrochemical (Potentiometric, Amperometric, and Conductometric) and optical (UV-Visible, Fluorescence) systems of measurement **(Fig. 1.9)**. Detection systems employing potentiometric measurement utilize changes in potential with corresponding changes in current which is the result of oxidation and reduction potential of the electrochemical reaction. On the other hand, amperometric detection systems work on the basis of changes in current according to changes in chemical concentrations of interest. They typically utilize two/three-electrode systems constituted as a reference, a working electrode, and an auxiliary electrode. Amperometric detection systems are believed to be superior due to the linear increase which solves the perils, such as salt screening and exponential or logarithmic increase with the concentration in a potentiometric detection system. The conductometric detection systems measure the electrical conductivity or resistivity of analyte samples based on the number of ions and electrons. The effect produced is also influenced by temperature and pH. Electrical impedance is another phenomenon utilized by detection systems wherein the resistance of biological components and ionic conductance across it is utilized for the measurement. The optical detection systems typically utilize photons as mediating components in electrical transduction in comparison to the direct use of electrons in electrochemical detectors. Intensity, decaying time, quenching efficiency, radiant energy transfer, anisotropy, etc. are the critical parameters measured while using absorption, reflectance, or fluorescence using ultraviolet (UV), visible, near-infrared radiations in photometric measurement. Some optical detection tools also work on the principle of evanescent waves and the total internal reflection phenomenon occurring due to the changes in the

refractive index. Some hybrid mechanisms like electrochemiluminescence, amperometric-potentiometric, piezoelectric, and magneto-elastic detection systems are also utilized in several reports of biosensors.

1.8 Biosensors for organophosphate detection

The currently accepted and utilized methods for detection and quantification of OPs such as liquid chromatography or immunoassay-based techniques have limitations of being time-consuming, non-suitable for infield determination, and online monitoring. Lately, biosensors have emerged as leading analytical techniques owing to miniaturization of transduction, development of microelectronic circuitry, and interfacing using bio-recognition units. Cost-effective and miniaturized analytical tools have led to the transformation of sophisticated instruments into point-of-care devices. Enzymes are the most commonly utilized biological recognition units considering the ease of application and translation. Analysis of OPs can best be investigated using OPH and OPAA as a biological recognition unit and converting the catalytic reaction to a measurable signal in a biosensor. The broad substrate specificity of OPH and OPAA makes them attractive enzymes of interest for researchers and professionals interested in monitoring and detoxification of OPs present in the environment. The OPH/OPAA catalyzed hydrolysis reaction of OPs generates two protons and an alcohol, which can be chromophoric or electro-active. This provides ample opportunities for use of OPH and OPAA in a variety of sensors ranging from fluorometric to electrochemical, or even a pH-based sensor that can quantify changes in pH based on the increase in protons generated during the hydrolysis process. A broad classification of the various biosensors employing OPH and OPAA for the detection of OPs is described here.

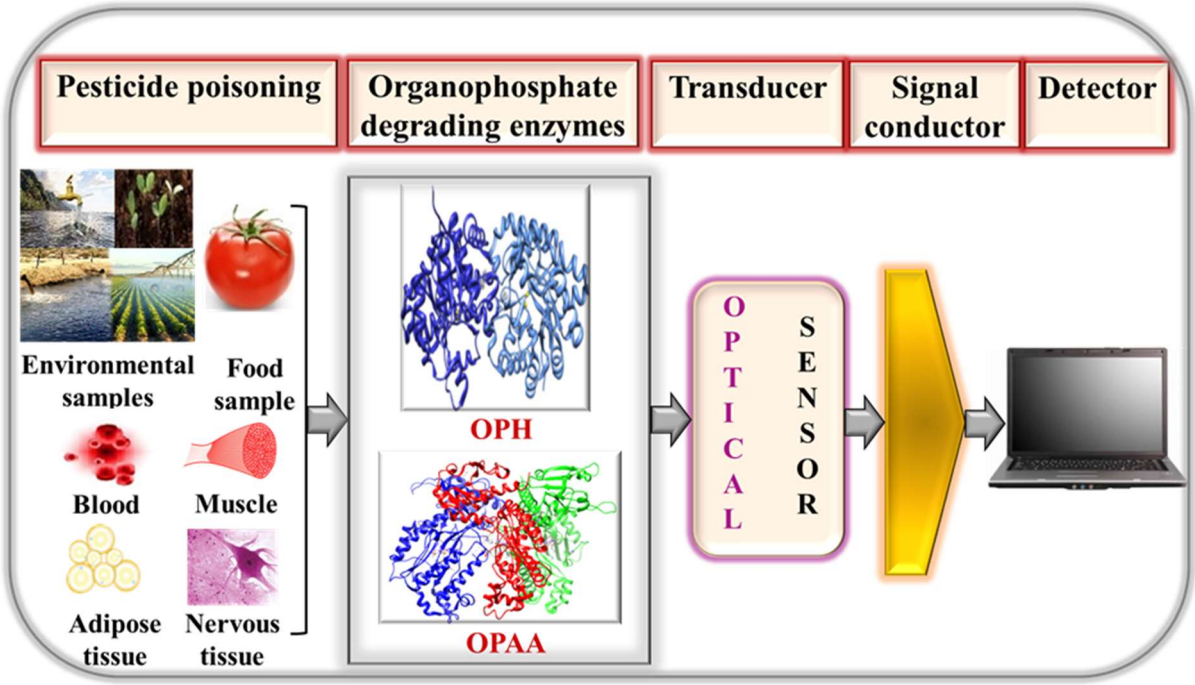

Figure 1.9. Schematic representation of enzymatic biosensor for detection of Organophosphorus pesticides: Microbial OP degrading enzymes degrades the organophosphate compounds present in environmental samples, food, water, tissue, muscle. The degradation process is monitored by a change in optical output through monitoring of by-products. Finally, the changes are logged on a computer, wherein the data is analysed to quantify the organophosphates present in the samples and the results are calibrated to standard scales. This method provides a direct, fast and effective way of quantifying organophosphate poisoning in common foods, crops, soil and water as well as diagnosis of severe pesticide poisoning in humans by means of tissue analysis.

1.8.1 Organophosphorus hydrolase sensors

1.8.1.1 Electrochemical

A typical electrochemical sensor is based on the processes occurring inside an electrochemical cell, in which the working electrode (usually glassy carbon electrode or a conductive strip) is coated with the compound of interest, while the analyte (or substrate) is inserted into the electrolyte of the electrochemical cell. Here, sensing is based on changes in current and/or voltages upon the addition of the analyte to the electrolyte. Additionally, a transducer, amplifier, and a data analysis system are other components included which define the biosensing performance of electrochemical biosensors. The property of electrodes is the key determining factor in the performance using this electrochemical catalysis. The basis of detection can be the changes in current or potential differences occurring at the biological receptor-electrode interface. In the case of OPH, OPs (such as methyl parathion or paraoxon) are the analytes introduced in specific concentrations into the electrolyte **(Fig. 1.10)**. The reaction of OPs with OPH results in the formation of PNP, which gives a current when oxidized that serves as the response of the electrochemical sensor.

1.8.1.2 Optical sensors

Most of the reports on optical sensors **(Table 1.2)** are based on the changes in absorbance or fluorescence during hydrolysis of OPs through the generation of byproducts like PNP and the resultant change in the pH of the medium, which can be measured by the output of a UV-Vis spectrophotometer or a fluorescence spectrophotometer. Changes in absorbance due to the production of PNP during the catalytic activity of OPH are the main mechanism of use of UV-Vis-based detection of OP compounds. Quenching of fluorescence due to pH changes and employing pH-sensitive fluorophores form the most common mechanism for the use of a fluorescence-based OPH biosensor **(Fig. 1.11)**.

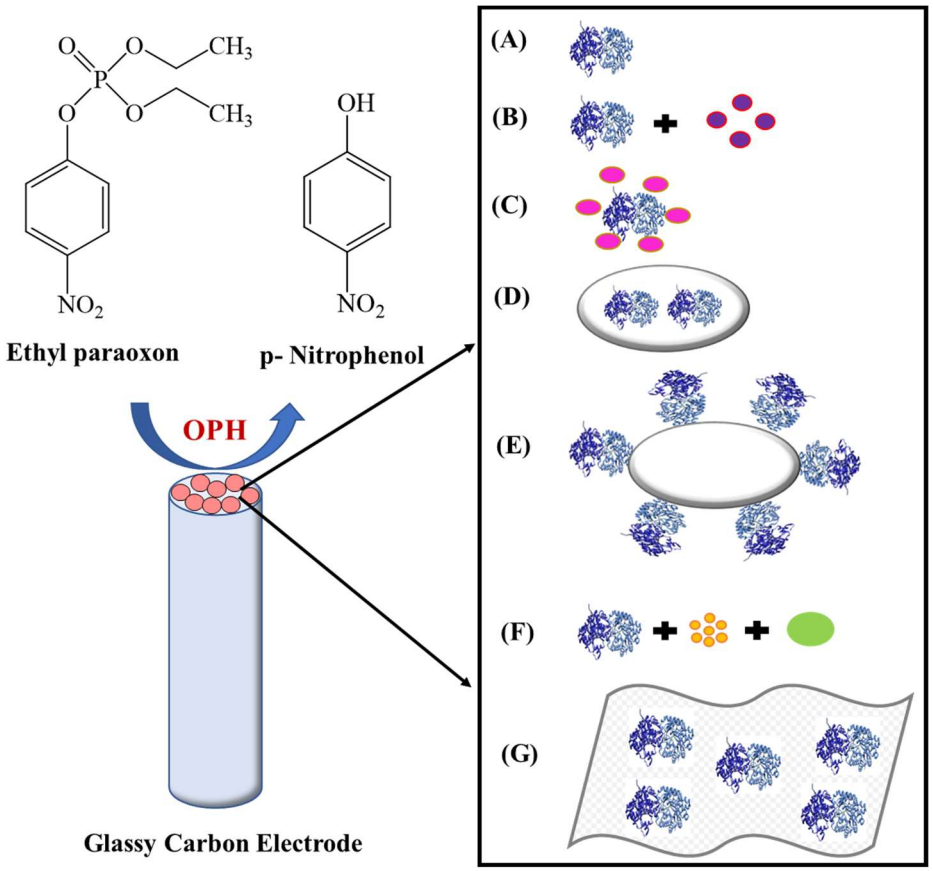

Figure 1.10. Schematic diagram of electrochemical sensing system: Glassy carbon electrode surface showing the conversion of OP compound into *p*-nitrophenol (PNP), in the presence of OPH and the various configurations for developing electrochemical biosensor found in contemporary literature. (A) OPH. (B) OPH with the nanoparticle. (C) OPH with quantum dots. (D) OPH inside bacterial cell (E) OPH on the bacterial cell surface. (F) OPH with gold nanoparticle and binder. (G) Encapsulated OPH.

Table 1.2: Characteristics of OPH based optical-based biosensors

Cell Type	Type (Material)	Substrate (LOD)	Linear Range	Sensitivity	Stability	Response time	Reference
1.2.1 UV Spectrophotometric biosensors							
E. coli	1. Reversible inhibition of OPH by copper complexed meso-tri (4-sulfonatophenyl)mono(4-carboxyphenyl)porphyrin (CuC_1TPP)	Paraoxon (2.5×10^{-5} µM)	10^{-2} - 10^{5} ppb	-	230 days	10 Sec (paraoxon)	(White and Harmon 2005)
		Diazinon (2.6×10^{-3} µM)	1 - 10^{5} ppb				
		Malathion (0.302×10^{-2} µM)	10-10^{4} ppb				
		Coumaphos (0.689 µM)	10-10^{5} ppb				
	2. *E. coli* whole cells harbouring plasmid pTInaPb-N/OPH	Paraxon (0.2 µM)	0.5 -150 µM	-	Approx. 30 days	<= 10 min.	(Tang et al. 2014)
		Parathion (0.4 µM)	1-200 µM				
		Methyl parathion (1 µM)	2.5-200 µM				
	3. OPH on nylon membrane connected to optical fibres	Paraoxon (2 µM)	0.01-0.48 mM (steady state) 0.02-0.5 mM (kinetic)	0.0022/µM (steady state); 0.00092/min/µM (kinetic)	10 days	14 min. (steady state), 2 min. (kinetic)	(Mulchandani et al. 1999)

		Parathion (2 µM)	0.01-0.2 mM (steady state)	0.002/µM (steady state)			
		Coumaphos (5 µM)	5-35 mM (kinetic)	0.0005/min/% (kinetic)			
	4. MAP based adhesion	Paraoxon (5 µM)	5-320 µM	-	28 days	5 min.	(Kim et al. 2013)
Flavobacterium sp. MTCC 2495	1. Glass fiber filter paper	Methyl parathion (0.3 µM)	4-80 µM	-	1 month	< 3 min.	(Kumar et al. 2006)
Sphingomonas sp. JK1	1. Glutaraldehyde as linker; direct deposition of *Spinghomonas* sp. JK1 on microplate reader wells	Methyl parathion (4 µM)	4-80 µM	-	18 days	5 min.	(Kumar and D'Souza 2010)
	2. Inner epidermis of onion bulb scale and glutaraldehyde	Methyl parathion (4 µM)	4-80 µM	-	32 days	5 min.	(Kumar and D'Souza 2011)
1.2.2 Fluorometric biosensors							
E. coli	1. CdSe QDs / OPH	Paraoxon (10^{-9} mol/L)	1 x 10^{-8} to 1 x 10^{-5} mol/L	-	-	~10 min.	(Constantine et al. 2003a)

	2. OPH with a histidine tail (OPH_{6His}) bioconjugated with pyranine—with the aid of silica-coated silver nanoparticles	Paraoxon (2 ppb)	5-100 ppb	-	-	<3 min.	(Thakur et al. 2013)
		Methyl parathion (10 ppb)	20-100 ppb				
	3. Fluorescein isothiocyanate covalently bound to OPH	Paraoxon (8 μM)	25-400 μM	-	90 days	-	(Rogers et al. 1999)
	4. OPH-conjugated gold nano particles with 7-hydroxy-9H-(1,3-dichloro9,9-dimethylacridin-2-one(DDAOphosphate) as decoy	Paraoxon (20 μM)	0-240 μM	-	-	-	(Simonian et al. 2005)
P. aeruginosa	1. OPH-conjugated gold nanoparticles with and without linking system (glutaraldehyde-cystamine) and cumarin1 as decoy	Paraoxon (5×10^{-5} μM)	50 – 1050 nM	-	-	-	(Kamelipour et al. 2014)
	2. Chitosan- gold nanoparticles organophosphorus hydrolase nano bio conjugate with Coumarin1 as decoy	Paraoxon (5×10^{-5} μM)	0–1050 nM	-	21 days, 80% activity	< 30 min.	(Karami et al. 2016)
P. diminuta	1. OPH-conjugated nano magnet-silica core-shell with coumarin 1 as decoy	Paraoxon (5×10^{-6} μM)	10-250 nM	-	-	-	(Khaksarinejad et al. 2015)
	2. Fluorescent dye/OPH	Paraoxon (5×10^{-9} mol/L)	5×10^{-9} - 1×10^{-5} M	-	-	30 s	(Zheng et al. 2005; Orbulescu et al. 2006)

1.2.3 Fiber optic microbial biosensor							
E. coli	1. *E. coli* cell suspension on fiber optic sensor strip	Paraoxon (3 µM)	0.0-0.6 mM	5.98×10^{-4} min^{-1} μM^{-1}	32 days	< 10 min.	(Mulchandani et al. 1998)
		Parathion (3 µM)	0.0-0.03 mM	3.4×10^{-4} min^{-1} μM^{-1}			

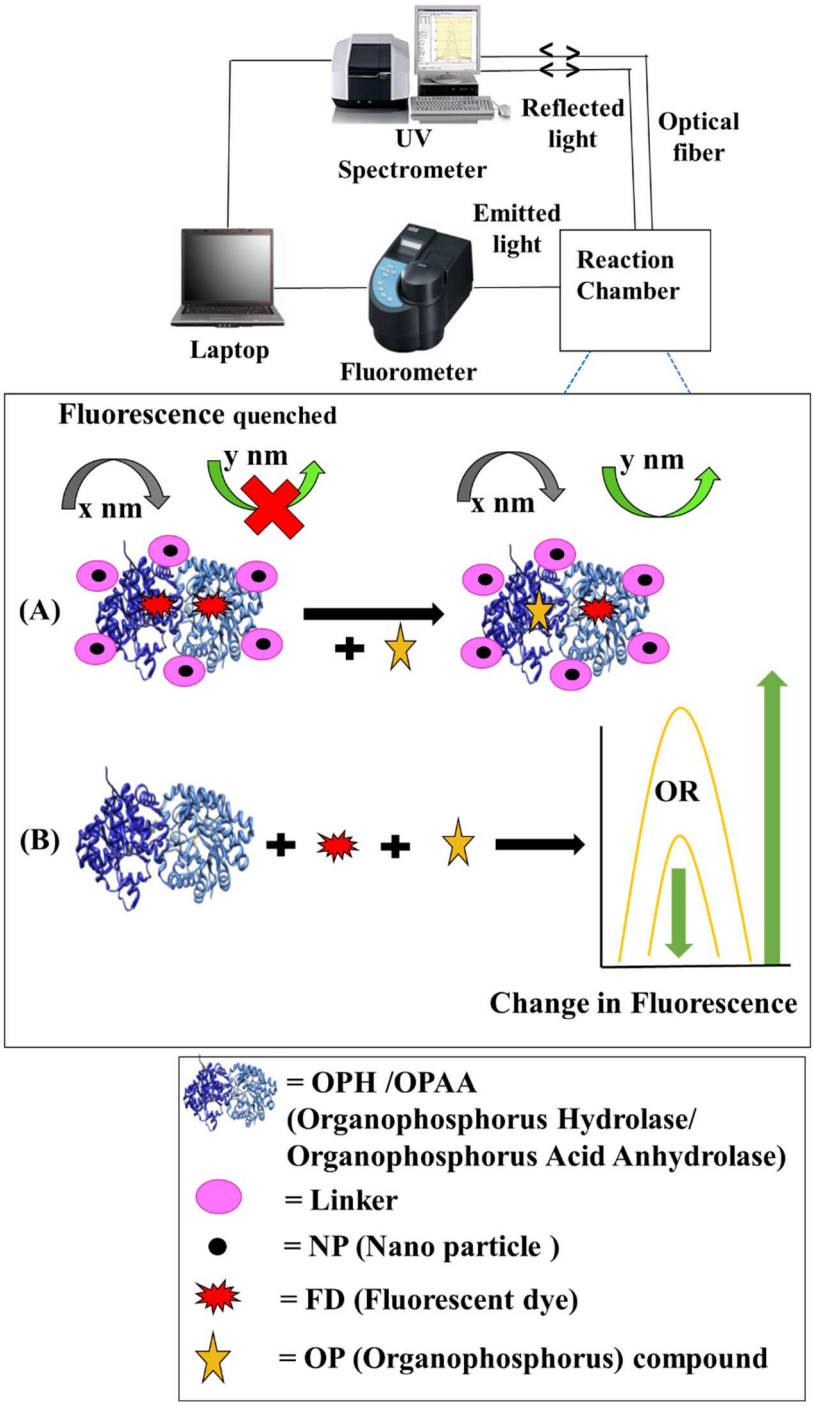

Figure 1.11. Schematic diagram of optical sensing system: Inset shows the mechanism of fluorescence as well as spectrophotometric-based sensing of OPH. (A) OPH/OPAA conjugated with nanoparticle, linker and the fluorescent dye does not exhibit fluorescence when excited at "x" nm, but exhibits fluorescence by emission at "y" nm when OP compound is added due to competitive binding of OP compound with OPH/OPAA. (B) OPH/OPAA in presence of a fluorescent dye exhibits fluorescence. Upon addition of the OP compound, binding of OPH/OPAA with OP compound may either increase or decrease the fluorescence emission.

1.8.1.2.1 UV-Vis based sensors

UV-Vis-based sensors refer to a type of optical sensing wherein a change in absorption upon creation of hydrolysis product of OPs is measured. In this case, however, the change is quantified either through measuring the signal from an optical fiber system or directly using UV-Visible spectrophotometers or plate readers. The principle of evanescent field optical fiber-based biosensors, in which an evanescent field is created by the presence of an extremely thin cladding on a dense core using total internal reflection at the interface, has also been used by several authors (Yang et al. 2008a) due to their convenience, lower cost and easy-to-deploy characteristics in various kinds of sensors. In terms of OPs detection and sensors, both enzymatic and cell-based detection methodologies have been investigated. Fiber-optic detection mechanisms are very commonly described in literature while investigating OPH-based UV-Vis or fluorescence-based sensors owing to their portability, cost, and ease of use. In a report of enzyme immobilization by Mulchandani et al., who used an optical fiber-based biosensor by immobilizing OPH on a nylon membrane attached to a sensor tip composed of a bundle of optical fibers. This system was attached to a measurement system comprising of a light source in which 400 nm light is delivered, a cutoff filter, reaction chamber, and an optical fiber system. The output measurement consists of a photomultiplier tube that can quantify changes in absorbance (at 400 nm) due to the generation of PNP. Using this assembly of sensor tips a detection limit of 2 μM for paraoxon and parathion and 5 μM for coumaphos was reported **(Table 1.2.1)** (Mulchandani et al. 1999). In another study, Zourob et al., described another way of using immobilized OPH in a pH-sensitive matrix and estimating using a waveguide sensor developed from absorber material-clad, using solvent blue and polythiophene as clad layers and a sol-gel layer as a wave-guide. The principle of detection here was the change in refractive index when the OPH enzyme was immobilized in a pH-sensitive matrix containing OPs. This sensor was able to achieve a detection limit of 4 nM for paraoxon and

parathion, with 81 nM for diazinon, with a linear range of 1 - 5 μM (Zourob et al. 2007b).

A direct whole cell-based biosensor utilizing *Flavobacterium* sp. expressing OPH was developed by Kumar et al., who immobilized the cells on the glass fiber filter paper discs and analyzed methyl parathion. The absorbance of PNP was measured in a specially designed reaction vessel connected through optical fibers to a UV-Vis spectrophotometer. The discs were inserted into the reaction medium in the presence of OP compounds, and the changes in absorbance were noted through the UV-Vis spectrophotometer. This method reported a detection limit of 0.3 μM and a linear range of 4 - 80 μM for methyl parathion **(Table 1.2.1)** (Kumar et al. 2006). White and Harmon developed a biosensor based on immobilization of *E. coli* expressing OPH on ProbeOn^{TM} Plus slides with glutaraldehyde as a linker and complexation with the porphyrin meso-tri(4-sulfonato phenyl) mono(4-carboxy phenyl) porphyrin (C1TPP) which is competitively bound to OPH. Upon introduction of OP compounds, the porphyrin is unbound and the reaction of OP compound with OPH generates PNP, which is measured by a change in absorbance at 412 nm, through an optical fiber-based UV-Vis spectrophotometer. This sensor was able to display a low detection limit of 7 ppt (25 pM) for paraoxon **(Table 1.2.1)** (White and Harmon 2005). Kim et al., developed a biosensor by immobilizing whole cells of recombinant *E. coli* expressing periplasmic OPH onto the surface of a 96-well microplate using mussel adhesive protein as a microbial cell immobilizing linker. The resultant setup was able to detect through changes in absorbance at 410 nm, paraoxon in quantities as low as 5 μM, with a linear range of 5 - 320 μM and good stability, 80% activity retention up to 28 days and reusability up to 20 times **(Table 1.2.1)** (Kim et al. 2013). Intending to improve the catalytic activity of substrates, researchers have investigated surface expression in cells. Tang X. et al., developed a sensor based on surface expression of *E. coli* bacteria expressing OPH with an anchored ice nucleation protein, which showed detection limits of 0.2 μM, 0.4 μM and 1 μM for paraoxon, parathion, and methyl parathion, respectively, based on monitoring of the production of PNP through absorption spectra at 410

nm, a principle that is followed for most studies in this category. The same sensor showed a broad linear range of 0.5 - 150 μM paraoxon, 1 - 200 μM parathion, and 2.5 - 200 μM methyl parathion, respectively **(Table 1.2.1)** (Tang et al. 2014). Thus, both periplasmic and surface-expressed bacteria have shown promise in achieving the detection of OPs. Another approach shown to be effective for improved detection of OPs is by mineralization of cells for attachment of OPH using $Co_3(PO_4)_2.8H_2O$. Han and Liu, developed a novel biosensor using $Co_3(PO_4)_2.8H_2O$ which was mineralized onto the surface of OPH fused bacteria expressing OPH. The embedding of OPH into $Co_3(PO_4)_2.8H_2O$ crystals greatly enhanced the activity through the allosteric effect. The resultant hybrids, when used as a sensor based on the change in absorbance at 410 nm in the presence of paraoxon, were found to have a detection limit of 0.08 μM and a linear range of 0.2 - 200 μM. Furthermore, this sensor was found to have greater recovery rates of 97% to 102% when used to detect paraoxon in real samples, such as seawater, tap water, and sewage water (Han and Liu 2017). In addition to the location of expression of OPH inside cells, advanced materials like nanomaterials, or nanofabricated chips, or solid crystals have also been described to be able to detect OPs. Kim et al., developed a MEMS chip with etched gaps between two electrodes wherein Single Walled Carbon Nanotube attached *E. coli* strain expressing periplasmic OPH was inserted. This chip was then attached to a 'chamber' containing the analyte solution (e.g., paraoxon), and then the reaction was allowed to proceed for up to 50 minutes. The absorbance of the analyte solution was then measured at 400 nm to determine the effect of OPH on the OPs. The authors reported a linear range of 20 - 500 μM and a detection limit of 5 μM for this sensor (Kim et al. 2015).

Absorbance based sensors developed by White and Harmon using copper complexed meso-tri (4-sulfonatophenyl) mono (4-carboxyphenyl) porphyrin as a reversible inhibitor for OPH displays encouraging results in terms of detection limit (2.5×10^{-5} μM for paraoxon), linear range (10^{-2} to 10^5 ppb), stability (~ 230 days) and response time (under 10 seconds) (White and Harmon 2005). In terms of sensitivity, the enzyme-modified fiber optic sensor developed by Mulchandani et al., displays a high

sensitivity of 0.0022/μM (steady-state) or 0.0092/μM (kinetic) and a linear range of 5000 - 35000 μM (Mulchandani et al. 1999). Although UV-vis absorbance-based sensing has some advantages concerning lower costs and potential to detect additional contaminants through other specific peaks, this method has limitations of poor signal-to-noise ratio which affects the sensitivity as well as selectivity. In cases where the costs are not a concern and highly specific and selective detection is required, fluorescence sensors are often considered to be a better choice (Nemzer and Epstein 2010).

1.8.1.2.2 Fluorescence-based sensors

Fluorescence-based sensors are either based on the quenching of fluorescence or an increase in fluorescence intensity when an analyte is converted into a product. Interaction of OPs with OPH leads to the formation of PNP with the release of protons which can very easily be linked to fluorescence-based estimation. The pH drop occurring during the catalytic reaction may be linked to pH-based fluorescent sensors (Chaudhari et al. 2017). Among the several methods of using OPH for the detection of OPs, the use of pH-sensitive fluorophores like FITC, coumarin 1, poly-thiophene-3-acetic acid (PTAA), etc., are the most common transduction mechanisms followed in the literature reports. An example of a fluorophore with pH-sensitive properties is FITC which causes a depletion of fluorescence intensity as the reaction of OPH progresses. Mulchandani et al., and Roger et al., used this principle to covalently immobilize FITC to OPH, and then adsorb the FITC-labelled OPH to poly-methyl methacrylate (PMMA) beads. The detection mechanism is based on the change of fluorescence due to the change in pH caused by the action of OPH on OPs, wherein existing fluorescence is quenched as a substrate for OPH (i.e., OPs) is introduced. The observed limit of detection was 8 μM for paraoxon and coumaphos, and up to 50 μM for crotoxyphos (Rogers et al. 1999; Mulchandani et al. 2001a) **(Table 1.2.2)**.

Another fluorescence quenching-based mechanism was employed using coumarin 1 in combination with OPH by Paliwal et al., who used an excitation wavelength of 343 nm for a solution containing 1:1 coumarin 1: OPH and fluorescence quenching measured at 465 nm after addition of OPs. A detection limit of 0.7 μM was observed for paraoxon with a linear range of 1 - 8 μM (Paliwal et al. 2007). Coumarin 1 was also utilized as an indirect assay by Karami et al. wherein electrostatically attached Au nanoparticles were immobilized along with OPH and coumarin 1 in chitosan. The method of sensing was the change in fluorescence of coumarin 1, wherein the fluorescence was quenched in the presence of OPH-Au nanoconjugate but was enhanced when paraoxon was introduced into the solution, due to the tendency of paraoxon to replace coumarin 1 as the substrate for OPH. The limit of detection in this study was as low as 50 pM **(Table 1.2.2)** (Karami et al. 2016). Constantine et al., developed a quartz substrate comprising of 5 bilayers of chitosan and PTAA on which OPH was deposited and the fluorescence spectrum of PTAA with chitosan was recorded at 575 nm (excitation wavelength 480 nm) in the absence and presence of paraoxon. The fluorescence was quenched by the presence of paraoxon and the limit of detection was found to be 1 nM (Constantine et al. 2003b). The use of nanomaterials for enhancing the sensitivity of detection is a very common approach used in all biosensors including fluorescent biosensors. Light responsive nanomaterials like gold nanoparticles, quantum dots, core-shell nanoparticles of silica, etc., are very commonly employed with OPH for detection. Kamelipour et al., used glutaraldehyde-cystamine as a linker to develop a conjugate of Au nanoparticles and OPH expressed in *Pseudomonas aeruginosa* and appropriately purified to detect paraoxon in human serum. The sensing mechanism is similar to that mentioned previously, and a detection limit of 50 pM was observed **(Table 1.2.2)** (Kamelipour et al. 2014). Ji et al., designed a conjugate of OPH with (CdSe) ZnS quantum dots, and detected paraoxon using the principle of photoluminescence quenching at 570 nm with a 350 nm excitation in the presence of paraoxon, which they concluded, was caused by a secondary structure change in OPH during the interaction with paraoxon, which in this case interacts with OPH as a

substrate rather than as an inhibitor. The detection limit was found to be 0.01 μM of paraoxon (Ji et al. 2005). Khaksarinejad et al., using OPH conjugated with APTES activated Fe_3O_4-SiO_2 core-shell nanoparticles wherein glutaraldehyde was used as a cross-linker. In this study, a low detection limit of 5 pM was reported **(Table 1.2.2)** (Khaksarinejad et al. 2015). The whole cell-based biosensors using OPH and fluorescence transduction mechanisms are meagre in literature. In one of the fluorescent whole cell-based biosensors described by Fleischauer et al., OPH expressing *E. coli* bacteria were immobilized in a hydrogel precursor and crosslinked by adding in mineral oil and crosslinked by photopolymerization in UV light for 5 seconds. The fluorescence intensity of a standard solution containing a pH sensitive fluorescent dye and a standard quantity of paraoxon was recorded with and without the beads. The reaction between OPs and OPH causes an increase in acidity, changing the pH and consequently the fluorescence intensity ratio. A detection limit of 3 μM was observed for this sensor (Fleischauer and Heo 2014).

In terms of linear range and detection limit, Khaksarinejad et al., have obtained the best results for their sensor based on competitive binding of coumarin 1 to OPH, with values of 10 - 250 nM and 5 pM, respectively **(Table 1.2.2)** (Khaksarinejad et al. 2015). Rogers et al., have obtained an impressive linear range of 25 - 400 μM and good stability of 90 days in their sensor based on fluorescence signal quenching of FITC bound OPH in the presence of paraoxon, but this study falls behind in terms of the detection limit (8 μM for paraoxon) **(Table 1.2.2)** (Rogers et al. 1999). Thakur et al., have reported a fast response time of less than 3 minutes in their study based on metal nanoparticle enhanced fluorescence of OPH conjugated with a pyranine complex **(Table 1.2.2)** (Thakur et al. 2013). Fluorometric sensors have the advantages of sensitivity. However, this method is dependent on the components and materials in the test setup, which can absorb or reflect the light and hence affect the readings. In practice, this necessitates an expensive setup and is not easily deployed in real-world scenarios and on-site detection methodology due to such limitations (Ryškevič et al. 2010).

1.8.1.3 Other methods of sensing

In addition to the methods described above, efforts have also been made towards utilizing new and upcoming principles of science towards the sensing and detection of organophosphorus compounds. For example, Walker et al., developed a photonic crystal-based sensing platform wherein a bimodular sensing motif was utilized in Intelligent Polymerized Crystalline Colloidal Array (IPCCA) with OPH as the first sensing material and 3-aminophenolate as the second sensing material, added as functionalizing agents in the IPCCA matrix. The IPCCAs comprise of colloidal nanoparticles polymerized in a hydrogel which diffracts light in the visible spectral region. The OPH degrades methyl parathion to PNP and dimethyl phosphate at pH 9.7, with two protons as a byproduct. The protons protonate the 3-aminophenolate, causing a change in the steady-state volume in the IPCCA. This causes a change in the wavelength of diffracted light, a blue-shift, and is directly proportional to the number of protons generated, i.e. the quantity of methyl parathion. In practice, the difference was measured by the change in reflectance using a UV-Vis spectrophotometer, in contrast to the measurement of absorbance of PNP in other studies concerning detection of OP compounds. A detection limit of 0.2 μM for methyl parathion was observed (Walker et al. 2007).

Magnetoelastic sensors have come up as new advanced sensors which are based on substrates made of amorphous ferromagnetic materials which vibrate when subjected to an AC (alternating current) signal. The resultant magnetic flux can be easily sensed by means of an excitation coil and an acoustic wave that can be monitored over several meters. Furthermore, one can also visualize the vibration of the magnetoelastic strip by observing the attenuation of a laser beam reflected from its surface. Zourob et al., developed a sensor based on the magnetoelastic concept wherein OPH was dropped on a pH-sensitive polymer layer coated on the top of a ribbon of a magnetoelastic material. On interaction with the target analyte, the reaction between OPH and the OP compound would induce changes in pH, causing the polymer layer to swell, which changes the density and elasticity of the composite strip comprising of a

magnetoelastic material, polymer layer, and OPH. The result is a change in fundamental frequency. The sensor was found to have a detection limit of 0.1 μM for paraoxon and 0.85 μM for methyl parathion, respectively (Zourob et al. 2007a).

1.8.2 Organophosphorus Acid Anhydrolase (OPAA) sensors

Biosensors have been designed to use integrated enzymes, antibodies, cellular and DNA-based biosensors to detect pesticides.

1.8.2.1 Electrochemical

Electrochemical OPAA-based biosensors are based on the enzyme's activity to hydrolyze pesticides, leading to the generation of electroactive byproducts that generate a current upon oxidation. Electrochemical sensors are usually based on an electrochemical cell, in which the enzyme would be loaded on one of the electrodes. The electrodes are usually made out of materials with high carrier mobility and conductivity, such as graphite, glassy carbon, gold, or carbon. In the case of OPAA, OPs (such as methyl parathion or paraoxon) are the analytes introduced in specific concentrations into the electrolyte. The reaction of OPs with OPAA results in the formation of PNP, which gives a current when oxidized that serves as the response of the electrochemical sensor. In principle, electrochemical methods are preferred due to relative ease of use, convenience, and speed of analysis. Commonly, electrochemical sensors are of two types - amperometric i.e., current-based, and potentiometric i.e. voltage-based. Recently, Harvey and Wang et al. designed an electrochemical sensor with a solid contact ion-selective electrode and OPAA for the detection of DFP with a detection limit of 100 μM and a linear range of 250-3000 μM (Goud et al. 2020).

1.8.2.2 Optical sensors

Optical sensors generally involve a fluorescent or luminescent output that is readily viewable through an instrument or to the naked eye. A representative mechanism for using a fluorescence-based OPAA

biosensor is the quenching of fluorescence due to pH changes and the use of pH-sensitive fluorophores **(Fig. 1.11)**. Fluorescence-based sensors are considered attractive in the present day due to their simplicity and advantages in terms of sensitivity, selectivity, and convenience of use (Choi et al. 2014). On the other hand, colorimetric sensing methods have been part of the analytical toolkit for a long time, due to the obvious advantage of naked-eye visual monitoring and relatively rapid response to analytes (Xiao-wei et al. 2018). UV-vis spectroscopy, in addition to serving as a sensing tool, can provide useful insights into the chemistry of the analyte. In the upcoming sections, we shall discuss the main types of optical sensors encountered in the literature. Reports about the use of OPAA in the optical sensor to detect OPs are limited in the literature.

1.8.2.2.1 UV-Vis based sensors

In UV-vis-based detection, absorbance changes are observed against the analyte concentration. This method has mainly a cost and time advantage over the fluorescence-based method. The current research in this area focuses on the production of certain compounds during enzymatic hydrolysis of organophosphates, which are detectable under UV-vis spectroscopic analysis. In the year 1993, Luqi pei et al., determined OPAA in blood using a colorimetric method to develop a pioneered approach in which OPAA was encapsulated in erythrocytes. OPAA activity was determined with paraoxon as a substrate. The activity was reported based on the amount of liberation of PNP and diethyl phosphoric acid formed during the reaction. The detection limit was reported 0.01 mM of PNP (Pei et al. 1993). Contemporarily, Reynolds and group designed a sensing platform for pesticides based on OPAA immobilized on luminescent porous silicon devices, which could detect a minimum concentration of 25 µM of *p*-nitrophenyl-soman (Létant et al. 2005). Future research is expected to explore the synergistic effect of nanoparticles functionalized with enzymes to enhance the absorption characteristics and increase the sensitivity of the sensor.

1.8.2.2.2 Fluorescence-based sensors

In terms of OPAA, reports too far have been limited, and are inclined towards emission-based sensing. Earlier in 2003, Sarita V. Mello and group built a fluorescence-based biosensor in which they developed a Langmuir and Langmuir-Blodgett monolayer film of OPAA. One layer of OPAA was labeled with fluorescein isothiocyanate (FITC), a fluorescent probe. It was deposited onto the quartz slide and tested against DFP as a sensor. The stability of the Langmuir and Langmuir-Blodgett film as a sensor showed the potential of the system as a biosensor and a clear pronounced response was reported (Mello et al. 2003). Two protons and an alcohol are generated upon hydrolysis of the OP compound, which are often electroactive or chromophoric (Pedrosa et al. 2010; Kirsch et al. 2013). The two protons produced reduce the pH of the environment and thus drop the intensity of the FITC (Choudhary et al. 2019). There exist many opportunities in the development of fluorescent biosensors using the OPAA enzyme, either through the construction of fusion proteins with known fluorophores, or by immobilization into nanostructures with the desired optical properties (Li et al. 2016).

1.8.2.3 Other methods of sensing

Wild and coworkers reported two approaches to biosensor development using OPAA, based on pH changes during P-X bond hydrolysis by the enzyme. The first approach was based on covalent immobilization of OPAA on silica gel, which was used in batch measurements with a flat glass pH electrode in order to sense changes due to P-X cleavage. In the second approach, OPAA was immobilized to porous silica-modified gate insulator of a pH-sensitive field-effect transistor (FET), and the changes in current relative to a second transistor without the enzyme coating were compared in stop-flow mode. Both approaches were used for the detection of DFP, with the FET-based method displaying a better limit of detection (Simonian et al. 2001). In 2004, Simonian and his group invented a new approach of using a multi-enzyme strategy for the detection of various classes of neurotoxins based

on the substrate specificity of the enzymes. OPAA was used in a modified pH-sensitive field-effect transistor. Sensor response of DFP was reported and linear order kinetics was reported between 12.5 to 500 μM concentration of DFP whereas barely any measurable signals were reported in the case of paraoxon (Simonian et al. 2004). On the other hand, Marc-Michael Blum and coworkers developed an in-situ FTIR-based organophosphate detection platform using a related enzyme, DFPase, to detect DFP, GB, GD, and GF, with observed detection limits of 0.5, 0.54, 0.78, and 0.74 mM respectively (Gäb et al. 2009). Based on these results, it can be surmised that several methods of detection are possible, including fiber optic-based, potentiometric and impedance-based sensors.

1.9 Strategies to improve performance of enzymatic sensors

Though enzymes such as OPH and OPAA have great potential for developing as biosensors, their *in-vivo* functioning is quite different than that used in the laboratory and industrial settings. To improve the substrate specificity, various mutants have been created by site-directed mutagenesis in the active site(s) of OPH and OPAA. By altering specific residues of amino acids, the electrostatic interaction between the side chain and hydrogen bond can be disrupted that decrease the affinity towards the smaller substrate, and add flexibility for the larger molecules that enter into the active site (Theriot and Grunden 2011). In the rational design approach, researchers use structural data and crystal structures to identify portions of a compound that may be mutated specifically to obtain certain designed characteristics. Alternatively, in the directed evolution approach, libraries of mutant genes are created through means of gene recombination and/or random mutagenesis. These mutant genes are cloned into expression vectors and inserted into microbes for protein expression. The expressed proteins are then identified and screened to be used as templates for the next rounds of development (Johannes and Zhao 2006). Both rational design and directed evolution approaches have been used in contemporary literature to try and improve the specificity, activity, and stability of OPH and OPAA.

Schofield and Di Novo created 8 OPH mutants using site-directed mutagenesis, displaying immensely improved activity for the degradation of demeton s-methyl with a 24 times improvement in specificity and established a correlation between enzymatic activity for demeton s-methyl degradation and VX (Schofield and DiNovo 2010). Similarly, Gopal et al., described a rationally designed L136Y mutant of OPH, based on similarities in structure to AChE, which displayed a 33% increase in hydrolysis rates of VX compared to the wild-type enzyme (Gopal et al. 2000). On similar lines, Reeves et al., also created several mutants, two of which displayed 10 and 39 times greater activity for the degradation of VX compared to the wild-type enzyme. They postulated that substitutions of histidines at the 254^{th} and 257^{th} position in the wild-type OPH with arginine and phenylalanine residues, respectively, have a significant impact on the catalytic activity towards hydrolysis of P-S bonds, bringing the best balance between higher catalytic activity and uncompromised stability (Reeves et al. 2008). On the other hand, Jeong et al., used a rational design based on substrate docking simulation and studies on the structure of OPH to design a double mutant L271/Y309A which delivered a striking 150 fold increase in catalytic efficiency for VX compared to the wild-type protein (Tokuriki and Tawfik 2009).

To enhance the protein expression at the cell surface, Cho et al., altered the OPH enzyme obtained from *P. diminuta* to include a truncated ice nucleation motif, in which the mutagenized variants were screened by checking for hydrolysis activity and production of a byproduct, PNP. The first study yielded an enzyme 22A11, which was found to break down methyl parathion 25 times faster than wild-type OPH (Cho et al. 2002). This variant was then used as a template in directed evolution to create a new variant (Cho et al. 2004) B3561, which was able to hydrolyze chlorpyrifos at a rate of 750 times greater than wild-type OPH. It was also observed that these variants were able to perform faster hydrolysis of parathion and its metabolic byproduct, paraoxon. These studies identified three key mutations that affected the hydrolysis activity of OPH - A80V, I274N, and K185R. The other substitutions found in variants 22A11 and B3561 had led Cho et al., to believe that conformational changes led to a

wider active site, which improved catalytic turnover and efficiency (Cho et al. 2006). Naqvi et al., described a variant of OPH from *Agrobacterium radiobacter* with S308L/T309A substitutions in the substrate-binding pocket, which displayed over 5000-fold increase in activity towards degradation of malathion. They confirmed that widening of the active site of OPH was responsible for the enhanced activity (Naqvi et al. 2014).

Cherny et al., used iterative computational modeling to design variants of OPH which resulted in a 5000 fold increase in catalytic efficiency for detoxification of V-series of nerve agents (VE, VG, VM, VR, and VX) and also was effective for detoxification of G-series of nerve agents (GA, GB, GD, GF, and GV) (Cherny et al. 2013). In another study, DiSioudi et al., replaced the histidine at position 254 with arginine (H254R) and the one at position 257 with leucine (H257L) independently, as well as double mutation (H254R/H257L) in the OPH enzyme. Interestingly, these mutants of OPH possessed only two metals per dimer, as compared to four per dimer in native OPH. All three of these altered enzymes demonstrated a 2 – 30 fold increase in substrate specificity (kcat/Km) for demeton S (P−S bond), an analogue for the chemical warfare agent VX. Furthermore, two of the altered enzymes, H257L and H254R/H257L, showed an 11- and 18-fold increase, respectively, in specificity for NPPMP, the analogue for the chemical warfare agent soman (diSioudi et al. 1999).

Interestingly, to increase the solubility of OPH, Tokuriki et al., expressed OPH in a strain in which chaperonins are overexpressed, as they assist in the proper folding of proteins. Their experiments showed that OPH solubility is 2.4 times enhanced in the presence of overexpressed chaperonins. Similarly, a few novel cloning strategies were explored to express OPH on the cell surface to increase its access to the substrate and thereby enhancement in its activity (Tokuriki and Tawfik 2009). Towards this approach, a new anchor system based on the ice nucleation protein from *Pseudomonas syringae* INA5 was employed to display functional OPH on the cell surface of *Moraxella* sp. The OPH activity for this new cell was reported to be 80-fold higher than in *E. coli* and thus offers potential for greatly improved biosensor performance (Mulchandani et al.

2001b). Mulchandani et al. developed a fiber optic sensor based on OPH expressed on *E. coli* cell surface. This method allowed for developing a sensor without the need to purify OPH. The developed sensor displayed a detection limit of 3 μm for paraoxon and parathion **(Table 1.2.3)** (Mulchandani et al. 1998)

Attempts have similarly been made to enhance the properties of OPAA in terms of enzymatic hydrolysis and potential sensor applications. Latifi's group performed in silico docking studies to demonstrate the increased catalytic activity of two mutants of OPAA, namely 4ZWU and 4ZWP, and detailed the importance of amino acids at positions 342 and 212 for the small pocket of OPAA (Heidari et al. 2019). Steven Harvey's group reported enhanced activity on sarin, soman, and GP nerve agent using an OPAA FL mutant, which is based on mutations at the aforementioned 212 and 342 sites (Bae et al. 2018). The same group also reported the FL, FLY and FLYD variants of OPAA with increased stereospecificity and enhanced activity for the hydrolysis of Russian VX (Daczkowski et al. 2015). In comparison to OPH, OPAA is less well-studied and there is much scope to study mutations as well as develop functional applications of both the wild type and mutated enzyme. Attempts are ongoing to develop recombinant strains of *E. coli* with high levels of OPH and OPAA expression for industrial-grade applications (Yair et al. 2008).

1.10 Advantages of fluorescent sensors

Fluorescent sensors are considered to have traditional advantages in terms of sensitivity, fast response, easy operation, and detection in aqueous/liquid solutions with the possibility of in-vitro as well as in-vivo experiments (Gao and Tang 2017; Fan et al. 2019). Research groups have explored the use of fluorescent proteins, for example, in in-situ monitoring and high-throughput screening applications (VanEngelenburg and Palmer 2008). Fluorescent sensors also deliver the benefits of tunable excitation and emission wavelengths and surface modification flexibility, which are instrumental for the design of substrate-specific sensing platforms. Some

of the approaches used include the use of nanomaterials, fluorescent dyes, or proteins as the signaling element, with the molecular recognition done by another compound or protein/enzyme. The use of fluorophores is of particular importance for the development of biosensors, due to the nature of biologically-relevant media to experience changes in pH during the course of a reaction, which necessitates the requirement of a pH-sensitive method of detection. In the following section, some important fluorophores of interest will be discussed in detail.

1.10.1 Common fluorophores

The reaction of an OP-degrading enzyme, such as OPH or OPAA, with an OP compound, involves the production of PNP and the generation of protons, which contribute to the pH of the medium. This presents an opportunity to develop fluorescent biosensors that track the generation of protons and modulate the optical output based on the infinitesimal and gradual changes in pH over time. Commonly used fluorophores for such purposes fall into the fluorescein derivatives category, the anthracene dye family, boron-dipyrromethene (BODIPY) based dyes, benzoxanthene dyes, cyanine-based dyes, quantum dot nanomaterials, and fluorescent proteins (Han and Burgess 2010). In this thesis, however, the main fluorophores used are fluorescein derivatives and fluorescent proteins.

Fluorescein is a xanthene fluorophore prepared from the $ZnCl_2$-catalyzed synthesis of resorcinol-phthalein from phthalic anhydride and 1,3-dihydroxybenzene (Lee et al. 1997). It exists in an equilibrium between a “closed” lactone and an “open” quinoid form, leading to pH-dependent absorption and emission characteristics in a pH range of 5 to 9. A number of fluorescein derivatives are reported in the literature and have been used for various purposes involving imaging, biosensing, and bioconjugation. The sensing mechanism is usually based on the enhancement or decrease of fluorescence upon interaction with the target analyte. This property is based on the aforementioned equilibrium between the “closed” and “open” forms, with the “closed”, non-fluorescent form being more dominant with increased protonation (Rajasekar 2021).

Several derivatives of fluorescein have been reported in the literature with the optical properties being dependent on the structural changes in the derivatives (Zhang et al. 2014). In the literature, fluorescein and its derivatives have largely been utilized for metal-ion, bacterial, and amino acid sensing (Panchompoo et al. 2012; Hong et al. 2013; Hu et al. 2016; Yan et al. 2017; Ma et al. 2019).

Fluorescent proteins are responsible for the luminescence of marine creatures. Green fluorescent protein (GFP) from jellyfish *Aequorea victoria* was originally cloned in 1992 (Prasher et al. 1992), and its first use as a fluorescent tag for in vivo labeling was reported in 1994 (Chalfie et al. 1994). Subsequently, many GFP-like proteins were discovered in bioluminescent *Hydrozoa and Anthozoa* species. Fluorescent proteins make it possible to observe the localization, movement, turnover, and even aging of proteins, allow the labeling of nucleic acids, and the visualization of cell morphology and basic processes like fusion/fission, cell division, etc. Much like fluorescein, structural modifications incorporated either by mutagenesis or by protein engineering are able to tune the optical properties of the green fluorescent protein. Apart from GFP, other fluorescent proteins are also available like Blue fluorescent protein (BFP), Cyan fluorescent protein (CFP), monomeric teal fluorescent protein1 (mTFP1), Yellow fluorescent protein (YFP), Orange fluorescent protein (OFP), Red fluorescent protein (RFP), and Far-red fluorescent protein (FRFP). GFP derivatives like CFPs are super folder GFP derivatives (Pédelacq et al. 2006) created by site-directed mutagenesis. mTFP1 also belongs to the GFP family and mTFP1 is engineered by a 31 amino acid replacement from naturally tetrameric *Clavularia* CFP wild type (WT) protein, to address the limitations of CFPs (Ai and Campbell 2008). mTFP1 is 3 times brighter than enhanced CFP (ECFP) and about twice as bright as enhanced GFP (EGFP). mTFP1 has high photostability, pH stability, quantum yield, and maturation rate and does not interfere with the function or localization of its fusion partner (Ai et al. 2008). Currently, modified variants of fluorescent proteins exist to cover the entire visible light spectrum (Chudakov et al. 2010). In the current literature, fluorescent proteins are majorly used for biological labeling and

imaging purposes (Wiedenmann et al. 2009; Liu et al. 2020), and the analytical/sensing applications are less commonly evaluated.

1.11 Background work and objectives of the research work presented in this thesis

Agricultural advancements and the urge to increase crop production have led to excessive usage of insecticides and pesticides across many countries. This eventually, resulted in the leaching and accumulation of these highly toxic chemicals in soil, water, and food-chain. Organophosphorus (OP) compounds are the most commonly used insecticides and pesticides, which cause a wide range of long-lasting and life-threatening conditions.

Continuous or prolonged exposure of the OPs leads to the deposition of these compounds at the human organ depot sites, from where they are uninterruptedly released into the blood. Subsequently, from blood, they reach the nervous system where one of their targets is the AChE enzyme (Masson et al. 1998). In addition to AChE, these compounds target other enzymes like lipases and esterases that are crucial for the proper functioning of the human body. Due to acute toxicity and long-term side effects of OP compounds, their timely, on-the-spot, and rapid detection can be of great importance, for effective healthcare management.

In this respect, several OP degrading enzymes have gained the spotlight in developing enzyme-based biosensors, owing to their high activity and broad specificity. Among these enzymes, OPAA and OPH have emerged as a promising candidate for the detection of OP compounds, due to their ability to act on a broad range of substrates having a variety of bonds, like P-F, P-O, P-S, and P-CN, as well as chemical warfare agents and nerve agents (Kang et al. 2008). Enzymatic hydrolysis is reportedly 40-2450 times faster compared to chemical hydrolysis (Shimazu et al. 2003), and thus attracts great interest from a scientific viewpoint for the remediation as well as detection of organophosphorus compounds.

There are many reports in the literature, on the sensing of organophosphorus compounds using OPAA and OPH through electrochemical, optical, and other methods (Xiong et al. 2018). However, an optimal sensor that achieves good enzymatic catalytic activity and low enough detection limits to detect organophosphorus compounds remains elusive, primarily due to reproducibility and cost concerns. This study focuses on colorimetric, as well as fluorescence-based sensing by using a known fluorescent dye FITC and fluorescent protein, mTFP1 of organophosphorus compounds, by the interaction of OPAA and OPH with OP compounds such as methyl parathion and ethyl paraoxon.

Thus, the main objectives of the present thesis are defined as follows and are covered in three major objectives:

1. Expression and purification of recombinant organophosphorus acid anhydrolase (OPAA)-FL variant, organophosphorus hydrolase (OPH), and organophosphorus acid anhydrolase (OPAA)-FL-monomeric teal fluorescent protein1 (mTFP1) fusion protein in *E. coli*.

2. Development of recombinant OPAA-FL variant, OPH, and OPAA-FL-mTFP1 fusion protein-based biosensors for detection of OP compounds.

3. Detection and quantification of pesticides using the recombinant OPAA-FL-variant, OPH, and OPAA-FL-mTFP1 fusion protein-based biosensor.

The thesis additionally includes the research experience on encapsulation of recombinant enzymes and the effects of such encapsulation on the hydrolysis performance of OPs. The experimentations and contents of this thesis are envisioned to be of great importance for researchers working in the area of enzymatic biosensor development.

Chapter 2

Chapter 2

Materials, Methods, and Instrumentation

2.1 Materials

2.1.1 Primers and enzymes

All oligos used in this study were procured from Sigma Aldrich Pvt. Ltd. **(Appendix B)**. All restriction enzymes used were purchased from New England Biolabs and Fermentas (Thermo Fisher).

2.1.2 Cloning vectors and competent cells

The bacterial cloning and expression vectors used are pET28a and pET43a vector (Novagen) containing a T7 promoter. Bacterial competent cells used were *E. coli* DH5α and Rosetta (DE3) cells **(Appendix A)**.

2.1.3 *E. coli* strains

An *opd* gene construct was received from Prof. D. Siddavattam (Dept. of Animal Biology, School of Life Sciences University of Hyderabad, Hyderabad-500046, India). In this study, an OPH gene without signal peptide was used. The *E. coli* cells, DH5α and Rosetta, were used as host cells and pET43a and pET28a vector (Novagen) were used for cloning and expression of OPH.

LB/ Amp plate streaked with OPAA FL was obtained from Prof. Steven Harvey, U.S. Army Edgewood Chemical Biological Center, MD, 21010-5424, USA.

2.1.4 Chemicals

The chemical agent used are: Trizma base, Glycine ($C_2H_5NO_2$), Ethylene diamine tetra acetic acid (EDTA), Sodium hydrogen phosphate (Na_2HPO_4), Sodium dihydrogen phosphate (NaH_2PO_4), Ethidium bromide

(EtBr), Manganese chloride ($MnCl_2$), Sodium chloride (NaCl), Cobalt chloride ($CoCl_2$), Calcium chloride ($CaCl_2$), Sodium hydroxide (NaOH), Sodium dodecyl sulphate or Sodium lauryl sulphate (SDS), Commassie brilliant blue G-250, β-mercaptoethanol ($HOCH_2CH_2SH$), Agarose, Luria-Bertani agar (LB-agar), Luria-Bertani broth (LB-broth), Ampicillin, Chloramphenichol, Kanamycin, Acrylamide (C_3H_5NO), *N, N′*-Methylene bisacrylamide (MBAA), Triethylenetetramine or Tetramethylethylene diamine (TEMED), Ammonium per sulphate ($(NH_4)_2S_2O_8$), bromophenol blue or 3′,3″,5′,5″-tetrabromophenol sulfonphthalein ($C_{19}H_{10}Br_4O_5S$), Bovine serum albumin (BSA), Isopropyl-β-D-thiogalactopyranoside ($C_9H_{18}O_5S$), Imidazole ($C_3H_4N_2$), Triton X-100 $C_{14}H_{22}O(C_2H_4O)_n$, Glycerol ($C_3H_8O_3$), RNase A, Methanol (CH_3OH), Glacial acetic acid (CH_3COOH), Ethanol (C_2H_5OH), Protease inhibitor cocktail, Bradford reagent, Lysozyme. Ethyl paraoxon ($O_2NC_6H_4OP(O)(OCH_5)_2$, Methyl parathion ($C_8H_{10}NO_5PS$), alginic acid sodium salt from brown algae or Sodium alginate and Fluorescein isothiocyanate-dextran 500 kDa, 1,3 Bis[tris(hydroxymethyl)methylamino]propane (Bis-Tris propane) $C_{11}H_{26}N_2O_6$, 2-(Cyclohexylamino)ethanesulfonic acid (CHES) ($C_8H_{17}NO_3S$).

All chemicals were of molecular biology grade and procured from different manufacturers like Sigma Aldrich Chemical Pvt. Ltd., Invitrogen Pvt. Ltd., MP Biomedical USA, Himedia Pvt. Ltd. India, Alfa Aesar Pvt. Ltd., Sisco Research Lab Pvt. Ltd. India, and Otto. Chemie Pvt. Ltd.

2.1.5 Reagents and Kits

Plasmid isolation kit, Gel extraction kit, and PCR purification kit were purchased from Thermo Fisher Scientific, USA, and Favorgen Biotech Corporation, Taiwan.

T4 DNA ligase10X Buffer with Mg^{++}, Deoxyribonucleoside triphosphates (dNTPs), *Taq* DNA Polymerase, Q5 DNA polymerase, *Nde*I, *Xho*I, *BamH*I, *Spe*I, 100bp DNA ladder, 1kb DNA ladder, unstained protein marker, prestained protein marker, were purchased from New England Biolabs, USA.

Dithiothreitol, dNTP mix, was purchased from Invitrogen Pvt. Ltd. Ni-NTA columns and Amicon ultra were purchased from GE Healthcare.

2.2 Methods and Instrumentation

2.2.1 *E. coli* competent cell preparation

Competent cells were prepared by using 0.1 M $CaCl_2$ solution. *E. coli* was grown on LB Agar plates and single colonies from overnight grown culture were transferred to LB broth medium. Cells were incubated in a bacterial incubator shaker at 250 rpm and 37 °C. After reaching optical density (OD) 0.45 at 600 nm, cells were treated with 0.1 M $CaCl_2$ solution and incubated for 45 min and then for 4 hrs on ice. Competent cells were stored in 15 % glycerol from 50 % stock solution.

2.2.2 Transformation of *E. coli* competent cells

E. coli strains DH5α were transformed with a gene construct. For each transformation, 10-50 ng of DNA were added to 200 µl of chemically competent cells and incubated on ice for 30 min followed by heat shock at 42 °C for 90 sec in a water bath and incubated on ice for 2 min. The cells were allowed to recover in 1 ml Luria-Bertani broth (LB broth: 1 % Bacto-Tryptone, 1 % NaCl, and 0.5 % Bacto-Yeast extract) and then incubated for 90 min at 37 °C in a water bath. Cells were plated on a LB-agar plate containing appropriate antibiotic (ampicillin, 100 µg/ml, or kanamycin, 20 µg/ml) and incubated at 37 °C overnight in a bacterial incubator to select the transformants.

2.2.3 Plasmid DNA isolation

Plasmid DNA was isolated from transformed cells by using Gene JET Plasmid Miniprep Kit (Thermo Scientific) and Plasmid isolation Miniprep kit (Favorgen). The isolated single colony from transformed cells was inoculated in 5 ml LB broth containing appropriate antibiotics and incubated at 250 rpm at 37 °C for overnight. Resuspension buffer was added to the overnight grown culture. Cells were lysed by lysis solution and neutralization buffer was added. After centrifuge, the upper aqueous

layer was collected in a spin column and washed by washing solution. Plasmid DNA was eluted by using elution buffer and stored at 4 °C.

2.2.4 Polymerase chain reaction

Gene sequences were amplified from genomic DNA by using PCR. Plasmid DNA was used as a positive control. A PCR reaction mixture of 20-50 µl containing 10X PCR Buffer with Mg^{++}(NEB), 2 mM dNTPs (Invitrogen), Primers (Forward and Reverse), *Taq* DNA Polymerase or Q5 DNA Polymerase (NEB). The thermal cycle was programmed for 5 min at 95 °C as initial denaturation, followed by 30 cycles of 30 sec at 92 °C for denaturation, annealing temperature based on primer, extension based on template size, and a final extension at 72 °C for 10 min.

2.2.5 Agarose gel electrophoresis

Gene sequences amplified by PCR were confirmed by using 0.7 % Agarose in 0.5X TAE Buffer. Ethidium bromide was added to the gel of 100 µg/ml from the stock concentration. Samples were loaded with 6X Loading Dye. 1 Kb DNA ladder and 100 bp DNA Ladder were used as a standard. Bands were visualized using a UV transilluminator and images were taken by Image Quant (GE Healthcare).

2.2.6 PCR purification

The PCR amplified product was purified by a PCR purification kit (Thermo scientific). Further, PCR purified DNA fragment was checked on agarose gel electrophoresis. PCR purified DNA was stored at -20 °C and used for cloning.

2.2.7 Restriction digestion

Appropriate amounts of plasmid DNA as a vector, and PCR product as an insert, were mixed with sterile ddH_2O to a final volume of 50 µl. Further, 10X CutSmart buffer was added in a 1X dilution. Finally, the mixture was supplemented with 1U of restriction enzyme per µg of DNA. Digestion was carried out for 1-2 hrs for plasmid DNA and PCR products at an appropriate temperature as recommended by the manufactures in a water

bath. The samples were gel electrophoresed and gel purified as described below.

2.2.8 Gel extraction

Restriction digested product of respective DNA fragment were gel eluted by Gel extraction kit (Thermo scientific). The eluted DNA fragment was further checked on agarose gel electrophoresis. Eluted DNA was stored at -20 °C and used for cloning with respective insert DNA.

2.2.9 Ligation

For a ligation reaction, the following solution was mixed in an appropriate molar ratio (linearized purified vector DNA: a purified insert DNA), 1 µl of 10X T4 DNA ligase buffer, 1 µl of T4 DNA ligase (NEB) to the total volume of 10 µl. Ligation control was without the insert DNA. The ligation mixture was incubated at 24 °C for 1 hr. 2-5 µl of ligation mixture and ligation control were used for transformation.

2.2.10 Cloning of OPH, OPAA-FL- variant, and OPAA-FL-mTFP1 in the pET expression vector

OPH, OPAA-FL-variant, and OPAA-FL-mTFP1 were cloned in appropriate pET expression vectors with respective restriction enzymes and DNA ligase as described below.

2.2.10.1 Cloning of OPAA-FL-variant with N- terminal His tag in pET28a expression vector

OPAA-FL -variant was cloned into pET28a expression vector by using *Nde*I and *BamH*I site with N-terminal 6X His tag. OPAA-FL-variant was amplified from the pSE420-OPAA-FL vector using primers PK702F and PK706R **(Appendix B)**, and *Pfu* DNA Polymerase. (Sigma Aldrich, USA). Thermal cycles were programmed for 2 minutes as initial denaturation, followed by 30 cycles of 30 seconds at 95 ºC for denaturation, 30 seconds at 59 ºC as annealing temperature, 2 minutes at 72 ºC for the extension, and a final extension at 72 ºC for 10 minutes. The resultant PCR product is 1320 bps and a clone was obtained with a size of

6649 bps. Insert and vector DNA were both double digested by *Nde*I and *BamH*I restriction enzymes. The vector and insert DNA were ligated in a 1:4 molar ratio, followed by the transformation of ligated samples into DH5 α cells. The presence of insert DNA in the plasmid construct was confirmed by colony PCR, further recombinant plasmids were isolated from the replica plates and then sequenced by Sanger sequencing (Eurofins). Recombinant clones designated as p28-His-OPAA-FL were then transformed into *E. coli* Rosetta (DE3) cells.

2.2.10.2 Cloning of OPH with N- terminal His tag in pET28a expression vector

OPH was cloned into pET28 expression vector by using *Nde*I and *Xho*I site with N-terminal 6X His tag. OPH was amplified by using *Pfu* DNA polymerase and primers PK671F and PK673R **(Appendix B)** (Sigma Aldrich, USA). Thermal cycles were programmed for 2 minutes as initial denaturation, followed by 30 cycles of 30 seconds at 95 ºC for denaturation, 30 seconds at 59 ºC as annealing temperature, 90 seconds at 72 ºC for the extension, and a final extension at 72 ºC for 10 minutes. The resultant PCR product is 1011 bps and a clone was obtained with a size of 6300 bps. Insert and vector DNA were both double digested by *Nde*I and *Xho*I restriction enzymes. The vector and insert DNA were ligated in a 1:4 molar ratio, followed by the transformation of ligated samples into DH5 α cells. The presence of insert DNA in the plasmid construct was confirmed by colony PCR, further recombinant plasmids were isolated from the replica plates and then sequenced by Sanger sequencing (Eurofins). Recombinant clones designated as p28-His-OPH were then transformed into *E. coli* Rosetta (DE3) cells.

2.2.10.3 Sequential cloning of OPH in pET43 and pET28 with N-terminal His tag and NusA tag

Briefly, OPH was initially cloned into pET43 by using *Spe*I and *Xho*I site with N-terminal NusA tag, with preScission protease site in between NusA tag and OPH to generate p43-Nus-OPH (8023 bps). Subsequently, the

Nus-OPH fragment was released using *Nde*I and *Xho*I sites and cloned into the pET28 expression vector to generate an N-terminal His-NusA tag. OPH was amplified by using *Pfu* DNA polymerase and primers PK672F and PK673R **(Appendix B)** and cloned into plasmid pET43. Thermal cycles were programmed for 5 minutes as initial denaturation, and subsequently 30 cycles of 30 seconds for denaturation at 95 ºC, 30 seconds at 73 ºC as annealing temperature, 90 seconds at 72 ºC for the extension, and a final extension at 72 ºC for 10 minutes. The resultant PCR product of the *oph* gene is 1011 bps. Insert and vector DNA were both double digested by using *Spe*I, *Xho*I restriction enzymes, and cloned into pET43 vector. Later, the Nus-OPH fusion gene fragment was excised using *Nde*I and *Xho*I sites, and cloned into pET28 vector, to generate p28-His-Nus-OPH (7819 bps). The presence of insert DNA in the plasmid construct was confirmed by colony PCR, recombinant plasmids were isolated from the replica plates and then sequenced by Sanger sequencing (Eurofins). Recombinant clones were then transformed into *E. coli* Rosetta cells.

2.2.10.4 Sequential cloning of OPAA-FL-variant with N- terminal His tag and C- terminal mTFP1 in pET28a expression vector

OPAA-FL -variant was cloned into pET28a expression vector by using *Nde*I and *BamH*I site with N-terminal 6X His tag. OPAA-FL-variant was amplified from the Hp28FLS1 vector using primers PK702F and PK765R **(Appendix B)**, and *Pfu* DNA Polymerase. (Sigma Aldrich, USA). Thermal cycles were programmed for 2 minutes as initial denaturation, followed by 30 cycles of 30 seconds at 95 ºC for denaturation, 30 seconds at 59 ºC as annealing temperature, 2 minutes at 72 ºC for the extension, and a final extension at 72 ºC for 10 minutes. The resultant PCR product is 1320 bps and a clone was obtained with a size of 6649 bps. Insert and vector DNA were both double digested by *Nde*I and *BamH*I restriction enzymes. The vector and insert DNA were ligated in a 1:4 molar ratio, followed by the transformation of ligated samples into DH5 α cells. The presence of insert DNA in the plasmid construct was confirmed by colony PCR, further recombinant plasmids were isolated from the replica plates

and then sequenced by Sanger sequencing (Eurofins). Recombinant clone designated as p28-His-OPAA-FL.

To sequentially clone mTFP1 at C-terminal, p28-His-OPAA-FL was used as a vector by using *BamH*I and *Not*I sites. mTFP1 was amplified from pcDNA3.1-mTFP1 clone using primers PK762F and PK780R **(Appendix B)**, and *Pfu* DNA Polymerase. (Sigma Aldrich, USA). Thermal cycles were programmed for 2 minutes as initial denaturation, followed by 30 cycles of 30 seconds at 95 ºC for denaturation, 30 seconds at 50 ºC as annealing temperature, 1.30 minutes at 72 ºC for the extension, and a final extension at 72 ºC for 10 minutes. The resultant PCR product is 711 bps and a clone was obtained with a size of 7328 bps. Insert and vector DNA were both double digested by *BamH*I and *Not*I restriction enzymes. The vector and insert DNA were ligated in a 1:3 molar ratio, followed by the transformation of ligated samples into DH5 α cells. The presence of insert DNA in the plasmid construct was confirmed by colony PCR, further recombinant plasmids were isolated from the replica plates and then sequenced by Sanger sequencing (Eurofins). Recombinant clone designated as p28-His-OPAA-FL-TFP was then transformed into *E. coli* Rosetta (DE3) cells.

2.2.10.5 Cloning of mTFP1 with N- terminal His tag in pET28a expression vector

mTFP1 was cloned into pET28 expression vector by using *Nde*I and *Xho*I site with N-terminal 6X His tag. mTFP1 was amplified by using *Pfu* DNA polymerase and primers PK810F and PK763R **(Appendix B)** (Sigma Aldrich, USA). Thermal cycles were programmed for 2 minutes as initial denaturation, followed by 30 cycles of 30 seconds at 95 ºC for denaturation, 30 seconds at 50 ºC as annealing temperature, 1.30 minutes at 72 ºC for the extension, and a final extension at 72 ºC for 10 minutes. The resultant PCR product is 711 bps and a clone was obtained with a size of 6000 bps. Insert and vector DNA were both double digested by *Nde*I and *Xho*I restriction enzymes. The vector and insert DNA were ligated in a 1:3 molar ratio, followed by the transformation of ligated samples into

DH5 α cells. The presence of insert DNA in the plasmid construct was confirmed by colony PCR, further recombinant plasmids were isolated from the replica plates and then sequenced by Sanger sequencing (Eurofins). Recombinant clone designated as p28-His-mTFP1 was then transformed into *E. coli* Rosetta (DE3) cells.

2.2.11 Expression of recombinant OPH, OPAA-FL, OPAA-FL-mTFP1 and mTFP1 proteins

A single colony of *E. coli* Rosetta transformed recombinant clone was inoculated into a 5 ml LB tube containing appropriate antibiotic (Kanamycin 10 µg/ml or Ampicillin 100 µg/ml) working concentration and was incubated at 37 °C and 200 rpm for 10-12 hrs, followed by re-inoculation of 50 µl overnight grown culture into a fresh 5 ml LB tube with appropriate antibiotic and incubated at 37 °C and 200 rpm for 2 to 3 hours till OD 600 reached 0.8. This culture was then induced with 0.1 mM IPTG and 0.1 mM $CoCl_2$ for all recombinant clones of OPH and 1 mM IPTG and 1 mM $MnCl_2$ for recombinant clones of OPAA-FL variant and 0.1 mM IPTG for recombinant clones of OPAA-FL-mTFP1 and mTFP1 and incubated at 180 rpm, with the conditions set at 37 °C/3 and 16 °C/16 hours for p28-His-OPH, and p28-His-Nus-OPH, 20 °C/20 hours for p28-His-OPAA-FL variant, p28-His-OPAA-FL-mTFP1 and p28-His-mTFP1. Subsequently, the cells were harvested at 10000 rpm at 4 °C for 10 minutes. The resultant pellet was washed and resuspended with 50 mM Tris-Cl (pH 7.4) with 10% glycerol. Afterwards, Lysozyme was added to a final concentration of 100 µg/ml and then incubated at 30 °C for 20 minutes, followed by sonication and centrifugation of cell lysate at 14000 rpm and 4 °C for 10 minutes. The lysate was then analysed on 8% SDS-PAGE (Sodium dodecyl sulphate polyacrylamide gel electrophoresis) for p28-His-Nus-OPH and on 12 % SDS-PAGE for p28-His-OPH, p28-His-OPAA-FL, p28-His-OPAA-FL-mTFP1, and p28-His-mTFP1.

2.2.12 Purification of recombinant OPH, OPAA-FL-variant, OPAA-FL-mTFP1 and mTFP1 proteins

All affinity chromatography steps (Ni NTA column) were performed at 4 °C using His-trap Ni-column (GE) with AKTA Unichromat 1500. After expression, the concentration of components in the input sample for purification was made equivalent to the equilibration buffer (50 mM Tris-Cl pH 8.0, 500 mM NaCl, and 10 mM imidazole). This input sample was loaded on a pre-equilibrated column at a flow rate of 1ml/minute. Subsequently, the column was washed with wash buffers comprising of 50 mM Tris-Cl pH 8.0 and 500 mM NaCl, with 50 mM and 90 mM imidazole for OPH and only with 50 mM imidazole for OPAA-FL variant, 30 mM and 50 mM imidazole for OPAA-FL-mTFP1 and only with 50 mM imidazole for mTFP1. The expression level of the 6X His tagged protein chiefly determines the number of wash steps required for a high level of purification. The sample was then eluted using elution buffer comprising of 50 mM Tris-Cl pH 8.0, 500 mM NaCl, and a fixed concentration of imidazole, i.e. with 150 mM imidazole for recombinant clones of OPH, OPAA-FL-variant, OPAA-FL-mTFP1, and mTFP1 clones. All fractions were analysed on SDS-PAGE.

2.2.13 Buffer exchange and concentration of the purified OPH, OPAA-FL-variant, OPAA-FL-mTFP1, and mTFP1 recombinant proteins

The purified protein was in 500 mM NaCl, 50 mM Tris-Cl of pH 8.0, and a fixed concentration of imidazole i.e. 150 mM for OPH, OPAA-FL variant, OPAA-FL-mTFP1, and mTFP1. It was then buffer exchanged and concentrated to 500 mM NaCl, 50 mM Tris-Cl of pH 8.0 with 15 mM Imidazole for OPH, and 50 mM NaCl, 50 mM Tris-Cl of pH 8.0 with 15 mM Imidazole for OPAA-FL-variant and OPAA-FL-mTFP1 and mTFP1. The purified protein was loaded (500 µl) into the amicon and centrifuged at 4000 g until the volume of the protein in the amicon reached 10 times lesser (50µl) than the loaded protein. The volume was again made up to the

initial volume using 50 mM Tris-Cl of pH 8.0 and 500 mM NaCl for OPH and 50 mM Tris-Cl of pH 8.0 and 50 mM NaCl for OPAA-FL-variant, OPAA-FL-mTFP1, and mTFP1 recombinant proteins. Amicons were again centrifuged at 4000 g until the volume was reduced to 10 times lesser than the initial volume. In the collection tube, amicon was inverted and centrifuged at 1000 g for 2 minutes for the collection of the desalted and concentrated sample. The temperature was maintained at 4° C throughout the procedure of buffer exchange and concentration. The buffer exchanged and concentrated proteins were then collected in a fresh autoclaved microcentrifuge tube and tested for its activity against OPs.

2.2.14 SDS-PAGE for recombinant OPH, OPAA-FL-variant, OPAA-FL-mTFP1 and mTFP1 proteins

Before purification, the cell pellet was dissolved in 50 mM Tris-Cl, pH-7.4, with 10% glycerol and treated with 100 µg/ml (final concentration) lysozyme for 20 min at 30 °C in a water bath followed by sonication of cell lysate. Lysed and the purified protein was mixed with 5X sample loading buffer (10% SDS, 0.05 M β mercapto-ethanol, 0.25 M Tris-Cl pH 6.8, 50 % glycerol, 0.5 % bromophenol blue), and boiled at 95 °C. Proteins were separated on an 8 % and 12 % SDS-PAGE gel in a mini protean tetra cell (Bio-Rad).

2.2.15 Activity assay of the recombinant proteins

2.2.15.1 Activity assay of the recombinant OPH protein

To perform OPH assay, 1µl of purified protein was mixed with 50 mM CHES [2-(N-cyclohexyl amino) ethane-sulfonic acid] buffer, pH 9.0, 0.1 mM $CoCl_2$, 1 mM methyl parathion and/or ethyl paraoxon (Sigma), and final volume was made up to 200 µl with SDW. A blank sample was made similarly except that methyl parathion and/or ethyl paraoxon were not added. The reaction mixtures were incubated at 37 ºC for 5 minutes in the case of solution-phase His-Nus-OPH, 10 minutes for encapsulated His-Nus-OPH with ethyl paraoxon, and 20 minutes for encapsulated His-Nus-OPH with methyl parathion. The activity was calculated by measuring the

absorbance of PNP produced due to the hydrolysis of methyl parathion and/or ethyl paraoxon at 400nm (ε400 = 17,000/M/cm for PNP (Cheng et al. 1996) by using a plate reader (SYNERGY H1 microplate reader). Specific activities were expressed as units (micromoles of methyl parathion and/or ethyl paraoxon hydrolyzed per minute) per milligram of total protein.

Enzymatic activity of encapsulated OPH protein was also performed in a similar manner by taking 330 µl encapsulated protein and making up to 500 µl.

The kinetic parameters of solution phase and encapsulated His-Nus-OPH with ethyl paraoxon and methyl parathion were determined using substrate concentrations of 0.1 to 9 mM. kinetic parameters for ethyl paraoxon and methyl parathion substrate (k_{cat}, K_m, V_{max}, k_{cat}/K_m) were calculated following the method described in previously published literature (Robinson 2015).

2.2.15.2 Activity assay of the recombinant OPAA-FL-variant and OPAA-FL-mTFP1 protein

1 µl of cell lysate or purified OPAA-FL-variant protein was mixed with 50 mM Bis-Tris propane buffer, pH 8.5, 1 mM methyl parathion and/or ethyl paraoxon (Sigma), 1 mM $MnCl_2$, and the final volume was made up to 200 µl with SDW and the reaction was incubated at 50 °C for 15 minutes. Similarly, to check the activity of OPAA-FL-mTFP1 on ethyl paraoxon, 1 µl of cell lysate or purified OPAA-FL-mTFP1 protein was mixed with Bis-Tris propane buffer, pH 8.5, 1 mM $MnCl_2$ was used at 65 °C for 15 minutes. A blank sample was made similarly except that methyl parathion and/or ethyl paraoxon were not added. OPAA-FL-variant and OPAA-FL-mTFP1 enzyme activity was calculated by measuring the increase in absorbance of PNP formed at 400 nm using extinction coefficient 17,000 M/cm for PNP (Hill et al. 2000). Specific activity was calculated as U/mg.

Enzymatic activity of encapsulated OPAA-FL-variant protein was also performed in a similar manner by taking 330 µl encapsulated protein and making up to 500 µl.

2.2.16 Effect of temperature and pH on the activity of recombinant OPH and OPAA-FL and OPAA-FL-mTFP1 proteins

To determine the optimal temperature for His-Nus-OPH with ethyl paraoxon, its activity at varying temperatures ranging from 20 to 45 ºC for 10 minutes, in 50 mM CHES buffer, pH 9.0, 0.1 mM $CoCl_2$, and 1 mM ethyl paraoxon was tested. To know the optimum temperature for OPAA-FL-variant and OPAA-FL-mTFP1 with ethyl paraoxon, its activity at various temperatures between 20 to 60 ºC and 30 to 80 ºC respectively for 15 minutes, in 50 mM Bis-Tris propane buffer, pH 8.5, 1 mM ethyl paraoxon, and 1 mM $MnCl_2$ was tested. To determine the pH optima for His-Nus-OPH with ethyl paraoxon, the activity tests were performed at a pH range of 6 – 10, at 37 ºC for 10 minutes, in either 50 mM sodium phosphate buffer (pH 6.0, 6.5, 7.0, 7.5 and 8.0, respectively) or 50 mM CHES buffer (pH 8.5, 9.0, 9.5 and 10.0, respectively), 0.1 mM $CoCl_2$, and 1 mM ethyl paraoxon. To know the optimum pH for OPAA-FL variant and OPAA-FL-mTFP1 with ethyl paraoxon, we tested its activity at various pH between 6 – 10, at 50 ºC and 65 ºC respectively for 15 minutes, in either 50 mM phosphate buffer (pH 6.0, 6.5, 7.0, 7.5 and 8.0, respectively) or 50 mM Bis-Tris propane buffer (pH 8.5, 9.0 and 10.0, respectively), 1 mM ethyl paraoxon and 1 mM $MnCl_2$. Enzymatic activity assays were performed similarly as described in the above section.

2.2.17 Encapsulation of recombinant OPH and OPAA-FL-variant proteins in alginate microspheres using an ultrasonic atomizer

Proteins (His-Nus-OPH, 0.2 to 0.65 mg/ml and OPAA-FL-variant 0.7 to 0.8 mg/ml) were encapsulated in 0.7% sodium alginate microspheres formulated via ionic gelation technique by using 4% calcium chloride to form Calcium alginate microspheres. The protein alginate mixtures were sprayed using an ultrasonic atomizer (Sonozap, USA) at optimized

instrumental parameters like frequency 130 kHz and 3.5 Watt of power with the flow rate of 0.3 ml/min using a syringe pump (Multi-phaserTM, model NE-300, New Era pump system, USA) and collected in 40 ml 4% w/v calcium chloride stirred on a magnetic stirrer at 1500 rpm. Particles prepared were separated using a refrigerated high-speed centrifuge (Kubota-7000, Japan) at 7000 X, after three washing cycles of 15 minutes. FITC dextran (1 mg)/His-Nus-OPH (0.5 mg) was encapsulated in alginate (0.7% w/v) microspheres formed by ionic gelation technique using an ultrasonic atomizer with optimized instrumental parameters as described above using 4% w/v calcium chloride as a crosslinker. FITC dextran (1 mg) was separately encapsulated in alginate (0.7% w/v) microspheres by the same technique to act as a control. Both dye-loaded particles and co-immobilized particles prepared were separated using a refrigerated high-speed centrifuge (Kubota-7000) at 7000 X, after three washing cycles of 15 minutes.

2.2.18 Characterization of microspheres and encapsulation efficiency of recombinant OPH and OPAA-FL-variant proteins

Morphological characterization was done by scanning electron microscopy (SEM) using a Zeiss Supra 55 (Germany) machine. A thin layer of microspheres was evenly spread onto the glass slide. The slide was kept on the desiccator for 3 hours in which silica adsorbed all the moisture present in the sample. The sample was coated with copper metal (Q150R Rotary-pumped sputter coater/ carbon coater) and observed at an operating voltage of 5 kV. Alginate encapsulated FITC-Dextran and FITC-Dextran/His-Nus-OPH high-resolution images were taken at 60 X magnification using a confocal laser scanning microscope (CLSM) (FluoView 1000, Olympus America Inc. USA). The fluorescence excitation and emission wavelengths were selected as 488 nm and 520 nm, respectively. Particle size distribution measurements were performed using ImageJ software. (Dhirhi et al. 2016). To confirm encapsulation of His-Nus-OPH and OPAA-FL variant, beads were boiled at 95 °C for 15 minutes and then loaded on the 8% and 12% SDS-PAGE, respectively.

2.2.19 Colorimetric bio-sensing studies of organophosphates with recombinant OP degrading enzymes

Colorimetric biosensing of ethyl paraoxon and methyl parathion in solution phase was performed by mixing His-Nus-OPH fusion protein with 50 mM CHES buffer, pH 9.0, 0.1 mM $CoCl_2$, and incubating at 37 °C for 5 minutes. On the other hand, for encapsulated protein, enzymatic activity was also performed in a similar manner that is, incubating at 10 minutes for His-Nus-OPH encapsulated alginate microspheres with ethyl paraoxon and 20 minutes for methyl parathion. The His-Nus-OPH enzyme activity was calculated by introducing different concentrations of ethyl paraoxon and methyl parathion (0.005 - 1 mM) and measuring the increase in absorbance of PNP formed at 400 nm using extinction coefficient 17,000 M/cm for PNP.

Colorimetric biosensing of ethyl paraoxon was performed by mixing OPAA-FL- variant protein or protein-containing alginate microspheres with 50 mM Bis-Tris propane buffer, pH 8.5, 1 mM $MnCl_2$ and incubating at 50 °C for 15 minutes. OPAA-FL-variant enzyme activity was calculated by exposing different concentrations of ethyl paraoxon (0.01 - 1 mM) for purified OPAA-FL variant and (0.025 - 1 mM) for encapsulated OPAA-FL variant and measuring the increase in absorbance of PNP formed at 400 nm using extinction coefficient 17,000 M/cm for PNP. For OPAA-FL-mTFP1, colorimetric biosensing of ethyl paraoxon was performed by mixing purified OPAA-FL-mTFP1 protein with 50 mM Bis-Tris propane buffer, pH 8.5, 1 mM $MnCl_2$ and incubating at 65 °C for 15 minutes. OPAA-FL-mTFP1 enzyme activity was calculated by exposing different concentrations of paraoxon (0.005 - 1 mM) and measuring the increase in absorbance of PNP formed at 400 nm using extinction coefficient 17,000 M/cm for PNP. Limits of detection and sensitivity values were calculated as per the standard practice (Arshak and Gaidan 2005; Yin and Guo 2014; Nieuwoudt et al. 2016)

2.2.20 Fluorometric bio-sensing studies of organophosphates with recombinant OP degrading enzymes

Fluorometric biosensing assay comprised of His-Nus-OPH fusion protein and FITC-dextran (1 mg/ml) which were mixed in ratio 1:12 (w/w) in solution phase. Initially, a solution comprising of His-Nus-OPH, sterile distilled water, and 0.1 mM $CoCl_2$ was prepared. Subsequently, FITC-dextran and ethyl paraoxon (0.001- 0.5 mM) / methyl parathion (0.005-0.5 mM) were added to the mixture and the volume was made up to 1 ml. A blank sample was made in a similar way except that ethyl paraoxon/methyl parathion was not added. The reaction mixture was incubated for 5 minutes at 37 °C, and the decrease in the fluorescence intensity was recorded at 488 nm excitation and 519 nm emission by using a fluorimeter (Horiba Fluoromax 4, Japan). Fluorescence changes in response to the catalytic activity of His-Nus-OPH in the solution phase were observed to evaluate the performance of His-Nus-OPH for the detection of OP compounds (Cao et al. 2004).

Fluorometric biosensing assay comprised of OPAA-FL-variant protein and FITC-dextran (1 mg/ml) were mixed in six ratios 0.25:1, 0.5:1, 0.75:1, 1:1, 3:1 and 5:1, respectively (w/w, 20 ug of OPAA-FL and FITC-dextran for 1:1 ratio). Initially, a solution comprising of OPAA-FL, sterile distilled water, and 1 mM $MnCl_2$ was prepared. Subsequently, FITC-dextran and ethyl paraoxon (0.1 mM - 1 mM) was added to the mixture of OPAA-FL-variant protein, and the volume was made up to 1 ml. A blank sample was made in a similar way except that ethyl paraoxon was not added. The reaction mixture was incubated for 5 minutes at 50 °C, and the decrease in the fluorescence intensity was recorded. Fluorescence excitation of FITC was performed at 488 nm, and emission was measured at 519 nm.

A temperature optimization experiment for OPAA-FL-mTFP1 was performed, taking the temperature range from 25 to 70 °C. OPAA-FL-mTFP1 protein was mixed with 1 mM $MnCl_2$, and the volume was made up to 1 ml with sterile distilled water. The reaction mixture was incubated for 5 minutes from 25 to 70 °C, and the decrease in the fluorescence intensity was recorded. Fluorescence excitation of mTFP1 was performed

at 462 nm, and emission was measured at 491 nm. In each of these experiments, the average of at least three separate repetitions was considered.

For fluorometric biosensing assay of OPAA-FL-mTFP1 fusion protein, initially, a solution comprising of 25 mM Bis-Tris-Propane buffer pH 8.0, 1 mM $MnCl_2$, and sterile distilled water was prepared. Subsequently, OPAA-FL-mTFP1 (80 µg) and ethyl paraoxon (0.1 -1 mM) were added to this mixture, and the volume was made up to 1 ml. A blank sample was made in a similar way except that ethyl paraoxon was not added, and mTFP1 was used as a control with the same experimental conditions. The reaction mixture was incubated for 10 minutes at 50 °C, and the decrease in the fluorescence intensity was recorded. Fluorescence excitation of mTFP1 was performed at 462 nm, and emission was measured at 491 nm. Fluorescence emission intensity ratios were plotted with respect to different concentrations of ethyl paraoxon and methyl parathion, and a linear regression analysis was performed to determine the calibration curves for estimation.

2.2.21 Fluorescent protein mTFP1 as a pH sensor

To determine the pH-dependence of the fluorescence emission of mTFP1, the protein (stock solution of 1 mg/ml in 5 mM Tris-Cl, pH 7.4 at room temperature) was diluted 1:100 in a corning half area black 96-well-plate containing 0.1 ml of buffer (100 mM) at pH values ranging from 2 to 8 (2.5- 5.5 citrate phosphate buffer and pH 6-8 Bis-Tris-Propane buffer). Fluorescence excitations of mTFP1 for each pH were acquired with a SYNERGY H1 plate reader (Biotech) at 462 nm, and emission was measured at 491 nm.

2.2.22 Statistical analysis

The statistical analysis was performed by one-way ANOVA and calculated by Graph-Pad Prism (****) $p<0.0001$, (***) $p<0.0002$, (**) $p<0.0021$, (*) $p<0.0332$, (ns) $p<0.123$, standard deviation (s.d.) was calculated as per the proper method.

.

Chapter 3

Chapter 3

A novel biosensor for the detection of organophosphorus (OP) based pesticides using Organophosphorus acid anhydrolase (OPAA) -FL variant

3.1 Introduction

The commonly used pesticides are classified mainly into three categories: organochlorines, carbamates, and organophosphates. Due to their low-cost synthesis and high efficacy, organophosphates are most widely used. Structurally, OPs have alkyl or aryl groups that are either bonded to phosphorous via oxygen or sulfur linkage, or such groups are directly bonded to the phosphorus. The leaving group attached to the phosphorus may be an aromatic group, halogen, aliphatic, or heterologous cyclic group (Jain et al. 2019). The central atom phosphorus, if bound to the Sulphur then the OPs are called as thions and if the central atom is bound to the oxygen then such OPs are called oxons (Peter et al. 2010). These OPs are extensively used as pesticides for the last several decades. These compounds inactivate the AChE enzyme and a variety of serine hydrolases (lipases and esterases) that are important for the proper functioning of the human body (Mangas et al. 2017). Incidentally, poisoning by OPs has a high mortality rate of up to 10 – 20 % (Eddleston 2000; Liu et al. 2012) and therefore is a serious cause of concern for healthcare professionals and clinicians (Kang et al. 2009). Thus, measures to facilitate fast, accurate, and convenient detection of OPs in humans, as well as other environmental samples, are necessary (Jain et al. 2019).

In recent times, enzymatic sensors based on the hydrolysis of OPs have emerged as important candidates for enzymatic detection of OP compounds. The first enzymatic sensor using the principle of hydrolysis of OP compounds was developed by Wild and group in 1996 (Rainina et al. 1996).

OPAA (EC 3.1.8.2) is one of the promising enzymes which can hydrolyze hazardous OPs (Li et al. 2016). The wild-type OPAA is reported to act on various OPs, including nerve agents of G-series (Jeong et al. 2012), and OPAA variants are reported to act on V-series nerve agents as well (Daczkowski et al. 2015). The OPAA enzyme isolated from an aerobic, short rod, gram-negative bacterium *Alteromonas* sp. has drawn a keen focus due to its efficiently high expression in *E. coli* as well as its high activity against nerve agent GD (DeFrank and Cheng 1991). Luqi Pei and group conducted some early research on encapsulation of OPAA into erythrocytes for the UV-vis spectrophotometric sensing of paraoxon poisoning in blood samples through the detection of PNP, with a detection limit of about 0.01 mM (Pei et al. 1993).

DeFrank's group, for example, demonstrated a Langmuir-Blodgett film of OPAA labeled with a fluorescent probe, FITC on a quartz slide as a platform for the sensing of DFP (Mello et al. 2003). Reports about the use of OPAA for the detection of paraoxon are meagre in literature.

In this study, a variant of OPAA-FL was expressed in *E. coli* and purified to study its kinetics against ethyl paraoxon. The colorimetric and fluorometric detection method was employed for the measurement of ethyl paraoxon based on the production of PNP and the interaction of protons produced in the catalytic reaction with FITC. Additionally encapsulated OPAA-FL variant matrices were developed using alginate microspheres and combined with the above optical measurements to quantify paraoxon concentration by observing changes in the fluorescence/absorption spectra with addition of the analyte (Mulchandani et al. 2001a).

3.2 Results

OPAA has been demonstrated as an effective and active catalyst for the hydrolysis of OPs and nerve agents, due to which it has attracted widespread attention for the purpose of both detection and remediation of OPs (Iyer and Iken 2015). **Fig. 3.1** shows the diagrammatic representation of using the OPAA-FL variant enzyme for the detection of ethyl paraoxon. OPAA, in presence of $MnCl_2$ (Vyas et al. 2010), hydrolyses ethyl paraoxon into diethyl phosphoric acid and PNP, a yellow-colored product, which can be detected colorimetrically (**Fig. 3.1**). This reaction also releases two protons, which eventually decreases pH and in conjunction with a pH-sensitive fluorophore like FITC can be used for indirect fluorometric detection of OP substrates.

3.2.1 Cloning of OPAA-FL variant in the pET expression vector

The wild-type gene coding for OPAA was initially cloned from *Alteromonas* sp. JD6.5 (Cheng et al. 1996). Subsequently, using site-directed mutagenesis, several mutants of OPAA were reported which have greater activity against various OPs. One of those mutants, FL, having unique Y212F and V342L mutations, shows 5 – 10 fold increased catalytic activity on nerve agents soman and GP (Bae et al. 2018). The amino acid sequence of the OPAA-FL variant is shown in **Fig. 3.2**.

In order to enhance the expression and simplify the purification, the variant of the OPAA-FL gene was cloned downstream of the strong promoter (T7) into the expression vector pET28. OPAA-FL variant gene was amplified from the pSE420-OPAA-FL vector using primers PK702F and PK706R (**Appendix B**), and *Pfu* DNA Polymerase. The OPAA-FL variant gene was digested with *Nde*I and *Bam*HI, respectively, and cloned into a pET28 vector. The cloning was performed in such a way that the recombinant protein codes for an N-terminal His-tag (**Fig. 3.3 A**). Cloning of OPAA-FL variant in pET28 was confirmed by restriction analysis followed by DNA sequencing. The resultant recombinant plasmid was then transformed into *E. coli* Rosetta (DE3) cells.

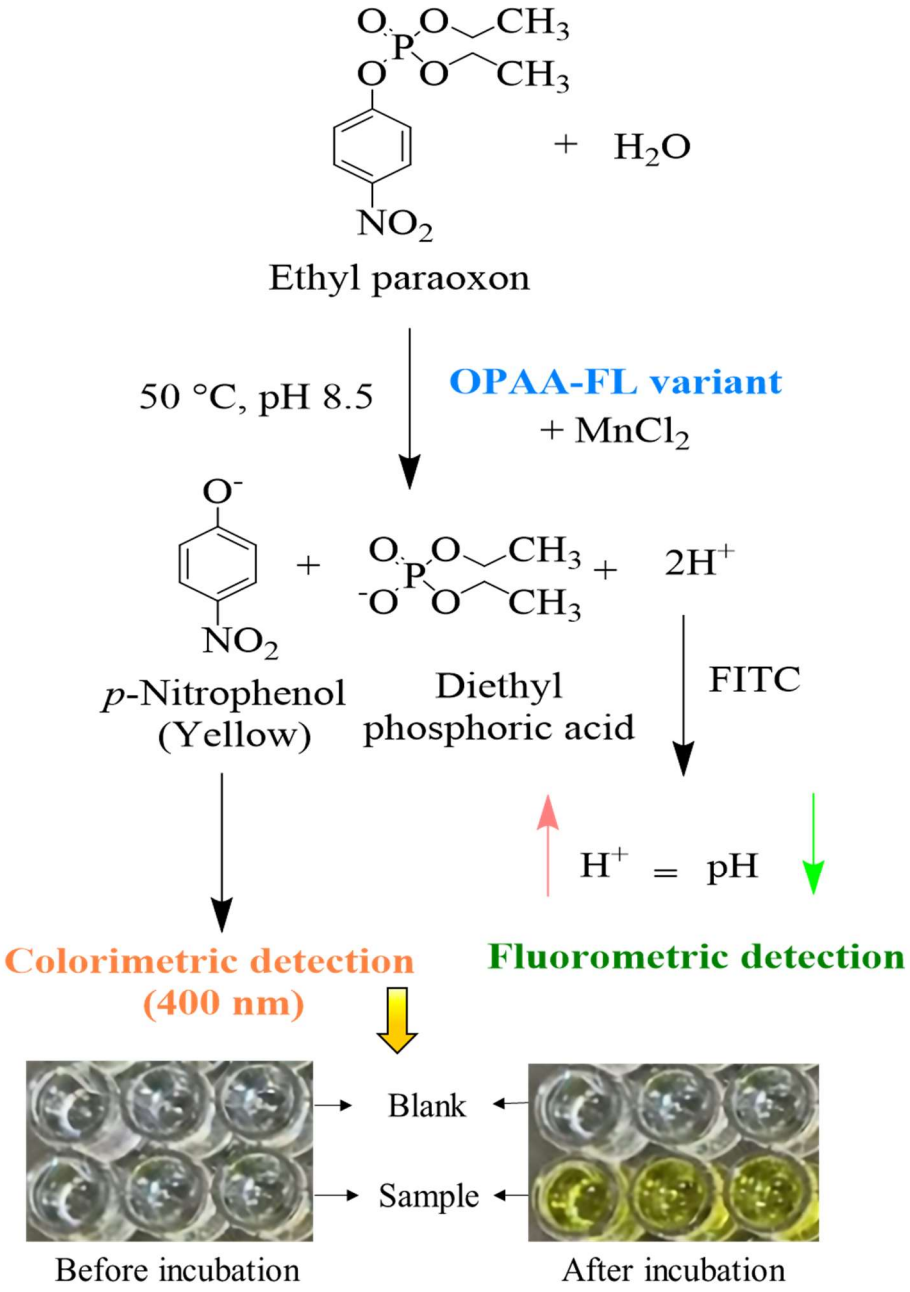

Figure 3.1. The reaction of the OPAA-FL variant with ethyl paraoxon. Sensing scheme of fluorometric and colorimetric detection of OP compound using OPAA-FL variant.

OPAA-FL variant sequence

```
MNKLAVLYAE HIATLQKRTR EIIERENLDG VVFHSGQAKR 40
QFLDDMYYPF KVNPQFKAWL PVIDNPHCWI VANGTDKPKL 80
IFYRPVDFWH KVPDEPNEYW ADYFDIELLV KPDQVEKLLP 120
YDKARFAYIG EYLEVAQALG FELMNPEPVM NFYHYHRAYK 160
TQYELACMRE ANKIAVQGHK AARDAFFQGK SEFEIQQAYL 200
LATQHSENDT PFGNIVALNE NCAILHYTHF DRVAPATHRS 240
FLIDAGANFN GYAADITRTY DFTGEGEFAE LVATMKQHQI 280
ALCNQLAPGK LYGELHLDCH QRVAQTLSDF NIVNLSADEI 320
VAKGITSTFF PHGLGHHIGL QLHDVGGFMA DEQGAHQEPP 360
EGHPFLRCTR KIEANQVFTI EPGLYFIDSL LGDLAATDNN 400
QHINWDKVAE LKPFGGIRIE DNIIVHEDSL ENMTRELELD 440
```

Figure 3.2. OPAA-FL variant amino acid sequence. OPAA-FL variant contains substitution mutations at Y212F and V342L. Additionally, 77 C-terminal amino acid residues are deleted compared to wild-type OPAA from *Alteromonas* sp. JD 6.5.

3.2.2 Expression and purification of recombinant OPAA-FL variant

E. coli Rosetta (DE3) cells with OPAA-FL variant expression vector were induced with 1 mM IPTG. Induced cells were harvested, washed, and resuspended in buffer containing 50 mM Tris-Cl, pH 7.4 with 10 % glycerol. Cells lysates were prepared and separated as supernatant and pellet to evaluate the amount of protein present in the soluble form. The results of the expression of the OPAA-FL variant in both pellet and supernatant are shown in **Fig. 3.3 B**. Most of the expression of 50 kDa OPAA-FL variant protein was observed in the soluble fraction (**Fig. 3.3 B**, lane 2).

Since the OPAA-FL variant carries an N-terminal His-tag, this study performed affinity purification of recombinant OPAA-FL variant protein on a Ni-NTA resin. The input sample was prepared in the equilibration buffer (50 mM Tris-Cl buffer, pH 8.0, 500 mM NaCl, and 10 mM imidazole), and loaded on the pre-equilibrated column at a flow rate of 1 ml/ minute. Subsequently, the column was washed with wash buffer comprising of 50 mM Tris-Cl, pH 8.0, 500 mM NaCl, with 50mM imidazole. The sample was eluted using elution buffer comprising of 50 mM Tris-Cl, pH 8.0, 500 mM NaCl, with 150mM imidazole. The samples were collected for analysis by SDS-PAGE. **Fig. 3.3 C** shows that the OPAA-FL variant protein was able to bind to the Ni-NTA resin, as most of the protein was absent in the flow-through (**Fig. 3.3 C**, lane 2). More than 95 % pure OPAA-FL variant protein was purified (**Fig. 3.3 C**, lane 6).

3.2.3 Activity assay of recombinant OPAA-FL variant

To know whether the purified OPAA-FL variant protein is indeed enzymatically active, the OPAA-FL variant enzyme assay with ethyl paraoxon was performed. To perform OPAA-FL variant assay, 1 µl of cell extract or purified protein was mixed with 50 mM Bis-Tris propane buffer, pH 8.5, 1 mM ethyl paraoxon, and 1 mM $MnCl_2$, and the final volume was made up to 250 µl with SDW and reaction mixtures were incubated at 50 ºC for 15 minutes.

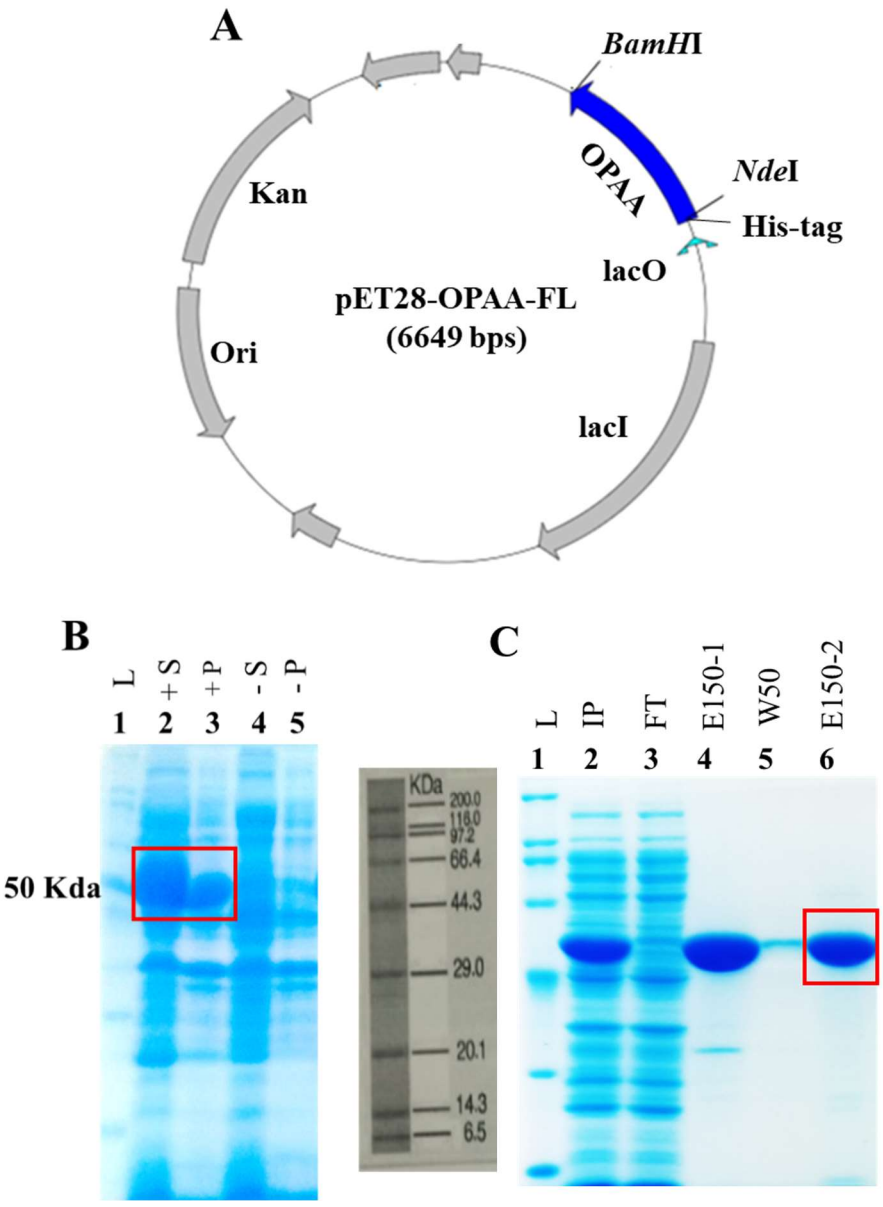

Figure 3.3. Cloning, expression and purification of OPAA-FL variant. **(A)** Map of pET28 with OPAA-FL variant, N-His tag. **(B)** Induction of recombinant OPAA-FL variant fusion protein. Induction of OPAA-FL variant was performed at 20 °C for 20 hrs. lane 1: Protein marker, lane 2: Induced supernatant, lane 3: Induced pellet, lane 4: Uninduced supernatant, lane 5: Uninduced pellet. **(C)** Purification of recombinant OPAA-FL variant fusion protein. Lane 1: Protein marker, lane 2: Lysate, lane 3: Flow-through, lane 4: Elution 1 with 150 mM Imidazole, lane 5: Wash 50 mM Imidazole, Lane 6: Elution 2 with 150 mM Imidazole.

OPAA-FL variant activity was calculated by measuring the absorbance of PNP produced due to the hydrolysis of ethyl paraoxon at 400 nm (ε400 = 17,000/M/cm for PNP, UV-Vis spectrum is shown in **Fig. 3.4**). Specific activities were expressed as units (micromoles of substrate hydrolysed per minute) per milligram of total protein.

Specific activities of various samples of OPAA-FL variant protein are mentioned in **Fig. 3.5 A**. As expected, induced cell lysate showed several folds higher specific activity as compared with the un-induced cell lysate. Furthermore, purified recombinant OPAA-FL variant protein demonstrated higher specific activity as compared to that in the induced cell lysate. The specific activity in the induced cell lysate was around 0.826 U/mg, and purified OPAA-FL variant showed even higher specific activity, that is, 1.96 U/mg.

Similarly, to know whether the purified protein is indeed enzymatically active against other OPs, an OPAA-FL variant enzyme assay with methyl parathion was done. To perform OPAA-FL variant assay, 1 µl of cell extract or purified protein was mixed with 50 mM Bis-Tris propane buffer, pH 8.5, 1 mM methyl parathion, and 1 mM $MnCl_2$, and final volume was made up to 250 µl with SDW and reaction mixtures were incubated at 50 ºC for 15 minutes. OPAA-FL variant activity was calculated by measuring the absorbance of PNP produced due to the hydrolysis of methyl parathion at 400 nm (ε400 = 17,000/M/cm for PNP). Specific activities were expressed as units (micromoles of substrate hydrolysed per minute) per milligram of total protein.

Specific activities of various samples of OPAA-FL variant protein with methyl parathion are mentioned in **Fig. 3.5 B**. Surprisingly, almost identical specific activity in both un-induced, as well as induced cell lysates, was observed. However, the purified recombinant OPAA-FL variant protein demonstrated a higher specific activity as compared to that in the induced cell lysate. The specific activity in the induced cell lysate was around 0.096 U/mg, and the purified OPAA-FL variant showed higher specific activity of 0.149 U/mg.

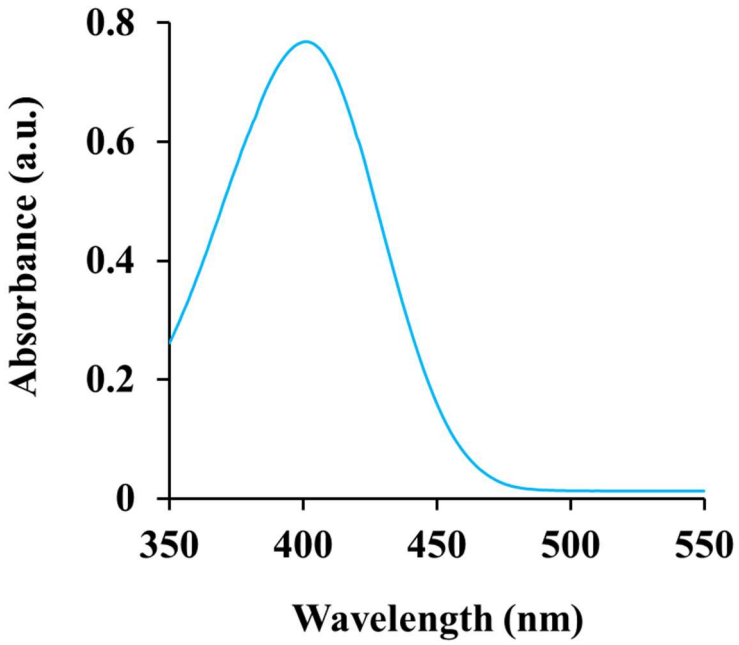

Figure 3.4. UV-Vis spectrum of *p*-nitrophenol in 50 mM Bis-Tris propane buffer at pH 8.5 using ethyl paraoxon as a substrate for OPAA-FL variant.

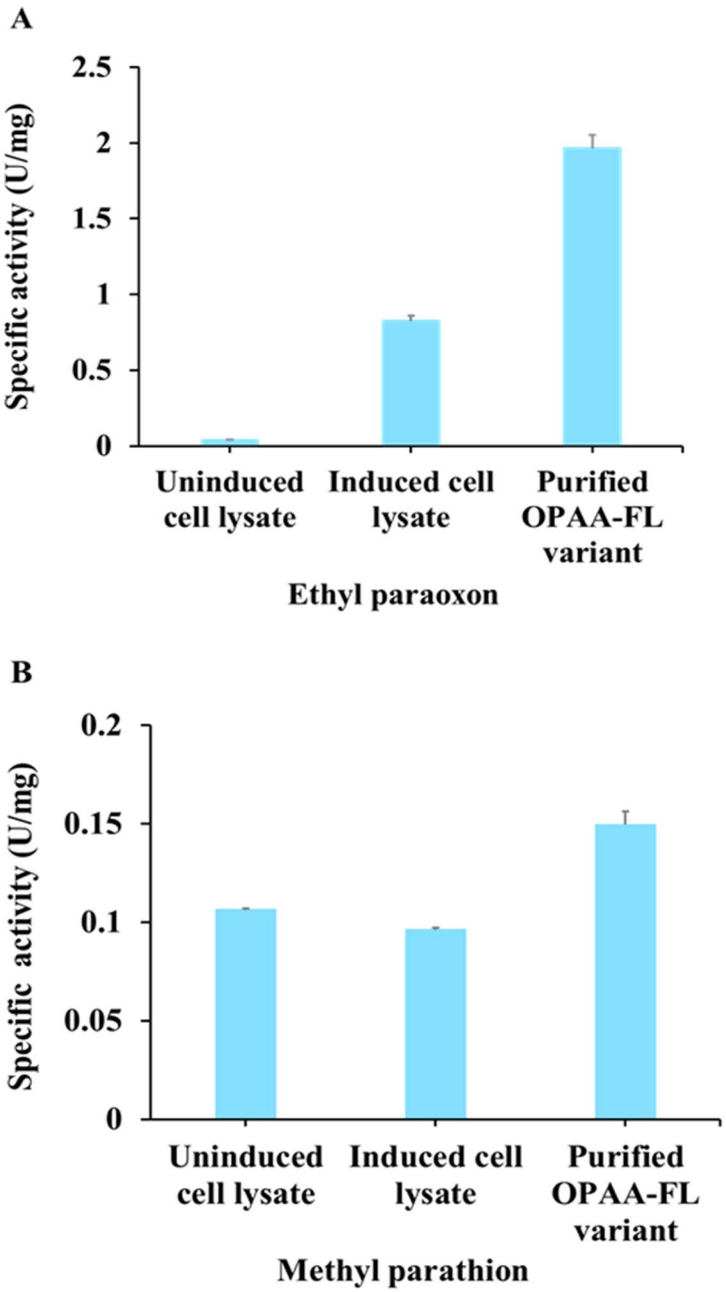

Figure 3.5. Colorimetric activity assay of OPAA-FL variant. OPAA-FL variant with 1 mM substrate in presence of Bis-tris propane buffer, pH 8.5, at 50 ºC for 15 minutes. **(A)** 1 mM of ethyl paraoxon, **(B)** 1 mM of methyl parathion. The values are an average of duplicate samples and error bars represent standard deviation. At least three independent experiments were performed, and a representative result is shown.

Considering the relatively low specific activities observed for methyl parathion substrate with OPAA-FL variant as compared to ethyl paraoxon substrate, further experiments were carried out using ethyl paraoxon as a substrate to develop a working biosensor. With this in mind, the kinetic parameters for ethyl paraoxon as substrate concentrations of 0.1 to 9 mM and 0.25 to 9 mM using purified as well as encapsulated OPAA-FL variant have been reported in **Fig. 3.6 A and B** respectively and **Table 3.1.** The enzyme kinetic parameters for ethyl paraoxon substrate (k_{cat}, K_m, V_{max}, k_{cat}/K_m) are calculated following the published literature (Robinson 2015).

3.2.4 Effect of pH and temperature on OPAA-FL variant activity

The study observed a significant specific activity with substrate ethyl paraoxon, the effect of pH and temperature on the activity of the OPAA-FL variant was examined. To know the optimum temperature for the OPAA-FL variant with ethyl paraoxon, tests were done on the activity at various temperatures between 20 – 60 ºC for 15 minutes, in 50 mM Bis-Tris propane buffer, pH 8.5, 1 mM ethyl paraoxon, and 1 mM $MnCl_2$. Similar to earlier reports (DeFrank and Cheng 1991), OPAA-FL variant activity was gradually increasing until 50 ºC, and any further increase in the temperature led to a decrease in the specific activity. The experiments suggested that 50 ºC is the optimum temperature for the OPAA-FL variant with ethyl paraoxon (**Fig. 3.7 A**).

To know the optimum pH for OPAA-FL variant with ethyl paraoxon, tests were done on activity at various pH between 6 – 10, at 50 ºC for 15 minutes, in either 50 mM phosphate buffer (pH 6.0, 6.5, 7.0, 7.5 and 8.0, respectively) or 50 mM Bis-Tris propane buffer (pH 8.5, 9.0 and 10.0, respectively), 1 mM ethyl paraoxon and 1 mM $MnCl_2$. The optimum activity was observed at pH 8.5 for the OPAA-FL variant (**Fig. 3.7 B**).

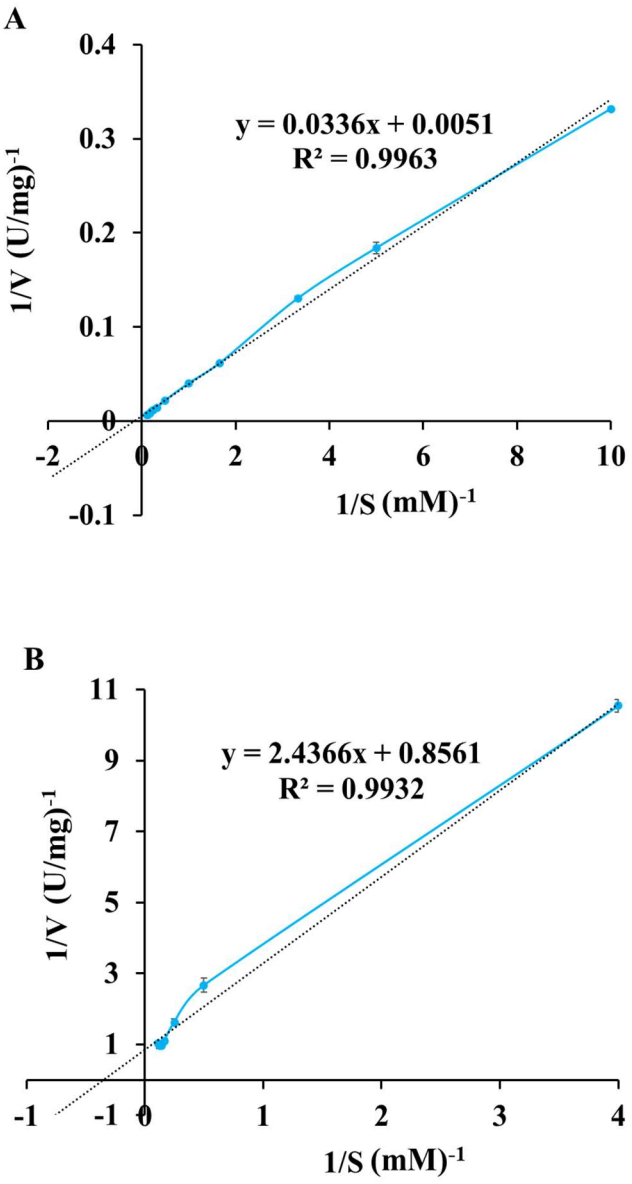

Figure 3.6. Lineweaver Burk plot for OPAA-FL variant using ethyl paraoxon. (A) For purified OPAA-FL variant, **(B)** For encapsulated OPAA-FL variant. The values are average of duplicate samples and error bars represent standard deviation.

Table 3.1 Kinetic parameters of OPAA-FL variant enzyme

Sample	Ethyl paraoxon (mM)	V_{max} (U/mg)	K_m (mM)	k_{cat} (min^{-1})	k_{cat} / K_m (mM^{-1} min^{-1})
Purified OPAA-FL	0.1 to 9	196	6.58	9800	1489.362
Encapsulated OPAA-FL	0.25 to 9	1.168	2.85	58.4	20.49

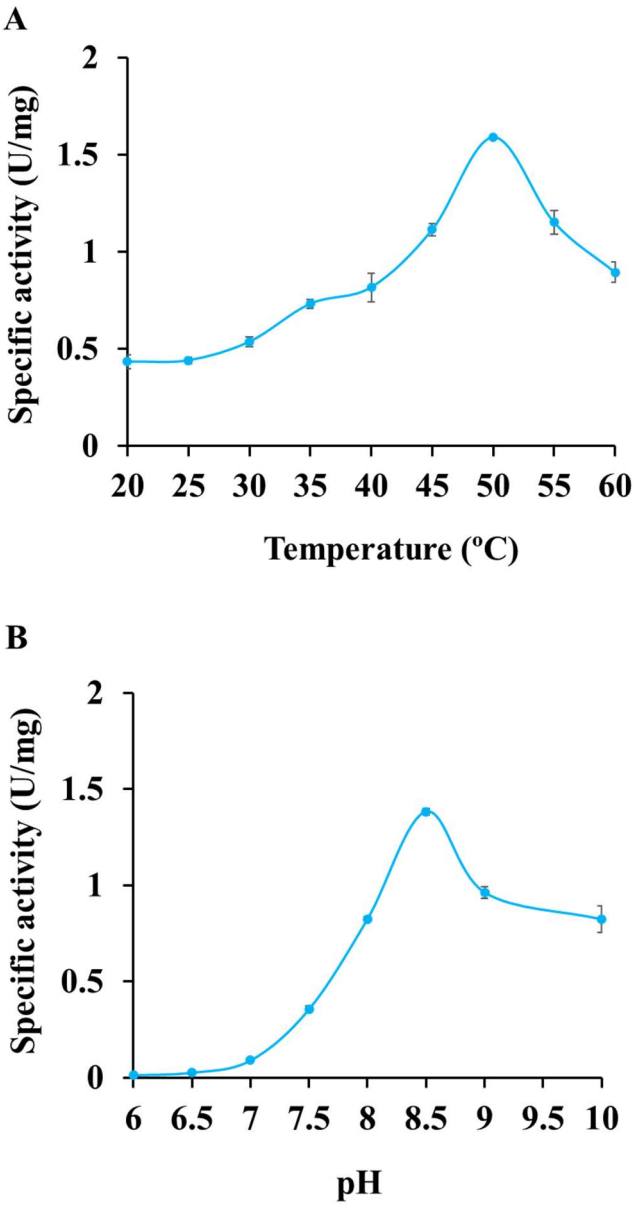

Figure 3.7. Effect of temperature and pH on the OPAA-FL variant activity. (A) Effect of temperature on the specific activity of the OPAA-FL variant with ethyl paraoxon. **(B)** Effect of pH on the specific activity of OPAA-FL variant ethyl paraoxon. The values are an average of duplicate samples and error bars represent standard deviation. At least three independent experiments were performed, and a representative result is shown.

3.2.5 Encapsulation of OPAA-FL variant in alginate microspheres

Typically, encapsulation of proteins in polymers is performed to maintain the activity and the function of the protein over a prolonged time, reduce the chances of interference and increase the sensitivity of the biosensor response (Yap et al. 2014). The OPAA-FL variant was encapsulated into the sodium alginate by using $CaCl_2$ as a crosslinker (**Fig. 3.8 A)**. Alginate was selected for encapsulation of the OPAA-FL variant as it is a natural polymer with numbers of favorable properties such as biocompatibility, ease of gelation, and it enables the protein to retain its activity for a longer period of time while maintaining its structure and function (Lee and Mooney 2012). Subsequently, the encapsulation efficiency of the OPAA-FL variant into the alginate microsphere was estimated, by boiling the alginate microspheres and running these on 12 % SDS-PAGE, along with input and wash controls (**Fig. 3.8 B**). In general, 25 – 30 % encapsulation efficiency was observed. After confirming the encapsulation of OPAA-FL variant protein in the alginate microsphere, the surface characterization using SEM was performed (**Fig. 3.8 C-E**). SEM analysis revealed the spherical-shaped microspheres ranging from 0.1 to 0.8μm.

3.2.6 Colorimetric biosensing of ethyl paraoxon

The bio-sensing activity of the OPAA-FL variant with ethyl paraoxon was evaluated colorimetrically using substrate concentrations ranging from 0.005 mM to 1 mM (**Fig. 3.9 A**). A linear range of 0.01 mM to 1 mM for the detection of ethyl paraoxon was observed with a LOD of 0.04 mM. The sensitivity of such estimation was found to be 1.44 U/mg/mM. For encapsulated OPAA-FL variant with ethyl paraoxon as the substrate, a linear range of 0.025 to 1 mM was observed (**Fig. 3.9 B**). The LOD of bio-sensing was 0.036 mM, and the sensitivity was 0.538 U/mg/ mM.

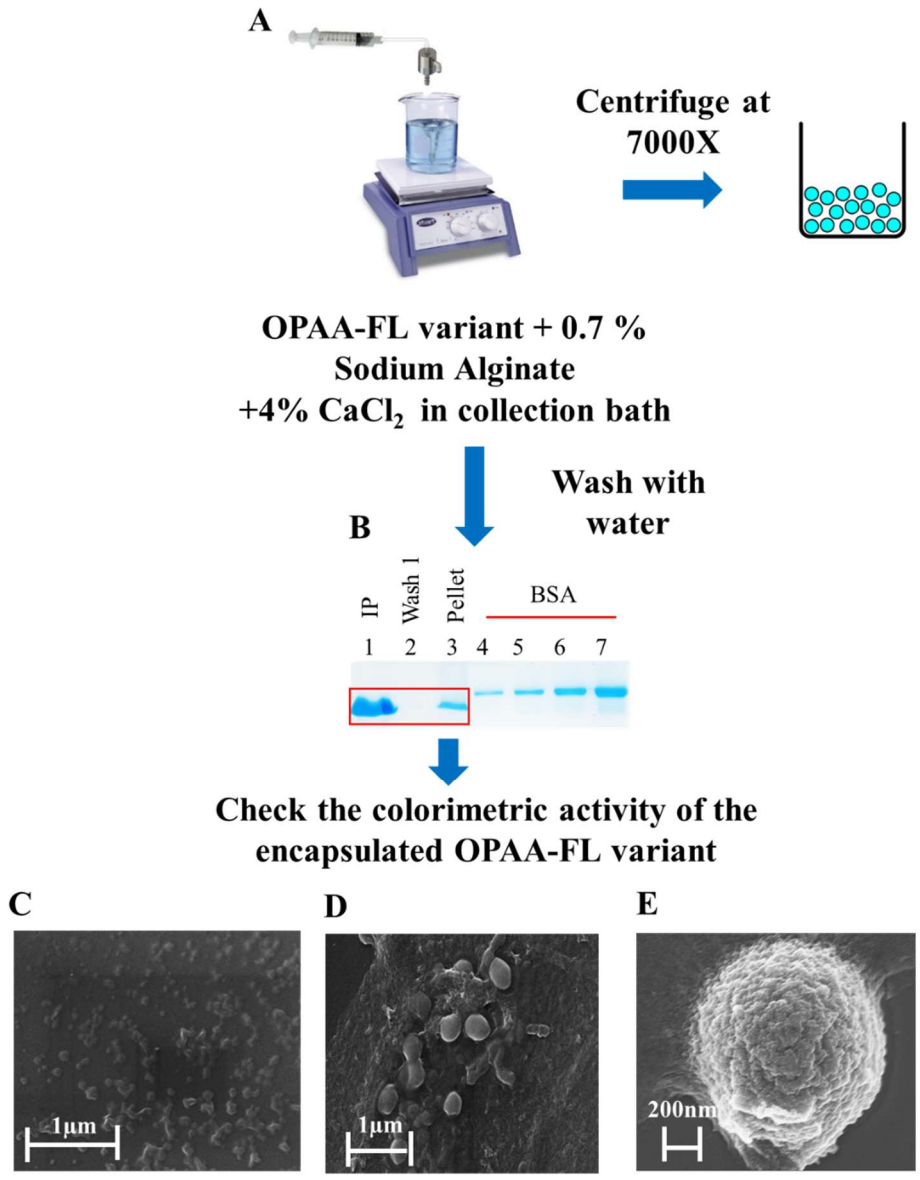

Figure 3.8. Encapsulation of the OPAA-FL variant enzyme. (A) Schematic representation of immobilization procedure for the OPAA-FL variant using an atomizer. **(B)** Analysis of OPAA-FL variant loaded alginate microspheres using SDS-PAGE. Lane 1: Input, lane 2: unloaded OPAA-FL variant in wash 1, lane 3: encapsulated OPAA-FL variant, lane 4 to 7: 0.5, 1, 2, 4 µg of BSA. **(C-E)** Characterization of microspheres: SEM images of OPAA-FL variant loaded alginate microspheres with 0.7% alginate. **(C)** At 6.32 K X magnification, **(D)** At 32.0 K X magnification, and **(E)** At 57.95 K X magnification.

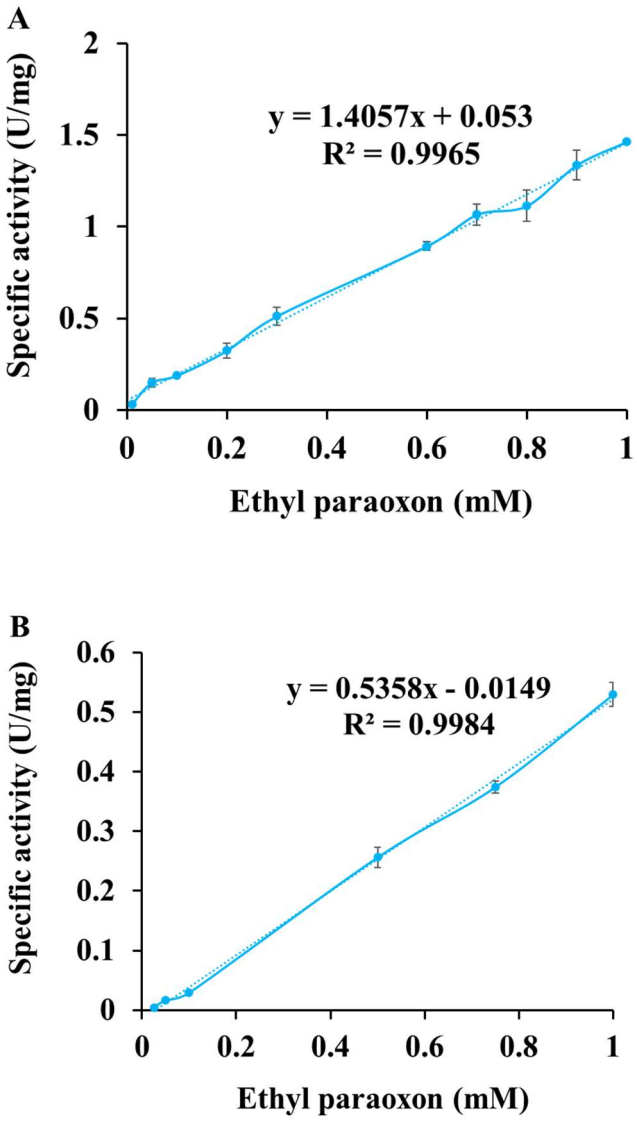

Figure 3.9. Colorimetric biosensing of ethyl paraoxon using the OPAA-FL variant enzyme. (A) Purified OPAA-FL variant **(B)** Encapsulated OPAA-FL variant. The values are an average of duplicate samples and error bars represent standard deviation. At least three independent experiments were performed, and a representative result is shown.

3.2.7 Fluorescent biosensing of ethyl paraoxon

OPAA-FL variant on hydrolysis of OPs release PNP as well as two protons. The protons released result in lowering the pH of the reaction mixture. A pH-sensitive fluorescent probe like FITC can be efficient in detecting such a reaction and indirectly quantify paraoxon. Fluorescence intensity of FITC decreases as the H^+ concentration of the reaction mixture increases, lowering pH results in quenching of fluorescence, and this phenomenon was exploited to detect the presence of OPs **(Fig. 3.10)**. FITC has known to exhibit a linear range of pH determination between pH 4–8. This property of FITC is exploited in most of the enzymatic reactions especially those producing and utilizing protons. The ionization of FITC in basic pH leads to an increase in fluorescence intensity and vice versa. The effects of ionization produced also are affected by the buffering of biological and environmental samples. Generally, the buffer system is responsible for maintaining the conditions under which the enzyme can express maximum activity and stability. A high buffer concentration leads to high buffering capacity, which can suppress pH changes in the medium and hence suppresses the sensitivity of the sensor (Głąb et al. 1994), thus explaining the better results observed for the fluorometric sensing of ethyl paraoxon with 0 mM buffer.

To know optimum buffer and reaction conditions for fluorometric detection of OPs using the OPAA-FL variant, initially, it was tested a decrease in fluorescence values of FITC in different buffer concentrations. The reaction mixture was prepared with 1 mM $MnCl_2$, 1 mM ethyl paraoxon, OPAA-FL variant, FITC-dextran, and sterile distilled water up to 1 ml. 0 mM, 25 mM, and 50 mM activity buffer (Bis-Tris propane) were used, respectively, and measured loss in the fluorescence values (**Fig. 3.11**). Interestingly, the maximum decrease in the fluorescence values was observed in the absence (0 mM) of activity buffer (P value= 0.0058), indicating that the higher buffering capacity of reaction inhibits the loss in fluorescence values.

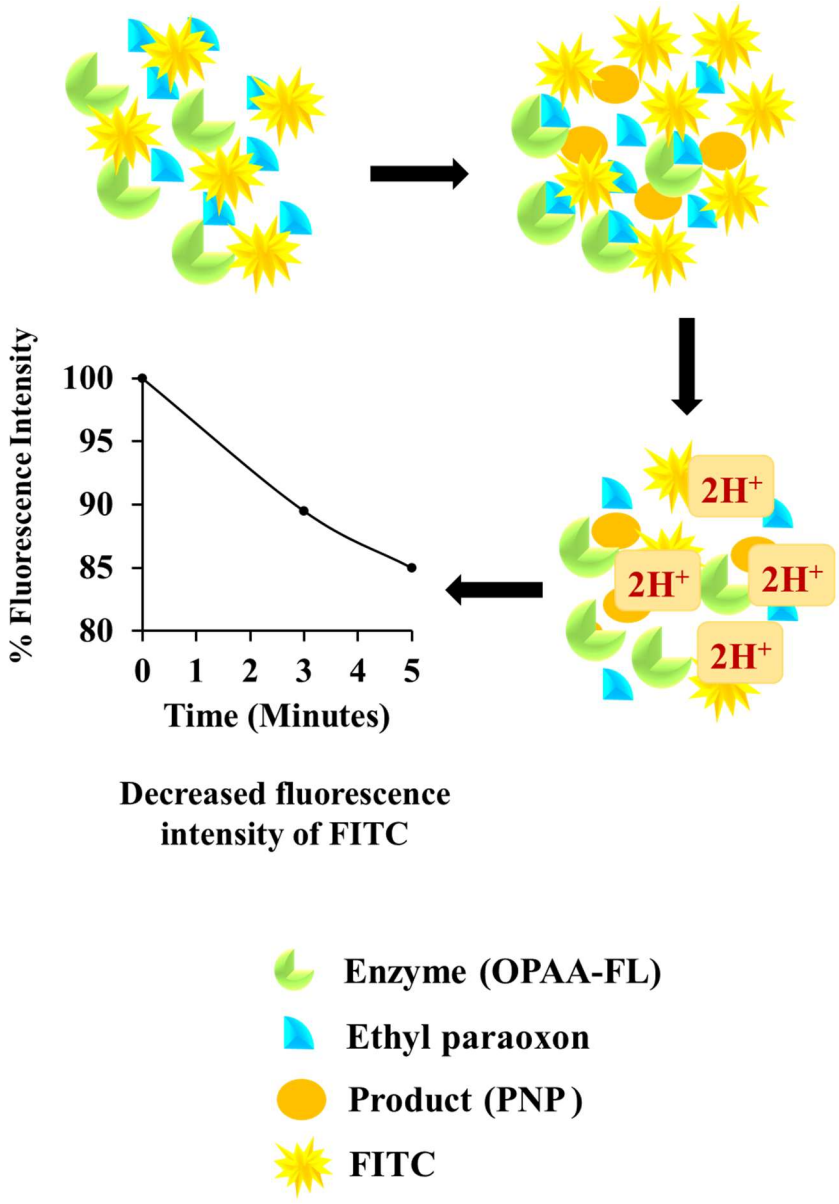

Figure 3.10 Depiction of fluorescence assay mechanism of OPAA-FL variant using FITC dextran for detection of organophosphorus compounds.

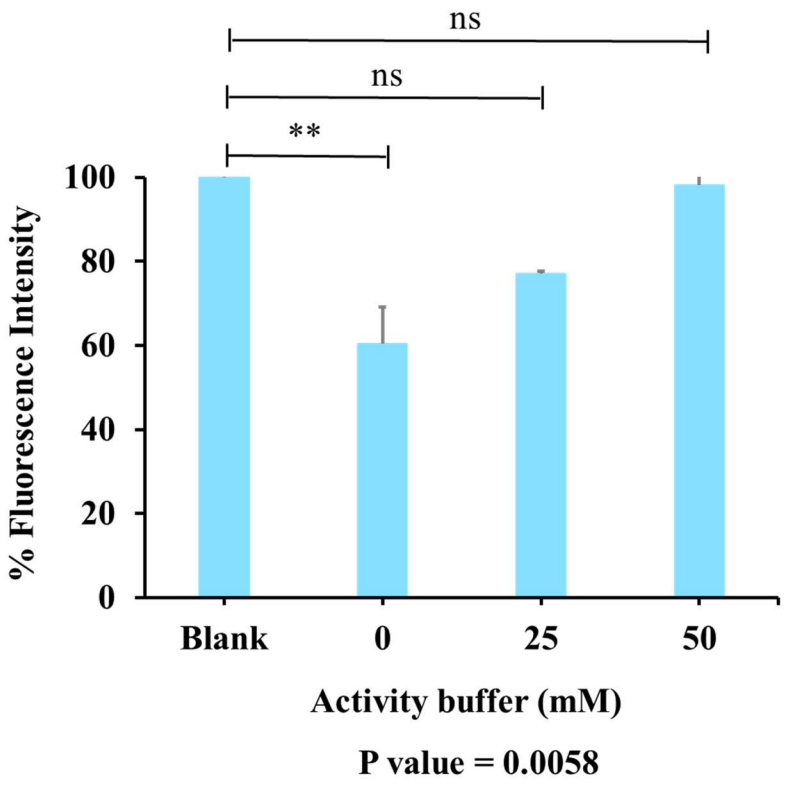

Figure 3.11. Optimization of concentration of Bis-tris propane buffer for OPAA-FL variant fluorescence assay. 0 mM, 25 mM, and 50 mM Bis-tris propane buffer were used at 50 ºC, pH 8.5 for 5 minutes with ethyl paraoxon. The values are an average of duplicate samples and error bars represent standard deviation. At least three independent experiments were performed, and a representative result is shown. The statistical analysis was performed by one-way ANOVA and calculated by Graph-Pad Prism (****) $p<0.0001$, (***) $p<0.0002$, (**) $p<0.0021$, (*) $p<0.0332$, (ns) $p<0.123$, Error bars, standard deviation (s.d.).

Subsequently, to identify an optimum ratio of OPAA-FL:FITC-dextran that gives a higher decrease in fluorescence values, six ratios, namely, OPAA-FL:FITC-dextran 0.25:1, 0.5:1, 0.75:1, 1:1, 3:1 and 5:1, were analyzed respectively (**Fig. 3.12 A-F**). A relative decrease in fluorescence values at three different concentrations of ethyl paraoxon, that is, 0.1 mM, 0.5 mM, and 1 mM, were tested, respectively. Incidentally, it was observed OPAA-FL:FITC-dextran ratio 1:1 gives a higher and consistent decrease in the fluorescence values of FITC ($P = < 0.0001$) (**Fig. 3.12 D**), possibly due to optimal labeling of FITC and protein (Chakraborty et al. 2015; Breen et al. 2016). In fact, with increasing the concentration of ethyl paraoxon, the fluorescence intensity of FITC decreased faster confirming that the higher number of H^+ released at higher substrate concentrations.

The fluorescence-based bio-sensing activity of the OPAA-FL variant with different concentrations of ethyl paraoxon showed that a linear range in 0.1 mM to 0.5 mM of paraoxon (**Fig. 3.13**). The LOD of bio-sensing was 0.038 mM, and the sensitivity was 104 % /mM. Incidentally, the encapsulated OPAA-FL variant microspheres did not show the expected biosensing response in the fluorescence assay.

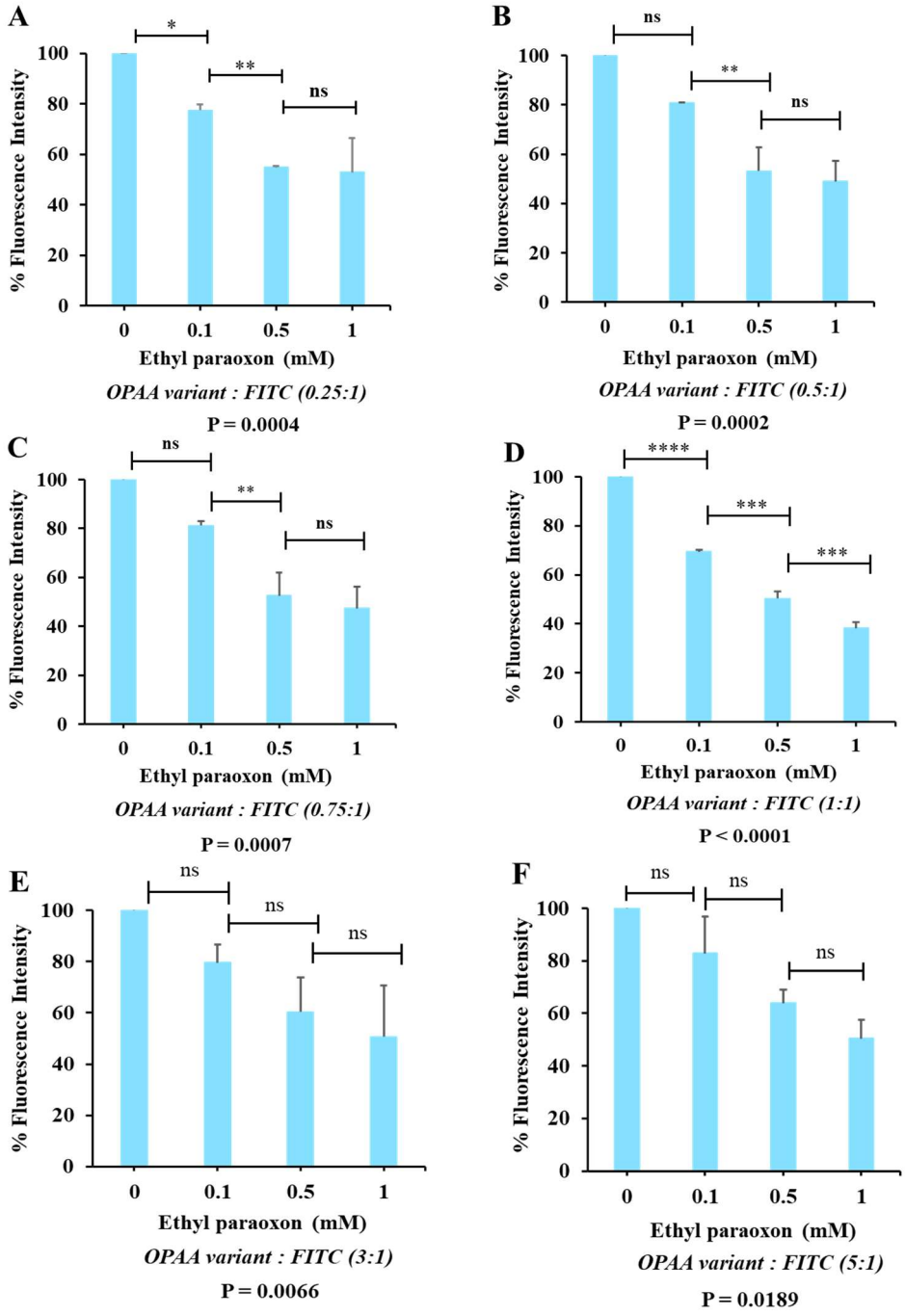

Figure 3.12. Optimization of the ratio of OPAA-FL variant protein: FITC-dextran in fluorescence assay. Three ratios of OPAA-FL variant protein: FITC-dextran **(A)** 0.25:1; **(B)** 0.5:1; **(C)** 0.75:1 **(D)** 1:1; **(E)** 3:1; **(F)** 5:1 were analyzed using 1 mM ethyl paraoxon at 50 ºC, for 5 minutes without activity buffer. The values are an average of duplicate samples and error bars represent standard deviation. At least three independent experiments were performed, and a representative result is shown. The statistical analysis was performed by one-way ANOVA and calculated by Graph-Pad Prism (****) $p<0.0001$, (***) $p<0.0002$, (**) $p<0.0021$, (*) $p<0.0332$, (ns) $p<0.123$, Error bars, standard deviation (s.d.).

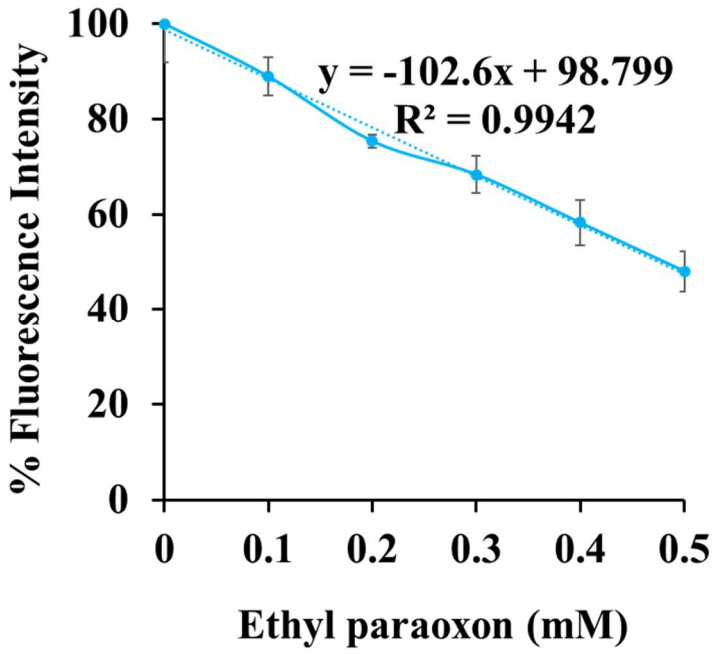

Figure 3.13. Bio-sensing of ethyl paraoxon using the OPAA-FL variant via fluorescence assay. 1:1 ratio of OPAA-FL variant and FITC-dextran were used with 1 mM paraoxon as the substrate at 50 ºC, for 3 minutes without activity buffer. The fluorescence intensity of FITC decreased linearly with an increase in the concentration of ethyl paraoxon. The values are an average of duplicate samples and error bars represent standard deviation. At least three independent experiments were performed, and a representative result is shown.

3.3 Summary

The detection methods for OPs commonly used so far are costly and have several limitations for infield analysis. Recombinant expression of OPAA-FL variant and deployment of OPAA-FL variant into a biosensing assay can help to quantify OPs effectively. The OPAA enzyme is reported to hydrolyze OP compounds with P-F, P-O, P-S, and P-CN bonds in the published literature. A representative comparison table of OPAA-FL with P-F and P-O bond containing OPs, OPAA WT with P-O bond containing compounds, as well as a comparison of OPAA FL and wild-type OPAA for the hydrolysis of P-S bond containing Russian VX is given in **Table 3.2** and **Table 3.3**, respectively. This chapter describes the utilization of the OPAA-FL variant for the development of a biosensing assay for ethyl paraoxon using a colorimetric and fluorometric estimation. OPAA-FL variant was successfully expressed and purified from *E. coli* Rosetta (DE3) cells. The purified OPAA-FL variant showed higher specific activity than the induced cell lysate and exhibited an optimum temperature of 50 °C and optimum pH of 8.5. Colorimetric estimation of ethyl paraoxon via the PNP method showed a capability of detection to an extent of 0.01 - 1 mM. OPAA-FL variant was also immobilized in alginate microspheres using a novel technique of ultrasonic atomization to enhance stability, activity, and biosensing. After encapsulation of the OPAA-FL variant, the microspheres also were able to detect ethyl paraoxon at similar detection limits. Fluorometric detection tests with ethyl paraoxon as the substrate showed a detection capability in the range of 0.1 - 0.5 mM after a short incubation time of 3 minutes. Both colorimetric and fluorometric methods can form the basis of new OPAA-FL variant-based optical biosensors and their transformation into point-of-care devices for in-field and facile analysis of insecticides and pesticides. This study, therefore, establishes the use of OPAA variants towards detection of common organophosphate pesticides and paves the way for the research community to develop sensitive, user friendly and portable point-of-care devices for the timely and accurate detection of these toxic compound.

Table 3.2 Kinetic parameters of OPAA-FL variant enzyme on P-F and P-O hydrolysis and OPAA-WT with P-O hydrolysis

Substrate	k_{cat}	K_m	k_{cat} / K_m	V_{max}	References
OPAA-FL variant P-F and P-O hydrolysis					
P-F bond hydrolysis					
Sarin / GB	4.52E + 04 ± 4.62E + 03 min^{-1}	5.31E + 03 ± 1.01E + 03 μM	8.50E + 06 ± 2.49E + 06 M^{-1} min^{-1}	-	(Bae et al. 2018)
Soman /GD	6.60E + 04 ± 3.40E + 03 min^{-1}	883.16 ± 156.395 μM	7.48E + 07 ± 1.71E + 07 M^{-1} min^{-1}	-	
GP	6.90E + 04 ± 3.08E + 03 min^{-1}	534.924 ± 6.78E + 01 μM	1.29E + 08 ± 2.21E + 07 M^{-1} min^{-1}	-	
Soman / GD	1.18E+05 ± 6.12E+03 min^{-1}	2.19E+03 ± 3.09E+02 μM	5.38 E+07 ± 1.04E+07 M^{-1} min^{-1}	-	(Guelta et al. 2018)

P-O bond hydrolysis					
Ethyl paraoxon	9800 min^{-1}	6580 µM	1489.362 mM^{-1} min^{-1}	196 U/mg	Our study

WT OPAA P-O hydrolysis

P-O bond hydrolysis					
Ethyl paraoxon	1.8 s^{-1}	>7.6 mM	280±10 M^{-1} s^{-1}	-	(Hill et al. 2000)
	3.0 ± 0.526 s^{-1}	3.203 ± 0.929 mM	0.000935 ± 0.089M^{-1} s^{-1}	10.277 ±1.803 µmol/min/ml	(Xiao et al. 2017)
	4.64 s^{-1}	0.6 mM	7.75 × 10^3 M^{-1} s^{-1}	-	(Simonian et al. 2001)
	-	14.2 mM	-	6.11 mmol/min/mg	(Petrikovics et al. 2000)

Table 3.3 Kinetic parameters of OPAA-WT and OPAA-FL variant enzyme on P-S bond (Russian VX) hydrolysis

Enzyme	k_{cat} (min^{-1})	K_m (μM)	k_{cat}/K_m (M^{-1} min^{-1})	Reference
WT OPAA	1.8 ± 0.12	3280 ± 551	548 ± 128	(Daczkowski et al. 2015)
OPAA-FL	21 ± 1.1	1767 ± 258	11894 ± 2349	

Chapter 4

Chapter 4

Recombinant organophosphorus hydrolase (OPH) expression in *E. coli* for the effective detection of organophosphate pesticides

4.1 Introduction

In modern times, due to the needs and demands of an increasing population, pesticides have gained popularity in different sectors, from agriculture to industry. Due to cost-effective synthesis and widespread and proven use as pesticides/insecticides, OPs are widespread, especially in developing countries. OPs have several nicotinic and muscarinic side effects on human health. The AChE in our nervous system is severely affected by OP poisoning, resulting in neurological complications - a problem that extends to all vertebrates including humans (Yang et al. 2008b; Watson et al. 2014; Ortiz-Delgado et al. 2019). OPs can enter the human body through the dermal, ocular, respiratory, and oral routes. Dermal exposure is more probable (49%) than other exposure routes (Toe et al. 2013). Long-term exposure of OPs leads to permanent inactivation of AChE enzyme, leading to muscarinic and nicotinic toxicity on account of accumulation of acetylcholine in the neuromuscular junctions and synapses. Combined with the relative ease and prevalence of exposure, these compounds present a significant risk of concern for interventions from the scientific community and healthcare processions.

Due to the concerns of pesticide toxicity and accumulation in environmental and biological systems, the development of a reliable, selective, sensitive detection and detoxification method for these compounds is necessary. Some soil microbiotas have been shown to have enzymes that can degrade these toxic compounds into non-toxic compounds (Laveglia and Dahm 1977). OPH enzyme isolated from *Flavobacterium sp.* and *Pseudomonas diminuta* has shown this activity of degradation of OPs. OPH has a broad substrate specificity, including the

cleavage of P-O, P-S, P-F, and P-CN bonds, it catalyzes the hydrolysis of organophosphorus compounds, such as methyl and ethyl parathion, paraoxon, chlorpyrifos, coumaphos, cyanophos, and diazinon as well as chemical warfare agents, such as sarin and soman (Kang et al. 2008). Enzymatic hydrolysis is reportedly 40-2450 times faster compared to chemical hydrolysis (Shimazu et al. 2003), and thus attracts great interest from a scientific viewpoint for the remediation as well as detection of organophosphorus compounds in the environment. The catalytic action of OPH is based on a reaction mechanism most similar to SN2 with the active site histidine residue acting as a water deprotonating base during the hydrolysis of OP compounds with PNP as a product (Thakur et al. 2012), as shown in **Fig. 4.1**. Detailed discussions on the reaction mechanism of OPH with OP compounds have been described in earlier reports (Jain et al. 2019; Bigley and Raushel 2019).

In the literature, there are several reports on the sensing of organophosphorus compounds using OPH through electrochemical, optical, and other methods (Xiong et al. 2018). However, an optimal sensor that achieves good enzymatic catalytic activity and low enough detection limits to detect organophosphorus compounds in practical use cases remains elusive primarily due to reproducibility and cost concerns. This study reported colorimetric, as well as fluorescence-based sensing using a known fluorescent dye FITC of organophosphorus compounds, by the interaction of His-Nus-OPH with OP compounds such as methyl parathion and ethyl paraoxon.

4.2 Results

OPH has attracted widespread attention of the scientific community due to its ability to hydrolyze a variety of organophosphate compounds, such as ethyl paraoxon and methyl parathion. **Fig. 4.1** shows a representative schematic of the hydrolysis of ethyl paraoxon and methyl parathion. The hydrolysis process in the presence of $CoCl_2$ (Cho et al. 2006) results in the production of PNP along with the release of two protons, which form the basis of the colorimetric and fluorometric

detection methods used in this study, with FITC-dextran as a fluorophore in the case of fluorometric detection of OPs.

4.2.1 Cloning and expression of OPH with N-terminal His tag in pET vector

The *oph* gene from *Pseudomonas diminuta* was cloned into a pET28 expression vector, giving p28-His-OPH **(Fig. 4.2 A).** The results of the expression of His-OPH in both pellet and supernatant are shown in Fig. 4.2 B, C. From Fig. 4.2 B at 37^{o}C for 3 hrs and Fig. 4.2 C at 16^{o}C for 16 hrs induction, no expression of His-OPH protein in the uninduced supernatant and pellet was observed but, surprisingly, it was found that on induction, the 38 kDa His-OPH protein was expressed in the pellet but not in the supernatant. Most likely, improper folding resulted in the formation of inclusion bodies (Itkonen et al. 2014), and hence more than 90% of the expression of His-OPH protein was observed in the pellet (**Fig. 4.2 B** and **C,** lane 4 and 5, respectively).

4.2.2 Cloning, expression, and purification of OPH with N-terminal His and NusA tag in pET vector

Several recombinant proteins demonstrate poor solubility when expressed in a heterologous host (Habibi et al. 2014). To overcome the problem of solubility, the NusA solubilization tag was used. To obtain soluble OPH by bringing the N-terminal NusA tag, the *oph* gene was sequentially cloned into pET43 and pET28 expression vectors to give p43-Nus-OPH and p28His-Nus-OPH respectively. In pET43, the *oph* gene was cloned in such a way that a preScission protease site is present in between the NusA tag and the OPH protein. The expression of these proteins along with the solubilization tag helps in getting expression in the soluble fraction (Bell et al. 2013). To explore the possibility that bringing His tag on the N-terminal will assist in the purification step (Spriestersbach et al. 2015), the *oph* gene along with the NusA tag was double digested from the p43-Nus-OPH clone and sequentially cloned into pET28a expression

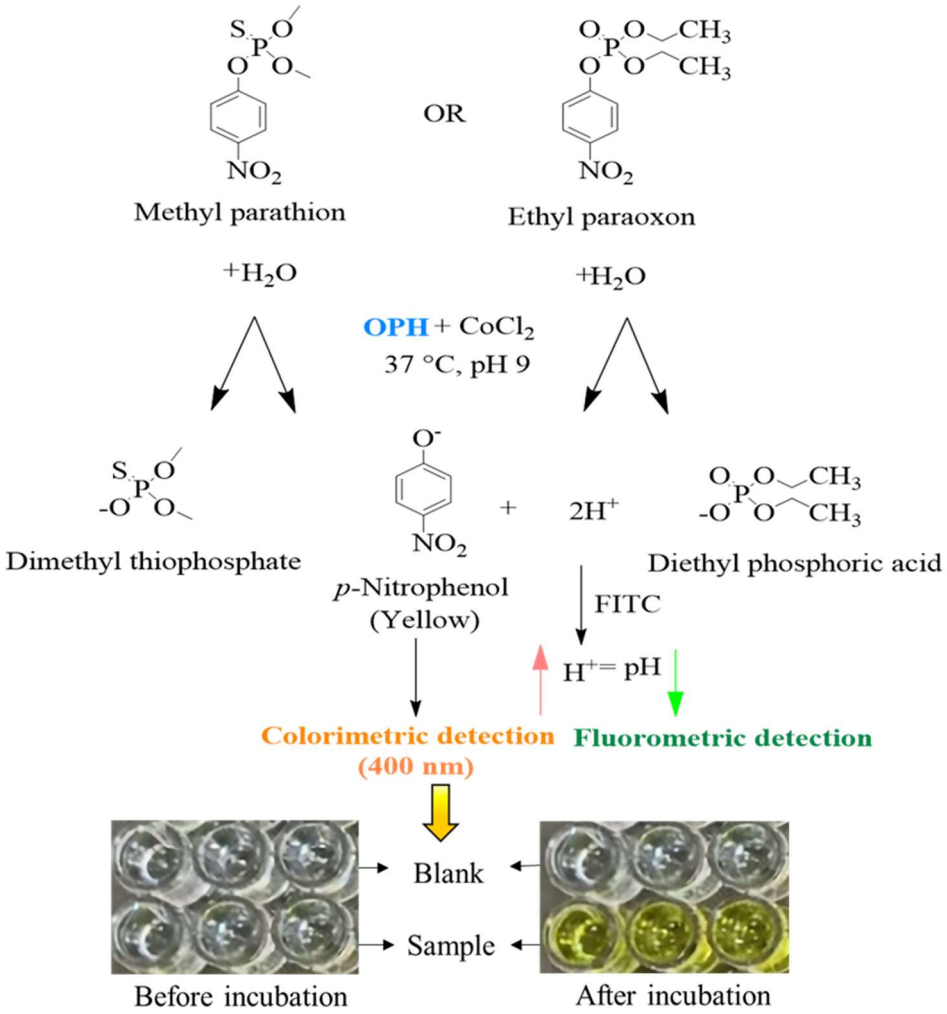

Figure 4.1. OPH reaction mechanism. Depiction of hydrolysis of OP compounds in presence of His-Nus-OPH with *p*-nitrophenol and H^+ as a product which can be detected by colorimetric and fluorometric detection methods, respectively.

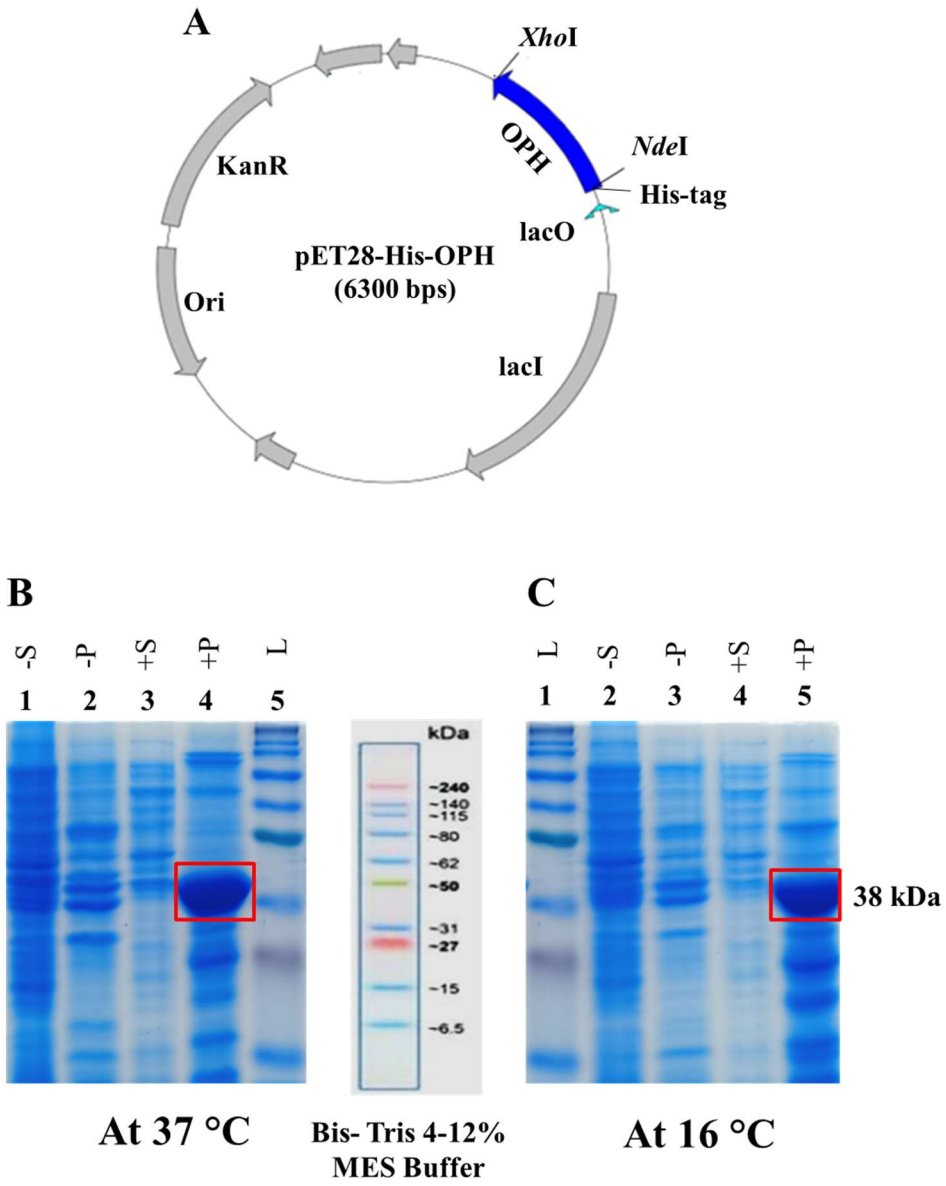

Figure 4.2. **Cloning and expression of OPH (p28-His-OPH) with N-terminal His tag in pET vector. (A)** Map of pET28a with OPH, N-His tag. **(B)** Induction of recombinant His-OPH fusion protein. Induction of His-OPH was performed with 0.1 mM IPTG at 37 °C for 3 hrs. Lane 1: Uninduced supernatant, lane 2: Uninduced pellet, lane 3: Induced supernatant, lane 4: Induced pellet, lane 5: Protein marker. **(C)** Induction of His-OPH was performed at 16 °C for 16 hrs. Lane 1: Protein marker, lane 2: Uninduced supernatant, lane 3: Uninduced pellet, lane 4: Induced supernatant, lane 5: Induced pellet.

vector by using *Nde*I and *Xho*I sites **(Fig. 4.3 A)**. The recombinant cloned plasmid was transformed into *E. coli* Rosetta cells and induced with 0.1 mM IPTG. Cell lysates were prepared and separated as supernatant and pellet to evaluate the amount of protein present in the soluble form. From Fig. 4.3 B at 37 ℃ for 3 hrs induction, no expression of His-Nus-OPH protein in the uninduced supernatant and pellet was observed but surprisingly, it was found that on induction, the His-Nus-OPH protein was expressed in the pellet but not in the supernatant **(Fig. 4.3 B,** lane 4 and 5**)**. To explore the possibility of getting soluble protein via induction at a lower temperature, cells were induced at 16 ℃. From Fig. 4.3 C at 16 ℃ for 16 hrs induction, no expression of His-Nus-OPH protein was observed in the uninduced supernatant and pellet, but it was found that on induction, the 93 kDa His-Nus-OPH protein expression was higher in the supernatant than the pellet **(Fig. 4.3 C,** lane 4 and 5**)**.

An induced band of 93 kDa for His-Nus-OPH fusion protein in the soluble fraction was observed, suggesting that low-temperature expression of OPH along with solubilization Nus-tag assists in getting His-Nus-OPH expressed in the soluble fraction. Since His-Nus-OPH carries an N-terminal His-tag, affinity purification of the recombinant His-Nus-OPH fusion protein was performed on a Ni-NTA resin. N-terminal His-tagged protein was able to bind to the Ni-NTA resin and His-Nus-OPH protein was eluted by using 150 mM Imidazole elution buffer **(Fig. 4.3 D,** lanes 6 to 8**)**. Moreover, more than 90% pure His-Nus-OPH fusion protein was purified due to the proper folding of protein facilitated by the presence of the NusA tag (Nallamsetty and Waugh 2006).

4.2.3 Activity assay of recombinant His-Nus-OPH

To determine whether the recombinant protein is indeed enzymatically active, an OPH enzyme assay was performed. Recombinant His-Nus-OPH fusion protein demonstrated activity in the induced cell lysate as well as in purified fraction. Induced cell lysates were observed to be significantly more active than uninduced cell lysates for methyl

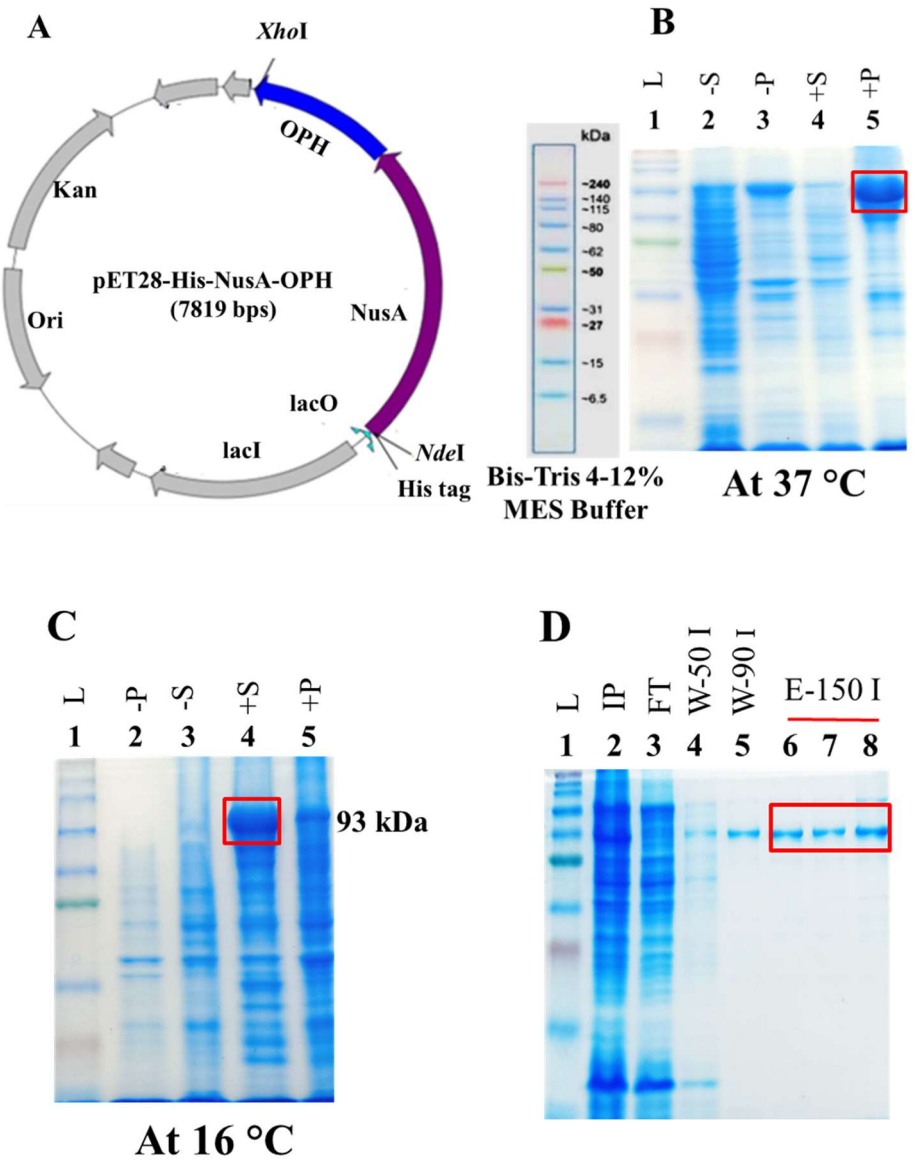

Figure 4.3. Cloning, expression, and purification of OPH (p28-His-Nus-OPH) with N-terminal His and NusA tag in pET vector. (A) Map of pET28a with OPH, N-His-Nus tag. **(B)** Induction of recombinant His-Nus-OPH fusion protein. Induction was performed with 0.1 mM IPTG at 37 °C for 3 hrs. Lane 1: Protein marker, lane 2: Uninduced supernatant, lane 3: Uninduced pellet, lane 4: Induced supernatant, lane 5: Induced pellet. **(C)** Induction of recombinant His-Nus-OPH fusion protein. Induction was performed at 16 °C for 16 hrs. Lane 1: Protein marker, lane 2: Uninduced pellet, lane 3: Uninduced supernatant, lane 4: Induced supernatant and lane 5: Induced pellet. **(D)** Purification of recombinant His-Nus-OPH fusion protein. Lane 1: Protein marker, lane 2: Induced cell extract, lane 3: Flow-through, lane 4, 5: Wash with 50, 90 mM Imidazole, lane 6 to 8: Elution with 150 mM Imidazole.

parathion and ethyl paraoxon. However, purified samples showed higher specific activity as compared with the induced cell lysate.

The specific activity of uninduced, induced, and purified His-Nus-OPH fusion protein was found to be 0.21 U/mg (± 0.006), 24.12 U/mg (± 1.22), and 333 U/mg (± 45.11), respectively, for ethyl paraoxon and 0.57 U/mg (± 0.003), 13.79 U/mg (± 0.89), and 90.2 U/mg (± 6.07), respectively, for methyl parathion **(Fig. 4.4 A and B)** using a 1 mM concentration of the substrates. Thus, it was observed that purified His-Nus-OPH has 13.8 and 6.5 times greater specific activity than the induced His-Nus-OPH with respect to ethyl paraoxon and methyl parathion, respectively, suggesting significant fold purification using affinity chromatography.

The kinetic parameters with ethyl paraoxon and methyl parathion as substrate using solution phase as well as encapsulated His-Nus-OPH have been reported in **Table 4.1** and **Fig. 4.5 and 4.6**. Kinetic parameters with ethyl paraoxon and methyl parathion as a substrate for OPH, as reported by other groups are listed in **Table 4.2.**

4.2.4 Effect of temperature and pH on recombinant His-Nus-OPH activity

Considering the significant specific activity with ethyl paraoxon, the effect of temperature and pH on the activity of His-Nus-OPH in the solution phase was studied. The effect of temperature on the activity of purified recombinant His-Nus-OPH was determined at varying temperatures ranging from 20 – 45 ºC with an interval of 5 ºC but also including 37 ºC. In concurrence with earlier studies (Liu et al. 2016), His-Nus-OPH activity was found to gradually increase until 37 ºC, and a subsequent rise in temperature decreased the activity. Hence, it is suggested that 37 ºC is the optimum temperature for His-Nus-OPH with ethyl paraoxon **(Fig. 4.7 A)**.

The effect of pH on the activity of purified recombinant His-Nus-OPH was determined at a pH range of 6 – 10 with an interval of 0.5 pH

units. These experiments showed the optimum activity at pH 9.0 for His-Nus-OPH **(Fig. 4.7 B)**.

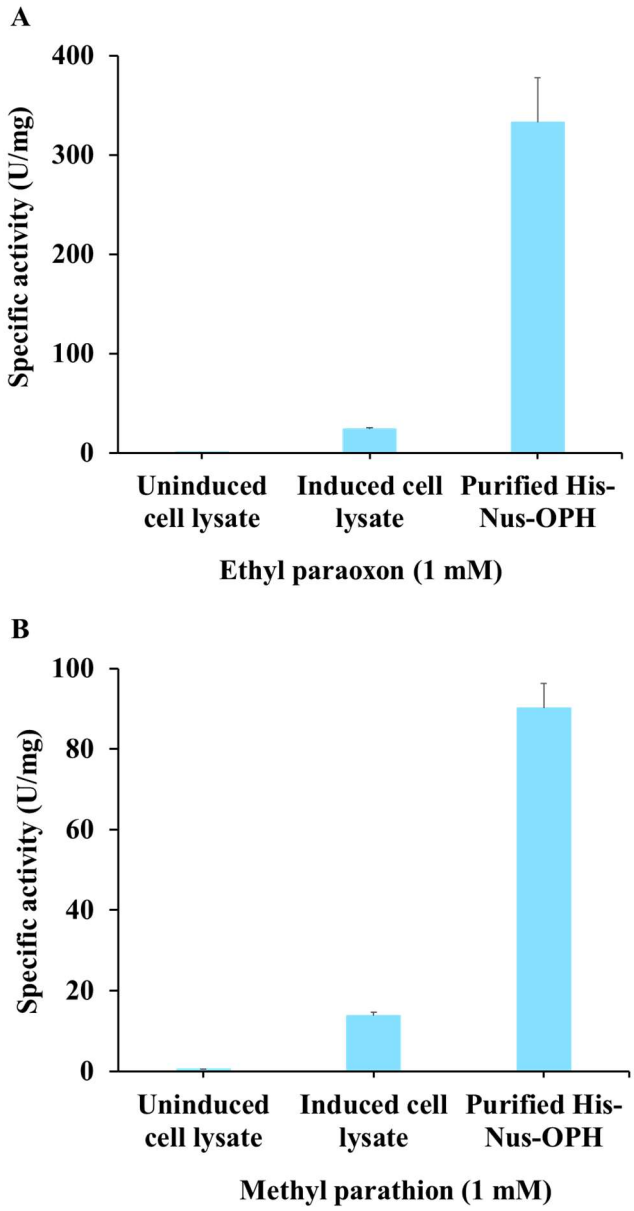

Figure 4.4. Colorimetric activity assay of solution-phase His-Nus-OPH with different substrates. His-Nus-OPH with 1 mM substrate in the presence of CHES buffer, pH 9.0, at 37 ºC for 5 minutes **(A)** 1 mM of ethyl paraoxon **(B)** 1 mM of methyl parathion. The values are represented as the average of duplicate samples and the standard deviation is indicated by error bars. A representative result is shown based on at least three separate experiments.

Table 4.1 Kinetic parameters of His-Nus-OPH with ethyl paraoxon and methyl parathion

Sample	Substrate Concentration (0.1 to 9 mM)	V_{max} (U/mg)	K_m (mM)	k_{cat} (min^{-1})	k_{cat} / K_m ($mM^{-1} min^{-1}$)
Solution phase His-Nus-OPH	Ethyl paraoxon	416.6	1.916	38743.8	20217.4
	Methyl parathion	45.248	1.217	4208.064	3457.249
Encapsulated His-Nus-OPH	Ethyl paraoxon	77.5	2.123	7207.5	3394.16
	Methyl parathion	6.281	0.538	584.133	1085.181

Table 4.2 Kinetic parameters of purified OPH with ethyl paraoxon and methyl parathion

S. No.	V_{max}	K_m	k_{cat}	k_{cat} / K_m	References
Kinetic parameters of purified OPH with ethyl paraoxon					
1		0.12 mM	11500 S^{-1}	9.6×10^7 M^{-1} S^{-1}	(Simonian et al. 2001)
2	2070 U/mg	0.05 mM			(Petrikovics et al. 2000)
3		0.12 ± 0.01 mM	15000 ± 300 S^{-1}	1.3 * 10^8 M^{-1} S^{-1}	(diSioudi et al. 1999)
4				1 * 10^8 M^{-1} S^{-1}	(Di Sioudi et al. 1999)
5				5.5 *10^7 M^{-1} ^{L} S^{-1}	(Karpouzas and Singh 2006)

6		2100 S^{-1}		(Dave et al. 1993)
7	0.058 mM	3170 S^{-1}	55,000 mM^{-1} S^{-1}	(Theriot and Grunden 2011)
8	0.12 mM	10,500 S^{-1}	8.75 * 10^{7} M^{-1} S^{-1}	(Grimsley et al. 2005)
9	0.40 ±0.02 mM	4010 ± 40 S^{-1}	10 *10^{6} M^{-1} S^{-1}	(Carletti et al. 2009)
10	0.12 ± 0.003 mM	11700 ± 580 S^{-1}	1.0 * 10^{8} M^{-1} S^{-1}	(Cho et al. 2006)
11	0.016 ± 0.5 mM	4900 ± 100 S^{-1}	(3.0 ± 0.2) * 10^{8} M^{-1} S^{-1}	(Votchitseva et al. 2006)

Kinetic parameters of purified OPH with methyl parathion					
S. No.	**V_{max}**	**K_m**	**k_{cat}**	**k_{cat} / K_m**	**References**
1		0.08 mM	189 S^{-1}	2400 mM^{-1} S^{-1}	(Theriot and Grunden 2011)
2	2.5 µM/min	0.2862 mM			(Maheshwari et al. 2017)
3	50 µM/min	0.28571 mM			(Gothwal et al. 2014)
4	508 U/ml	0.599 mM	369.7 S^{-1}		(Rowland et al. 1991)
5		1.22 ± 0.03 mM	2300 ± 130 S^{-1}	1.9 * 10^6 M^{-1} S^{-1}	(Cho et al. 2006)
6		0.21 ± 10 mM	75 ± 5 S^{-1}	(3.5 ± 0.2) * 10^5 M^{-1} S^{-1}	(Votchitseva et al. 2006)

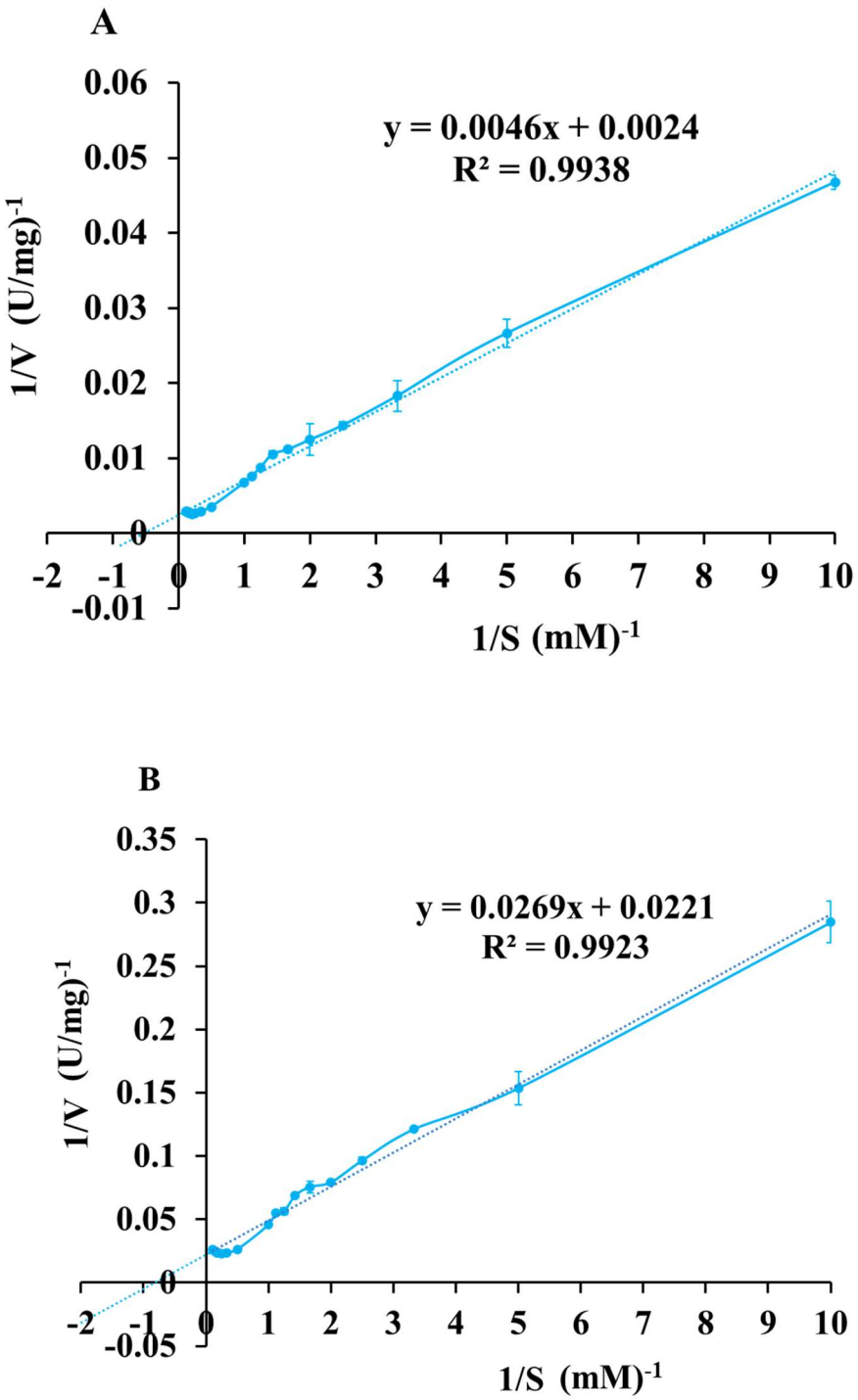

Figure 4.5. Lineweaver burk plot for solution phase His-Nus-OPH. **(A)** Ethyl paraoxon. **(B)** Methyl parathion. The values are average of duplicate samples and error bars represent standard deviation.

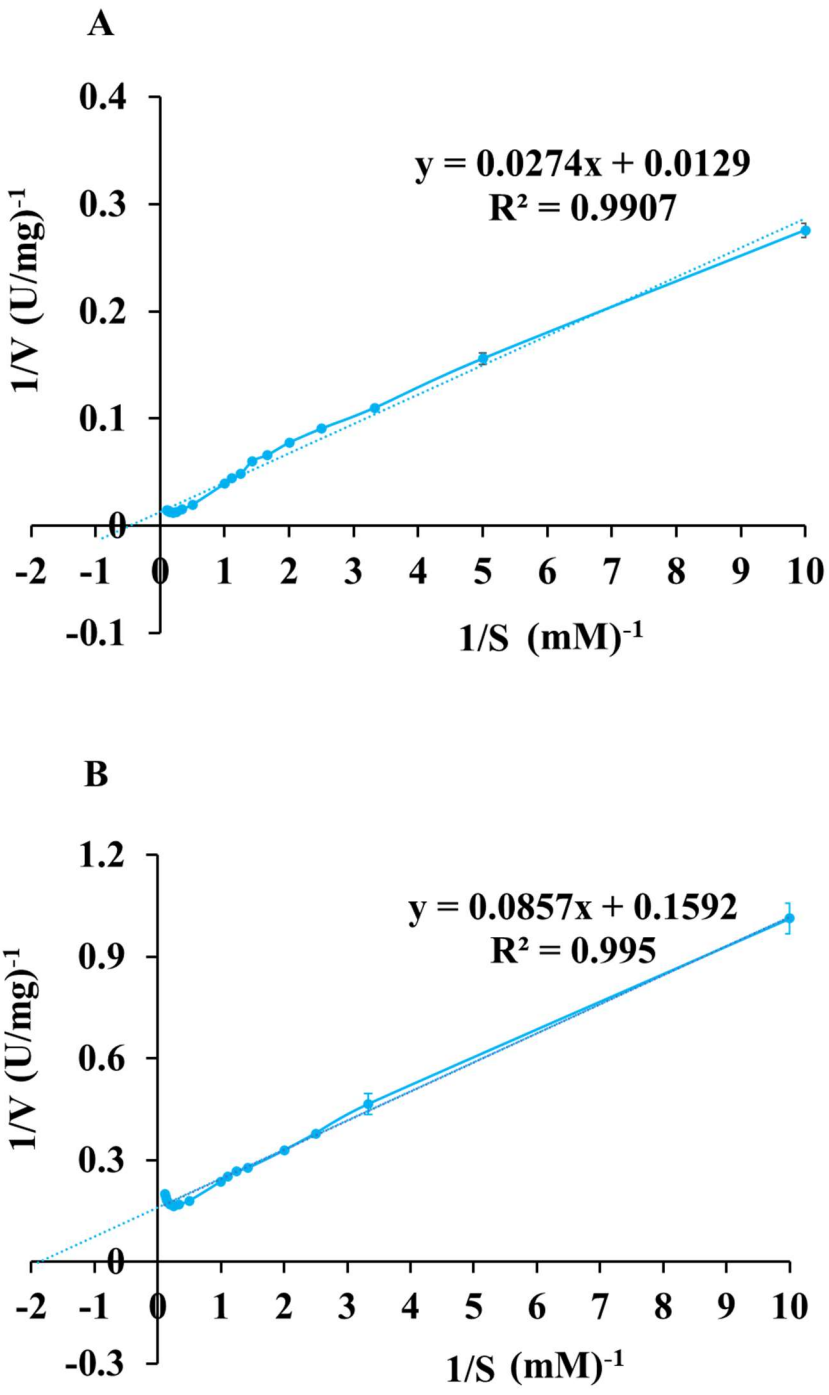

Figure 4.6. Lineweaver burk plot for encapsulated His-Nus-OPH. **(A)** Ethyl paraoxon. **(B)** Methyl parathion. The values are average of duplicate samples and error bars represent standard deviation.

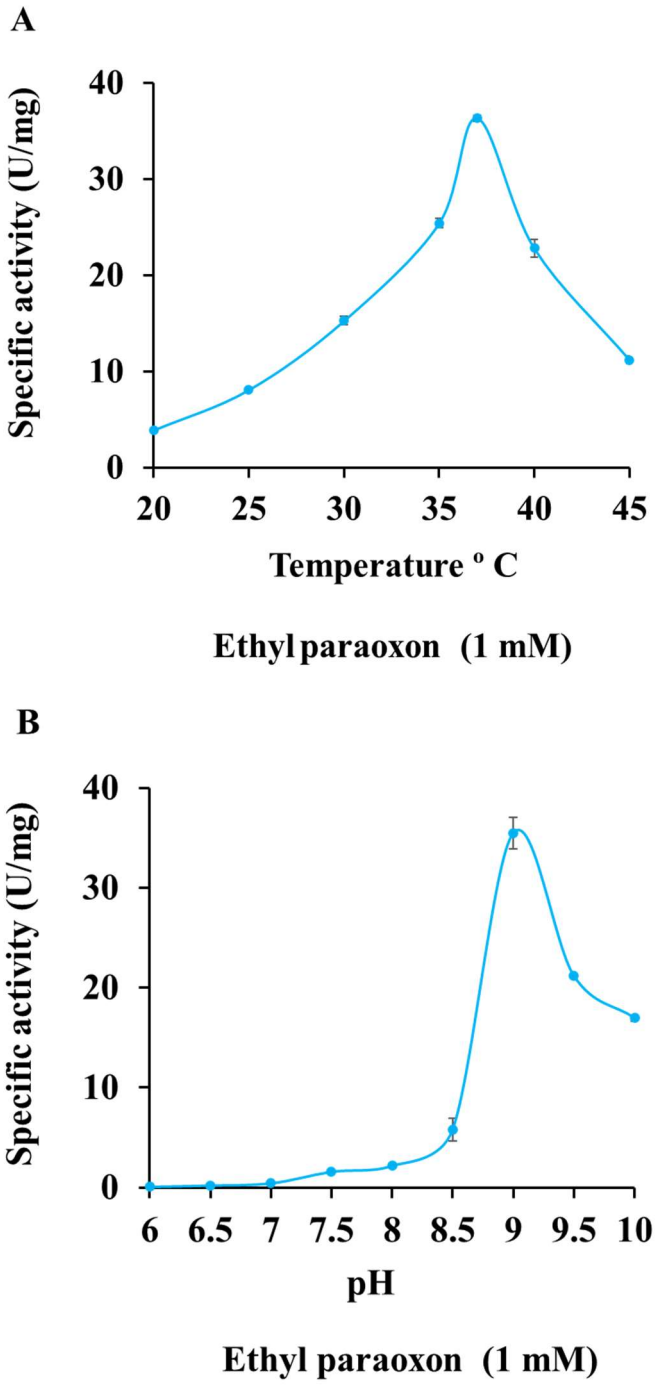

Figure 4.7. Effect of temperature and pH on solution-phase His-Nus-OPH activity. (A) Effect of temperature on the specific activity of solution-phase His-Nus-OPH with ethyl paraoxon. **(B)** Effect of pH on the specific activity of solution-phase His-Nus-OPH ethyl paraoxon. The values are represented as the average of duplicate samples and the standard deviation is indicated by error bars. A representative result is shown based on at least three separate experiments.

4.2.5 Encapsulation of His-Nus-OPH and FITC-dextran/His-Nus-OPH in alginate microspheres using an ultrasonic atomizer

In recent times, encapsulation of proteins and cells are increasingly being explored in order to protect biomolecules from detrimental environmental factors such as pH changes, salts, or reactive oxygen species, etc. (Dong et al. 2013). To this end, materials such as polysaccharides and lipids have been used as encapsulants.

Among these, alginate-based encapsulation has gained prominence due to its favourable properties such as good immobilization capacity, mechanical stability, water retention capability, heat stability, controllable porosity, low toxicity, and biocompatibility (A. Chaudhari et al. 2015). Proteins are encapsulated in different natural/synthetic polymers with an aim to maintain enzyme activity and increase stability. His-Nus-OPH protein was encapsulated in 0.7% sodium alginate by using an ultrasonic atomizer, chosen for reasons of high productivity, biocompatibility, mild gelation and formation conditions, industrial relevance, and good particle size distribution (Joshi et al. 2010; Leong et al. 2016). 4% $CaCl_2$ was used as a cross-linker to maximize bead formation and achieve a smaller particle size (Park et al. 2012; Jiang et al. 2015; Kim et al. 2016). Ionic gelation is the main principle behind the formation of alginate microspheres from atomized droplets created using the ultrasonic atomizer due to ultrasonic waves. To optimize the particle size distribution of alginate microspheres different instrumental parameters like frequency, flow rate, the distance of crosslinking were evaluated. Ultrasonic atomizer was utilized as described previously to co-immobilize FITC-dextran which acts as a pH-sensitive fluorophore along with His-Nus-OPH.

4.2.6 Characterization of alginate microspheres

SEM analysis was performed to observe the encapsulation of His-Nus-OPH into the alginate microspheres revealing the spherical-shaped porous microspheres of His-Nus-OPH ranging from 7 to 37 µm, and the average size of the particle was found to be 18.8 µm **(Fig. 4.8 A and B)**. Moreover, the spherical morphology has been reported to enhance the

stability and mechanical strength of the constituents (Sandoval-Castilla et al. 2010). Higher porosity of the alginate microsphere aids in the transport of analyte and product across the beads for continuous catalysis by the enzymes. The encapsulated FITC-Dextran and FITC-Dextran/His-Nus-OPH were characterized by CLSM, which confirmed the successful incorporation of FITC-Dextran/His-Nus-OPH in the alginate microspheres **(Fig. 4.8 C and D).** The CLSM analysis revealed that FITC-Dextran and FITC-Dextran/Nus-OPH microcarriers have typical particle sizes ranging from 3 to 22 µm and 10.7 to 30.4 µm, respectively, and average particle sizes of 13.0 µm and 20.5 µm, respectively.

Encapsulation efficiency is the percentage of protein that is successfully entrapped into the microspheres, which was determined in this study **(Fig. 4.8 E,** lanes 3 and 4 to 6**)**. Subsequently, it was estimated that the encapsulation efficiency of His-Nus-OPH into the alginate microspheres by boiling the alginate microspheres and running these on 8% SDS-PAGE, along with input and wash controls **(Fig. 4.8 E)**. In general, 10 – 20% encapsulation efficiency was observed, and this value was used to calculate the amount of protein present inside alginate microspheres after encapsulation.

4.2.7 Colorimetric biosensing of ethyl paraoxon and methyl parathion

Colorimetric biosensing of His-Nus-OPH was performed with 0.005, 0.01, 0.05, 0.1, 0.2, 0.3, 0.4, 0.5, 0.6, 0.8, 0.9 and 1 mM of ethyl paraoxon and 0.005, 0.01, 0.05, 0.1, 0.2, 0.3, 0.4, 0.5, 0.6, 0.8 and 1 mM methyl parathion and specific activity with respect to the aforementioned concentrations was found to be 10.04, 12.49, 14.23, 21.38, 37.64, 55.02, 69.64, 81.61, 89.78, 114.53, 131.30, 148.68 U/mg with ethyl paraoxon and 0.16, 0.23, 2.39, 3.51, 6.53, 8.24, 10.37, 12.62, 13.25, 17.74, 21.86 U/mg for methyl parathion **(Fig. 4.9 A and B)**. Colorimetric biosensing of encapsulated His-Nus-OPH was performed with 0.005, 0.01, 0.1, 0.2, 0.3, 0.4, 0.5, 0.6, 0.8, 0.9, and 1 mM of ethyl paraoxon and 0.005, 0.01, 0.025, 0.05, 0.2, 0.3, 0.6, 0.8, 1 mM methyl parathion, respectively, and specific activity with respect to the after mentioned concentrations was found to be 1.69, 2.09, 3.62, 6.42, 9.07, 11.03, 12.9, 15.11, 20.76, 22.57 and 25.39

U/mg with ethyl paraoxon **(Fig. 4.10 A),** and 0.07, 0.12, 0.34, 0.72, 1.67, 2.97, 4.77, 6.37 and 8.66 U/mg for methyl parathion **(Fig. 4.10 B)**. The detailed parameters such as linear range, sensitivity, LOD, and linearity of the solution-phase, as well as encapsulated His-Nus-OPH used in the colorimetric assay for ethyl paraoxon and methyl parathion, are given in **Table 4.3 A**. The linear range for the detection of ethyl paraoxon was found to be 0.005-1 mM for both the solution-phase and encapsulated phase, of the His-Nus-OPH enzyme.

Similarly, for methyl parathion linear range was 0.005-1 mM in the case of purified His-Nus-OPH enzyme in both solution-phase and encapsulated forms. In general, better detection limits are observed for encapsulated His-Nus-OPH compared to solution-phase His-Nus-OPH, that is, 0.024 and 0.049 mM for encapsulated His-Nus-OPH compared to 0.034 and 0.06 mM for solution-phase His-Nus-OPH, w.r.t. ethyl paraoxon and methyl parathion, respectively. It is observed that the assay with solution-phase and encapsulated His-Nus-OPH is more sensitive with greater linearity and lower LOD for ethyl paraoxon compared to methyl parathion. Response time for the purified enzyme was found to be about 5 min, for both paraoxon and methyl parathion, in the solution phase. For the encapsulated enzyme, however, the response time for ethyl paraoxon and methyl parathion respectively was 10 minutes and 20 minutes. The increase in response time in the encapsulated phase is likely due to the additional diffusion barrier of alginate microspheres for interaction with the substrates.

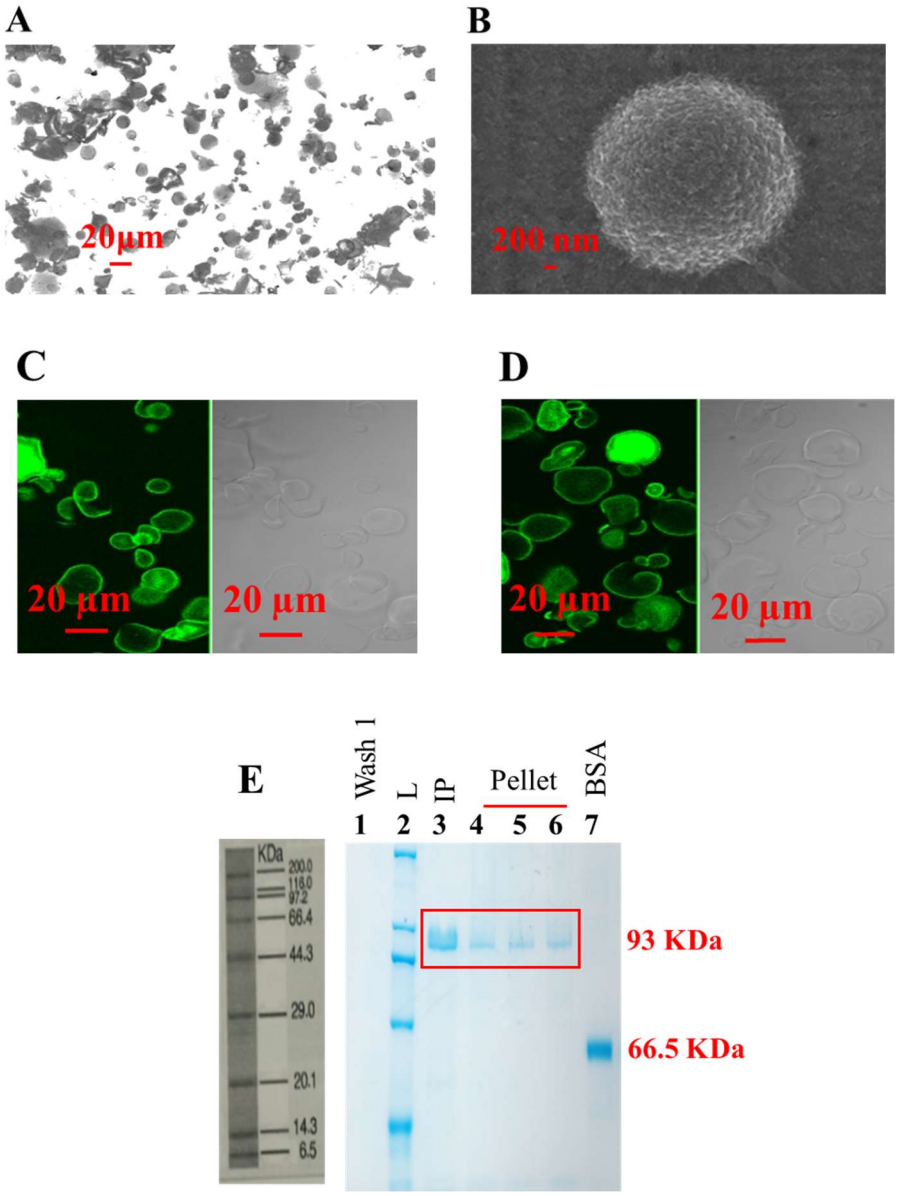

Figure 4.8. Encapsulation and characterization of His-Nus-OPH and FITC-dextran/His-Nus-OPH. SEM images of His-Nus-OPH loaded alginate microspheres with 0.7% alginate. Spherical-shaped beads were observed in SEM. **(A-B)** His-Nus-OPH loaded alginate microspheres at 513 X and 55 K X magnification respectively. **(C)** CLSM image of FITC-Dextran loaded alginate microcarriers at 60 X. **(D)** CLSM image of FITC-Dextran/His-Nus-OPH loaded alginate microcarriers at 60 X. At least three independent experiments were performed, and a representative result is shown. **(E)** Analysis of His-Nus-OPH loaded alginate microspheres using SDS-PAGE. Lane 1: Unencapsulated His-Nus-OPH in wash 1 after buffer exchange, lane 2: protein marker, lane 3: input sample, lane 4 to 6: encapsulated His-Nus-OPH, lane 7: 2 µg of BSA.

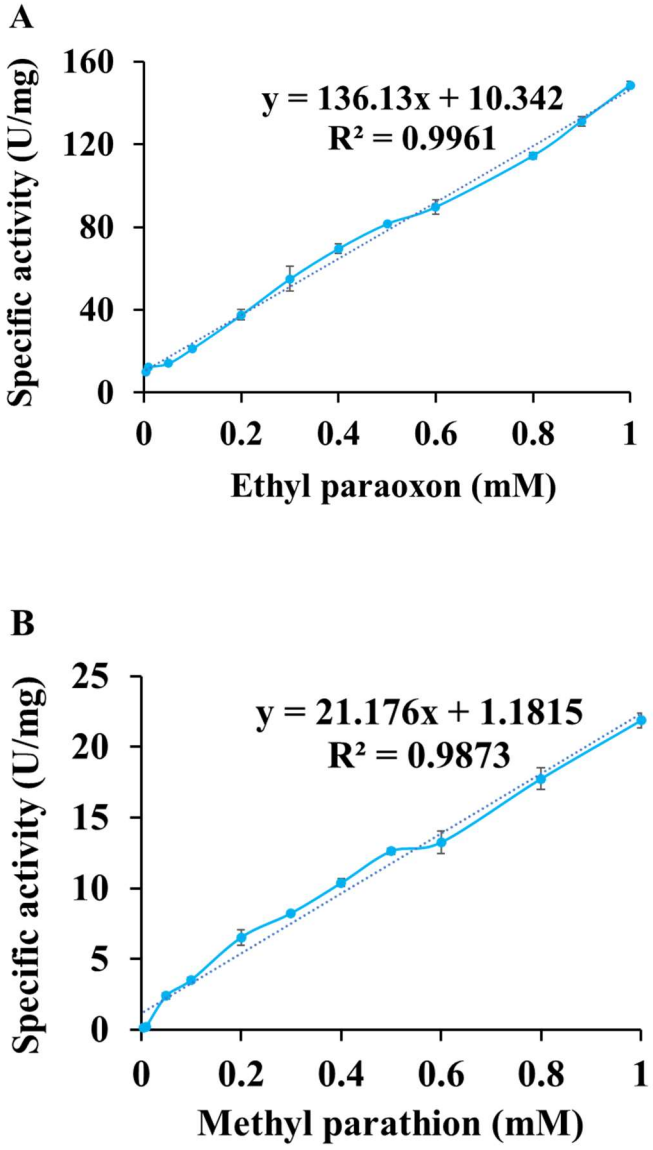

Figure 4.9. Colorimetric activity assay of solution-phase His-Nus-OPH with different substrate concentrations. His-Nus-OPH with 0.005 to 1 mM of the substrate in the presence of CHES buffer pH 9.0, at 37 ºC for 5 minutes. **(A)** With ethyl paraoxon **(B)** With methyl parathion. The values are represented as the average of duplicate samples and the standard deviation is indicated by error bars. A representative result is shown based on at least three separate experiments.

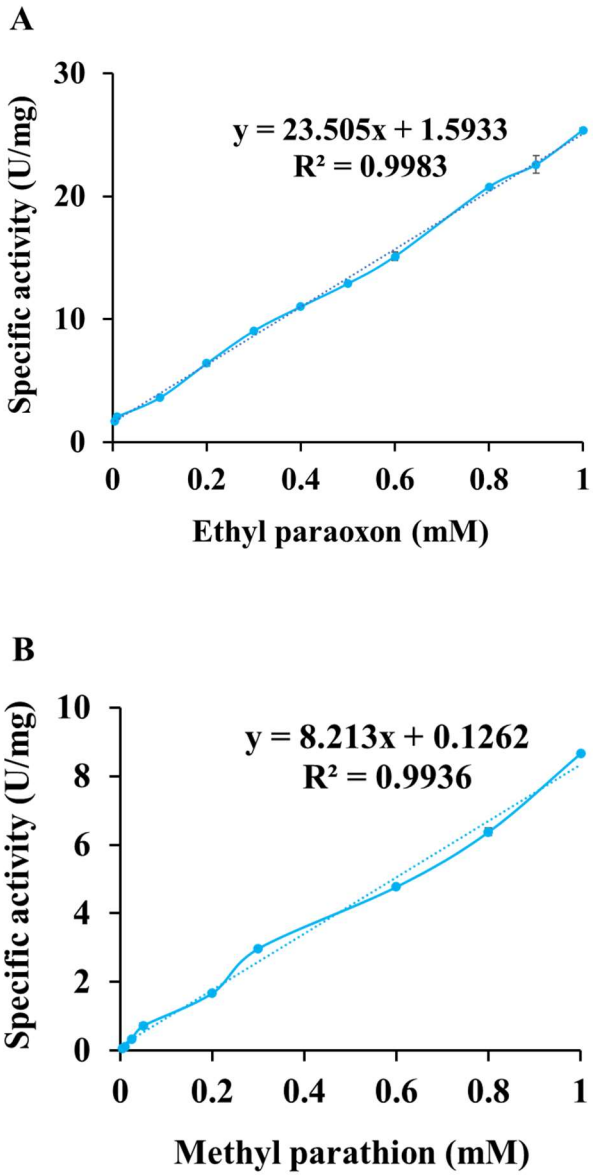

Figure 4.10. Colorimetric activity assay of encapsulated His-Nus-OPH with different substrate concentrations. (A) Activity assay of His-Nus-OPH with 0.005, 0.01, 0.1, 0.2, 0.3, 0.4, 0.5, 0.6, 0.8, 0.9, and 1 mM of ethyl paraoxon, CHES buffer at 37 ºC for 10 minutes. **(B)** Activity assay of His-Nus-OPH with 0.005, 0.01, 0.025, 0.05, 0.2, 0.3, 0.6, 0.8 and 1 mM of methyl parathion, CHES buffer at 37 ºC for 20 minutes. The values are represented as the average of duplicate samples and the standard deviation is indicated by error bars. A representative result is shown based on at least three separate experiments.

4.2.8 Fluorescence biosensing of ethyl paraoxon and methyl parathion

The assay was developed based on a decrease in fluorescence intensity of pH-sensitive fluorophore FITC-dextran (Chen et al. 2015). Upon the interaction of OPH with OP compounds a decrease in pH of the solution occurs due to the release of protons with the concurrent release of PNP (Prieto-Simón et al. 2006). The resultant drop in pH causes protonation of negatively charged FITC results in quenching of fluorescence, and this phenomenon was exploited to detect the presence of OPs (Chaudhari et al. 2017). To know optimum buffer and reaction conditions for fluorometric detection of OPs using His-Nus-OPH in solution-phase initially, it was tested for a decrease in the fluorescence values (if any) of FITC in the different buffer concentrations. The reaction mixture was prepared with 0.1 mM $CoCl_2$, 1 mM ethyl paraoxon, His-Nus-OPH, FITC-dextran, and sterile distilled water up to 1 ml. 0 mM, 10 mM, and 50 mM activity buffer (CHES), was used respectively, and measured loss in the fluorescence values. It was observed that the reaction mixture with 0 mM CHES buffer showed a greater decrease in the intensity in comparison to the reaction mixture with the 10 and 50 mM concentration of CHES buffer in it. This could be because the presence of buffer neutralized the H^+ ions released during the reaction due to the inherent buffering capacity of the buffers. It is observed that the interaction of His-Nus-OPH with OP compounds such as ethyl paraoxon result in a decrease in fluorescence intensity of FITC dye over a time period of 0-20 minutes due to the progressive release of H^+ ions by the hydrolysis of OP compounds **(Fig. 4.11 A and B)**. Thus, for all fluorescent sensing experiments, no CHES buffer was used. Moreover, when His-Nus-OPH:FITC (1:12) was used in solution-phase with 0.001, 0.005, 0.025, 0.05, 0.1, 0.3, 0.5 mM of ethyl paraoxon and 0.005, 0.025, 0.05, 0.1, 0.5 mM of methyl parathion, respectively, the rate of fluorescence decay increased with the concentration of substrate **(Fig. 4.12 A and B)**. The 1:12 ratio of His-Nus-OPH : FITC was selected to optimize for good sensitivity (Wischke and Borchert 2006).

Fluorescence-based bio-sensing of His-Nus-OPH with different concentrations of ethyl paraoxon and methyl parathion showed a linear range of 0.001 to 0.5 mM and 0.005 to 0.5 mM, respectively. The LOD of bio-sensing was 0.014 mM for ethyl paraoxon and 0.044 mM for methyl parathion, and the sensitivity defined as the slope of the linear concentration curve, (Gauglitz 2018) was 95.96 % / mM for ethyl paraoxon and 47.18 % / mM for methyl parathion, respectively. The fluorescence intensity of FITC decreased linearly with an increase in the concentration of ethyl paraoxon or methyl parathion. Due to the increase in enzymatic activity, there is a decrease in pH, which eventually results in a decrease in the fluorescence intensity of FITC. The detailed parameters such as linear range, sensitivity, LOD, and linearity of the solution-phase His-Nus-OPH used in fluorescence assay with ethyl paraoxon and methyl parathion are given in **Table 4.3 B**. It is observed that the assay with His-Nus-OPH is more sensitive with greater linearity and lower LOD for ethyl paraoxon compared to methyl parathion. Incidentally, the encapsulated His-Nus-OPH microspheres did not show expected biosensing response in the fluorescence assay which can be postulated to be because of interference of polymer in pH-based detection.

Table 4.3 Biosensing parameters of His-Nus-OPH

Table 4.1 A Colorimetric biosensing parameters of solution-phase and encapsulated His-Nus-OPH

S. No.	Sample	Substrate	LOD (mM)	Sensitivity (U/ mg/ mM)	Linear range (mM)	Response time (Minutes)	Linearity (R^2)
1	Solution-phase His-Nus-OPH	Ethyl paraoxon	0.034	139.3	0.005-1	5	0.9961
		Methyl parathion	0.06	21.8	0.005-1	5	0.9873
2	Encapsulated His-Nus-OPH	Ethyl paraoxon	0.024	23.8	0.005-1	10	0.9983
		Methyl parathion	0.049	8.6	0.005-1	20	0.9936

Table 4.1 B Fluorometric biosensing parameters of solution-phase His-Nus-OPH

S. No.	Sample	Substrate	LOD (mM)	Sensitivity (% / mM)	Linear range (mM)	Response time (Minutes)	Linearity (R2)
1	Solution-phase His-Nus-OPH	Ethyl paraoxon	0.014	95.96	0.001-0.5	5	0.9982
		Methyl parathion	0.044	47.2	0.005-0.5	5	0.9898

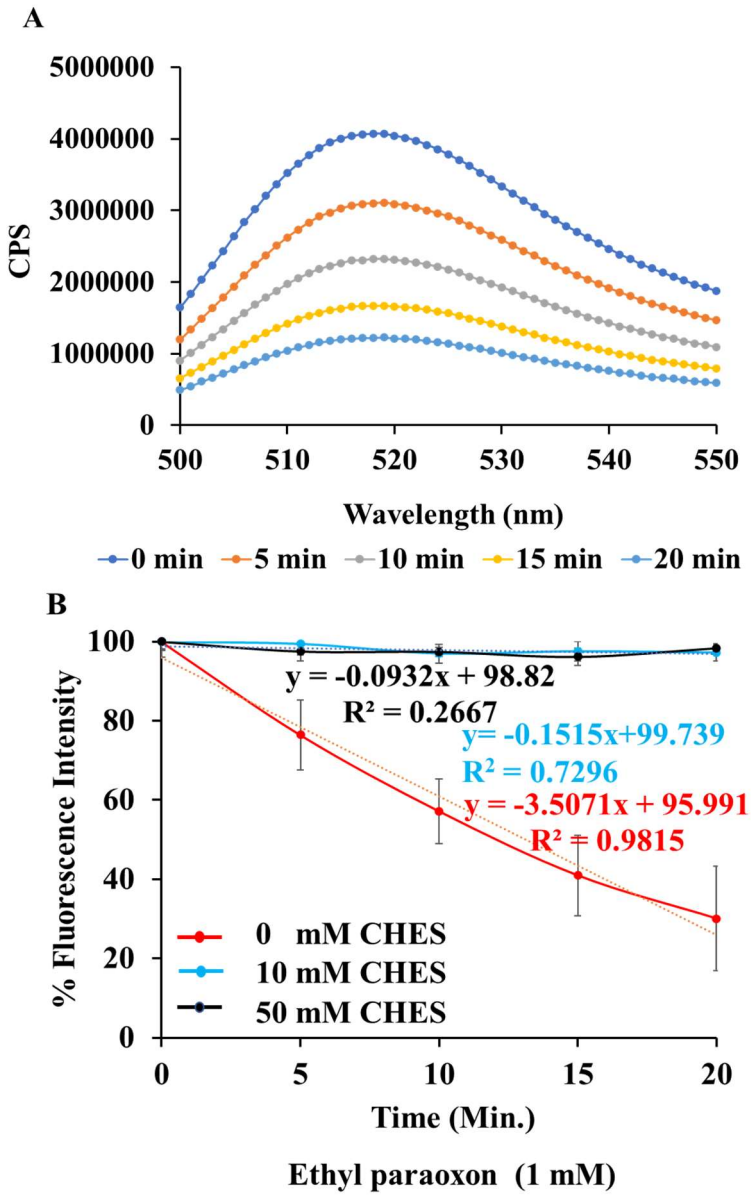

Figure 4.11. Optimization of the concentration of CHES buffer for solution-phase His-Nus-OPH fluorescence assay. Fluorescence activity assay of solution-phase His-Nus-OPH enzyme detected using FITC, a pH-sensitive dye. With an increase in enzymatic activity, there is a decrease in pH which eventually results in a decrease in fluorescence intensity of FITC. **(A)** 0 mM CHES buffer was used at 37 ºC, pH 9.0 for 20 minutes with an interval of 5 minutes with ethyl paraoxon, and with an increase in time fluorescence intensity was decreased. **(B)** 0 mM, 10 mM, and 50 mM CHES buffer were used at 37 ºC, pH 9.0 for 20 minutes with an interval of 5 minutes with ethyl paraoxon. The decrease in the intensity of FITC was more in the case of the reaction mixture in which a 0 mM CHES buffer was used. The values are represented as the average of duplicate samples and the standard deviation is indicated by error bars. A representative result is shown based on at least three separate experiments.

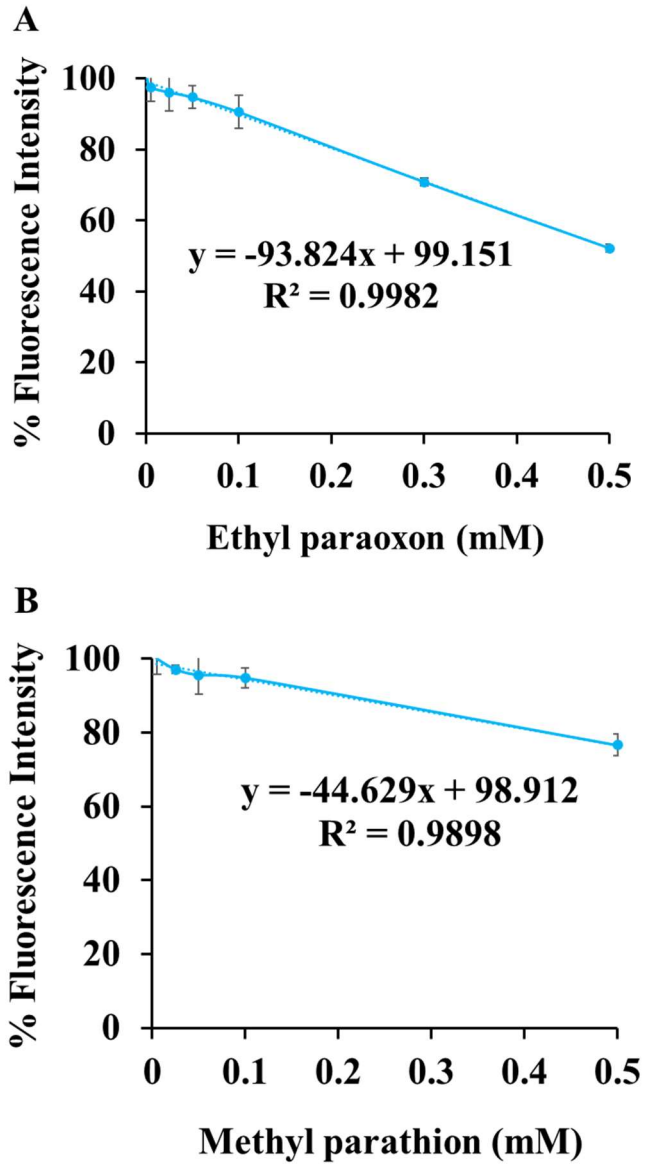

Figure 4.12. **Bio-sensing of OPs using solution-phase His-Nus-OPH via fluorescence assay.** The 1:12 ratio of His-Nus-OPH and FITC-dextran was used at 37 ºC, without activity buffer. **(A)** Fluorescence assay of His-Nus-OPH with 0.001, 0.005, 0.025, 0.05, 0.1, 0.3 mM, 0.5 mM of ethyl paraoxon, for 5 minutes. **(B)** Fluorescence assay of His-Nus-OPH with 0.005, 0.025, 0.05, 0.1, 0.5 mM of methyl parathion, for 5 minutes. The values are represented as the average of duplicate samples and the standard deviation is indicated by error bars. A representative result is shown based on at least three separate experiments.

4.3 Summary

This chapter demonstrated that NusA-tagged OPH (His-Nus-OPH) was found to be soluble and hence purified to be used in colorimetric and fluorometric assays for organophosphate detection. The study also demonstrated that His-Nus-OPH yields enhanced enzymatic activity for the degradation of organophosphate compounds while being a good candidate for use as a colorimetric biosensor when encapsulated with alginate microspheres. This study indicates good specific activity for the purified His-Nus-OPH, i.e., 333 U/mg and 90.2 U/mg for ethyl paraoxon and methyl parathion, respectively. Solution phase His-Nus-OPH protein and protein encapsulated using a novel method of ultrasonic atomization used in a colorimetric assay where encapsulated protein gave improved LOD than solution-phase His-Nus-OPH with a same linear range of substrates. A fluorescence-based method was also established using FITC dextran for solution-phase His-Nus-OPH. Fluorescence emission drop suggested a linear decrease over a concentration range of 0.001-0.5 mM in the case of ethyl paraoxon, and 0.005-0.5 mM in the case of methyl parathion, respectively. As expected, the limit of detection was found to superior for fluorescence assay than a colorimetric assay for ethyl paraoxon and methyl parathion. The results indicate that the NusA-tagged OPH enzyme can be used in both colorimetric and fluorescence-based sensor systems with good detection limits, response time, and linearity. Future research efforts to further enhance the performance should be focused on structural modifications to enhance the catalytic activity, as well as enhancing the long-term stability of the sensor.

Chapter 5

Chapter 5

Fluorometric biosensing of organophosphates using a recombinant organophosphorus acid anhydrolase (OPAA)-FL variant with monomeric teal fluorescent (mTFP) fusion protein expressed in *E. coli*.

5.1 Introduction

In the previous chapters, the structure, properties, and benefits of the OPAA enzyme for biosensor development have been discussed in detail. In continuous efforts to explore the development of sensing platforms, the use of fusion proteins with OPAA-FL and a fluorescent protein that is a mTFP1 was done. Unlike several widely used fluorescent proteins, mTFP1 is a true monomer and possibly does not interfere with its fusion partner's function. Fusion proteins have advantages in terms of stability, repeatability easier purification, and avoid the requirement of specific labelling and complex processing while providing enhanced fluorescent outputs for analytical and sensing applications (Wu et al. 2018). In the current chapter, the use of mTFP1 has been explored as the fluorophore, and a fusion protein has been developed with OPAA-FL and mTFP1. mTFP1 is one of several known and popular fluorescent proteins in the life sciences, belongs to the green fluorescent protein (GFP) family, and is popularly used for imaging applications (Ai et al. 2008; Topol et al. 2010). Corals are among the most common and frequently encountered sources of fluorescent proteins. mTFP1 is a codon-optimized and monomeric version of cFP484, a tetrameric cyan FP (CFP) from Clavularia coral, developed for narrower and single-peaked emission characteristics, photostability, pH sensitivity, and improved brightness (Ai et al. 2008). It is desirable to combine the molecular recognition element with a signal output element for sensor development. With this in mind, a fluorescent fusion protein of OPAA-FL-mTFP1 was designed, which was

utilized in one of very few known studies with fusion proteins for analytical purposes (Wu et al. 2018). This chapter describes the first use of an OPAA-FL-mTFP1 fluorescent fusion protein for the sensing of organophosphate compounds with the use of a fluorescent mTFP1 fusion partner. This study indicated that OPAA-FL-mTFP1 works favourably for the detection of OP compound ethyl paraoxon, with detection limits as low as 0.0254 mM and 0.098 mM, and a linear range of 0.005 – 1 mM and 0.05 – 0.75 mM for colorimetric and fluorometric sensing, respectively. A detailed experimental procedure of cloning, expression, purification, kinetics, and interpretation is provided in the following sections, along with the colorimetric and fluorometric sensing results.

5.2 Results

5.2.1 Cloning, expression, and purification of mTFP1, N- terminal His tag fusion protein in pET vector

A gene for the mTFP1 was cloned into a pET28 expression vector giving pET28-His-mTFP1 **(Fig. 5.1 A)** and subsequently transformed into expression host *E. coli* Rosetta (DE3) cells with the mTFP1 expression vector were induced with 0.1 mM IPTG at 20 ^{o}C for 20 hrs. The results of the expression of mTFP1 in both pellet and supernatant are shown in **Fig. 5.1 B**, no expression of mTFP1 protein was observed in the uninduced supernatant and pellet. As expected, it was found that on induction, the mTFP1 protein was expressed more in the supernatant. **(Fig. 5.1 B,** lane 5**)**. The soluble form of 27 kDa His-mTFP1 was obtained, and subsequently, affinity purified on a Ni-NTA resin as mTFP1 protein has an N-terminal His tag with an affinity towards Ni-NTA resin and eluted in 150 mM imidazole elution buffer. **(Fig. 5.1 C,** lane 5**)**.

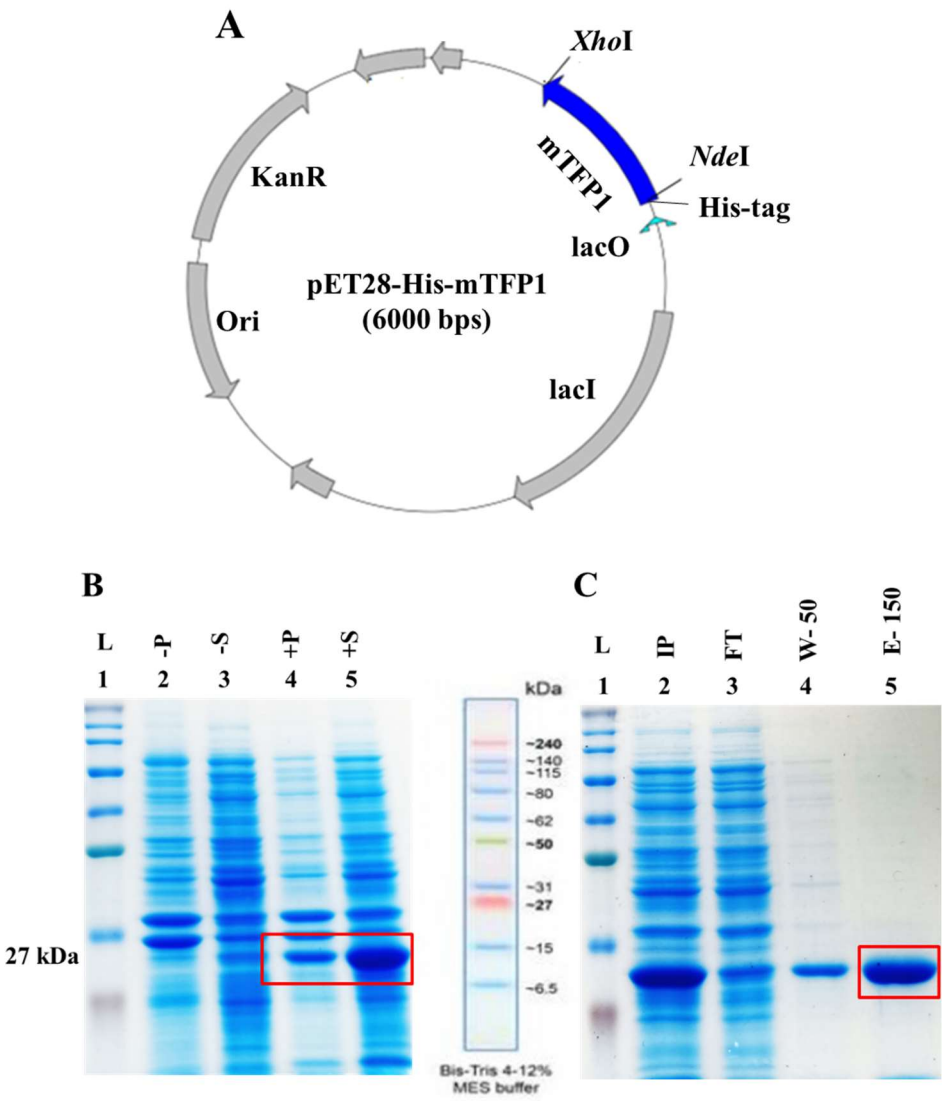

Figure 5.1 Cloning, expression, and purification of His-mTFP1. (A) Map of pET28 with mTFP1, N-His tag. **(B)** Induction of His-mTFP1 protein. Induction of His-mTFP1 was performed at 20 °C for 20 hrs. lane 1: Protein marker, lane 2: Uninduced pellet, lane 3: Uninduced supernatant, lane 4: Induced pellet, lane 5: Induced supernatant. **(C)** Purification of recombinant His-mTFP1 protein. Lane 1: Prestained protein marker, lane 2: Input, lane 3: Flow-through, lane 4: Wash 50 mM Imidazole, lane 5: Elution with 150 mM Imidazole.

5.2.2 Cloning, expression, and purification of recombinant OPAA-FL-mTFP1 fusion protein

A gene for the OPAA-FL variant without stop codon was cloned into a pET28 expression vector, sequentially mTFP1 gene was cloned after OPAA-FL sequence giving pET28-OPAA-FL-mTFP1 **(Fig. 5.2 A).** and subsequently transformed into expression host *E. coli* Rosetta (DE3) cells. *E. coli* Rosetta (DE3) cells with the OPAA-FL-mTFP1 expression vector were induced with 0.1 mM IPTG at 20 ^{o}C for 20 hrs. The results of the expression of OPAA-FLmTFP1 in both pellet and supernatant are shown in **Fig. 5.2 B**, no expression of OPAA-FL-mTFP1 protein was observed in the uninduced supernatant and pellet. As expected, it was found that on induction, the OPAA-FL-mTFP1 protein was expressed more in the supernatant (**Fig. 5.2 B,** lane 4). The soluble form of 77 kDa OPAA-FL-mTFP1 was obtained, and subsequently, affinity purified on a Ni-NTA resin as this fusion protein has an N-terminal His tag with an affinity towards Ni-NTA resin and eluted in 150 mM imidazole elution buffer. (**Fig. 5.2 C,** lane 4).

5.2.3 Activity assay of recombinant OPAA-FL-mTFP1

An OPAA-FL-mTFP1 enzyme assay was done to know whether the recombinant protein is enzymatically active or not. In both the induced cell lysate and the purified fraction, the recombinant OPAA-FL-mTFP1 fusion protein showed activity with ethyl paraoxon. The induced cell lysate was significantly more active than uninduced cell lysates. However, when compared with the induced cell lysate, purified samples displayed higher specific activity. The specific activity of uninduced, induced, and purified OPAA-FL-mTFP1 fusion protein was found to be 0.006 U/mg (± 0.0007), 0.02 U/mg (± 0.002), and 0.668 U/mg (± 0.199), respectively, for 1 mM ethyl paraoxon **(Fig. 5.3)**. It was observed that purified OPAA-FL-mTFP1 has 33.4 times greater specific activity than the induced OPAA-FL-mTFP1 for ethyl paraoxon, suggesting significant fold purification using affinity chromatography

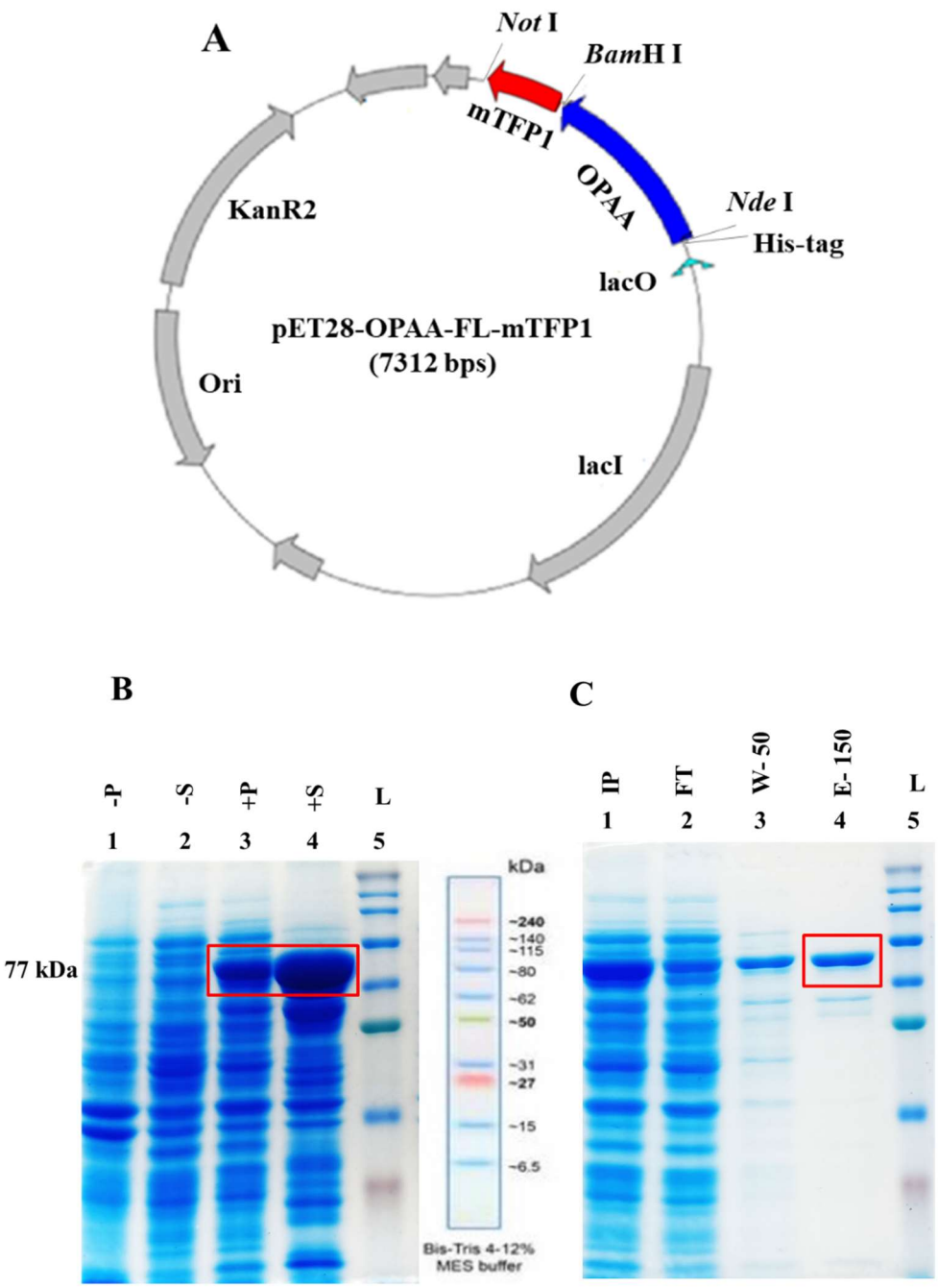

Figure 5.2 Cloning, expression, and purification of OPAA-FL-mTFP1. (A) Map of pET28 with OPAA-FL-mTFP1, N-His tag. **(B)** Induction of recombinant OPAA-FL-mTFP1 fusion protein. Induction of OPAA-FL-mTFP1 was performed at 20 °C for 20 hrs. Lane 1: Uninduced pellet, lane 2: Uninduced supernatant, lane 3: Induced pellet, lane 4: Induced supernatant lane 5: Protein marker. **(C)** Purification of recombinant OPAA-FL-mTFP1 fusion protein. Lane 1: Input, lane 2: Flow-through, lane 3: Wash 50 mM Imidazole, lane 4: Elution with 150 mM Imidazole, Lane 5: Prestained protein marker.

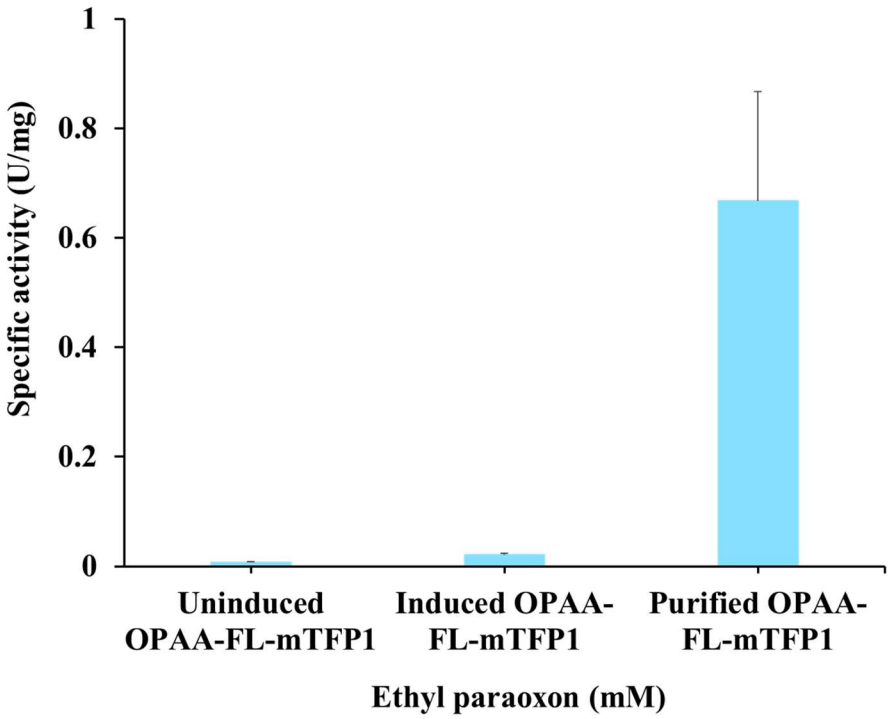

Figure 5.3. Colorimetric activity assay of OPAA-FL-mTFP1. OPAA-FL-mTFP1 with 1 mM ethyl paraoxon as a substrate in presence of Bis-tris propane buffer, pH 8.5, at 65 ºC for 15 minutes. The values are an average of duplicate samples and error bars represent standard deviation. At least three independent experiments were performed, and a representative result is shown.

The kinetic parameters for ethyl paraoxon from 0.05 to 9 mM as a substrate using purified OPAA-FL-mTFP1 fusion protein have been reported in **Fig. 5.4** and **Table 5.1**. Table 5.1 describes the comparative kinetic analysis of OPAA-FL-mTFP1 and OPAA-FL-variant. As per the observed data, the catalytic efficiency of OPAA-FL-mTFP1 is lower compared to the OPAA-FL-variant enzyme, possibly due to the fusion of mTFP1. The enzyme kinetic parameters for ethyl paraoxon substrate (k_{cat}, K_m, V_{max}, k_{cat}/K_m) are calculated by curve fitting to Lineweaver Burk plot following the published literature (Robinson 2015).

5.2.4 Effect of pH and temperature on recombinant OPAA-FL-mTFP1 activity

The effect of pH and temperature on the activity of the OPAA-FL-mTFP1 fusion protein was studied. To know the optimum temperature for the OPAA-FL-mTFP1 fusion protein with ethyl paraoxon, its activity was tested at various temperatures between 30 – 80 ºC for 15 minutes, in 50 mM Bis-Tris propane buffer, pH 8.5, 1 mM ethyl paraoxon, and 1 mM $MnCl_2$. OPAA-FL-mTFP1 fusion protein activity was gradually increasing until 65 ºC, and any further increase in the temperature led to a decrease in the specific activity. Our experiments suggested that 65 ºC is the optimum temperature for the OPAA-FL-mTFP1 fusion protein with ethyl paraoxon (**Fig. 5.5 A**).

To know the optimum pH for OPAA-FL-mTFP1 fusion protein with ethyl paraoxon, its activity was tested at various pH between 6 – 10, at 65 ºC for 15 minutes, in either 50 mM phosphate buffer (pH 6.0, 6.5, 7.0, 7.5 and 8.0, respectively) or 50 mM Bis-Tris propane buffer (pH 8.5, 9.0 and 10.0, respectively), 1 mM ethyl paraoxon and 1 mM $MnCl_2$. Optimum activity for OPAA-FL-mTFP1 fusion protein was observed at pH 8.5 (**Fig. 5.5 B**).

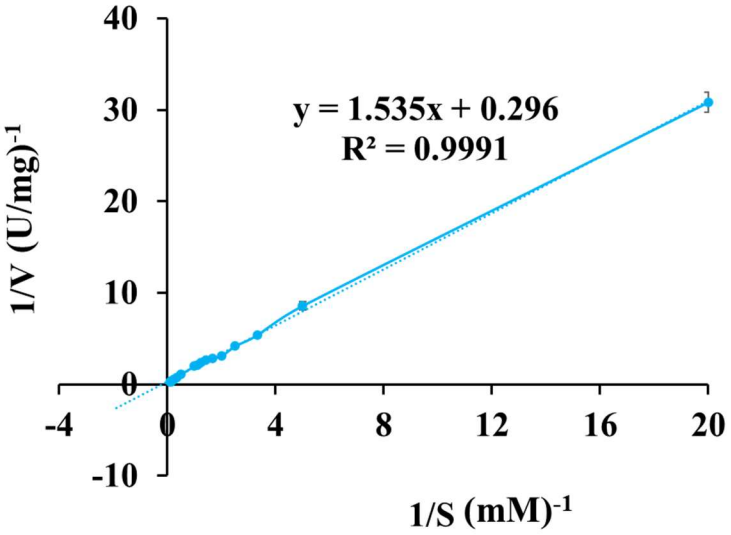

Figure 5.4. Lineweaver Burk plot for purified OPAA-FL-mTFP1 using ethyl paraoxon. The values are average of duplicate samples and error bars represent standard deviation.

Table 5.1 Kinetic parameters of OPAA-FL-mTFP1 enzyme

Sample	Ethyl paraoxon (mM)	V_{max} (U/mg)	K_m (mM)	k_{cat} (min^{-1})	k_{cat} / K_m ($mM^{-1} min^{-1}$)
Purified OPAA-FL-mTFP1	0.05 to 9	3.374	5.18	261.86	5.055
Purified OPAA-FL-variant	0.1 to 9	196	6.58	9800	1489.362

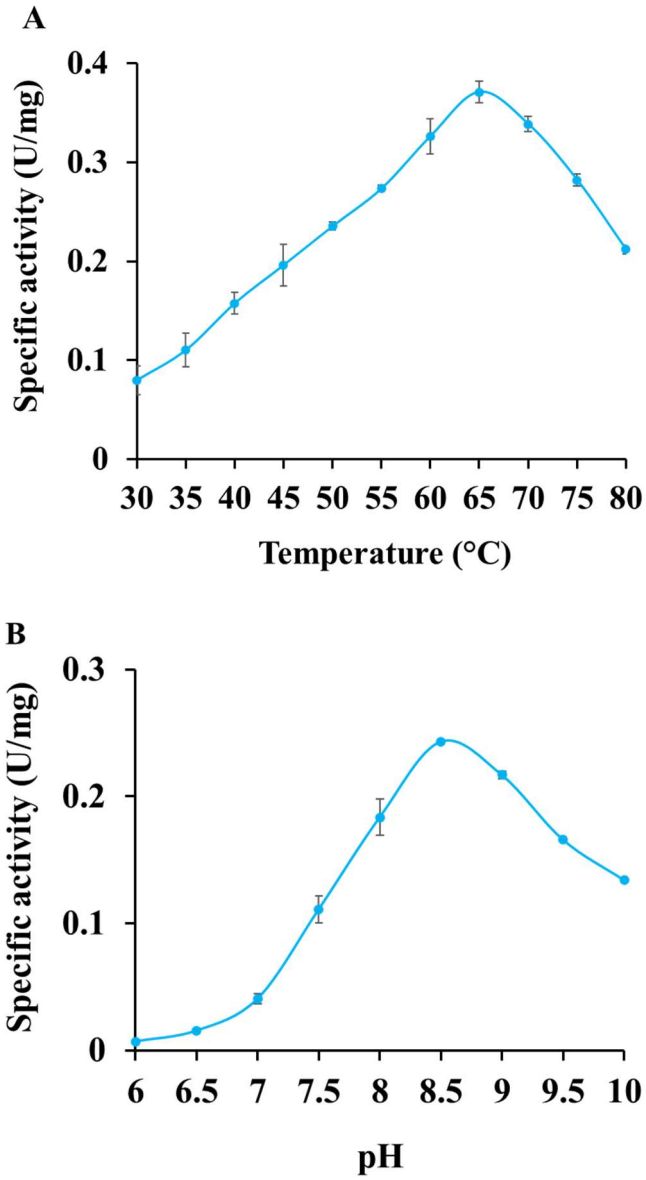

Figure 5.5. Effect of temperature and pH on the OPAA-FL-mTFP1 activity. (A) Effect of temperature on the specific activity of the OPAA-FL-mTFP1 with ethyl paraoxon. **(B)** Effect of pH on the specific activity of OPAA-FL-mTFP1 with ethyl paraoxon. The values are an average of duplicate samples and error bars represent standard deviation. At least three independent experiments were performed, and a representative result is shown.

5.2.5 Colorimetric biosensing of ethyl paraoxon

Colorimetric biosensing of OPAA-FL-mTFP1 fusion protein was performed with 0.005, 0.01, 0.05, 0.1, 0.2, 0.3, 0.4, 0.5, 0.6, 0.7, 0.8, 0.9, and 1 mM of ethyl paraoxon, and specific activity with respect to the aforementioned concentrations was found to be 0.004, 0.005, 0.032, 0.053, 0.116, 0.164, 0.221, 0.275, 0.325, 0.374, 0.420, 0.473, and 0.502 U/mg with ethyl paraoxon **(Fig. 5.6)**. The linear range for detection of ethyl paraoxon was found to be 0.005 - 1 mM with a LOD of 0.0254 mM. The sensitivity of such estimation was found to be 0.499 U/mg/ mM.

5.2.6 Fluorescence biosensing of ethyl paraoxon

The assay was developed based on a decrease of fluorescence intensity of pH-sensitive fluorescent protein mTFP1 (Ai et al. 2006). Upon the interaction of OPAA-FL-mTFP1 with OP compounds a decrease in pH of solution occurs due to the release of protons with the concurrent release of PNP (Prieto-Simón et al. 2006). The fluorescence of mTFP1 is dependent on protons. In acidic conditions, the mTFP1 signal decreased, with fluorescence quenching below pH 3.5. In less acidic buffer conditions of pH 5-6, mTFP1 showed increasing brightness with fluorescence plateauing above pH 6.0 (Chin et al. 2020) **(Fig. 5.7)**.

To know optimum buffer and reaction conditions for fluorometric detection of OPs using OPAA-FL-mTFP1 fusion protein, initially, it was tested for a decrease in the fluorescence values of OPAA-FL-mTFP1 in the different buffer concentrations. The reaction mixture was prepared with 1 mM $MnCl_2$, 1 mM ethyl paraoxon, OPAA-FL-mTFP1, and sterile distilled water up to 1 ml. 0 mM, 5mM, 10 mM, 25 mM, and 50 mM, Bis-Tris propane activity buffer (pH 8.0), was used respectively, and measured loss in the fluorescence values. It was observed that the reaction mixture with 25 mM Bis-Tris propane buffer showed a greater decrease in the intensity in comparison to the reaction mixture with the 0, 5, and 10 mM concentration of Bis-Tris propane buffer in it **(Fig. 5.8).** Further increase in buffer concentration did not result in a significant change in the fluorescence output, as seen in **Figure 5.8**.

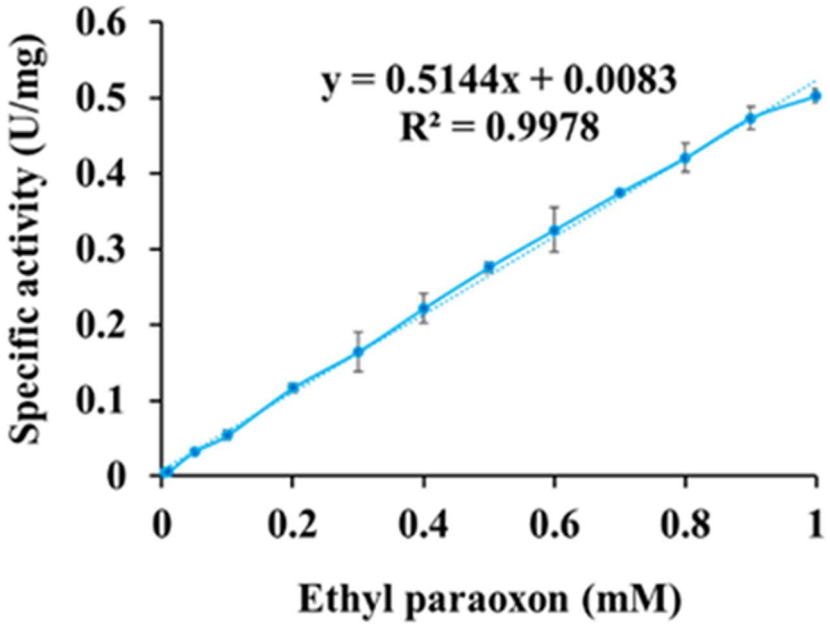

Figure 5.6. Colorimetric biosensing of ethyl paraoxon using OPAA-FL-mTFP1 fusion protein. Colorimetric activity assay of OPAA-FL-mTFP1 with 0.005 to 1 mM of the substrate with Bis-Tris propane buffer pH 8.5, at 65 °C for 15 minutes. The values are represented as the average of duplicate samples and the standard deviation is indicated by error bars. A representative result is shown based on at least three separate experiments.

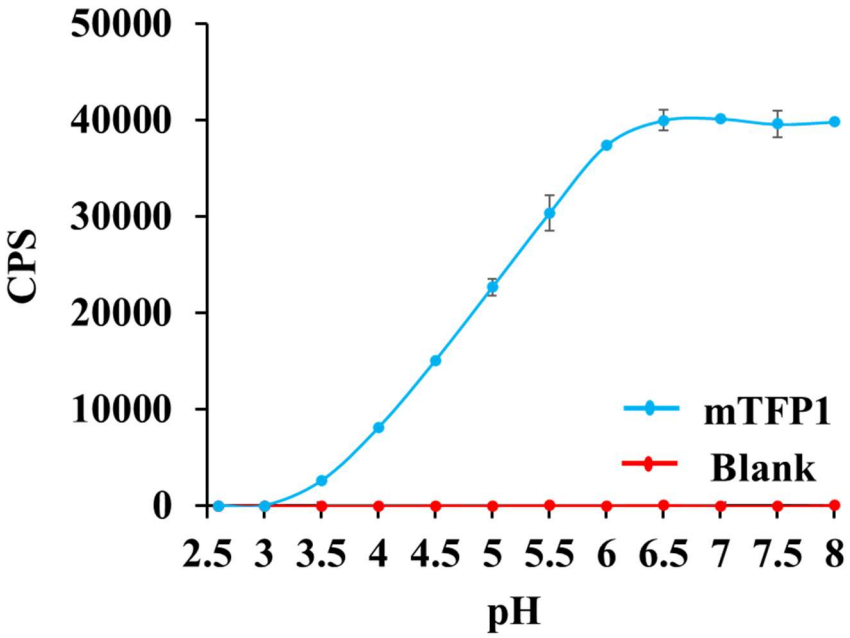

Figure 5.7. pH dependence of mTFP1 fluorescent proteins. pH sensing of mTFP1 was examined using citrate phosphate buffer, pH 2.6 to 5.5 and bis tris propane buffer, pH 6 to 8. The values are an average of duplicate samples and error bars represent standard deviation. At least three independent experiments were performed, and a representative result is shown.

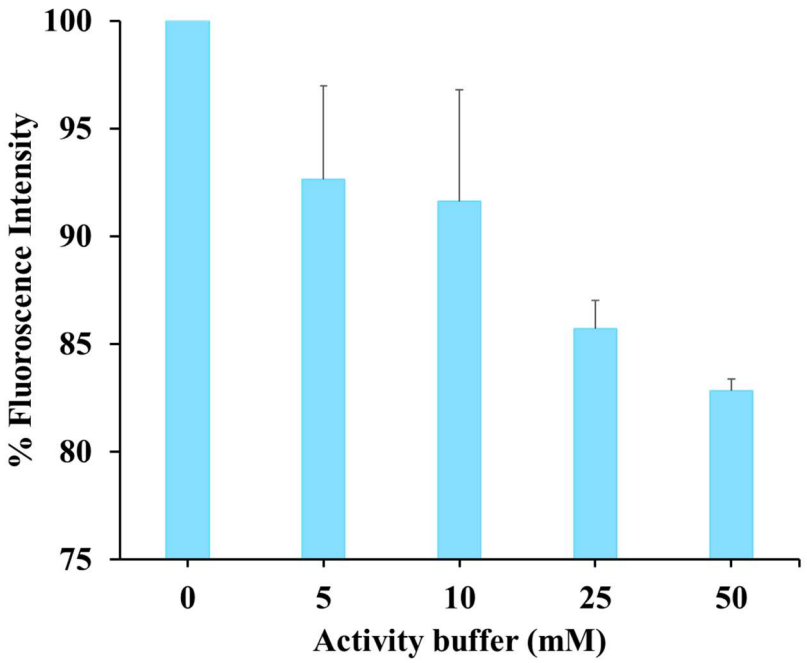

Figure 5.8. Optimization of concentration of Bis-tris propane buffer for OPAA-FL-mTFP1 fluorescence assay. 0 mM, 5 mM, 10 mM, 25 mM, and 50 mM Bis-tris propane buffer were used at 50 ºC, pH 8.0 for 10 minutes with ethyl paraoxon. The values are an average of duplicate samples and error bars represent standard deviation. At least three independent experiments were performed, and a representative result is shown.

It is observed that the interaction of OPAA-FL-mTFP1 with ethyl paraoxon result in a decrease in fluorescence intensity of mTFP1 fluorescent protein over a time period of 0-10 minutes due to the progressive release of H^+ ions by the hydrolysis of ethyl paraoxon.

To know the optimum temperature for the OPAA-FL-mTFP1 fluorescence assay, temperature optima experiment was performed from 25 to 70 °C, in 1 mM $MnCl_2$ and sterile distilled water. OPAA-FL-mTFP1 fusion protein fluorescence intensity was gradually decreasing until 70 ºC **(Fig. 5.9).** As reported earlier, mTFP1 is a temperature-sensitive protein (Nakano et al. 2017). To maintain the functional property of mTFP1 in the OPAA-FL-mTFP1 fusion protein, an optimum temperature of 50 °C was used for the OPAA-FL-mTFP1 fusion protein considering the maximum activity OPAA-FL and functional activity of mTFP1 for fluorescence sensing purpose at this temperature.

It is observed that the interaction of OPAA-FL-mTFP1 with OP compounds such as ethyl paraoxon result in a decrease in fluorescence - intensity of mTFP1 over a time of 0-10 minutes due to progressive release of H^+ ions by the hydrolysis of OP compounds, which does not occur in the control comprised of mTFP1 only. Thus, for all fluorescent sensing experiments, 50 °C temperature and 25 mM Bis-Tris propane buffer pH 8.0 was used. Moreover, when OPAA-FL-mTFP1 was used with 0.1, 0.25, 0.4, 0.5, 0.6, 0.75, 1 mM of ethyl paraoxon the rate of fluorescence decay increased with the concentration of substrate **(Fig. 5.10)**.

Fluorescence-based bio-sensing of OPAA-FL-mTFP1 with different concentrations of ethyl paraoxon showed a linear range of 0.1 to 1 mM. The LOD of bio-sensing was 0.066 mM for ethyl paraoxon, and the sensitivity defined as the slope of the linear concentration curve (Gauglitz 2018) was 36.9 % / mM for ethyl paraoxon. The fluorescence intensity of OPAA-FL-mTFP1 decreased linearly with an increase in the concentration of ethyl paraoxon. Due to the increase in enzymatic activity, there is a decrease in pH, which eventually results in a decrease in fluorescence intensity of mTFP1.

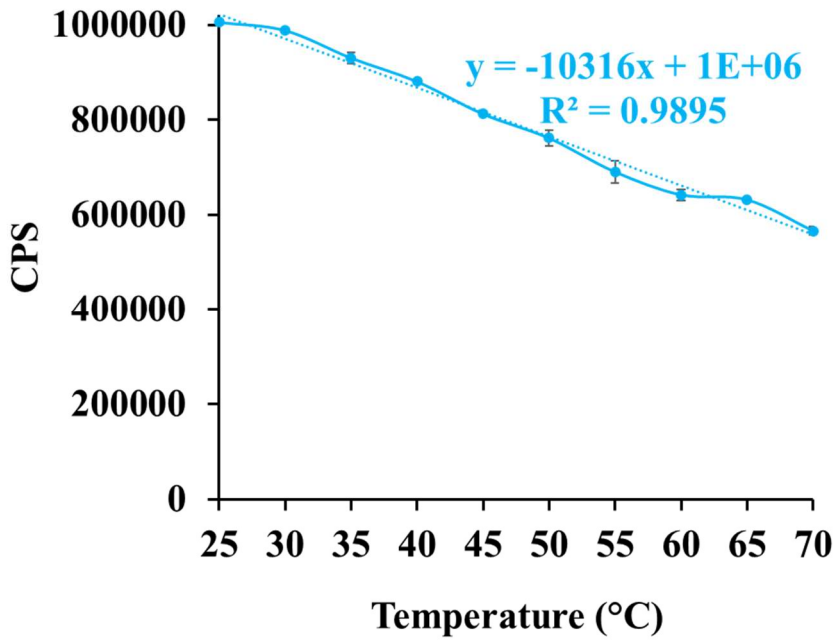

Figure 5.9. Optimization of temperature for OPAA-FL-mTFP1 fluorescence assay. The assay was performed with OPAA-FL-mTFP1 in the absence of substrate between 25 to 70 °C. The values are an average of duplicate samples and error bars represent standard deviation. At least three independent experiments were performed, and a representative result is shown.

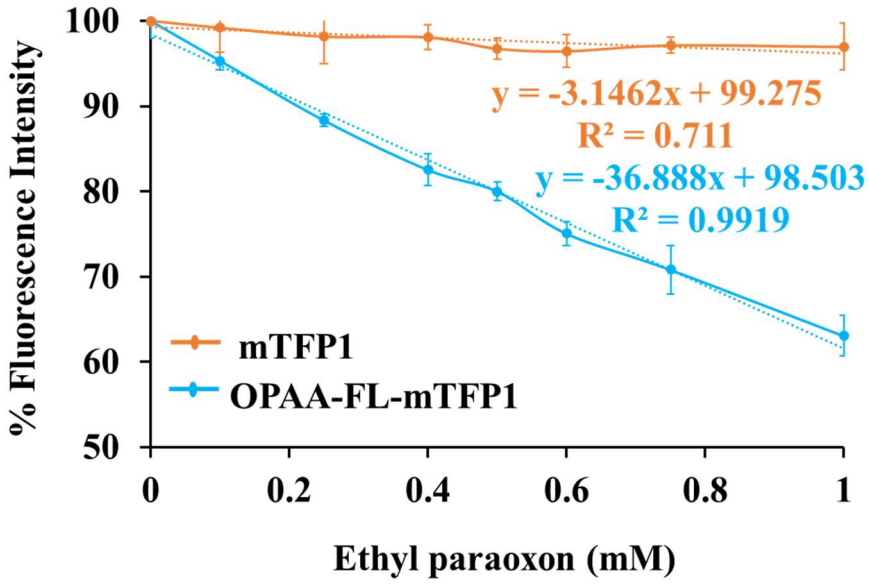

Figure. 5.10. Fluorometric bio-sensing of ethyl paraoxon using OPAA-FL-mTFP1 fusion protein. Bio-sensing of ethyl paraoxon using the OPAA-FL-mTFP1 via fluorescence assay with 0.1 to 1 mM ethyl paraoxon as the substrate at 50 ºC, for 10 minutes with bis tris propane activity buffer. The fluorescence intensity of OPAA-FL-mTFP1 decreased linearly with an increase in the concentration of ethyl paraoxon. while no significant changes of fluorescence were observed in the mTFP1 control. The values are an average of duplicate samples, and error bars represent standard deviation. At least three independent experiments were performed, and a representative result is shown.

5.3 Summary

The chapter demonstrated the fusion of OPAA-FL-variant, an OP degrading enzyme, with a pH-sensitive fluorescent protein called mTFP1. mTFP1 was used as a fluorophore and fusion partner because it is pH sensitive, and it does not interfere with the function of its fusion partner. This property was used to make OPAA-FL-mTFP1 fusion protein for enzymatic biosensing of OPs. The OPAA-FL-mTFP1 fusion protein was expressed, purified, and further used to test its enzymatic activity using colorimetric and fluorometric assays for organophosphate detection.

The results indicate good specific activity for the OPAA-FL-mTFP1, i.e., 0.668 U/mg for ethyl paraoxon. It was demonstrated that OPAA-FL-mTFP1 yields an enhanced limit of detection and good linear range for the detection of organophosphate compounds while being a good candidate for use as a colorimetric biosensor. This chapter discusses the use of mTFP1 as a pH-sensitive fluorophore to test the enzymatic activity of OPAA-FL-mTFP1 as a biosensing platform for the sensitive detection of ethyl paraoxon. In the case of the fluorometric method, the linear range was found to be 0.05 - 0.75 mM with a limit of detection of 0.098 mM. The results specify that the OPAA-FL-mTFP1 fusion protein can be used in both colorimetric and fluorescence-based sensor systems with good linear range, the limit of detection, response time, and linearity. It is the first known experimental evaluation of biosensing of ethyl paraoxon using OPAA-FL-mTFP1 fluorescent fusion protein.

Chapter 6

Chapter 6
Conclusion and scope for future work

6.1 Introduction

In modern times, pesticides have gained prominence in various sectors, from agriculture to the industry, due to a growing population's needs and expectations. The global usage of pesticides stands at around 3 million tons annually (Silva et al. 2019). Of the known pesticides, four classes are most prominent: organophosphates (OPs), organochlorines, pyrethroids, and carbamates (Clarke et al. 1997; Karami-Mohajeri and Abdollahi 2011). Among these, OPs are very popular, especially in developing countries, due to cost-efficient synthesis, ubiquitous and widespread proven usage as pesticides/insecticides. From a clinical point of view, there are some major concerns related to OPs, like blockage of the active site of acetylcholinesterase (AChE), which is an important enzyme of the nervous system required for breakdown of acetylcholine. The build-up of acetylcholine resulting from inhibition of AChE results in neurological complications and the problems can extend to all vertebrates, including humans (Yang et al. 2008b; Watson et al. 2014; Ortiz-Delgado et al. 2019). Long-term OP exposure results in an “ageing effect” on neuropathy target esterase (loss of alkyl group bound to phosphorus), which progressively and irreversibly inhibits the esterase over time, leading to OP-induced neuropathy (Jokanović et al. 2011). OP poisoning has a high rate of mortality. Various studies have documented it to be between 22% and 50% (Sungur and Güven 2001; Munidasa et al. 2004; Sungurtekin et al. 2006) irrespective of the economic status of the country or its patients (Hrabetz et al. 2013). Combined with the relative ease of exposure, these compounds pose a high risk for healthcare professionals to mitigate effectively.

Initially, separation methods like chromatography were used for pesticide analysis in the environment, however, these techniques

prevented adequate monitoring and had several limitations (Van Dyk and Pletschke 2011). Additionally, it involves a prior clean-up procedure of the instruments and requires a tedious extraction process, thereby making it not so suitable for the detection of OPs and nerve agents for wide and frequent usage. An alternative method of pesticide detection was promoted many years back using enzymes. The mainly utilized enzymes were AChE and BChE; and using the same the first enzymatic sensors for detection of organophosphates were developed (Kulys and D'Costa 1991; Marty et al. 1992). Both enzymes play a key role in the nervous system's functioning (Van Dyk and Pletschke 2011). The OPs and nerve agents were detected based on the inactivation of enzymes in proportion to the OPs and nerve agents. Based on this property of OPs, various inhibition-based biosensors have been designed to accurately detect the OPs (Pundir and Chauhan 2012; Pohanka 2013). Nevertheless, AChE and BChE are also inhibited by various other chemical agents apart from nerve agents and OPs, such as hypochlorite, detergents, carbamates, heavy metals, fluoride, and nicotine, and therefore, one cannot rely on the detection of inhibition based biosensors using AChE and BChE (Karami et al. 2016). Thus, there is a need to develop a rapid, selective, and sensitive biosensor for the detection of OPs and nerve agents. In this thesis, OP degrading enzymes, OPH and OPAA-FL, are cloned in the pET expression vector to express recombinant proteins. Subsequently, these recombinant proteins are purified by affinity chromatography and used as enzymatic biosensors to detect and quantify OPs based on optical sensing methods that are rapid, selective, and sensitive for the detection of common OP compounds such as ethyl paraoxon and methyl parathion used in this study.

6.2 Optical biosensor for the detection of OP based pesticides using OPAA-FL-variant

An enzyme-based biosensor that is safe, non-corrosive, cheap, user-friendly, rapid, stable, sensitive, selective, and environmentally friendly is needed. Microbial enzymes have proven to be attractive because of economic and environmental considerations. Whereby, OPs degrading enzymes have attracted widespread attention because of the toxicity of pesticides and the use of nerve agents as chemical warfare agents. In this study, an OPAA-FL variant enzyme-based biosensor was presented, which is safe, user-friendly, and environmentally benign to detect ethyl paraoxon. This work provides information about the cloning, expression, purification, encapsulation of the OPAA-FL variant into alginate, and developing a colorimetric as well as a pH-based biosensor.

Out of 517 amino acids of OPAA from *Alteromonas* sp., only 440 are found to affect the activity of enzyme. Truncation of 77 amino acids from the C-terminal is found to not affect the activity of enzyme (DeFrank and Cheng 1991). Before 2015, there was no report of OPAA action against V-type nerve agents and there were no previous reports of its engineering. OPAA structure was engineered by Steven P. Harvey's group to improve the catalytic efficiency of the enzyme. Using site-directed mutagenesis, they created few mutations in the small pocket in order to increase specific activity of the enzyme. Four mutants of OPAA, namely, F (Y212F), FL (Y212F & V342L), FLY (Y212F, V342L & I215Y), and FLYD (Y212F, V342L, I215Y, and H343D) were produced (Daczkowski et al. 2015), of which OPAA FL variant displayed a 20-fold increase in catalytic efficiency for the hydrolysis of Russian VX over wild-type OPAA, whereas the FLY mutant of OPAA displayed more than 30-fold enhancement in the catalytic activity on VR racemic. In literature, OPAA enzyme is reported to hydrolyze OP compounds with P-F, P-O, P-S, and P-CN bonds. A representative comparison table of OPAA-FL with P-F and P-O bond containing OPs, OPAA WT with P-O bond containing compounds, as well as a comparison of OPAA-FL and wild-type OPAA for the hydrolysis of P-S bond containing Russian VX is given in **Table**

3.2 and **Table 3.3**, respectively. A group of scientists in year 2000, proved that by encapsulating OPAA hydrolyzing enzyme in conjugation with 2-PAM and atropine in lysosome to provide 23 LD50s of protection against DFP (Petrikovics et al. 2000). This report attempts to evaluate the OPAA-FL variant as a potential candidate for the enzymatic hydrolysis of ethyl paraoxon, and this study thus would contribute towards developing effective sensors and/or mutant enzymes for detection and/or degradation of organophosphates, especially ones with P-O bond, such as ethyl paraoxon.

In this study, the OPAA-FL variant gene was cloned into pET28 expression vector with N-terminal His-tag. The recombinant OPAA-FL variant was expressed in *E. coli* cells, then purified and tested for its activity against methyl parathion and ethyl paraoxon. The specific activity of the OPAA-FL variant using colorimetric assay was observed to be 1.96 U/mg against ethyl paraoxon with an incubation time of 15 minutes, which is around 1.2 fold higher compared to previously reported OPAA from marine bacterium *Pseudoalteromonas* sp. SCSIO 04301 (1.6 U/mg) by Xiao Yunzhu and his group (Xiao et al. 2017). In 2017, Xiao Yunzhu and his group showed that OPAA obtained from the sediment of coastal areas of south China, specifically the bacterium *Pseudoalteromonas* sp. SCSIO 04301 (GIMCC 1.828) expressed activity against methyl paraoxon and ethyl paraoxon. They reported specific activity OPAA against methyl paraoxon of approximately 0.0314 U/mg and specific activity against ethyl paraoxon of about 1.604 U/mg.

The activity was further validated using fluorometric assay using pH-sensitive fluorophore, FITC. For the OPAA-FL variant, the observed fluorescence intensity of FITC dropped within a response time of 3 minutes giving a good linear range and detection limit. The protein was encapsulated into alginate using an ultrasonic atomizer. The bead morphology was observed by SEM. The average size of the microspheres so formed was around 0.2 μm. Microspheres were further used for the detection of OPs using a colorimetric assay.

In the colorimetric and fluorescence assays, a buffer solution of Bis-Tris propane was used, which acts as an activity buffer to provide

optimal conditions for maximum enzyme activity (Bisswanger 2014). Colorimetric estimation using the OPAA-FL variant provided a linear range of 0.01 - 1 mM whereas encapsulated OPAA-FL variant provided a linear range of 0.025 - 1 mM. The results indicate that both OPAA-FL variant and encapsulated OPAA-FL variant colorimetric estimation exhibit a limit of detection of ethyl paraoxon of 0.04 mM and 0.036 mM, respectively, with ethyl paraoxon as the substrate and response time of 15 minutes. Thus, encapsulation results in a decrease in the linear range, however with a slight improvement in the detection limit. In the case of the fluorometric method, the linear range was found to be 0.1 - 0.5 mM with a similar limit of detection of 0.038 mM. Incidentally, the encapsulated OPAA-FL variant microspheres did not show the expected biosensing response in the fluorescence assay. This could be because of the interference of alginate in enzymatic reaction or pH response. This study establishes use of the OPAA-FL variant for organophosphate pesticide detection and provides avenues for the development of sensitive real-time sensing platforms.

6.3 Organophosphate pesticides detection using recombinant OPH expressed in *E. coli*

This study demonstrated that His-Nus-OPH can show improved solubilization by including a NusA tag and yields enhanced enzymatic activity for degradation of organophosphate compounds. It was also observed that soluble protein was obtained when induction was performed at a lowered temperature of 16 ºC compared to 37 ºC. This is attributed to increased solubility of protein at lower temperatures owing to increased expression of chaperones in *E. coli* (Ferrer et al. 2003), reduced effect of heat shock proteases, and increased stability favouring proper folding patterns (Vera et al. 2007; Sahdev et al. 2008). Additionally, growth at lower temperatures from 15–23 °C, brings a significant reduction in degradation of the expressed protein (Spiess et al. 1999; Hunke and Betton 2003). These factors allowed proper solubilization of protein when induction was performed at 16 ºC.

Alginate encapsulation is used in a variety of applications, such as controlled drug release, oil encapsulation, nanoparticles, cells, and enzymes (Haider and Husain 2009; Yeh et al. 2009; Mandal and Kundu 2009; Ren et al. 2010; Chan et al. 2011; Stojanovic et al. 2012; Duarte et al. 2013; Yadav et al. 2018). Many of these reports have focused on encapsulation with calcium alginate. In this report, FITC Dextran with or without His-Nus-OPH was successfully encapsulated in sodium alginate beads, which posed an important advantage in terms of water solubility when compared to calcium alginate (Shilpa et al. 2003), resulting in decreased fluorescence quenching, higher fluorescence intensity when used with fluorescent dyes, and enhanced chemical availability for the encapsulated enzyme (Realdon et al. 2001; Koner and Nau 2007). FITC has been known to be a versatile fluorophore with properties like pH sensitivity, the capability to conjugating polymer matrices, and ease of characterization by fluorometry and fluorescence microscopy. FITC-dextran (500 kDa) is also known to have similar fluorescence properties as FITC itself while having advantages in terms of water solubility, inert nature, non-toxicity, and reduced leachability from alginate matrices (Alvarez et al. 1996; Lanz et al. 1997). Co-immobilization of FITC-dextran with His-Nus-OPH has been shown in this report to aid in developing a fluorescent assay for the detection of OP compounds. The fluorescence of FITC-dextran is pH-dependent; at pH 0-3, fluorescence intensity is minimum. At pH 4 and above, there is a linear increase in fluorescence intensity, which saturates at pH 8-9. In essence, acidic pH leads to loss of fluorescence intensity due to protonation of FITC, and basic pH leads to higher fluorescence intensity due to conversion into a mono-anionic or di-anionic form (Chaudhari et al. 2016; Chaudhari et al. 2017).

With respect to the colorimetric assay, an increase in the specific activity is observed with an increase in substrate concentration of ethyl paraoxon and methyl parathion due to the progressive access of substrate to the active sites of His-Nus-OPH. Consequently, the intensity of the yellow colour observed due to the production of PNP also increases. Interestingly, it is observed that in the colorimetric tests, the sensitivity of

the encapsulated His-Nus-OPH is lower than that of soluble His-Nus-OPH. Moreover, a higher response time was seen for the encapsulated His-Nus-OPH compared to the soluble enzyme. This may be due to the loss of some enzyme activity to the substrate after encapsulation (Plekhanova et al. 2019). Nevertheless, the encapsulated enzyme does exhibit improvements in terms of LOD while maintaining similar linearity as the solution-phase His-Nus-OPH.

Typically, using fluorescence techniques for detection of OP compounds provide a lower detection limit, which can also be seen in the current study. Use of His-Nus-OPH enzyme in the fluorescence assay demonstrated a lower LOD of 0.014 mM and 0.044 mM for ethyl paraoxon and methyl parathion, respectively, which was found to be superior compared to the colorimetric biosensing. The linear range and response time in both colorimetric and fluorescent sensing are comparable (5 min), which is mainly a function of enzyme activity of His-Nus-OPH. The results also clearly indicate that, although both colorimetric and fluorometric methods can be used for estimation, due to sensitivity, FITC dextran-based estimation would be preferable for the development of biosensor assays and devices.

6.4 Fluorometric biosensing of ethyl paraoxon using a recombinant OPAA-FL-mTFP fluorescent fusion protein

Fusion proteins, consisting of a protein of interest and a fluorescent protein are used to achieve improved association between the fluorescent molecule and the enzyme for sensing applications in continuing efforts to investigate enzymatic processes and sensing platforms for the detection of organophosphorus compounds. Effective devices and methods are needed to sensitively detect and/or degrade organophosphorus compounds for enzymatic bioremediation. Monomeric teal fluorescent protein from *Clavularia* coral (mTFP1) is a monomeric variant of the tetrameric CFP (cyan FP) cFP484 from Clavularia coral family with favorable fluorescence and stability characteristics for functional applications (Topol et al. 2010). An alternative known as mTFP1 was engineered to fix

the shortcomings of CFPs (Ai and Campbell 2008). It has high photostability, high brightness of fluorescence, pH stability, quantum yield, and maturation rate. Unlike several widely used fluorescent proteins, mTFP1 is a true monomer and possibly does not interfere with its fusion partner's function or localization. To test the enzymatic behaviour of OPAA-FL-mTFP1 as a biosensor based on the OPAA-FL-mTFP1 fusion protein for the sensitive detection of ethyl paraoxon, mTFP1 is investigated here as a pH-sensitive fluorophore in the fluorometric assay. mTFP1, a cyan fluorescent protein variant (pKa of 4.3), has been chosen for this purpose. In vitro, mTFP1 has a strong sigmoidal pH response over a large spectrum of pH 2.0 ± 9.0 (Ai et al. 2006). It also has a brightness (54 units) and displays good photostability (t1/2 = 163.0 s) (Shaner et al. 2004; Ai et al. 2006; Cranfill et al. 2016). Hence, mTFP1 provides the preferred combination of desirable characteristics for the pH-sensitive feature of a pH sensor. mTFP1 has a pH-sensing domain that enables pH measurements within the highly acidic range even in physiological lysosomes. The fluorescence of mTFP1 is dependent on protons. During acidic conditions, the mTFP1 signal decreased, with fluorescence quenching below pH 3.5. In less acidic buffer conditions of pH 5-6, mTFP1 showed increasing brightness with fluorescence plateauing above pH 6.0 (Chin et al. 2020).

The OPAA-FL-variant gene was cloned into pET28 expression vector with N-terminal His-tag and mTFP1 sequentially cloned at C-terminal in pET28-OPAA-FL vector. The recombinant OPAA-FL-mTFP1 was expressed in *E. coli* cells, then purified and tested for its activity against ethyl paraoxon. The specific activity of OPAA-FL-mTFP1 using colorimetric assay was observed to be 0.668 U/mg against ethyl paraoxon with an incubation time of 15 minutes.

OPAA-FL-mTFP1 was further used in a colorimetric assay for the detection of OPs. Colorimetric estimation using OPAA-FL-mTFP1 provided a linear range of 0.005 - 1 mM. The result indicates that the OPAA-FL-mTFP1 colorimetric estimation exhibits a limit of detection of 0.025 mM, with ethyl paraoxon as the substrate. The activity was further analysed through a fluorometric assay using the pH-sensitive fluorescent

protein, mTFP1. For OPAA-FL-mTFP1, it was observed the intensity of mTFP1 dropped with a response time of 10 minutes giving a linear range of detection between 0.1 mM - 1 mM and a detection limit of 0.066 mM with ethyl paraoxon. Although the linear range and limit of detection of fluorometric estimation are observed to be lower compared to the colorimetric method, this method can enable reduced interference in complex environmental samples. This chapter represents one of the first studies for enzymatic sensing applications with potential mTFP1 and is intended to further push research efforts towards the production of sensitive, selective, user-friendly organophosphorus pesticide estimation probes for in-field determination of OPs.

6.5 Conclusion

This thesis explores the activity of recombinant OPH, OPAA-FL-variant and OPAA-FL-mTFP1 for the enzymatic sensing of organophosphate compounds. Significantly, it establishes the use of OPAA-FL-variant and OPAA-FL-mTFP1 as a competitive enzymatic biosensor for organophosphate detection. The studies with His-Nus-OPH serve as a reference point for other researchers for exploiting enzymes towards novel sensing applications for organophosphates.

This thesis establishes the activity of OPAA-FL-variant and OPAA-FL-mTFP1 towards the hydrolysis of the P-O bond and also shows the applicability of OPAA-FL-variant and OPAA-FL-mTFP1 for use as a sensor for ethyl paraoxon. Combined with the well-known analysis in literature of the efficacy of OPAA towards the hydrolysis of P-S, P-F, and P-CN bonds, this study establishes grounds for the development of engineered recombinant OPAA-FL enzymes with highly broad substrate activity. It is believed that site-directed mutagenesis can further open avenues for enhancing the activity of the OPAA enzyme and its substrate-specific interactions.

Similarly, a His-Nus-OPH fusion protein is demonstrated to act as an effective sensor for ethyl paraoxon and methyl parathion, with a specific mention that His-Nus-tagging significantly enhances the

solubility of protein. His-Nus-OPH protein has demonstrated a competitive sensing performance to other studies. This thesis thus establishes the effectiveness of the OPAA-FL variant and His-Nus-OPH fusion protein towards enhanced hydrolysis of OPs and also presents important advances on the sensing of organophosphate pesticides.

Moreover, this thesis explores the possibility of using mTFP1 as the fluorophore in an OPAA-FL-mTFP1 fusion protein, which is demonstrated to display significant and competitive detection abilities in fluorometric and colorimetric assays for the detection of ethyl paraoxon.

In this thesis, sensing activity using a fluorometric and colorimetric assay is demonstrated with low limits of detection, good sensitivity, good linearity and high linear range, good response time when tested on ethyl paraoxon **(Table 6.1).** Table 6.1 summarizes comparative biosensing parameters of OP degrading enzymes. In the case of colorimetric sensing, OPAA-FL-mTFP1 showed better LOD than OPH and OPAA-FL, while OPH and OPAA-FL showed similar LOD. In terms of sensitivity and response time, OPH exhibits a better performance compared to OPAA-FL and OPAA-FL-mTFP1. For colorimetric biosensing, OPH is better than OPAA-FL and OPAA-FL-mTFP1 in most parameters, except the LOD. In the case of fluorometric biosensing, OPH exhibits the best performance for linear range and LOD compared to OPAA-FL and OPAA-FL-mTFP1, and has similar sensitivity and response time as OPAA-FL. Based on table 6.1, it can be concluded that OPH is more suitable for major sensing parameters compared to OPAA-FL and OPAA-FL-mTFP1 recombinant protein, but when it comes to organophosphate pesticide sensing, OPAA-FL protein has a significantly wider substrate scope, being effective on a series of nerve agents **(Table 3.2 and 3.3)** other than the OP compounds **(Table 3.1)**, making it more practically useful.

The studies in this thesis are expected to provide useful insight on the development of enzymatic biosensing platforms and the utility of recombinant enzymes and fusion proteins towards functional applications.

Table 6.1 Comparative biosensing parameters of recombinant OP degrading enzymes with ethyl paraoxon.

Colorimetric biosensing				
Protein	**Linear Range (mM)**	**LOD (mM)**	**Sensitivity (U/mg/mM)**	**Response time (minutes)**
His-Nus-OPH	**0.005-1**	**0.034**	**139.3**	**5**
OPAA-FL	0.01-1	0.04	1.44	15
OPAA-FL-mTFP1	**0.005-1**	**0.0254**	0.5	15
Fluorometric biosensing				
Protein	**Linear Range (mM)**	**LOD (mM)**	**Sensitivity (% / mM)**	**Response time (minutes)**
His-Nus-OPH	**0.001-0.5**	**0.014**	95.96	5
OPAA-FL	0.1-0.5	0.038	**104**	**3**
OPAA-FL-mTFP1	0.1-1	0.066	36.9	10

6.6 Future directions

This thesis has explored the use of recombinant OPAA-FL-variant, an OPAA-FL-mTFP1 fusion protein, and His-Nus-OPH as enzymatic sensing elements for the detection and potential remediation of organophosphorus compounds. The results indicate great potential for the simultaneous use of both enzymes for synergistic degradation of a broad spectrum of pesticide compounds. Encapsulation strategies can be adopted to improve the stability and lifetime of the enzymatic sensors. In terms of microbial remediation, it may be a possibility to utilize two different pathways i.e. catabolic and co-metabolic in bacterial strains to remediate OP contamination in the environment. Similarly, for sensors – other than the enzymatic sensor, it is also possible to develop microbial sensing systems based on co-expression of both OPH and OPAA. There are now many nanoparticle-based systems reported in the literature which can function as enzyme mimics. An important future direction for research work would be to utilize bio-mimetic nanoparticles in conjunction with enzymes in encapsulated particles to achieve sensitive, linear and precise detection of OP compounds (the so-called "nanozyme" system). Similarly, enzymes can be embedded among nanoparticles in hydrogel systems, which can then be utilized for sensitive and selective detection of OP compounds. In terms of analytical protocol, fluorescence, UV spectrophotometric, and electrochemical methods are suggested to be best suited for developing point-of-care devices, due to their easily accessible and visually detectable results. For fluorescent sensors, either or both enzymes (OPH and OPAA) may be used along with a suitable fluorescent dye (such as FITC-dextran, TFP, GFP, etc.) to achieve highly sensitive detection with low detection limits. OPH and OPAA separately and together can be used with different fluorescent dyes/proteins like TFP, Coumarin, FITC dextran, and FITC isomer, etc. to check the effect of dyes/protein on sensing parameters.

APPENDIX A

Vector Maps

A I. pET28a

A II. pET43a

APPENDIX A I

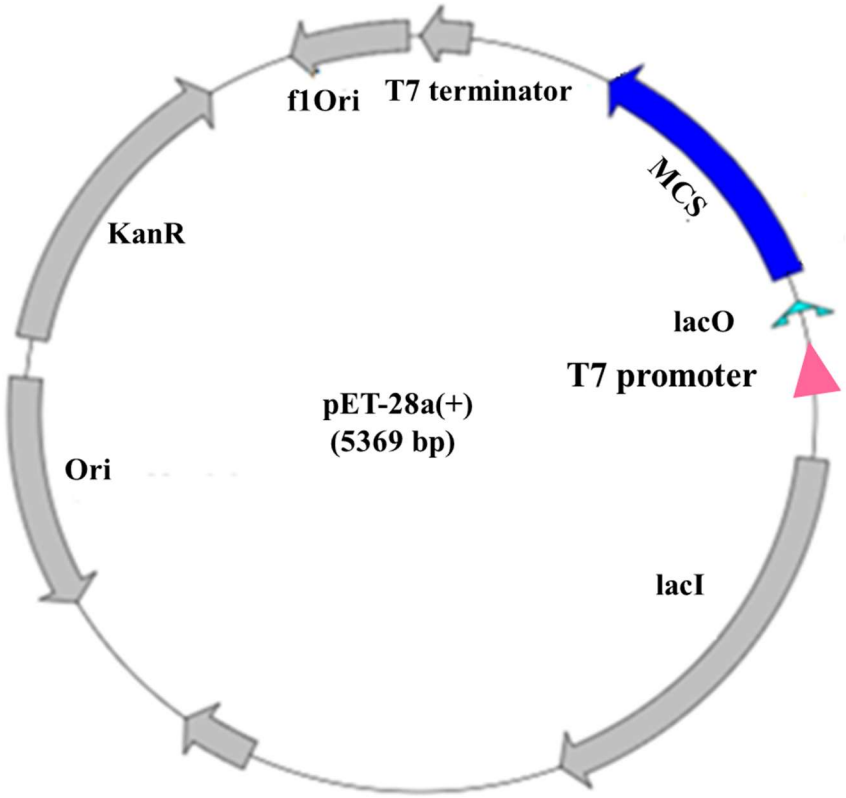

A I. pET28a null vector

APPENDIX A II

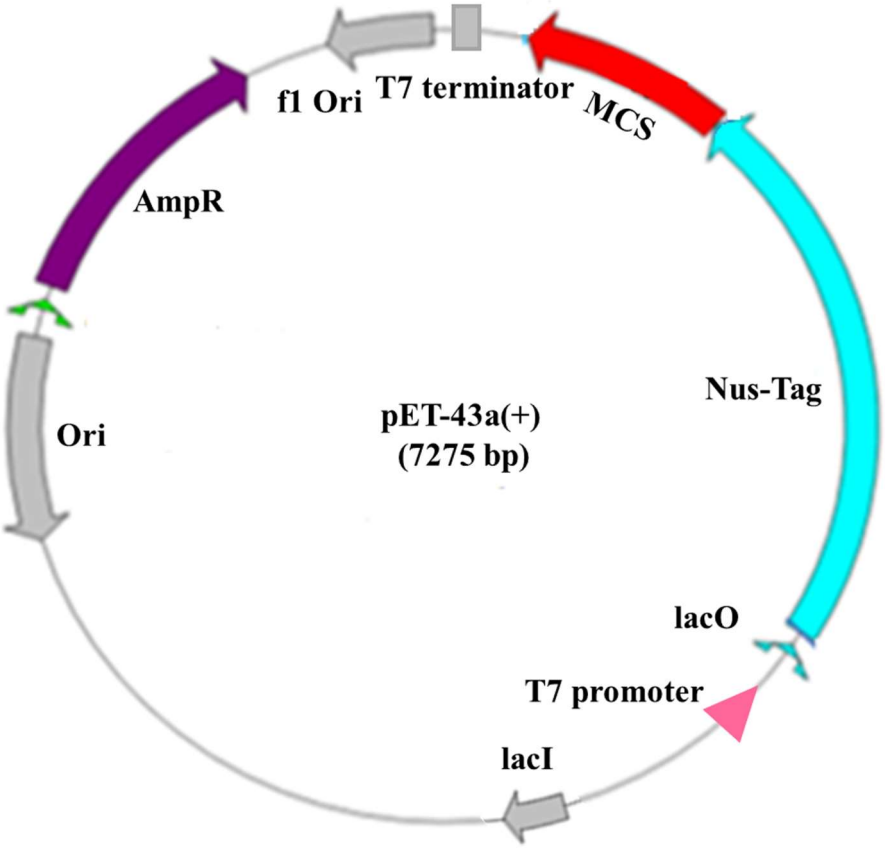

A II. pET43a null vector

Appendix B

List of primers used in cloning

Primer	Sequences (5' to 3')
PK671F	ACT **CATatg** tcg atc ggc aca ggc gat cgg
PK672F	TATAT **ACTAGT** ctg gaa gtt ctg ttc cag ggg ccc tcg atc ggc aca ggc gat cgg
PK673R	TATAT **CTCGAG** tta tga cgc ccg caa ggt cgg
PK702F	GCGCG **CATatg** aat aaa tta gcg gtg tta tac gct gaa c
PK706R	ATAT **GGATCC** tta atc gag ctc tag ctc gcg
PK762F	ATGC **GGATCC** atg gtg agc aag ggc gag gag
PK763R	ATGC **CTCGAG** tta ctt gta cag ctc gtc cat gcc
PK765R	ATAT **GGATCC** atc gag ctc tag ctc gcg ag
PK780R	ATAT **GCGGCCGC** tta ctt gta cag ctc gtc cat gcc
PK810F	GTC **CATatg** gtg agc aag ggc gag gag

a. Nucleotides in the small case are complementary to the genome sequence.

b. Underlined (bold case) in the corresponding sequence.

APPENDIX C

Permissions and Copyright

The chapters in this thesis adapt or reproduce certain published works, for which appropriate permissions have been obtained from the copyright holder, or are covered under open-access CC-BY license. The specific details are listed below.

Chapter	Details
Chapter 1: Introduction and Literature review	**Text:** Portions adapted from Monika Jain, Priyanka Yadav, Abhijeet Joshi & Prashant Kodgire (2019) Advances in detection of hazardous organophosphorus compounds using organophosphorus hydrolase-based biosensors, Critical Reviews in Toxicology, 49:5, 387-410, DOI: 10.1080/10408444.2019.1626800 with permission from Taylor & Francis **Figure 1.1:** Adapted from Md. Wasim Aktar, Dwaipayan Sengupta & Ashim Chowdhury (2009) Impact of pesticides use in agriculture: their benefits and hazards, Interdisc. Toxicol. 2, 1-12, DOI: 10.2478/v10102-009-0001-7

	Figure 1.2: Adapted from Meghdad Pirsaheb & Neghin Moradi (2020) Sonochemical degradation of pesticides in aqueous solution: investigation on the influence of operating parameters and degradation pathway – a systematic review, RSC Advances 10, 7396–7423, DOI: 10.1039/C9RA11025A - Published by the Royal Society of Chemistry **Figure 1.3:** Adapted from Miguel A. Sogorb & Eugenio Vilanova (2002) Enzymes involved in the detoxification of organophosphorus, carbamate and pyrethroid insecticides through hydrolysis, Toxicology Letters 128 (1-3), 215-228, DOI: 10.1016/S0378-4274(01)00543-4 with permission from Elsevier Also adapted from John R. Barr & W. Jack Driskell (2004) Quantitation of Metabolites of the Nerve Agents Sarin, Soman, Cyclohexylsarin, VX, and Russian VX in Human Urine Using Isotope-Dilution Gas Chromatography-Tandem Mass Spectrometry, Journal of Analytical Toxicology 28 (5), 372-378, DOI: 10.1093/jat/28.5.372 with permission from Oxford University Press **Figure 1.4 (C):** Adapted from the US Department of Agriculture (http://www.usda.gov)

	Figure 1.5: Adapted from Patrick Masson, Denis Josse, Oksana Lockridge, Nathalie Viguié, Claire Taupin & Cyril Buhler (1998) Enzymes hydrolyzing organophosphates as potential catalytic scavengers against organophosphate poisoning, Journal of Physiology-Paris, 92 (5-6), 357-362, DOI: 10.1016/S0928-4257(99)80005-9 with permission from Elsevier **Figure 1.6:** Adapted from Frank M. Raushel (2002) Bacterial detoxification of organophosphate nerve agents, Current Opinion in Microbiology, 5 (3), 288-295, DOI: 10.1016/s1369-5274(02)00314-4 with permission from Elsevier
Chapter 3: A novel biosensor for the detection of organophosphorus (OP) based pesticides using Organophosphorus acid anhydrolase (OPAA) -FL-variant	**Text:** Portions adapted from Monika Jain, Priyanka Yadav, Bhavana Joshi, Abhijeet Joshi & Prashant Kodgire (2021) A novel biosensor for the detection of organophosphorus (OP)-based pesticides using organophosphorus acid anhydrolase (OPAA)-FL variant, Applied Microbiology and Biotechnology, 105, 389-400, DOI: 10.1007/s00253-020-11008-w with permission from Springer Nature Customer Service GmbH

REFERENCES

A. Chaudhari S, R. Kar J, S. Singhal R (2015) Immobilization of Proteins in Alginate: Functional Properties and Applications. Curr Org Chem 19:1732–1754. https://doi.org/10.2174/1385272819666150429232110

Abdel Rasoul GM, Abou Salem ME, Mechael AA, Hendy OM, Rohlman DS, Ismail AA (2008) Effects of occupational pesticide exposure on children applying pesticides. Neurotoxicology 29:833–838. https://doi.org/10.1016/j.neuro.2008.06.009

Abou-Donia MB (1995) Involvement of cytoskeletal proteins in the mechanisms of organophosphorus ester-induced delayed neurotoxicity. Clin Exp Pharmacol Physiol 22:358–359. https://doi.org/10.1111/j.1440-1681.1995.tb02015.x

Ai H-W, Campbell RE (2008) Teal fluorescent proteins: characterization of a reversibly photoswitchable variant. Small Anim Whole-Body Opt Imaging Based Genet Eng Probes 6868:68680D. https://doi.org/10.1117/12.761423

Ai HW, Henderson JN, Remington SJ, Campbell RE (2006) Directed evolution of a monomeric, bright and photostable version of Clavularia cyan fluorescent protein: Structural characterization and applications in fluorescence imaging. Biochem J 400:531–540. https://doi.org/10.1042/BJ20060874

Ai HW, Olenych SG, Wong P, Davidson MW, Campbell RE (2008) Hue-shifted monomeric variants of Clavularia cyan fluorescent protein: Identification of the molecular determinants of color and applications in fluorescence imaging. BMC Biol 6:13. https://doi.org/10.1186/1741-7007-6-13

Aktar W, Sengupta D, Chowdhury A (2009) Impact of pesticides use in agriculture: Their benefits and hazards. Interdiscip Toxicol 2:1–12. https://doi.org/10.2478/v10102-009-0001-7

Alvarez FJ, Herráez A, Tejedor MC (1996) Fluorescence analysis of

carrier rat and human erythrocytes loaded with FITC-Dextran. Cytometry 24:181–189. https://doi.org/10.1002/(SICI)1097-0320(19960601)24:2<181::AID-CYTO11>3.0.CO;2-N

Amitai G, Gaidukov L, Adani R, Yishay S, Yacov G, Kushnir M, Teitlboim S, Lindenbaum M, Bel P, Khersonsky O, Tawfik DS, Meshulam H (2006) Enhanced stereoselective hydrolysis of toxic organophosphates by directly evolved variants of mammalian serum paraoxonase. FEBS J 273:1906–1919. https://doi.org/10.1111/j.1742-4658.2006.05198.x

Arora K, Mickelson SK, Helmers MJ, Baker JL (2010) Review of Pesticide Retention Processes Occurring in Buffer Strips Receiving Agricultural Runoff1. JAWRA J Am Water Resour Assoc 46:618–647. https://doi.org/10.1111/J.1752-1688.2010.00438.X

Arshak K, Gaidan I (2005) Development of a novel gas sensor based on oxide thick films. Mater Sci Eng B Solid-State Mater Adv Technol 118:44–49. https://doi.org/10.1016/j.mseb.2004.12.061

Atwood D, Paisley-Jones C (2017) Pesticides Industry Sales and Usage: 2008–2012 Market Estimates. United States Environ Prot Agency Washington, DC, USA

Bae SY, Myslinski JM, McMahon LR, Height JJ, Bigley AN, Raushel FM, Harvey SP (2018) An OPAA enzyme mutant with increased catalytic efficiency on the nerve agents sarin, soman, and GP. Enzyme Microb Technol 112:65–71. https://doi.org/10.1016/j.enzmictec.2017.11.001

Barak D, Ordentlich A, Segall Y, Velan B, Benschop HP, De Jong LPA, Shafferman A (1997) Carbocation-mediated processes in biocatalysts. Contribution of aromatic moieties. J Am Chem Soc 119:3157–3158. https://doi.org/10.1021/ja963861+

Barimani M, Pethybridge SJ, Vaghefi N, Hay FS, Taylor PWJ (2013) A new anthracnose disease of pyrethrum caused by *Colletotrichum tanaceti* sp. nov. Plant Pathol 62:1248–1257. https://doi.org/10.1111/ppa.12054

Barr JR, Driskell WJ, Aston LS, Martinez RA (2004) Quantitation of

metabolites of the nerve agents sarin, soman, cyclohexylsarin, VX, and Russian VX in human urine using isotope-dilution gas chromatography-tandem mass spectrometry. J Anal Toxicol 28:372–378. https://doi.org/10.1093/jat/28.5.372

Behrooz RD, Esmaili-Sari A, Ghasempouri SM, Bahramifar N, Covaci A (2009) Organochlorine pesticide and polychlorinated biphenyl residues in feathers of birds from different trophic levels of South-West Iran. Environ Int 35:285–290. https://doi.org/10.1016/j.envint.2008.07.001

Beketov MA, Kefford BJ, Schäfer RB, Liess M (2013) Pesticides reduce regional biodiversity of stream invertebrates. Proc Natl Acad Sci U S A 110:11039–11043. https://doi.org/10.1073/pnas.1305618110

Belenguer V, Martinez-Capel F, Masiá A, Picó Y (2014) Patterns of presence and concentration of pesticides in fish and waters of the júcar river (eastern spain). J Hazard Mater 265:271–279. https://doi.org/10.1016/j.jhazmat.2013.11.016

Bell MR, Engleka MJ, Malik A, Strickler JE (2013) To fuse or not to fuse: What is your purpose? Protein Sci 22:1466–1477. https://doi.org/10.1002/pro.2356

Benning MM, Shim H, Raushel FM, Holden HM (2001) High resolution X-ray structures of different metal-substituted forms of phosphotriesterase from Pseudomonas diminuta. Biochemistry 40:2712–2722. https://doi.org/10.1021/bi002661e

Bigley AN, Raushel FM (2013) Catalytic mechanisms for phosphotriesterases. Biochim Biophys Acta (BBA)-Proteins Proteomics 1834:443–453. https://doi.org/10.1016/j.bbapap.2012.04.004

Bigley AN, Raushel FM (2019) The evolution of phosphotriesterase for decontamination and detoxification of organophosphorus chemical warfare agents. Chem Biol Interact 308:80–88. https://doi.org/10.1016/j.cbi.2019.05.023

Birch H, Mikkelsen PS, Jensen JK, Holten Lützhøft HC (2011)

Micropollutants in stormwater runoff and combined sewer overflow in the Copenhagen area, Denmark. Water Sci Technol 64:485–493. https://doi.org/10.2166/wst.2011.687

Bisswanger H (2014) Enzyme assays. Perspect Sci 1:41–55. https://doi.org/10.1016/j.pisc.2014.02.005

Bjørling-Poulsen M, Andersen HR, Grandjean P (2008) Potential developmental neurotoxicity of pesticides used in Europe. Environ Heal A Glob Access Sci Source 7:1–22. https://doi.org/10.1186/1476-069X-7-50

Blum MM, Timperley CM, Williams GR, Thiermann H, Worek F (2008) Inhibitory potency against human acetylcholinesterase and enzymatic hydrolysis of fluorogenic nerve agent mimics by human paraoxonase 1 and squid diisopropyl fluorophosphatase. Biochemistry 47:5216–5224. https://doi.org/10.1021/bi702222x

Breen CJ, Raverdeau M, Voorheis HP (2016) Development of a quantitative fluorescence-based ligand-binding assay. Sci Rep 6:1–9. https://doi.org/10.1038/srep25769

Cao X, Mello S V., Leblanc RM, Rastogi VK, Cheng TC, DeFrank JJ (2004) Detection of paraoxon by immobilized organophosphorus hydrolase in a Langmuir-Blodgett film. Colloids Surfaces A Physicochem Eng Asp 250:349–356. https://doi.org/10.1016/j.colsurfa.2004.01.043

Carletti E, Jacquamet L, Loiodice M, Rochu D, Masson P, Nachon F (2009) Update on biochemical properties of recombinant Pseudomonas diminuta phosphotriesterase. J Enzyme Inhib Med Chem 24:1045–1055. https://doi.org/10.1080/14756360802608518

Chakraborty S, Hu S-Y, Wu S-H, Karmenyan A, Chiou A (2015) The Interaction Affinity between Vascular Cell Adhesion Molecule-1 (VCAM-1) and Very Late Antigen-4 (VLA-4) Analyzed by Quantitative FRET. PLoS One 10:e0121399. https://doi.org/10.1371/journal.pone.0121399

Chalfie M, Tu Y, Euskirchen G, Ward WW, Prasher DC (1994) Green

fluorescent protein as a marker for gene expression. Science (80-) 263:802–805. https://doi.org/10.1126/science.8303295

Chan ES, Wong SL, Lee PP, Lee JS, Ti TB, Zhang Z, Poncelet D, Ravindra P, Phan SH, Yim ZH (2011) Effects of starch filler on the physical properties of lyophilized calcium-alginate beads and the viability of encapsulated cells. Carbohydr Polym 83:225–232. https://doi.org/10.1016/j.carbpol.2010.07.044

Chattopadhyay S, Chattopadhyay D (2015) Remediation of DDT and Its Metabolites in Contaminated Sediment. Curr Pollut Reports 1:248–264. https://doi.org/10.1007/s40726-015-0023-z

Chaudhari R, Joshi A, Srivastava R (2017) PH and Urea Estimation in Urine Samples using Single Fluorophore and Ratiometric Fluorescent Biosensors. Sci Rep 7:5840. https://doi.org/10.1038/s41598-017-06060-y

Chaudhari RD, Joshi AB, Pandya K, Srivastava R (2016) pH based urea biosensing using fluorescein isothiocyanate (FITC)-dextran encapsulated micro-carriers of calcium alginate. Sens Lett 14:451–459. https://doi.org/10.1166/sl.2016.3663

Chen Y, Zhu C, Cen J, Bai Y, He W, Guo Z (2015) Ratiometric detection of pH fluctuation in mitochondria with a new fluorescein/cyanine hybrid sensor. Chem Sci 6:3187–3194. https://doi.org/10.1039/c4sc04021j

Chen ZM, Wang YH (1996) Chromatographic methods for the determination of pyrethrin and pyrethroid pesticide residues in crops, foods and environmental samples. J Chromatogr A 754:367–395. https://doi.org/10.1016/S0021-9673(96)00490-6

Cheng T-C, Defrank JJ (2000) Hydrolysis of Organophosphorus Compounds by Bacterial Prolidases. Enzym Action 243–261. https://doi.org/10.1007/978-94-010-0924-9_12

Cheng TC, DeFrank JJ, Rastogi VK (1999) Alteromonas prolidase for organophosphorus G-agent decontamination. Chem Biol Interact 119–120:455–462. https://doi.org/10.1016/S0009-2797(99)00058-7

Cheng TC, Harvey SP, Chen GL (1996) Cloning and expression of a gene encoding a bacterial enzyme for decontamination of organophosphorus nerve agents and nucleotide sequence of the enzyme. Appl Environ Microbiol 62:1636–1641. https://doi.org/10.1128/aem.62.5.1636-1641.1996

Cheng TC, Harvey SP, Stroup AN (1993) Purification and properties of a highly active organophosphorus acid anhydrolase from Alteromonas undina. Appl Environ Microbiol 59:3138–3140. https://doi.org/10.1128/aem.59.9.3138-3140.1993

Cheng TC, Liu L, Wang B, Wu J, DeFrank JJ, Anderson DM, Rastogi VK, Hamilton AB (1997) Nucleotide sequence of a gene encoding an organophosphorus nerve agent degrading enzyme from Alteromonas haloplanktis. J Ind Microbiol Biotechnol 18:49–55. https://doi.org/10.1038/sj.jim.2900358

Cherny I, Greisen P, Ashani Y, Khare SD, Oberdorfer G, Leader H, Baker D, Tawfik DS, Greisen Jr P, Ashani Y, Khare SD, Oberdorfer G, Leader H, Baker D, Tawfik DS (2013) Engineering V-type nerve agents detoxifying enzymes using computationally focused libraries. ACS Chem Biol 8:2394–2403. https://doi.org/10.1021/cb4004892

Chin MY, Patwardhan AR, Ang KH, Wang AL, Alquezar C, Welch M, Grabe M, Arkin MR, Kao AW (2020) Genetically encoded ratiometric biosensor for probing lysosomal pH in mammalian cells and C. elegans. bioRxiv. https://doi.org/10.1101/2020.11.04.368654

Chiron F, Chargé R, Julliard R, Jiguet F, Muratet A (2014) Pesticide doses, landscape structure and their relative effects on farmland birds. Agric Ecosyst Environ 185:153–160. https://doi.org/10.1016/j.agee.2013.12.013

Chishti Z, Hussain S, Arshad KR, Khalid A, Arshad M (2013) Microbial degradation of chlorpyrifos in liquid media and soil. J Environ Manage 114:372–380. https://doi.org/10.1016/j.jenvman.2012.10.032

Cho CM-HH, Mulchandani A, Chen W (2002) Bacterial cell surface

display of organophosphorus hydrolase for selective screening of improved hydrolysis of organophosphate nerve agents. Appl Environ Microbiol 68:2026–2030. https://doi.org/10.1128/AEM.68.4.2026-2030.2002

Cho CM-HH, Mulchandani A, Chen W (2004) Altering the substrate specificity of organophosphorus hydrolase for enhanced hydrolysis of chlorpyrifos. Appl Environ Microbiol 70:4681–4685. https://doi.org/10.1128/AEM.70.8.4681-4685.2004

Cho CMH, Mulchandani A, Chen W, Mee-Hie Cho C, Mulchandani A, Chen W (2006) Functional analysis of organophosphorus hydrolase variants with high degradation activity towards organophosphate pesticides. Protein Eng Des Sel 19:99–105. https://doi.org/10.1093/protein/gzj007

Choi YW, Park GJ, Na YJ, Jo HY, Lee SA, You GR, Kim C (2014) A single schiff base molecule for recognizing multiple metal ions: A fluorescence sensor for Zn(II) and Al(III) and colorimetric sensor for Fe(II) and Fe(III). Sensors Actuators, B Chem 194:343–352. https://doi.org/10.1016/j.snb.2013.12.114

Choudhary S, Joshi B, Pandey G, Joshi A (2019) Application of single and dual fluorophore-based pH sensors for determination of milk quality and shelf life using a fibre optic spectrophotometer. Sensors Actuators B Chem 298:126925. https://doi.org/10.1016/j.snb.2019.126925

Chu X, Zhang X, Chen Y, Liu H, Song D (2003) Study on the properties of methyl parathion hydrolase from Pseudomonas sp. WBC-3. Wei sheng wu xue bao= Acta Microbiol Sin 43:453–459

Chudakov DM, Matz M V, Lukyanov S, Lukyanov KA (2010) Fluorescent proteins and their applications in imaging living cells and tissues. Physiol Rev 90:1103–1163. https://doi.org/10.1152/physrev.00038.2009

Clarke EEK, Levy LS, Spurgeon A, Calvert IA (1997) The problems associated with pesticide use by irrigation workers in Ghana. Occup Med

(Chic Ill) 47:301–308. https://doi.org/10.1093/occmed/47.5.301

Constantine CA, Gattás-Asfura KM, Mello S V., Crespo G, Rastogi V, Cheng T-CC, DeFrank JJ, Leblanc RM (2003a) Layer-by-layer biosensor assembly incorporating functionalized quantum dots. Langmuir 19:9863–9867. https://doi.org/10.1021/la035237y

Constantine CA, Mello S V., Dupont A, Cao X, Santos D, Oliveira ON, Strixino FT, Pereira EC, Cheng TC, Defrank JJ, Leblanc RM (2003b) Layer-by-layer self-assembled chitosan/poly(thiophene-3-acetic acid) and organophosphorus hydrolase multilayers. J Am Chem Soc 125:1805–1809. https://doi.org/10.1021/ja028691h

Cooper J, Dobson H (2007) The benefits of pesticides to mankind and the environment. Crop Prot 26:1337–1348. https://doi.org/10.1016/j.cropro.2007.03.022

Cranfill PJ, Sell BR, Baird MA, Allen JR, Lavagnino Z, De Gruiter HM, Kremers GJ, Davidson MW, Ustione A, Piston DW (2016) Quantitative assessment of fluorescent proteins. Nat Methods 13:557–562. https://doi.org/10.1038/nmeth.3891

Cycoń M, Piotrowska-Seget Z (2009) Changes in bacterial diversity and community structure following pesticides addition to soil estimated by cultivation technique. Ecotoxicology 18:632–642. https://doi.org/10.1007/s10646-009-0321-6

Daczkowski CM, Pegan SD, Harvey SP (2015) Engineering the Organophosphorus Acid Anhydrolase Enzyme for Increased Catalytic Efficiency and Broadened Stereospecificity on Russian VX. Biochemistry 54:6423–6433. https://doi.org/10.1021/acs.biochem.5b00624

Daly GL, Lei YD, Teixeira C, Muir DCG, Castillo LE, Wania F (2007) Accumulation of current-use pesticides in neotropical montane forests. Environ Sci Technol 41:1118–1123. https://doi.org/10.1021/es0622709

Dave KI, Miller CE, Wild JR (1993) Characterization of organophosphorus hydrolases and the genetic manipulation of the

phosphotriesterase from Pseudomonas diminuta. Chem Biol Interact 87:55–68. https://doi.org/10.1016/0009-2797(93)90025-T

Deering K, Spiegel E, Quaisser C, Nowak D, Schierl R, Bose-O'Reilly S, Garí M (2019) Monitoring of arsenic, mercury and organic pesticides in particulate matter, ambient air and settled dust in natural history collections taking the example of the Museum für Naturkunde, Berlin. Environ Monit Assess 191:1–17. https://doi.org/10.1007/s10661-019-7495-z

DeFrank JJ, Beaudry WT, Cheng TC, Harvey SP, Stroup AN, Szafraniec LL (1993) Screening of halophilic bacteria and Alteromonas species for organophosphorus hydrolyzing enzyme activity. Chem Biol Interact 87:141–148. https://doi.org/10.1016/0009-2797(93)90035-W

DeFrank JJ, Cheng TC (1991) Purification and properties of an organophosphorus acid anhydrase from a halophilic bacterial isolate. J Bacteriol 173:1938–43. https://doi.org/10.1128/jb.173.6.1938-1943.1991

Dhirhi R, Prasad K, Shukla AK, Sarkar S, Renganathan T, Pushpavanam S, Kaza M (2016) Experimental study of rotating dry slag granulation unit: Operating regimes, particle size analysis and scale up. Appl Therm Eng 107:898–906. https://doi.org/10.1016/j.applthermaleng.2016.07.049

Di Sioudi BD, Miller CE, Lai K, Grimsley JK, Wild JR (1999) Rational design of organophosphorus hydrolase for altered substrate specificities. Chem Biol Interact 119–120:211–223. https://doi.org/10.1016/S0009-2797(99)00030-7

Ding G, Shi R, Gao Y, Zhang Y, Kamijima M, Sakai K, Wang G, Feng C, Tian Y (2012) Pyrethroid pesticide exposure and risk of childhood acute lymphocytic leukemia in Shanghai. Environ Sci Technol 46:13480–13487. https://doi.org/10.1021/es303362a

diSioudi B, Grimsley JK, Lai K, Wild JR (1999) Modification of near active site residues in organophosphorus hydrolase reduces metal stoichiometry and alters substrate specificity. Biochemistry 38:2866–

2872. https://doi.org/10.1021/bi9825302

Dong Q-Y, Chen M-Y, Xin Y, Qin X-Y, Cheng Z, Shi L-E, Tang Z-X (2013) Alginate-based and protein-based materials for probiotics encapsulation: a review. Int J Food Sci Technol 48:1339–1351. https://doi.org/10.1111/ijfs.12078

Dong Y-JJ, Bartlam M, Sun L, Zhou Y-FF, Zhang Z-PP, Zhang C-GG, Rao Z, Zhang X-EE (2005) Crystal structure of methyl parathion hydrolase from Pseudomonas sp. WBC-3. J Mol Biol 353:655–663. https://doi.org/10.1016/j.jmb.2005.08.057

Duarte JC, Rodrigues JAR, Moran PJS, Valença GP, Nunhez JR (2013) Effect of immobilized cells in calcium alginate beads in alcoholic fermentation. AMB Express 3:1–8. https://doi.org/10.1186/2191-0855-3-31

Dudley N, Attwood SJ, Goulson D, Jarvis D, Bharucha ZP, Pretty J (2017) How should conservationists respond to pesticides as a driver of biodiversity loss in agroecosystems? Biol Conserv 209:449–453. https://doi.org/10.1016/j.biocon.2017.03.012

Duysen EG, Li B, Xie W, Schopfer LM, Anderson RS, Broomfield CA, Lockridge O (2001) Evidence for nonacetylcholinesterase targets of organophosphorus nerve agent: supersensitivity of acetylcholinesterase knockout mouse to VX lethality. J Pharmacol Exp Ther 299:528–535

Eddleston M (2000) Patterns and problems of deliberate self-poisoning in the developing world. QJM 93:715–731. https://doi.org/10.1093/qjmed/93.11.715

Eddleston M, Buckley NA, Eyer P, Dawson AH (2008) Management of acute organophosphorus pesticide poisoning. Lancet 371:597–607. https://doi.org/10.1016/S0140-6736(07)61202-1

Ekinci D, Beydemir Ş (2010) Risk assessment of pesticides and fungicides for acid-base regulation and salt transport in rainbow trout tissues. Pestic Biochem Physiol 97:66–70. https://doi.org/10.1016/j.pestbp.2009.12.006

Fan J, Ding L, Fang Y (2019) Surfactant Aggregates Encapsulating and Modulating: An Effective Way to Generate Selective and Discriminative Fluorescent Sensors. Langmuir 35:326–341. https://doi.org/10.1021/acs.langmuir.8b02111

Farnoosh G, Latifi AM (2014) A review on engineering of organophosphorus hydrolase (OPH) enzyme. J Appl Biotechnol Reports 1:1–10

Ferrer M, Chernikova TN, Yakimov MM, Golyshin PN, Timmis KN (2003) Chaperonins govern growth of Escherichia coli at low temperatures. Nat Biotechnol 21:1266–1267. https://doi.org/10.1038/nbt1103-1266

Fleischauer V, Heo J (2014) An Organophosphate Sensor Based on Photo-crosslinked Hydrogel-entrapped E. coli. Anal Sci 30:937–942. https://doi.org/10.2116/analsci.30.937

Forbes VE, Galic N, Schmolke A, Vavra J, Pastorok R, Thorbek P (2016) Assessing the risks of pesticides to threatened and endangered species using population modeling: A critical review and recommendations for future work. Environ Toxicol Chem 35:1904–1913. https://doi.org/10.1002/etc.3440

Fukuto TR (1990) Mechanism of action of organophosphorus and carbamate insecticides. Environ Health Perspect 87:245–254. https://doi.org/10.1289/ehp.9087245

Gäb J, Melzer M, Kehe K, Richardt A, Blum MM (2009) Quantification of hydrolysis of toxic organophosphates and organophosphonates by diisopropyl fluorophosphatase from Loligo vulgaris by in situ Fourier transform infrared spectroscopy. Anal Biochem 385:187–193. https://doi.org/10.1016/j.ab.2008.11.012

Gao M, Tang BZ (2017) Fluorescent Sensors Based on Aggregation-Induced Emission: Recent Advances and Perspectives. ACS Sensors 2:1382–1399. https://doi.org/10.1021/acssensors.7b00551

Gauglitz G (2018) Analytical evaluation of sensor measurements. Anal Bioanal Chem 410:5–13. https://doi.org/10.1007/s00216-017-0624-z

Ghanem E, Raushel FM (2005) Detoxification of organophosphate nerve agents by bacterial phosphotriesterase. Toxicol Appl Pharmacol 207:459–470. https://doi.org/10.1016/j.taap.2005.02.025

Gilden RC, Huffling K, Sattler B (2010) Pesticides and health risks. JOGNN - J Obstet Gynecol Neonatal Nurs 39:103–110. https://doi.org/10.1111/j.1552-6909.2009.01092.x

Głąb S, Koncki R, Kopczewska E, Wałcerz I, Hulanicki A (1994) Urea sensors based on PVC membrane pH electrode. Talanta 41:1201–1205. https://doi.org/10.1016/0039-9140(94)80092-8

Gopal S, Rastogi V, Ashman W, Mulbry W (2000) Mutagenesis of organophosphorus hydrolase to enhance hydrolysis of the nerve agent VX. Biochem Biophys Res Commun 279:516–519. https://doi.org/10.1006/bbrc.2000.4004

Gothwal A, Dahiya M, Beniwal P, Hooda V (2014) Purification and kinetic studies of organophosphorus hydrolase from B. diminuta. Int J Pharm Pharm Sci 6:341–344

Goud KY, Teymourian H, Sandhu SS, Tostado N, Mishra RK, Moore LC, Harvey SP, Wang J (2020) OPAA/fluoride biosensor chip towards field detection of G-type nerve agents. Sensors Actuators B Chem 320:128344. https://doi.org/https://doi.org/10.1016/j.snb.2020.128344

Graham SC, Bond CS, Freeman HC, Guss JM (2005) Structural and functional implications of metal ion selection in aminopeptidase P, a metalloprotease with a dinuclear metal center. Biochemistry 44:13820–13836. https://doi.org/10.1021/bi0512849

Grimsley JK, Calamini B, Wild JR, Mesecar AD (2005) Structural and mutational studies of organophosphorus hydrolase reveal a cryptic and functional allosteric-binding site. Arch Biochem Biophys 442:169–179. https://doi.org/10.1016/j.abb.2005.08.012

Guelta MA, Dixon MM, Harvey SP (2018) OPAA FL—a mutant enzyme with increased catalytic efficiency on organophosphorus compound GD

Guo JX, Wu JJQ, Wright JB, Lushington GH (2006) Mechanistic insight into acetylcholinesterase inhibition and acute toxicity of organophosphorus compounds: A molecular modeling study. Chem Res Toxicol 19:209–216. https://doi.org/10.1021/tx050090r

Habibi N, Mohd Hashim SZ, Norouzi A, Samian MR (2014) A review of machine learning methods to predict the solubility of overexpressed recombinant proteins in Escherichia coli. BMC Bioinformatics 15:134. https://doi.org/10.1186/1471-2105-15-134

Haider T, Husain Q (2009) Hydrolysis of milk/whey lactose by β galactosidase: A comparative study of stirred batch process and packed bed reactor prepared with calcium alginate entrapped enzyme. Chem Eng Process Process Intensif 48:576–580. https://doi.org/10.1016/j.cep.2008.02.007

Han J, Burgess K (2010) Fluorescent indicators for intracellular pH. Chem Rev 110:2709–2728. https://doi.org/10.1021/cr900249z

Han L, Liu A (2017) Novel cell–inorganic hybrid catalytic interfaces with enhanced enzymatic activity and stability for sensitive biosensing of paraoxon. ACS Appl Mater Interfaces 9:6894–6901. https://doi.org/10.1021/acsami.6b15992

Harari R, Julvez J, Murata K, Barr D, Bellinger DC, Debes F, Grandjean P (2010) Neurobehavioral Deficits and Increased Blood Pressure in School-Age Children Prenatally Exposed to Pesticides. Environ Health Perspect 118:890–896. https://doi.org/10.1289/ehp.0901582

Harel M, Aharoni A, Gaidukov L, Brumshtein B, Khersonsky O, Meged R, Dvir H, Ravelli RBG, McCarthy A, Toker L, Silman I, Sussman JL, Tawfik DS (2004) Structure and evolution of the serum paraoxonase family of detoxifying and anti-atherosclerotic enzymes. Nat Struct Mol Biol 11:412–419. https://doi.org/10.1038/nsmb767

Hartleib J, Rüterjans H (2001) Insights into the reaction mechanism of the diisopropyl fluorophosphatase from Loligo vulgaris by means of kinetic studies, chemical modification and site-directed mutagenesis. Biochim Biophys Acta - Protein Struct Mol Enzymol 1546:312–324. https://doi.org/10.1016/S0167-4838(01)00153-4

Harvey SP, McMahon LR, Berg FJ (2020) Hydrolysis and enzymatic degradation of Novichok nerve agents. Heliyon 6:e03153. https://doi.org/10.1016/j.heliyon.2019.e03153

Hayoun MA, Smith ME, Swoboda HD (2020) V-Series (Ve, Vg, Vm, Vx) Toxicity. StatPearls Publishing

Headley DB (1982) Effects of Atropine Sulfate and Pralidoxime Chloride on Visual, Physiological, Performance, Subjective, and Cognitive Variables in Man: A Review. Mil Med 147:122–133. https://doi.org/10.1093/milmed/147.2.122

Heidari MF, Arab SS, Noroozi-Aghideh A, Tebyanian H, Latifi AM (2019) Evaluation of the substitutions in 212, 342 and 215 amino acid positions in binding site of organophosphorus acid anhydrolase using the molecular docking and laboratory analysis. Bratislava Med J 120:139–143. https://doi.org/10.4149/BLL_2019_022

Hill CM, Li WS, Cheng TC, DeFrank JJ, Raushel FM (2001) Stereochemical specificity of organophosphorus acid anhydrolase toward p-nitrophenyl analogs of soman and sarin. Bioorg Chem 29:27–35. https://doi.org/10.1006/bioo.2000.1189

Hill CM, Wu F, Cheng TC, Defrank JJ, Raushel FM (2000) Substrate and stereochemical specificity of the organophosphorus acid anhydrolase from Alteromonas sp. JD6.5 toward p-nitrophenyl phosphotriesters. Bioorganic Med Chem Lett 10:1285–1288. https://doi.org/10.1016/S0960-894X(00)00213-4

Holt E, Audy O, Booij P, Melymuk L, Prokes R, Klánová J (2017) Organochlorine pesticides in the indoor air of a theatre and museum in the

Czech Republic: Inhalation exposure and cancer risk. Sci Total Environ 609:598–606. https://doi.org/10.1016/j.scitotenv.2017.07.203

Hong KH, Lim SY, Yun MY, Lim JW, Woo JH, Kwon H, Kim HJ (2013) Selective detection of cysteine over homocysteine and glutathione by a bis(bromoacetyl)fluorescein probe. Tetrahedron Lett 54:3003–3006. https://doi.org/10.1016/j.tetlet.2013.03.119

Hoskin FCG, Prusch RD (1983) Characterization of a DFP-hydrolyzing enzyme in squid posterior salivary gland by use of soman, DFP and manganous ion. Comp Biochem Physiol Part C, Comp 75:17–20. https://doi.org/10.1016/0742-8413(83)90004-X

Hrabetz H, Thiermann H, Felgenhauer N, Zilker T, Haller B, Nährig J, Saugel B, Eyer F (2013) Organophosphate poisoning in the developed world – A single centre experience from here to the millennium. Chem Biol Interact 206:561–568. https://doi.org/10.1016/j.cbi.2013.05.003

Hu RR, Yin ZZ, Zeng YB, Zhang J, Liu HQ, Shao Y, Ren S Bin, Li L (2016) A novel biosensor for Escherichia coli O157: H7 based on fluorescein-releasable biolabels. Biosens Bioelectron 78:31–36. https://doi.org/10.1016/j.bios.2015.11.018

Hunke S, Betton J-M (2003) Temperature effect on inclusion body formation and stress response in the periplasm of Escherichia coli. Mol Microbiol 50:1579–1589. https://doi.org/10.1046/j.1365-2958.2003.03785.x

Iranzo M, Sainz-Pardo I, Boluda R, Sánchez J, Mormeneo S (2001) The use of microorganisms in environmental remediation. Ann Microbiol 51:135–143

Itkonen JM, Urtti A, Bird LE, Sarkhel S (2014) Codon optimization and factorial screening for enhanced soluble expression of human ciliary neurotrophic factor in Escherichia coli. BMC Biotechnol 14:92. https://doi.org/10.1186/s12896-014-0092-x

Iyer R, Iken B (2015) Protein engineering of representative hydrolytic

enzymes for remediation of organophosphates. Biochem Eng J 94:134–144. https://doi.org/10.1016/j.bej.2014.11.010

Jacquet P, Daudé D, Bzdrenga J, Masson P, Elias M, Chabrière E (2016) Current and emerging strategies for organophosphate decontamination: special focus on hyperstable enzymes. Environ Sci Pollut Res 23:8200–8218. https://doi.org/10.1007/s11356-016-6143-1

Jain M, Yadav P, Joshi A, Kodgire P (2019) Advances in detection of hazardous organophosphorus compounds using organophosphorus hydrolase based biosensors. Crit Rev Toxicol 49:. https://doi.org/10.1080/10408444.2019.1626800

Jao S-C, Huang L-F, Tao YS, Li W-S (2004) Hydrolysis of organophosphate triesters by Escherichia coli aminopeptidase P. J Mol Catal B Enzym 27:7–12. https://doi.org/https://doi.org/10.1016/j.molcatb.2003.09.002

Jeong YS, Choi SL, Kyeong HH, Kim JH, Kim EJ, Pan JG, Rha E, Song JJ, Lee SG, Kim HS (2012) High-throughput screening system based on phenolics-responsive transcription activator for directed evolution of organophosphate-degrading enzymes. Protein Eng Des Sel 25:725–731. https://doi.org/10.1093/protein/gzs071

Ji X, Zheng J, Xu J, Rastogi VK, Cheng T-CC, DeFrank JJ, Leblanc RM (2005) (CdSe) ZnS quantum dots and organophosphorus hydrolase bioconjugate as biosensors for detection of paraoxon. J Phys Chem B 109:3793–3799. https://doi.org/10.1021/jp044928f

Jiang H, Tian R, Hu W, Jia Y, Yuan P, Wang J, Zhang L (2015) Formulation and evaluation of gastroretentive floating drug delivery system of dipyridamole. Drug Dev Ind Pharm 41:674–680. https://doi.org/10.3109/03639045.2014.893355

Johannes TW, Zhao H (2006) Directed evolution of enzymes and biosynthetic pathways. Curr Opin Microbiol 9:261–267. https://doi.org/10.1016/j.mib.2006.03.003

Jokanović M, Kosanović M, Brkić D, Vukomanović P (2011) Organophosphate induced delayed polyneuropathy in man: An overview. Clin Neurol Neurosurg 113:7–10. https://doi.org/10.1016/j.clineuro.2010.08.015

Joshi A, Keerthiprasad R, Jayant RD, Srivastava R (2010) Nano-in-micro alginate based hybrid particles. Carbohydr Polym 81:790–798. https://doi.org/10.1016/j.carbpol.2010.03.050

Kamelipour N, Mohsenifar A, Tabatabaei M, Rahmani-Cherati T, Khoshnevisan K, Allameh A, Milani MM, Najavand S, Etemadikia B (2014) Fluorometric determination of paraoxon in human serum using a gold nanoparticle-immobilized organophosphorus hydrolase and coumarin 1 as a competitive inhibitor. Microchim Acta 181:239–248. https://doi.org/10.1007/s00604-013-1103-7

Kang DG, Li L, Ha JH, Choi SS, Cha HJ (2008) Efficient cell surface display of organophosphorous hydrolase using N-terminal domain of ice nucleation protein in Escherichia coli. Korean J Chem Eng 25:804–807. https://doi.org/10.1007/s11814-008-0132-0

Kang EJ, Seok SJ, Lee KH, Gil HW, Yang JO, Lee EY, Hong SY (2009) Factors for determining survival in acute organophosphate poisoning. Korean J Intern Med 24:362–367. https://doi.org/10.3904/kjim.2009.24.4.362

Karami-Mohajeri S, Abdollahi M (2011) Toxic influence of organophosphate, carbamate, and organochlorine pesticides on cellular metabolism of lipids, proteins, and carbohydrates: A systematic review. Hum Exp Toxicol 30:1119–1140. https://doi.org/10.1177/0960327110388959

Karami R, Mohsenifar A, Mesbah Namini SM, Kamelipour N, Rahmani-Cherati T, Roodbar Shojaei T, Tabatabaei M (2016) A novel nanobiosensor for the detection of paraoxon using chitosan-embedded organophosphorus hydrolase immobilized on Au nanoparticles. Prep Biochem Biotechnol 46:559–566.

https://doi.org/10.1080/10826068.2015.1084930

Karpouzas DG, Singh BK (2006) Microbial degradation of organophosphorus xenobiotics: metabolic pathways and molecular basis. Adv Microb Physiol 51:119–225. https://doi.org/10.1016/S0065-2911(06)51003-3

Katsemi V, Lücke C, Koepke J, Löhr F, Maurer S, Fritzsch G, Rüterjans H (2005) Mutational and structural studies of the diisopropylfluorophosphatase from Loligo vulgaris shed new light on the catalytic mechanism of the enzyme. Biochemistry 44:9022–9033. https://doi.org/10.1021/bi0500675

Khaksarinejad R, Mohsenifar A, Rahmani-Cherati T, Karami R, Tabatabaei M (2015) An organophosphorus hydrolase-based biosensor for direct detection of paraoxon using silica-coated magnetic nanoparticles. Appl Biochem Biotechnol 176:359–371. https://doi.org/10.1007/s12010-015-1579-1

Kim CS, Choi B-HH, Seo JH, Lim G, Cha HJ (2013) Mussel adhesive protein-based whole cell array biosensor for detection of organophosphorus compounds. Biosens Bioelectron 41:199–204. https://doi.org/10.1016/j.bios.2012.08.022

Kim ES, Lee J-S, Lee HG (2016) Calcium-alginate microparticles for sustained release of catechin prepared via an emulsion gelation technique. Food Sci Biotechnol 25:1337–1343. https://doi.org/10.1007/s10068-016-0210-8

Kim I, Kim GH, Kim CS, Cha HJ, Lim G (2015) Optical detection of paraoxon using single-walled carbon nanotube films with attached organophosphorus hydrolase-expressed Escherichia coli. Sensors 15:12513–12525. https://doi.org/10.3390/s150612513

Kim KH, Kabir E, Jahan SA (2017) Exposure to pesticides and the associated human health effects. Sci Total Environ 575:525–535. https://doi.org/10.1016/j.scitotenv.2016.09.009

Kirsch J, Siltanen C, Zhou Q, Revzin A, Simonian A (2013) Biosensor technology: Recent advances in threat agent detection and medicine. Chem Soc Rev 42:8733–8768. https://doi.org/10.1039/c3cs60141b

Kitchener RL, Grunden AM (2012) Prolidase function in proline metabolism and its medical and biotechnological applications. J Appl Microbiol 113:233–247. https://doi.org/10.1111/j.1365-2672.2012.05310.x

Koner AL, Nau WM (2007) Cucurbituril encapsulation of fluorescent dyes. Supramol Chem 19:55–66. https://doi.org/10.1080/10610270600910749

Kulys J, D'Costa EJ (1991) Printed amperometric sensor based on TCNQ and cholinesterase. Biosens Bioelectron 6:109–115. https://doi.org/10.1016/0956-5663(91)87034-9

Kumar J, D'Souza SF (2010) An optical microbial biosensor for detection of methyl parathion using Sphingomonas sp. immobilized on microplate as a reusable biocomponent. Biosens Bioelectron 26:1292–1296. https://doi.org/10.1016/j.bios.2010.07.016

Kumar J, D'Souza SF (2011) Immobilization of microbial cells on inner epidermis of onion bulb scale for biosensor application. Biosens Bioelectron 26:4399–4404. https://doi.org/10.1016/j.bios.2011.04.049

Kumar J, Jha SK, D'Souza SF (2006) Optical microbial biosensor for detection of methyl parathion pesticide using Flavobacterium sp. whole cells adsorbed on glass fiber filters as disposable biocomponent. Biosens Bioelectron 21:2100–2105. https://doi.org/10.1016/j.bios.2005.10.012

Kumar S, KAUSHIK G, DAR MA, NIMESH S, LÓPEZ-CHUKEN UJ, VILLARREAL-CHIU JF (2018) Microbial Degradation of Organophosphate Pesticides: A Review. Pedosphere 28:190–208. https://doi.org/10.1016/S1002-0160(18)60017-7

Lamberth C (2004) Sulfur chemistry in crop protection. J Sulfur Chem 25:39–62. https://doi.org/10.1080/17415990310001612290

Lanz E, Gregor M, Slavík J, Kotyk A (1997) Use of FITC as a Fluorescent Probe for Intracellular pH Measurement. J Fluoresc 7:317–319. https://doi.org/10.1023/A:1022586127784

Laveglia J, Dahm PA (1977) Degradation of Organophosphorus and Carbamate Insecticides in the Soil and by Soil Microorganisms. Annu Rev Entomol 22:483–513. https://doi.org/10.1146/annurev.en.22.010177.002411

Lee KY, Mooney DJ (2012) Alginate: Properties and biomedical applications. Prog Polym Sci 37:106–126. https://doi.org/10.1016/j.progpolymsci.2011.06.003

Lee LG, Spurgeon SL, Heiner CR, Benson SC, Rosenblum BB, Menchen SM, Graham RJ, Constantinescu A, Upadhya KG, Cassel JM (1997) New energy transfer dyes for DNA sequencing. Nucleic Acids Res 25:2816–2822. https://doi.org/10.1093/nar/25.14.2816

Leong JY, Lam WH, Ho KW, Voo WP, Lee MFX, Lim HP, Lim SL, Tey BT, Poncelet D, Chan ES (2016) Advances in fabricating spherical alginate hydrogels with controlled particle designs by ionotropic gelation as encapsulation systems. Particuology 24:44–60. https://doi.org/10.1016/j.partic.2015.09.004

Létant SE, Kane SR, Hart BR, Hadi MZ, Cheng TC, Rastogi VK, Reynolds JG (2005) Hydrolysis of acetylcholinesterase inhibitors - Organophosphorus acid anhydrolase enzyme immobilization on photoluminescent porous silicon platforms. Chem Commun 851–853. https://doi.org/10.1039/b412215a

Li P, Moon SY, Guelta MA, Harvey SP, Hupp JT, Farha OK (2016) Encapsulation of a Nerve Agent Detoxifying Enzyme by a Mesoporous Zirconium Metal-Organic Framework Engenders Thermal and Long-Term Stability. J Am Chem Soc 138:8052–8055. https://doi.org/10.1021/jacs.6b03673

Liu J, Liu J, Cui Z, Cui Z (2020) Fluorescent Labeling of Proteins of

Interest in Live Cells: Beyond Fluorescent Proteins. Bioconjug Chem 31:1587–1595. https://doi.org/10.1021/acs.bioconjchem.0c00181

Liu N, Cai X, Lei Y, Zhang Q, Chan-Park MB, Li C, Chen W, Mulchandani A (2007) Single-Walled Carbon Nanotube Based Real-Time Organophosphate Detector. Electroanal An Int J Devoted to Fundam Pract Asp Electroanal 19:616–619

Liu SH, Lin JL, Weng CH, Yang HY, Hsu CW, Chen KH, Huang WH, Yen TH (2012) Heart rate-corrected QT interval helps predict mortality after intentional organophosphate poisoning. PLoS One 7:. https://doi.org/10.1371/journal.pone.0036576

Liu XY, Chen FF, Li CX, Luo XJ, Chen Q, Bai YP, Xu JH (2016) Improved efficiency of a novel methyl parathion hydrolase using consensus approach. Enzyme Microb Technol 93–94:11–17. https://doi.org/10.1016/j.enzmictec.2016.07.005

Lorenz S, Rasmussen JJ, Süß A, Kalettka T, Golla B, Horney P, Stähler M, Hommel B, Schäfer RB (2017) Specifics and challenges of assessing exposure and effects of pesticides in small water bodies. Hydrobiologia 793:213–224. https://doi.org/10.1007/s10750-016-2973-6

Lupi L, Bedmar F, Wunderlin DA, Miglioranza KSB (2016) Organochlorine pesticides in agricultural soils and associated biota. Environ Earth Sci 75:1–11. https://doi.org/10.1007/s12665-015-5140-x

Ma T, Zhao X, Matsuo Y, Song J, Zhao R, Faheem M, Chen M, Zhang Y, Tian Y, Zhu G (2019) Fluorescein-based fluorescent porous aromatic framework for Fe 3+ detection with high sensitivity. J Mater Chem C 7:2327–2332. https://doi.org/10.1039/c8tc06288a

Macneale KH, Kiffney PM, Scholz NL (2010) Pesticides, aquatic food webs, and the conservation of Pacific salmon. Front Ecol Environ 8:475–482. https://doi.org/10.1890/090142

Maheshwari DT, Thygaraj V, Kumar NS, T. MD, Varsha T, Kumar NS (2017) Extraction and Purification of Organophosphorus Hydrolase

Enzyme from Soil Microorganism Pseudomonas diminuta. Def Life Sci J 2:416–421. https://doi.org/10.14429/dlsj.2.12272

Mandal BB, Kundu SC (2009) Calcium alginate beads embedded in silk fibroin as 3D dual drug releasing scaffolds. Biomaterials 30:5170–5177. https://doi.org/10.1016/j.biomaterials.2009.05.072

Mangas I, Estevez J, Vilanova E, França TCC (2017) New insights on molecular interactions of organophosphorus pesticides with esterases. Toxicology 376:30–43. https://doi.org/10.1016/j.tox.2016.06.006

Marty J -L, Sode K, Karube I (1992) Biosensor for detection of organophosphate and carbamate insecticides. Electroanalysis 4:249–252. https://doi.org/10.1002/elan.1140040217

Masson P, Josse D, Lockridge O, Viguié N, Taupin C, Buhler C (1998) Enzymes hydrolyzing organophosphates as potential catalytic scavengers against organophosphate poisoning. J Physiol Paris 92:357–362. https://doi.org/10.1016/S0928-4257(99)80005-9

Masson P, Nachon F, Lockridge O (2010) Structural approach to the aging of phosphylated cholinesterases. Chem Biol Interact 187:157–162. https://doi.org/10.1016/j.cbi.2010.03.027

Matula M, Kucera T, Soukup O, Pejchal J (2020) Enzymatic Degradation of Organophosphorus Pesticides and Nerve Agents by EC: 3.1.8.2. Catalysts 10:1365. https://doi.org/10.3390/catal10121365

Meeker JD, Barr DB, Hauser R (2009) Pyrethroid insecticide metabolites are associated with serum hormone levels in adult men. Reprod Toxicol 27:155–160. https://doi.org/10.1016/j.reprotox.2008.12.012

Meijer M, Hamers T, Westerink RHS (2014) Acute disturbance of calcium homeostasis in PC12 cells as a novel mechanism of action for (sub)micromolar concentrations of organophosphate insecticides. Neurotoxicology 43:110–116. https://doi.org/10.1016/j.neuro.2014.01.008

Mello S V., Mabrouki M, Cao X, Leblanc RM, Cheng TC, DeFrank JJ (2003) Langmuir and Langmuir - Blodgett films of organophosphorus acid anhydrolase. Biomacromolecules 4:968–973. https://doi.org/10.1021/bm025775+

Moshiri M, Darchini-Maragheh E, Balali-Mood M (2012) Advances in toxicology and medical treatment of chemical warfare nerve agents. DARU, J Pharm Sci 20:. https://doi.org/10.1186/2008-2231-20-81

Mueller-Beilschmidt D (1990) Toxicology and environmental fate of synthetic pyrethroids. J Pestic Reform 10:32–37

Mulchandani A, Chen W, Mulchandani P, Wang J, Rogers KR (2001a) Biosensors for direct determination of organophosphate pesticides. Biosens Bioelectron 16:225–230. https://doi.org/10.1016/S0956-5663(01)00126-9

Mulchandani A, Kaneva I, Chen W (1998) Biosensor for direct determination of organophosphate nerve agents using recombinant Escherichia coli with surface-expressed organophosphorus hydrolase. 2. Fiber-optic microbial biosensor. Anal Chem 70:5042–5046. https://doi.org/10.1021/ac9806431

Mulchandani A, Pan S, Chen W (1999) Fiber-optic enzyme biosensor for direct determination of organophosphate nerve agents. Biotechnol Prog 15:130–134. https://doi.org/10.1021/bp980111q

Mulchandani P, Chen W, Mulchandani A, Wang J, Chen L (2001b) Amperometric microbial biosensor for direct determination of organophosphate pesticides using recombinant microorganism with surface expressed organophosphorus hydrolase. Biosens Bioelectron 16:433–437. https://doi.org/10.1016/S0956-5663(01)00157-9

Muley A, Shah C, Lakhani J, Bapna M, Mehta J (2014) To identify morbidity and mortality predictors in acute organophosphate poisoning. Indian J Crit Care Med 18:297

Munidasa UADD, Gawarammana IB, Kularatne SAM, Kumarasiri PVR,

Goonasekera CDA (2004) Survival Pattern in Patients with Acute Organophosphate Poisoning Receiving Intensive Care. J Toxicol Clin Toxicol 42:343–347. https://doi.org/10.1081/CLT-120039539

Muñoz-Quezada MT, Lucero BA, Barr DB, Steenland K, Levy K, Ryan PB, Iglesias V, Alvarado S, Concha C, Rojas E, Vega C (2013) Neurodevelopmental effects in children associated with exposure to organophosphate pesticides: A systematic review. Neurotoxicology 39:158–168. https://doi.org/10.1016/j.neuro.2013.09.003

Murray DL, Taylor PL (2000) Claim no easy victories: Evaluating the pesticide industry's Global Safe Use campaign. World Dev 28:1735–1749. https://doi.org/10.1016/S0305-750X(00)00059-0

Nakano M, Arai Y, Kotera I, Okabe K, Kamei Y, Nagai T (2017) Genetically encoded ratiometric fluorescent thermometer with wide range and rapid response. PLoS One 12:. https://doi.org/10.1371/journal.pone.0172344

Nallamsetty S, Waugh DS (2006) Solubility-enhancing proteins MBP and NusA play a passive role in the folding of their fusion partners. Protein Expr Purif 45:175–182. https://doi.org/10.1016/j.pep.2005.06.012

Naqvi T, Warden AC, French N, Sugrue E, Carr PD, Jackson CJ, Scott C (2014) A 5000-fold increase in the specificity of a bacterial phosphotriesterase for malathion through combinatorial active site mutagenesis. PLoS One 9:e94177. https://doi.org/10.1371/journal.pone.0094177

Nath I, Chakraborty J, Verpoort F (2016) Metal organic frameworks mimicking natural enzymes: a structural and functional analogy. Chem Soc Rev 45:4127–4170. https://doi.org/10.1039/c6cs00047a

Nemzer LR, Epstein AJ (2010) A polyaniline-based optical biosensing platform using an entrapped oxidoreductase enzyme. Sensors Actuators, B Chem 150:376–383. https://doi.org/10.1016/j.snb.2010.06.054

Nieuwoudt MK, Holroyd SE, McGoverin CM, Simpson MC, Williams DE

(2016) Raman spectroscopy as an effective screening method for detecting adulteration of milk with small nitrogen-rich molecules and sucrose. J Dairy Sci 99:2520–2536. https://doi.org/10.3168/jds.2015-10342

Orbulescu J, Constantine CA, Rastogi VK, Shah SS, DeFrank JJ, Leblanc RM (2006) Detection of organophosphorus compounds by covalently immobilized organophosphorus hydrolase. Anal Chem 78:7016–7021. https://doi.org/10.1021/ac061118m

Ortiz-Delgado JB, Funes V, Sarasquete C (2019) The organophosphate pesticide -OP- malathion inducing thyroidal disruptions and failures in the metamorphosis of the Senegalese sole, Solea senegalensis. BMC Vet Res 15:3–21. https://doi.org/10.1186/s12917-019-1786-z

Paliwal S, Wales M, Good T, Grimsley J, Wild J, Simonian A (2007) Fluorescence-based sensing of p-nitrophenol and p-nitrophenyl substituent organophosphates. Anal Chim Acta 596:9–15. https://doi.org/10.1016/j.aca.2007.05.034

Panchompoo J, Aldous L, Baker M, Wallace MI, Compton RG (2012) One-step synthesis of fluorescein modified nano-carbon for Pd(ii) detection via fluorescence quenching. Analyst 137:2054–2062. https://doi.org/10.1039/c2an16261j

Pang L, Ge L, Yang P, He H, Zhang H (2018) Degradation of organophosphate esters in sewage sludge: Effects of aerobic/anaerobic treatments and bacterial community compositions. Bioresour Technol 255:16–21. https://doi.org/10.1016/j.biortech.2018.01.104

Paraíba LC, de Castro VLSS, de Holanda A, Maia N (2009) Insecticide distribution model in human tissues viewing worker's health monitoring programs. Brazilian Arch Biol Technol 52:875–881. https://doi.org/10.1590/S1516-89132009000400011

Park H, Kim PH, Hwang T, Kwon OJ, Park TJ, Choi SW, Yun CO, Kim JH (2012) Fabrication of cross-linked alginate beads using electrospraying for adenovirus delivery. Int J Pharm 427:417–425.

https://doi.org/10.1016/j.ijpharm.2012.01.050

Pédelacq JD, Cabantous S, Tran T, Terwilliger TC, Waldo GS (2006) Engineering and characterization of a superfolder green fluorescent protein. Nat Biotechnol 24:79–88. https://doi.org/10.1038/nbt1172

Pedrosa VA, Paliwal S, Balasubramanian S, Nepal D, Davis V, Wild J, Ramanculov E, Simonian A (2010) Enhanced stability of enzyme organophosphate hydrolase interfaced on the carbon nanotubes. Colloids Surfaces B Biointerfaces 77:69–74. https://doi.org/10.1016/j.colsurfb.2010.01.009

Pei L, Mcguinn GD, Petrikovics I, Pu L, Cannon EP, Way JL (1993) Determination of organophosphorus acid anhydrase in blood. Toxicol Mech Methods 3:261–267. https://doi.org/10.3109/15376519309068443

Peter JV, Jerobin J, Nair A, Bennett A, Samuel P, Chrispal A, Abraham OC, Mathews KP, Fleming JJ, Oommen A (2010) Clinical profile and outcome of patients hospitalized with dimethyl and diethyl organophosphate poisoning. Clin Toxicol 48:916–923. https://doi.org/10.3109/15563650.2010.528425

Peterson MW, Fairchild SZ, Otto TC, Mohtashemi M, Cerasoli DM (2011) VX Hydrolysis by Human Serum Paraoxonase 1: A Comparison of Experimental and Computational Results. PLoS One 6:e20335. https://doi.org/10.1371/journal.pone.0020335

Petrikovics I, Cheng TC, Papahadjopoulos D, Hong K, Yin R, DeFrank JJ, Jaing J, Song ZH, McGuinn WD, Sylvester D, Pei L, Madec J, Tamulinas C, Jaszberenyi JC, Barcza T, Way JL (2000) Long circulating liposomes encapsulating organophosphorus acid anhydrolase in diisopropylfluorophosphate antagonism. Toxicol Sci 57:16–21. https://doi.org/10.1093/toxsci/57.1.16

Pirsaheb M, Moradi N (2020) Sonochemical degradation of pesticides in aqueous solution: Investigation on the influence of operating parameters and degradation pathway-a systematic review. RSC Adv 10:7396–7423.

https://doi.org/10.1039/c9ra11025a

Pita R, Marco-Contelles J, Ramos E, Del Pino J, Romero A (2013) Toxicity induced by chemical warfare agents: Insights on the protective role of melatonin. Chem Biol Interact 206:134–142. https://doi.org/10.1016/j.cbi.2013.09.001

Plekhanova Y V., Tikhonenko SA, Dubrovsky A V., Kim AL, Musin E V., Wang GJ, Kuznetsova IE, Kolesov V V., Reshetilov AN (2019) Comparative study of electrochemical sensors based on enzyme immobilized into polyelectrolyte microcapsules and into chitosan gel. Anal Sci 35:1037–1043. https://doi.org/10.2116/analsci.19P131

Pohanka M (2013) Cholinesterases in Biorecognition and Biosensors Construction: A Review. Anal Lett 46:1849–1868. https://doi.org/10.1080/00032719.2013.780240

Porzio E, Bettazzi F, Mandrich L, Del Giudice I, Restaino OF, Laschi S, Febbraio F, De Luca V, Borzacchiello MG, Carusone TM, Worek F, Pisanti A, Porcaro P, Schiraldi C, De Rosa M, Palchetti I, Manco G (2018) Innovative Biocatalysts as Tools to Detect and Inactivate Nerve Agents. Sci Rep 8:1–13. https://doi.org/10.1038/s41598-018-31751-5

Prasher DC, Eckenrode VK, Ward WW, Prendergast FG, Cormier MJ (1992) Primary structure of the Aequorea victoria green-fluorescent protein. Gene 111:229–233. https://doi.org/10.1016/0378-1119(92)90691-H

Prieto-Simón B, Campàs M, Andreescu S, Marty JL (2006) Trends in flow-based biosensing systems for pesticide assessment. Sensors 6:1161–1186. https://doi.org/10.3390/s6101161

Proudfoot AT (2005) Poisoning due to pyrethrins. Toxicol Rev 24:107–113. https://doi.org/10.2165/00139709-200524020-00004

Pundir CS, Chauhan N (2012) Acetylcholinesterase inhibition-based biosensors for pesticide determination: A review. Anal Biochem 429:19–31. https://doi.org/10.1016/j.ab.2012.06.025

Quinn DM, Topczewski J, Yasapala N, Lodge A (2017) Why is aged acetylcholinesterase so difficult to reactivate? Molecules 22:1464

Rainina EII, Efremenco ENN, Varfolomeyev SDD, Simonian ALL, Wild JRR (1996) The development of a new biosensor based on recombinant E. coli for the direct detection of organophosphorus neurotoxins. Biosens Bioelectron 11:991–1000. https://doi.org/10.1016/0956-5663(96)87658-5

Rajasekar M (2021) Recent development in fluorescein derivatives. J Mol Struct 1224:129085. https://doi.org/10.1016/j.molstruc.2020.129085

Rasmussen JJ, Baattrup-Pedersen A, Larsen SE, Kronvang B (2011) Local physical habitat quality cloud the effect of predicted pesticide runoff from agricultural land in Danish streams. J Environ Monit 13:943–950. https://doi.org/10.1039/c0em00745e

Raushel FM (2002) Bacterial detoxification of organophosphate nerve agents. Curr Opin Microbiol 5:288–295. https://doi.org/10.1016/S1369-5274(02)00314-4

Raushel FM, Holden HM (2000) Phosphotriesterase: an enzyme in search of its natural substrate. Adv Enzymol Relat Areas Mol Biol 74:51–93. https://doi.org/10.1002/9780470123201.ch2

Realdon N, Ragazzi E, Ragazzi E (2001) Effect of drug solubility on in vitro availability rate from suppositories with polyethylene glycol excipients. Pharmazie 56:163–167

Reeves TE, Wales ME, Grimsley JK, Li P, Cerasoli DM, Wild JR (2008) Balancing the stability and the catalytic specificities of OP hydrolases with enhanced V-agent activities. Protein Eng Des Sel 21:405–412. https://doi.org/10.1093/protein/gzn019

Ren PW, Ju XJ, Xie R, Chu LY (2010) Monodisperse alginate microcapsules with oil core generated from a microfluidic device. J Colloid Interface Sci 343:392–395. https://doi.org/10.1016/j.jcis.2009.11.007

Richardt A, Blum MM (2008) Decontamination of Warfare Agents: Enzymatic Methods for the Removal of B/C Weapons. 1–293. https://doi.org/10.1002/9783527621620

Robinson PK (2015) Enzymes: principles and biotechnological applications. Essays Biochem 59:1–41. https://doi.org/10.1042/BSE0590001

Rogers KR, Wang Y, Mulchandani A, Mulchandani P, Chen W (1999) Organophosphorus hydrolase-based assay for organophosphate pesticides. Biotechnol Prog 15:517–521. https://doi.org/10.1021/bp990034e

Rowland SS, Speedie MK, Pogell BM (1991) Purification and characterization of a secreted recombinant phosphotriesterase (parathion hydrolase) from Streptomyces lividans. Appl Environ Microbiol 57:440–444. https://doi.org/10.1128/aem.57.2.440-444.1991

Ryškevič N, Juršnas S, Vitta P, Bakien E, Gaska R, Žukauskas A (2010) Concept design of a UV light-emitting diode based fluorescence sensor for real-time bioparticle detection. Sensors Actuators, B Chem 148:371–378. https://doi.org/10.1016/j.snb.2010.05.042

Sahdev S, Khattar SK, Saini KS (2008) Production of active eukaryotic proteins through bacterial expression systems: A review of the existing biotechnology strategies. Mol Cell Biochem 307:249–264. https://doi.org/10.1007/s11010-007-9603-6

Sandoval-Castilla O, Lobato-Calleros C, García-Galindo HS, Alvarez-Ramírez J, Vernon-Carter EJ (2010) Textural properties of alginate-pectin beads and survivability of entrapped Lb. casei in simulated gastrointestinal conditions and in yoghurt. Food Res Int 43:111–117. https://doi.org/10.1016/j.foodres.2009.09.010

Santillan JY, Rojas NL, Ghiringhelli PD, Nóbile ML, Lewkowicz ES, Iribarren AM (2020) Organophosphorus compounds biodegradation by novel bacterial isolates and their potential application in bioremediation of contaminated water. Bioresour Technol 317:124003.

https://doi.org/10.1016/j.biortech.2020.124003

Scharff EI, Koepke J, Fritzsch G, Lücke C, Rüterjans H (2001a) Crystal structure of diisopropylfluorophosphatase from Loligo vulgaris. Structure 9:493–502. https://doi.org/10.1016/S0969-2126(01)00610-4

Scharff EI, Lücke C, Fritzsch G, Koepke J, Hartleib J, Dierl S, Rüterjans H (2001b) Crystallization and preliminary X-ray crystallographic analysis of DFPase from Loligo vulgaris. Acta Crystallogr Sect D Biol Crystallogr 57:148–149. https://doi.org/10.1107/S0907444900014232

Schofield DA, DiNovo AA (2010) Generation of a mutagenized organophosphorus hydrolase for the biodegradation of the organophosphate pesticides malathion and demeton-S. J Appl Microbiol 109:548–557. https://doi.org/10.1111/j.1365-2672.2010.04672.x

Shaner NC, Campbell RE, Steinbach PA, Giepmans BNG, Palmer AE, Tsien RY (2004) Improved monomeric red, orange and yellow fluorescent proteins derived from Discosoma sp. red fluorescent protein. Nat Biotechnol 22:1567–1572. https://doi.org/10.1038/nbt1037

Shilpa A, Agrawal SS, Ray AR (2003) Controlled delivery of drugs from alginate matrix. J Macromol Sci - Polym Rev 43:187–221. https://doi.org/10.1081/MC-120020160

Shimazu M, Chen W, Mulchandani A (2003) Biological Detoxification of Organophosphate Pesticides. ACS Symp Ser 863:25–36. https://doi.org/10.1021/bk-2004-0863.ch003

Siddavattam D (2017) Evolution of Phosphotriesterases (PTEs): How Bacteria Can Acquire New Degradative Functions? Proc Indian Natl Sci Acad 83:865–875. https://doi.org/10.16943/ptinsa/2017/49140

Sidell FR, Borak J (1992) Chemical warfare agents: II. nerve agents. Ann Emerg Med 21:865–871. https://doi.org/10.1016/S0196-0644(05)81036-4

Sidhu GK, Singh S, Kumar V, Dhanjal S, Datta S, Singh J, Singh Dhanjal D (2019) Critical Reviews in Environmental Science and Technology

Toxicity, monitoring and biodegradation of organophosphate pesticides: A review Toxicity, monitoring and biodegradation of organophosphate pesticides: A review. https://doi.org/10.1080/10643389.2019.1565554

Silva E, Daam MA, Cerejeira MJ (2015) Aquatic risk assessment of priority and other river basin specific pesticides in surface waters of Mediterranean river basins. Chemosphere 135:394–402. https://doi.org/10.1016/j.chemosphere.2015.05.013

Silva V, Mol HGJ, Zomer P, Tienstra M, Ritsema CJ, Geissen V (2019) Pesticide residues in European agricultural soils – A hidden reality unfolded. Sci Total Environ 653:1532–1545. https://doi.org/10.1016/j.scitotenv.2018.10.441

Simonian AL, Flounders AW, Wild JR (2004) FET-based biosensors for the direct detection of organophosphate neurotoxins. Electroanalysis 16:1896–1906. https://doi.org/10.1002/elan.200403078

Simonian AL, Good TA, Wang S-SS, Wild JR (2005) Nanoparticle-based optical biosensors for the direct detection of organophosphate chemical warfare agents and pesticides. Anal Chim Acta 534:69–77. https://doi.org/10.1016/j.aca.2004.06.056

Simonian AL, Grimsley JK, Flounders AW, Schoeniger JS, Cheng TC, DeFrank JJ, Wild JR (2001) Enzyme-based biosensor for the direct detection of fluorine-containing organophosphates. Anal Chim Acta 442:15–23. https://doi.org/10.1016/S0003-2670(01)01131-X

Singh BK, Walker A (2006) Microbial degradation of organophosphorus compounds. FEMS Microbiol Rev 30:428–471. https://doi.org/10.1111/j.1574-6976.2006.00018.x

Smith HG, Dänhardt J, Lindström Å, Rundlöf M (2010) Consequences of organic farming and landscape heterogeneity for species richness and abundance of farmland birds. Oecologia 162:1071–1079. https://doi.org/10.1007/s00442-010-1588-2

Sogorb MA, Vilanova E (2002) Enzymes involved in the detoxification of

organophosphorus, carbamate and pyrethroid insecticides through hydrolysis. Toxicol Lett 128:215–228. https://doi.org/10.1016/S0378-4274(01)00543-4

Spiess C, Beil A, Ehrmann M (1999) A temperature-dependent switch from chaperone to protease in a widely conserved heat shock protein. Cell 97:339–347. https://doi.org/10.1016/S0092-8674(00)80743-6

Spriestersbach A, Kubicek J, Schäfer F, Block H, Maertens B (2015) Purification of His-Tagged Proteins. Methods Enzymol 559:1–15. https://doi.org/10.1016/bs.mie.2014.11.003

Stojanovic R, Belscak-Cvitanovic A, Manojlovic V, Komes D, Nedovic V, Bugarski B (2012) Encapsulation of thyme (Thymus serpyllum L.) aqueous extract in calcium alginate beads. J Sci Food Agric 92:685–696. https://doi.org/10.1002/jsfa.4632

Strekopytov S, Brownscombe W, Lapinee C, Sykes D, Spratt J, Jeffries TE, Jones CG (2017) Arsenic and mercury in bird feathers: Identification and quantification of inorganic pesticide residues in natural history collections using multiple analytical and imaging techniques. Microchem J 130:301–309. https://doi.org/10.1016/j.microc.2016.10.009

Sungur M, Güven M (2001) Intensive care management of organophosphate insecticide poisoning. Crit Care 5:211–215. https://doi.org/10.1186/cc1025

Sungurtekin H, Gürses E, Balci C (2006) Evaluation of several clinical scoring tools in organophosphate poisoned patients. Clin Toxicol 44:121–126. https://doi.org/10.1080/15563650500514350

Syed JH, Malik RN, Liu D, Xu Y, Wang Y, Li J, Zhang G, Jones KC (2013) Organochlorine pesticides in air and soil and estimated air-soil exchange in Punjab, Pakistan. Sci Total Environ 444:491–497. https://doi.org/10.1016/j.scitotenv.2012.12.018

Tang X, Liang B, Yi T, Manco G, IlariaPalchetti, Liu A (2014) Cell surface display of organophosphorus hydrolase for sensitive

spectrophotometric detection of p-nitrophenol substituted organophosphates. Enzyme Microb Technol 55:107–112. https://doi.org/10.1016/j.enzmictec.2013.10.006

Thakur S, Kumar P, Reddy MV, Siddavattam D, Paul AK (2013) Enhancement in sensitivity of fluorescence based assay for organophosphates detection by silica coated silver nanoparticles using organophosphate hydrolase. Sensors Actuators B Chem 178:458–464. https://doi.org/10.1016/j.snb.2013.01.010

Thakur S, Venkateswar Reddy M, Siddavattam D, Paul AK (2012) A fluorescence based assay with pyranine labeled hexa-histidine tagged organophosphorus hydrolase (OPH) for determination of organophosphates. Sensors Actuators, B Chem 163:153–158. https://doi.org/10.1016/j.snb.2012.01.024

Theriot CM, Grunden AM (2011) Hydrolysis of organophosphorus compounds by microbial enzymes. Appl Microbiol Biotechnol 89:35–43. https://doi.org/10.1007/s00253-010-2807-9

Tien CJ, Lin MC, Chiu WH, Chen CS (2013) Biodegradation of carbamate pesticides by natural river biofilms in different seasons and their effects on biofilm community structure. Environ Pollut 179:95–104. https://doi.org/10.1016/j.envpol.2013.04.009

Toe AM, Ouedraogo M, Ouedraogo R, Ilboudo S, Guissou PI (2013) Pilot study on agricultural pesticide poisoning in Burkina Faso. Interdiscip Toxicol 6:185–191. https://doi.org/10.2478/intox-2013-0027

Tokuriki N, Tawfik DS (2009) Chaperonin overexpression promotes genetic variation and enzyme evolution. Nature 459:668–673. https://doi.org/10.1038/nature08009

Topol I, Collins J, Nemukhin A (2010) Modeling spectral tuning in monomeric teal fluorescent protein mTFP1. Biophys Chem 149:78–82. https://doi.org/10.1016/j.bpc.2010.04.002

US EPA O (2015) Protect Yourself from Pesticides: Guide for Agricultural

Workers (English-Spanish). US EPA

Van Dyk JS, Pletschke B (2011) Review on the use of enzymes for the detection of organochlorine, organophosphate and carbamate pesticides in the environment. Chemosphere 82:291–307. https://doi.org/10.1016/j.chemosphere.2010.10.033

VanEngelenburg SB, Palmer AE (2008) Fluorescent biosensors of protein function. Curr Opin Chem Biol 12:60–65. https://doi.org/10.1016/j.cbpa.2008.01.020

Vera A, González-Montalbán N, Arís A, Villaverde A (2007) The conformational quality of insoluble recombinant proteins is enhanced at low growth temperatures. Biotechnol Bioeng 96:1101–1106. https://doi.org/10.1002/bit.21218

Vilanova E, Sogorb MA (1999) The role of phosphotriesterases in the detoxication of organophosphorus compounds. Crit Rev Toxicol 29:21–57. https://doi.org/10.1080/10408449991349177

Votchitseva YA, Efremenko EN, Aliev TK, Varfolomeyev SD (2006) Properties of hexahistidine-tagged organophosphate hydrolase. Biochem 71:167–172. https://doi.org/10.1134/S0006297906020088

Vyas NK, Nickitenko A, Rastogi VK, Shah SS, Quiocho FA (2010) Structural insights into the dual activities of the nerve agent degrading organophosphate anhydrolase/prolidase. Biochemistry 49:547–559. https://doi.org/10.1021/bi9011989

Wagner-Schuman M, Richardson JR, Auinger P, Braun JM, Lanphear BP, Epstein JN, Yolton K, Froehlich TE (2015) Association of pyrethroid pesticide exposure with attention-deficit/hyperactivity disorder in a nationally representative sample of U.S. children. Environ Heal 14:. https://doi.org/10.1186/s12940-015-0030-y

Wales ME, Reeves TE (2012) Organophosphorus hydrolase as an in vivo catalytic nerve agent bioscavenger. Drug Test Anal 4:271–281. https://doi.org/10.1002/dta.381

Walker JP, Kimble KW, Asher SA (2007) Photonic crystal sensor for organophosphate nerve agents utilizing the organophosphorus hydrolase enzyme. Anal Bioanal Chem 389:2115–2124. https://doi.org/10.1007/s00216-007-1599-y

Wang J, Zhu Y, Cai X, Yu J, Yang X, Cheng J (2011) Abnormal glucose regulation in pyrethroid pesticide factory workers. Chemosphere 82:1080–1082. https://doi.org/10.1016/j.chemosphere.2010.10.065

Watson FL, Schmidt H, Turman ZK, Hole N, Garcia H, Gregg J, Tilghman J, Fradinger EA (2014) Organophosphate pesticides induce morphological abnormalities and decrease locomotor activity and heart rate in Danio rerio and Xenopus laevis. Environ Toxicol Chem 33:1337–1345. https://doi.org/10.1002/etc.2559

Weston DP, Holmes RW, Lydy MJ (2009) Residential runoff as a source of pyrethroid pesticides to urban creeks. Environ Pollut 157:287–294. https://doi.org/10.1016/j.envpol.2008.06.037

White BJ, Harmon HJ (2005) Optical solid-state detection of organophosphates using organophosphorus hydrolase. Biosens Bioelectron 20:1977–1983. https://doi.org/10.1016/j.bios.2004.08.019

Wiedenmann J, Oswald F, Nienhaus GU (2009) Fluorescent proteins for live cell imaging: Opportunities, limitations, and challenges. IUBMB Life 61:1029–1042. https://doi.org/10.1002/iub.256

Wischke C, Borchert HH (2006) Fluorescein isothiocyanate labelled bovine serum albumin (FITC-BSA) as a model protein drug: Opportunities and drawbacks. Pharmazie 61:770–774

Wu T, Zhang Y, Hou T, Zhang Y, Wang S (2018) A simple and sensitive fluorescence method for detection of telomerase activity using fusion protein bouquets. Anal Chim Acta 1038:120–125. https://doi.org/10.1016/j.aca.2018.07.009

Wymore T, Field MJ, Langan P, Smith JC, Parks JM (2014) Hydrolysis of DFP and the nerve agent (S)-sarin by DFPase proceeds along two different

reaction pathways: Implications for engineering bioscavengers. J Phys Chem B 118:4479–4489. https://doi.org/10.1021/jp410422c

Xiao-wei H, Xiao-bo Z, Ji-yong S, Zhi-hua L, Jie-wen Z (2018) Colorimetric sensor arrays based on chemo-responsive dyes for food odor visualization. Trends Food Sci Technol 81:90–107. https://doi.org/10.1016/j.tifs.2018.09.001

Xiao Y, Yang J, Tian X, Wang X, Li J, Zhang S, Long L (2017) Biochemical basis for hydrolysis of organophosphorus by a marine bacterial prolidase. Process Biochem 52:141–148. https://doi.org/10.1016/j.procbio.2016.10.008

Xiong S, Deng Y, Zhou Y, Gong D, Xu Y, Yang L, Chen H, Chen L, Song T, Luo A, Deng X, Zhang C, Jiang Z (2018) Current progress in biosensors for organophosphorus pesticides based on enzyme functionalized nanostructures: A review. Anal Methods 10:5468–5479. https://doi.org/10.1039/c8ay01851k

Yadav SK, Khan G, Bonde GV, Bansal M, Mishra B (2018) Design, optimization and characterizations of chitosan fortified calcium alginate microspheres for the controlled delivery of dual drugs. Artif Cells, Nanomedicine, Biotechnol 46:1180–1193. https://doi.org/10.1080/21691401.2017.1366331

Yair S, Ofer B, Arik E, Shai S, Yossi R, Tzvika D, Amir K (2008) Organophosphate degrading microorganisms and enzymes as biocatalysts in environmental and personal decontamination applications. Crit Rev Biotechnol 28:265–275. https://doi.org/10.1080/07388550802455742

Yan F, Fan K, Bai Z, Zhang R, Zu F, Xu J, Li X (2017) Fluorescein applications as fluorescent probes for the detection of analytes. TrAC - Trends Anal Chem 97:15–35. https://doi.org/10.1016/j.trac.2017.08.013

Yang G, White IM, Fan X (2008a) An opto-fluidic ring resonator biosensor for the detection of organophosphorus pesticides. Sensors Actuators, B Chem 133:105–112.

https://doi.org/10.1016/j.snb.2008.02.004

Yang J, Yang C, Jiang H, Qiao C (2008b) Overexpression of methyl parathion hydrolase and its application in detoxification of organophosphates. Biodegradation 19:831–839. https://doi.org/10.1007/s10532-008-9186-2

Yap WT, Kelsey Song W, Chauhan N, Nina Scalise P, Agarwal R, Miller SD, Shea LD (2014) Quantification of particle-conjugated or particleencapsulated peptides on interfering reagent backgrounds. Biotechniques 57:39–44. https://doi.org/10.2144/000114190

Yeh CH, Zhao Q, Lee SJ, Lin YC (2009) Using a T-junction microfluidic chip for monodisperse calcium alginate microparticles and encapsulation of nanoparticles. Sensors Actuators, A Phys 151:231–236. https://doi.org/10.1016/j.sna.2009.02.036

Yin XT, Guo XM (2014) Selectivity and sensitivity of Pd-loaded and Fe-doped SnO2 sensor for CO detection. Sensors Actuators, B Chem 200:213–218. https://doi.org/10.1016/j.snb.2014.04.026

Yoshimoto T, Tone H, Honda T, Osatomi R, Kobayashi R, Tsuru D (1989) Sequencing and high expression of aminopeptidase P gene from Escherichia coli HB101. J Biochem 105:412–416. https://doi.org/10.1093/oxfordjournals.jbchem.a122678

Zhang XF, Zhang J, Liu L (2014) Fluorescence properties of twenty fluorescein derivatives: Lifetime, quantum yield, absorption and emission spectra. J Fluoresc 24:819–826. https://doi.org/10.1007/s10895-014-1356-5

Zheng J, Constantine CA, Zhao L, Rastogi VK, Cheng TC, DeFrank JJ, Leblanc RM (2005) Molecular interaction between organophosphorus acid anhydrolase and diisopropylfluorophosphate. Biomacromolecules 6:1555–1560. https://doi.org/10.1021/bm049199o

Zimmer LA, Ennis M, Shipley MT, Wiley RG (1998) Nerve gas-induced seizures: Role of acetylcholine in the rapid induction of Fos and glial

fibrillary acidic protein in piriform cortex. J Neurosci 18:3897–3908. https://doi.org/10.1523/JNEUROSCI.18-10-03897.1998

Zourob M, Ong KG, Zeng K, Mouffouk F, Grimes CA (2007a) A wireless magnetoelastic biosensor for the direct detection of organophosphorus pesticides. Analyst 132:338–343. https://doi.org/10.1039/b616035b

Zourob M, Simonian A, Wild J, Mohr S, Fan X, Abdulhalim I, Goddard NJ (2007b) Optical leaky waveguide biosensors for the detection of organophosphorus pesticides. Analyst 132:114–120. https://doi.org/10.1039/b612871h